

University of Alberta

**The Tectonothermal History of the Split Lake Block, Superior Province,
Manitoba**

by

Melissa Sue Bowerman



A thesis submitted to the Faculty of Graduate Studies and Research
in partial fulfillment of the requirements for the degree of

Master of Science

Department of Earth and Atmospheric Sciences

**Edmonton, Alberta
Spring 2008**



Library and
Archives Canada

Published Heritage
Branch

395 Wellington Street
Ottawa ON K1A 0N4
Canada

Bibliothèque et
Archives Canada

Direction du
Patrimoine de l'édition

395, rue Wellington
Ottawa ON K1A 0N4
Canada

Your file Votre référence

ISBN: 978-0-494-45779-5

Our file Notre référence

ISBN: 978-0-494-45779-5

NOTICE:

The author has granted a non-exclusive license allowing Library and Archives Canada to reproduce, publish, archive, preserve, conserve, communicate to the public by telecommunication or on the Internet, loan, distribute and sell theses worldwide, for commercial or non-commercial purposes, in microform, paper, electronic and/or any other formats.

The author retains copyright ownership and moral rights in this thesis. Neither the thesis nor substantial extracts from it may be printed or otherwise reproduced without the author's permission.

In compliance with the Canadian Privacy Act some supporting forms may have been removed from this thesis.

While these forms may be included in the document page count, their removal does not represent any loss of content from the thesis.

AVIS:

L'auteur a accordé une licence non exclusive permettant à la Bibliothèque et Archives Canada de reproduire, publier, archiver, sauvegarder, conserver, transmettre au public par télécommunication ou par l'Internet, prêter, distribuer et vendre des thèses partout dans le monde, à des fins commerciales ou autres, sur support microforme, papier, électronique et/ou autres formats.

L'auteur conserve la propriété du droit d'auteur et des droits moraux qui protège cette thèse. Ni la thèse ni des extraits substantiels de celle-ci ne doivent être imprimés ou autrement reproduits sans son autorisation.

Conformément à la loi canadienne sur la protection de la vie privée, quelques formulaires secondaires ont été enlevés de cette thèse.

Bien que ces formulaires aient inclus dans la pagination, il n'y aura aucun contenu manquant.



Canada

Abstract

This thesis reports the results of a comprehensive field, metamorphic, and geochronologic study of the Split Lake Block, northern Manitoba aimed to further our understanding of its origin and tectonothermal history. The Split Lake Block is a granulite terrane at the northwest margin of the Superior Province dominated by 2.8-3.1 Ga orthogneisses with rare metasediment that contain Paleoarchean detritus. The Split Lake Block has also been affected by three major episodes of deformation at 2702 Ma, 2695 Ma, and 2620 Ma with possible older metamorphic zircon growth at 2720 Ma and 2770 Ma. The first known conditions of metamorphism reported for the Split Lake Block are between 8-10 kbar and 750-920°C. The similarities between the nearby Pikwitonei Granulite Domain and the Split Lake Block suggest that these two areas share a common history.

Acknowledgements

This research was made possible through significant contributions from Manitoba Hydro, Manitoba Industry, Trades and Mines: Manitoba Geological Survey, and a National Sciences and Engineering Research Council of Canada grant awarded to Dr. Larry Heaman. Bill Reynolds and Lawrence Norquay from Manitoba Hydro provided exceptional field and technical support to the summer field excursions.

First, I would like to thank my supervisor Dr. Larry Heaman for his patience and positive outlook during the entire project. A very large thank you goes to Dr. Tom Chacko, for being the most exceptionally hard working co-supervisor I never had. A great deal of support during the field season and research was given by Dr. Christian Bohm, from the Manitoba Geological Survey as well as Dr. Russell Hartlaub, formerly of the University of Alberta. There are many people at the University of Alberta to thank for their assistance with the laboratory and analytical techniques used in this study. Instruction and data reduction help with LA-ICP-MS was patiently provided by Dr. Tony Simonetti. Dr. Sergei Matveev was very helpful during the electron microprobe sessions. Training and sample preparation was provided by Judy Schultz, Mark Labbe, and Don Resultay. These support people should be considered some of the greatest assets in the EAS Department.

The field crews that I was a part of for both field seasons consisted of a host of people who were geologically proficient as well as competent in ensuring that there was never a dull moment. Excellent field support was provided by Neill Brandson with the Manitoba Geological Survey in Thompson, Manitoba. Thank you to Matt Downey and Dr. Yvette Kuiper as well as our numerous assistants (Trevor Allen, Drew Heasman, Tara Penner, Geoff Speers, Jen Vinck, Tashia Dzikowski, and Todd Middleton) who were excellent companions and geologists. Our many visitors from the Manitoba Geological Survey (Tim Corkery, Alan Bailes and Ric Syme) provided helpful suggestions from their own vast field knowledge.

At the University of Alberta I have been lucky to be a part of an entire society of supportive and positive fellow graduate students and in particular thanks should go out to Shannon Zurevinski, Michael Schultz, and Jen Parks (of the University of Waterloo) who have been excellent sounding boards and friends. To my Parents I say thanks for your unwavering support and belief in me, I know that along the way I have had many doubts but those were often alleviated by you. My entire family has been very patient and I promise to become a fully functioning member very soon. Lastly to Micheal Moroskat, the best cheerleader a person could ask for and I hope that I can return the favour when you go on to write your own thesis in the near future.

Table of Contents

1.0 Introduction	1
1.1 Review of Ancient Crust Occurrences	4
1.2 Assean Lake Crustal Complex and the Northern Superior Superterrane	5
2.0 Geological Background	6
2.1 Pikwitonei Granulite Domain	6
2.2 Split Lake Block	9
2.2.1 Mafic Granulite	9
2.2.2 Amphibolite	11
2.2.3 Metasediment	11
2.2.4 Aluminous Granulite	11
2.2.5 Felsic Intrusive Units	14
2.2.6 Mafic Dykes	15
2.3 Gull Rapids Study Area	15
2.3.1 Metamorphic History	16
2.3.2 Previous Research	16
3.0 Analytical Techniques	18
3.1 Geochemistry	18
3.2 Mineral Chemistry, Imaging, and Chemical Ages	18
3.3 Thermobarometry	18
3.4 Mineral Separation	20
3.5 Tracer Isotopes	20
3.6 U-Pb Laser Ablation MC-ICP-MS	21
3.7 Thermal Ionization Mass Spectrometry	23
4.0 Results	23
4.1 Geochemistry	23

4.1.1	Metasediment	23
4.1.2	Mafic Igneous Units	24
4.1.3	Aluminous Granulite	28
4.1.4	Felsic Orthogneiss	30
4.1.5	Granitoid Injection	30
4.2	Petrography	30
4.2.1	Mafic Granulite	32
4.2.2	Aluminous Garnet-bearing Granulite	32
4.3	Mineral Chemistry	32
4.3.1	Garnet	34
4.3.2	Feldspar	35
4.3.3	Clinopyroxene	35
4.3.4	Orthopyroxene	35
4.3.5	Accessory Minerals	35
4.4	Thermobarometry	36
4.4.1	Thermodynamic System	36
4.4.2	Mafic Granulite	36
4.4.3	Aluminous Garnet-bearing Granulite	40
4.5	Radiogenic Isotope Analyses	43
4.5.1	Samarium-Neodymium	43
4.5.2	Uranium-Lead Geochronology	43
4.5.3	Electron Microprobe Analysis	45
4.5.4	Uranium-Lead Laser Ablation Inductively Coupled Plasma Mass Spectrometry	45
4.5.4.1	Sample 9703-6365 (Grain Mount)	45
4.5.4.2	Sample 9704-7069 (Grain Mount)	59
4.5.4.3	Sample 9704-7069 (Thin Section)	60

4.5.4.4 Sample 9704-7054 (Thin Section)	69
4.5.4.5 Sample GAR01 (Thin Section)	73
4.5.5 Thermal Ionization Mass Spectrometry	73
5.0 Discussion	75
5.1 Tectonothermal History	75
5.2 Timing of Events	76
5.3 Origin of Orthogneiss	81
5.4 Origin of Supracrustal Assemblage	81
5.5 Comparison with the Assean Lake Crustal Complex	86
5.6 Comparison with the Pikwitonei Granulite Domain	87
6.0 Conclusions	89
7.0 Future Research	91
8.0 References	92

List of Tables

Table 1 – Thermobarometric Systems	19
Table 2 – Thermobarometric Results	39
Table 3 – Petrographic Information for Zircons used for Geochronology	79

List of Figures

Figure 1 A map of the tectonic provinces of Canada	2
Figure 2 a) Subdivisions of the Western Superior Province.	3
b) Close-up of the Northern Superior Superterrane.	3
Figure 3 A map of the Nelson River from Gull Rapids to Split Lake	7
Figure 4 a) Photograph of mafic and aluminous granulite at Gull Rapids	10
b) Photograph of amphibolite at Gull Rapids	10
Figure 5 a) Photograph of metasediment and leucocratic injection at Gull Rapids	12
b) Photograph of metasediment and leucocratic injection at Gull Rapids	12
Figure 6 a) Photograph of mafic dyke and metasediment from Gull Rapids	13
b) Photograph of augen gneiss at Gull Rapids	13
Figure 7 a) Discrimination diagram of metasediment analyses	25
b) Diagram of REE analyses of metasediment	25
Figure 8a) Spider diagram of analyses of amphibolite	26
b) Tectonic association diagram for amphibolite and mafic granulite	26
Figure 9 Spider diagram of analyses of mafic granulite	27
Figure 10 a) Spider diagram of felsic orthogneiss	29
b) Spider diagram of leucogranite	29
Figure 11a) Photo micrograph of garnet porphyroblasts	31
b) Photomicrograph of a sample of mafic granulite	31
c) Photomicrograph of a sample of mafic granulite	31
d) Photomicrograph of clinopyroxene rimmed by hornblende	31
e) Photomicrograph of clinopyroxene rimmed by hornblende	31
Figure 12 a) Backscattered electron image of a hercynite symplectite	33
b) Backscattered electron image of quartz in aluminous granulite	33
Figure 13 a) Metamorphic equilibria for mafic granulite sample 9704-7069	38

b) Metamorphic equilibria for mafic granulite sample 9704-7142D	38
Figure 14 a) Metamorphic equilibria for aluminous granulite sample Garnetite GR	41
b) Metamorphic equilibria for aluminous granulite sample GAR03	41
c) Metamorphic equilibria for aluminous granulite sample 9704-7086	41
Figure 15 A plot of ϵ_{Nd} versus Time	44
Figure 16 A histogram of the distribution of monazite chemical ages	46
Figure 17 a) Photomicrograph of zircon separated from sample 9703-6365	47
Figure 18 a-aa) Backscattered electron images of zircons from sample 9703-6365 ..	48-52
Figure 19 a) LA-ICP-MS data for sample 9703-6365 displayed in a histogram	53
b) A Concordia diagram for LA-ICP-MS data for sample 9703-6365	53
Figure 20 a) Photomicrograph of zircon separated from sample 9704-7069	56
b) Photomicrograph of zircon separated from sample 9704-7069	56
Figure 21 a-f) Backscattered electron images of zircons from sample 9704-7069	57
Figure 22 a) LA-ICP-MS data for sample 9704-7069 in a Concordia diagram	58
b) LA-ICP-MS data for sample 9704-7069 in a histogram	59
Figure 23 a) Photomicrograph of zircon in thin section 9704-7069a	61
b) Photomicrograph of zircon in thin section 9704-7069a	61
Figure 24 a-f) Backscattered electron images of zircons from sample 9704-7069a	62
Figure 25 a) LA-ICP-MS data for sample 9704-7069a in a Concordia diagram	63
b) LA-ICP-MS data for sample 9704-7069a in a histogram.....	63
Figure 26 a) LA-ICP-MS data for sample 9704-7069b in a Concordia diagram	64
b) LA-ICP-MS data for sample 9704-7069b displayed in a histogram	64
Figure 27 a-c) Photomicrographs of zircon in thin-section 9704-7054	66
Figure 28 a-f) Backscattered electron images of zircons from sample 9704-7054	67
Figure 29 a) LA-ICP-MS data for sample 9704-7054 in a Concordia diagram	68
b) LA-ICP-MS data for sample 9704-7054 in a histogram	68
Figure 30 a-d) Backscattered electron images of zircons from sample GAR03	70

Figure 31 a) LA-ICP-MS data for sample GAR01 in a Concordia diagram	71
b) LA-ICP-MS data for sample GAR01 in a histogram	71
Figure 32 a) Concordia diagram of TIMS analyses of zircon	72
b) Concordia diagram of two TIMS analyses of zircon	72
Figure 33 Compilation diagram of geochronological data from the northwestern Superior Province	84

List of Appendices

Appendix 1 – Sample Description and Location.....	107
Appendix 2 – Whole Rock Geochemistry.....	112
2.1 Metasediment Geochemistry.....	113
2.2 Amphibolite Geochemistry.....	117
2.3 Mafic Granulite Geochemistry.....	121
2.4 Aluminous Granulite Geochemistry.....	125
2.5 Orthogneiss Geochemistry.....	129
2.6 Granitoid Geochemistry.....	133
Appendix 3 – Mineral Chemistry.....	137
3.1 Mineral analyses used for Thermobarometry.....	138
3.2 Garnet Mineral Chemistry.....	140
3.3 Plagioclase Mineral Chemistry.....	151
3.4 Clinopyroxene Mineral Chemistry.....	160
3.5 Orthopyroxene Mineral Chemistry.....	164
3.6 Accessory Mineral Chemistry.....	168
Appendix 4 – Geochronology Data.....	170
4.1 Samarium-Neodymium Analyses.....	171
4.2 Monazite Electron Microprobe Analyses	172
4.3 Uranium-Lead Analyses by Laser Ablation	178
4.3.1 Sample 9703-6365	178
4.3.2 Sample 9704-7069	181
4.3.3 Sample 9704-7069A	185

4.3.4 Sample 9704-7069B	186
4.3.5 Sample 9704-7054	187
4.3.6 Sample GAR01	188
4.4 Uranium-Lead Analyses by Thermal Ionization Mass Spectrometry.....	189
Appendix 5 –	
Geology of the Gull Rapids area, Manitoba (part of NTS 54D6)	Map Pocket

Mineral (Abbreviation)

Almandine (Alm)

Alpha-Quartz (aQtz)

Aluminous-Orthopyroxene (aOpx)

Anorthite (An)

Clinopyroxene (Cpx)

Cordierite (Cord)

Diopside (Di)

Enstatite (En)

Feldspar (Fsp)

Garnet (Gar)

Grossular (Gr)

Hedenbergite (Hed)

Hercynite (Herc)

Ilmenite (Ilm)

Orthopyroxene (Opx)

Plagioclase (Plag)

Pyrope (Py)

Quartz (Qtz)

Rutile (Rt)

Sillimanite (Si)

Spessartine (Sp)

Zircon (Zr)

1.0 Introduction

The geological history of Precambrian continents is largely derived from exposures of mid- to upper crust, but important aspects of continental growth are also recorded in rare exposures of middle to lower crust. Tectonic models for Precambrian cratons are often based on minimal information regarding the timing of magmatism and metamorphism and rarely consider the nature of the lower crust. The basement of cratons is often where ancient crust is hidden, therefore, exposures of the mid- to lower-crust offer a unique opportunity to decipher the tectonothermal history of a craton and gain information on the origins of continental crust.

The North American Continent is composed of a number of Archean cratons sutured by Paleoproterozoic Orogenes (Hoffman 1989). The largest of these Archean terranes is the Superior Province (Figure 1), which is blessed by an abundance of high-precision geochronological information (Card 1994). This wealth of age data in the Superior Province has allowed for a working hypothesis of the origin and growth of the entire craton to be formulated by a number of authors (e.g. Card 1990, Percival *et al.* 2006). One of the most striking features of the Superior Province geology is the dominance of 3.0-2.7 Ga east - west trending granite-greenstone terranes built on ~3.0 Ga stable crust and separated by metasedimentary terranes (Card 1990). These belts were amalgamated from 2.72-2.68 Ga and the age of last volcanism progressively youngs from north to south (Card 1990; Percival *et al.*, 2006). Major subdivisions of the Superior Province have been defined by a number of researchers (Card 1990, Percival *et al.* 2006) but the definition of the interior of these superterraneis is not well understood. Recent discoveries of previously unknown ancient crust in the Superior Province (e.g. Assean Lake, Manitoba and Porpoise Cove, Quebec (Bohm *et al.* 2000; David *et al.* 2003)) indicates that the Superior Province could be host to considerably more ancient crust occurrences than previously thought.

In particular, the Northern Superior Superterrane (Figure 2a), located at the northwestern margin of the Superior Province, is a high-grade terrane that hosts ancient

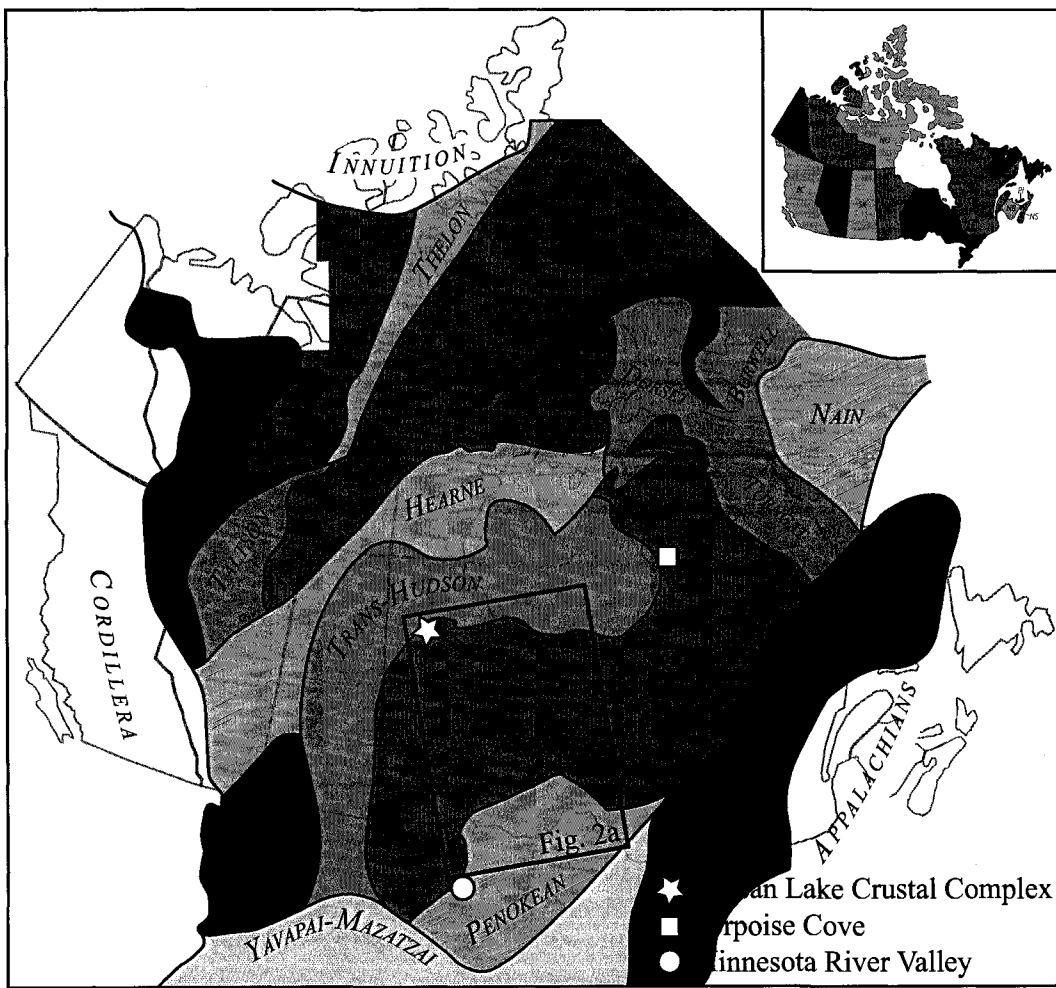


Figure 1: Map of the tectonic provinces of Canada. Figure simplified from Hoffman 1989 and Percival *et al.* 2006.

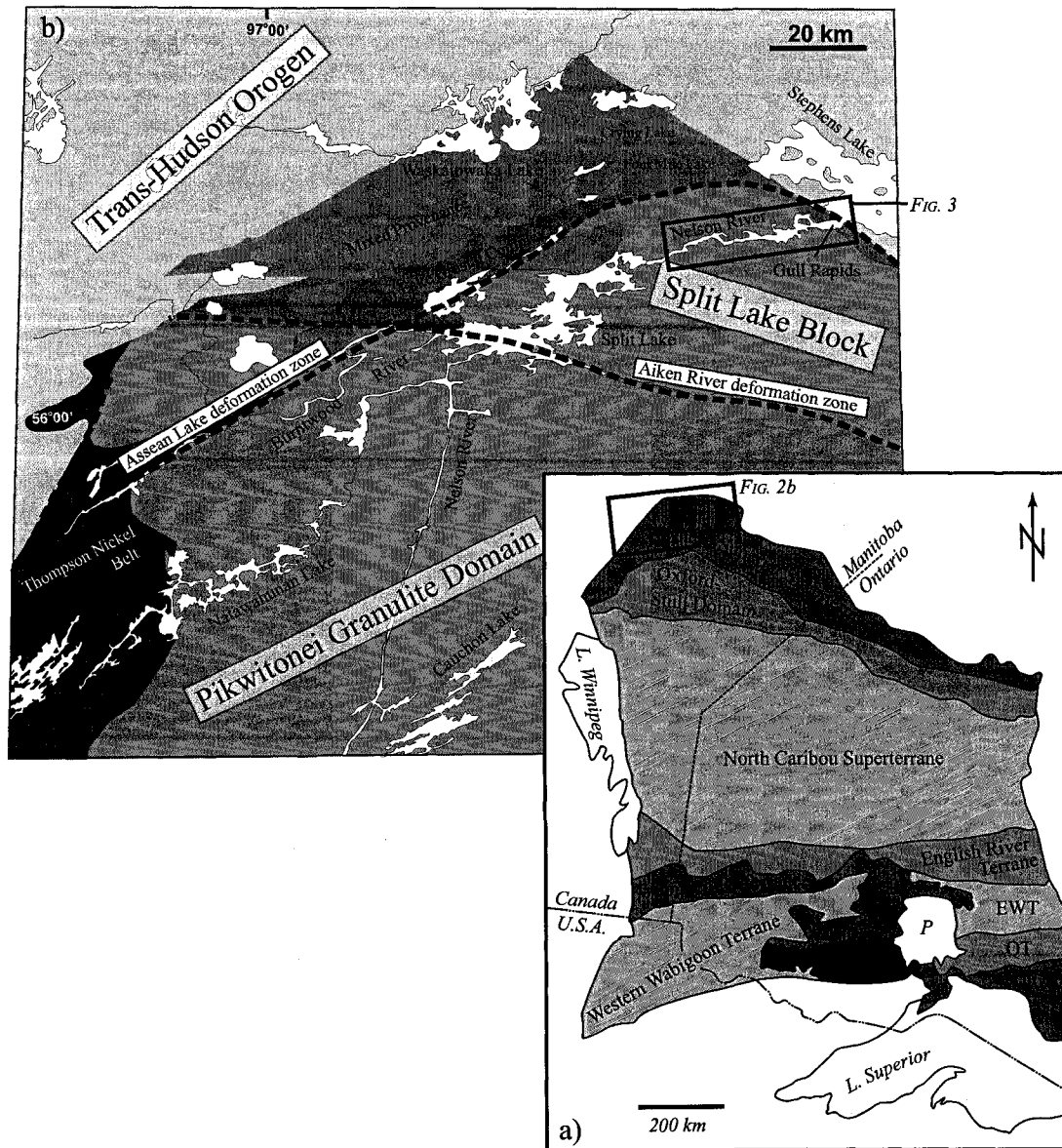


Figure 2: a) Subdivisions of the western Superior Province. EWT: Eastern Wabigoon Terrane QT: Quetico Terrane WT: Wawa-Abitibi Terrane. Redrawn from Percival *et al.* 2006. b) Close-up of the northwestern margin of the Superior Province. Redrawn from Böhm *et al.* 2000.

Mesoarchean crust, including the Assean Lake Crustal Complex (Bohm *et al.* 2003) and the Pikwitonei Granulite Domain (Percival *et al.* 2006). The recent discovery of ancient crust at Assean Lake (Bohm *et al.* 2000) has led to a search for ancient rocks throughout the Northern Superior Superterrane. As part of this search for ancient crust, a targeted initiative involving geoscientists from various institutions (the Universities of Waterloo and Alberta as well as Manitoba Hydro and the Manitoba Geological Survey) was implemented to understand the nature of the crust in the Northern Superior Superterrane as well as deciphering the history of Neoarchean terrane assembly in the Superior Province.

The objectives of this study are to:

- 1) Determine the timing and conditions of high-grade metamorphism in the Split Lake Block
- 2) Investigate the geochemistry and tectonic affiliation of units within the Split Lake Block
- 3) Compare the tectonothermal history of the Split Lake Block with adjacent terranes, such as the Pikwitonei Granulite Domain, to determine whether or not there is a common geological history
- 4) Investigate the crustal assembly history of the northwestern Superior Province

1.1 Review of Ancient Crust Occurrences

Although the Archean represents a major portion (>40%) of the time since Earth's formation and is when the majority of the large stable cratons were formed, our knowledge of the processes and events that occurred during this time are limited because there are relatively few known exposures of ancient (pre-3.0 Ga) crust. A few localities that preserve ancient crust are known in Canada, with a number of new discoveries in the past two decades. Located on the western edge of the Slave Province, the Acosta gneisses are considered to be the oldest known intact rocks on Earth with metamorphosed granitoids as old as 4012 ± 6 Ma (Bowring and Williams 1999) and xenocrystic zircons up to 4203 ± 58

Ma (Iizuka *et al.* 2006). A number of ancient crust exposures have been identified along the margins of the Superior Province in Minnesota, Quebec and Manitoba. For example, the Minnesota River Valley, Minnesota (Figure 1) exposes tonalite gneiss (e.g. Morton Gneiss) that has a U-Pb crystallization age of 3524 ± 9 Ma (Bickford *et al.* 2006). Recently, a sliver of ancient crust has been discovered along the northern margin of the Superior Province in the area of Porpoise Cove, Quebec (Figure 1; David *et al.* 2003). Zircons from a felsic tuff unit within the supracrustal package at Porpoise Cove yielded an an age of 3825 ± 16 Ma (David *et al.* 2003; Bedard *et al.* 2003).

1.2 Assean Lake Crustal Complex and the Northern Superior Superterrane

On the northwestern edge of the Superior Province, a sliver of pre-3.2 Ga ancient crust known as the Assean Lake Crustal Complex has recently been discovered (Heaman *et al.* 1999; Böhm *et al.* 2000; 2003; 2007). A number of amphibolite-grade crustal segments together form the Assean Lake Crustal Complex and these are bounded by the Assean Lake and Aiken River shear zones (Figure 2b). The Assean Lake Crustal Complex consists of 3.1-3.2 Ga tonalitic to granitic orthogneisses that intrude two domains of supracrustal rocks, the Clay River and Lindal Bay packages (Böhm *et al.* 2003). Samples of 3.2-3.1 Ga orthogneiss from the Assean Lake Crustal Complex have a range of Nd model ages from ~3.5 to 3.7 Ga, interpreted to represent the maximum age of their protoliths (Böhm *et al.* 2003). The Nd model ages obtained for the metasedimentary samples range from ~3.5 to 3.9 Ga and are interpreted to represent an average provenance age (Böhm *et al.* 2003). The U-Pb isotopic composition of detrital zircons isolated from supracrustal units (e.g. Lindal Bay metagreywacke) within the Assean Lake Crustal Complex were analysed by ID-TIMS (isotope dilution thermal ionization mass spectrometry; Böhm *et al.* 2000) and SHRIMP (Sensitive High Resolution Ion Microprobe; Böhm *et al.* 2003) and contain grains as old as 3900.4 ± 5.7 and 3905.3 ± 36.5 Ma.

Another exposure of possible ancient metasedimentary rocks occurs ~50 km further

east along strike from Assean Lake at Gull Rapids (Figure 3). The rocks in this region share many similarities to the ancient crust within the Assean Lake Crustal Complex. Based on a reconnaissance study (Bohm *et al.* unpubl. data), initial Nd isotopic data gathered at Gull Rapids indicate that ancient (>3.0 Ga) components exist in the area. Further investigation revealed orthogneisses in the Gull Rapids area with U-Pb zircon crystallization ages between 2.86 and 3.18 Ga and detrital zircon grains in metasedimentary rocks to be as old as 3.8 Ga (Hartlaub *et al.* 2005). The youngest crosscutting intrusion in the Gull Rapids field area is an unmetamorphosed mafic dyke with an emplacement age of 2072 ± 3 Ma (Heaman and Corkery 1996) that effectively is a minimum age constraint for the supracrustal rocks in this area.

2.0 Geological Background

2.1 Pikwitonei Granulite Domain

The northwestern corner of the Superior Province is marked by a large (>9000 km²) granulite terrane, known as the Pikwitonei Granulite Domain (Figure 2b). The Thompson Nickel Belt is adjacent to the western margin of the Pikwitonei Granulite Domain. The contact between these two terranes is defined by the Assean Lake deformation zone, which has a dextral, southeast side-up sense of movement (Kuiper *et al.* 2003). To the north, the Pikwitonei Granulite Domain is separated from the Split Lake Block and the Northern Superior Superterrane by the Aiken River deformation zone, with a dextral, north side-up sense of displacement (Kuiper *et al.* 2004b). The southeast margin of the Pikwitonei Granulite Domain is defined by an orthopyroxene isograd (Bell 1971) that divides the North Caribou terrane from the Pikwitonei Granulite Domain. In the area between Cross and Sipiwersk lakes, mafic volcanics and granodiorite can be traced from the amphibolite-grade North Caribou terrane in the east across this isograd into the granulite-grade Pikwitonei Granulite Domain in the west (Hubregtse 1980).

Felsic orthopyroxene-bearing orthogneiss is the dominant lithology exposed in

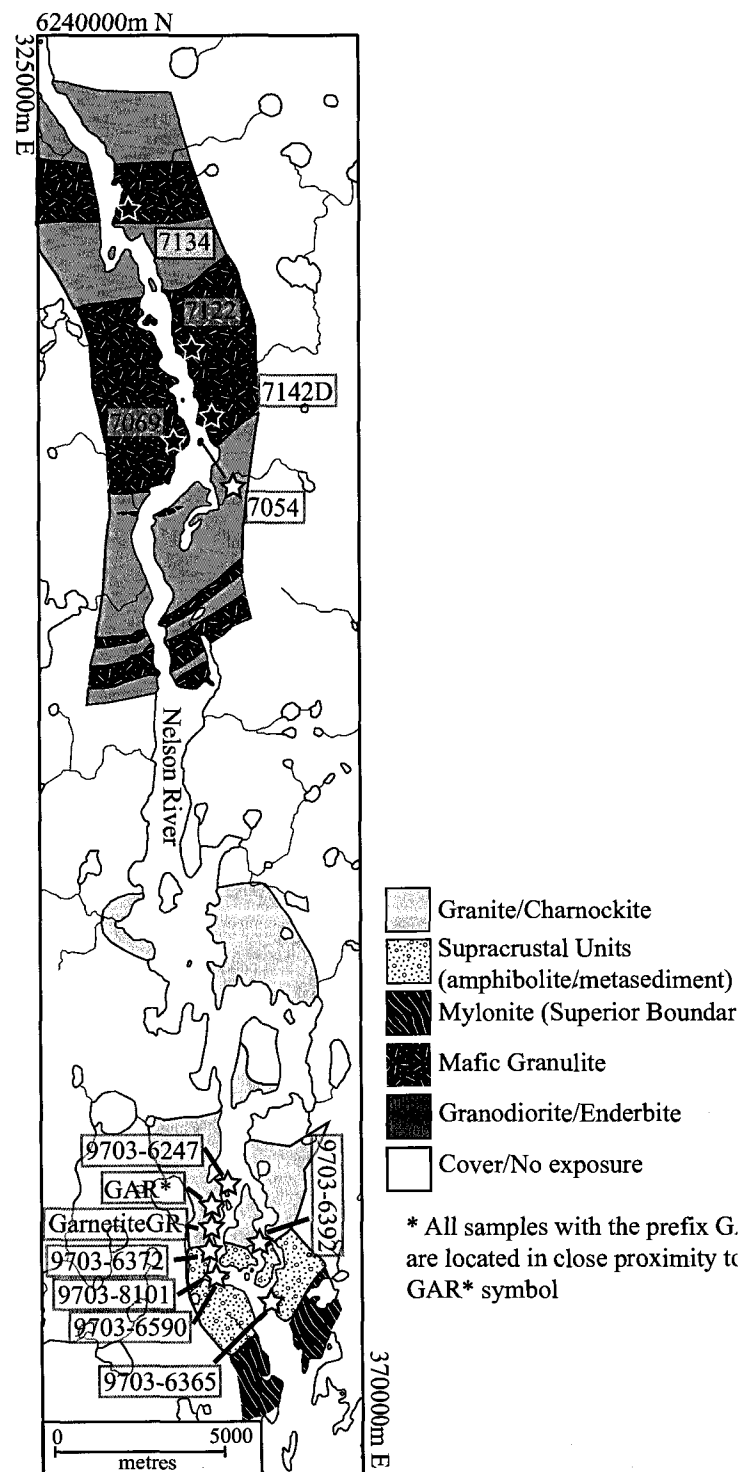


Figure 3: A map of the Nelson River in between Gull Rapids and Split Lake. North is to the right. Modified from Hartlaub *et al.* 2004.

the Pikwitonei Granulite Domain, with lenses of various other lithologies such as mafic granulite, anorthosite, pelite, iron formation, and rare occurrences of sapphirine-bearing gneisses (Hubregtse 1980, Arima and Barnett 1984).

Previous authors have delineated three main episodes of deformation and metamorphism that have affected the Pikwitonei Granulite Domain (Hubregtse 1980). The earliest metamorphic event, M_1 , attained amphibolite and locally granulite conditions and produced quartz-feldspathic mobilizates and migmatites (Hubregtse 1980). This was followed by a granulite-grade event (M_2) that reactivated M_1 migmatites and produced orthopyroxene-bearing mobilizates. A third metamorphic event (M_3) was localized in shear zones that retrogress granulites to amphibolite facies assemblages (Hubregtse 1980, Vry *et al.* 1992).

Very few firm age constraints exist for the Pikwitonei Granulite Domain. Cross-cutting granitoid dykes have returned U-Pb zircon ages of 2695 ± 2 Ma and 2637 ± 2 Ma (Heaman *et al.* 1986), interpreted to coincide with the timing of granulite and amphibolite metamorphic events, respectively. The younger age of granitic dykes agrees with the age of metamorphic zircon overgrowth in an enderbite from Cauchon Lake (Heaman *et al.* 1986).

Characterizing the conditions attained during metamorphism has been approached by a number of methods. The data suggest that both pressure and temperature of peak metamorphism increase from the interior of the Pikwitonei Granulite Domain to the western margin (Weber 1980, Fountain and Salisbury 1987), from 575°C and 7 kbar at Cauchon Lake to 9 kbar 860°C near the Thompson Belt (Arima and Barnett 1984, Patunc and Baer 1986, Mezger *et al.* 1990). At the western margin of the Pikwitonei Granulite Domain, sapphirine-bearing granulites provide an estimate of peak metamorphic conditions up to 11 kbar and $860\text{-}890^{\circ}\text{C}$ (Arima and Barnett 1984). This information combined with U-Pb geochronology suggests an anti-clockwise P-T-t path for the Pikwitonei Granulite Domain (Mezger 1990).

2.2 Split Lake Block

The Split Lake Block is a granulite-grade block dominated by orthogneisses but also contains subordinate mafic granulite and metasediment. The Split Lake Block is bounded to the south by the Aiken River shear zone, which has a north side up sense of movement (Kuiper 2004b), and to the north the Assean Lake shear zone (Figure 2) with a south side up sense of motion (Kuiper 2003). The interior of the block displays a number of major deformation and metamorphic events and is variably retrogressed (Corkery 1985). Three main high-grade events have been identified by previous authors (Corkery 1985, Böhm *et al.* 1999) on the basis of field observations, petrography, and geochronology. At the northeastern margin of the Split Lake Block, an exceptionally large exposure of supracrustal rocks is exposed at Gull Rapids on the Nelson River (Figure 3). The origin of these supracrustal rocks and their relation to the Split Lake Block was unknown prior to this study.

2.2.1 Mafic Granulite

Sporadic outcroppings of mafic granulite (e.g. Figure 4a) occur along the Nelson River, and commonly occur as lenses within felsic orthogneiss units. The mafic granulites are variably retrogressed but feature the basic mineralogy of plagioclase ± clinopyroxene ± orthopyroxene ± garnet ± ilmenite. The modal mineralogy is variable and is due in part to the greenschist-grade overprint as well as original compositional differences. Evidence of partial melt pods and stringers within the mafic granulite are known and commonly feature a more felsic composition and coarser texture than the host granulite. Zircon from these leucosomes in a sample of mafic granulite from the Split Lake Block has been dated by ID-TIMS and yields an age of $2695 +4/-1$ Ma (Böhm *et al.* 1999). Although the crystallization age of the mafic granulite protolith is unknown, a similar minimum formation age constraint is given by a metamorphic zircon age of 2684 ± 35 Ma from a sample of mafic granulite determined by U-Pb Laser Ablation-Inductively Coupled Plasma Mass Spectrometry (LA-

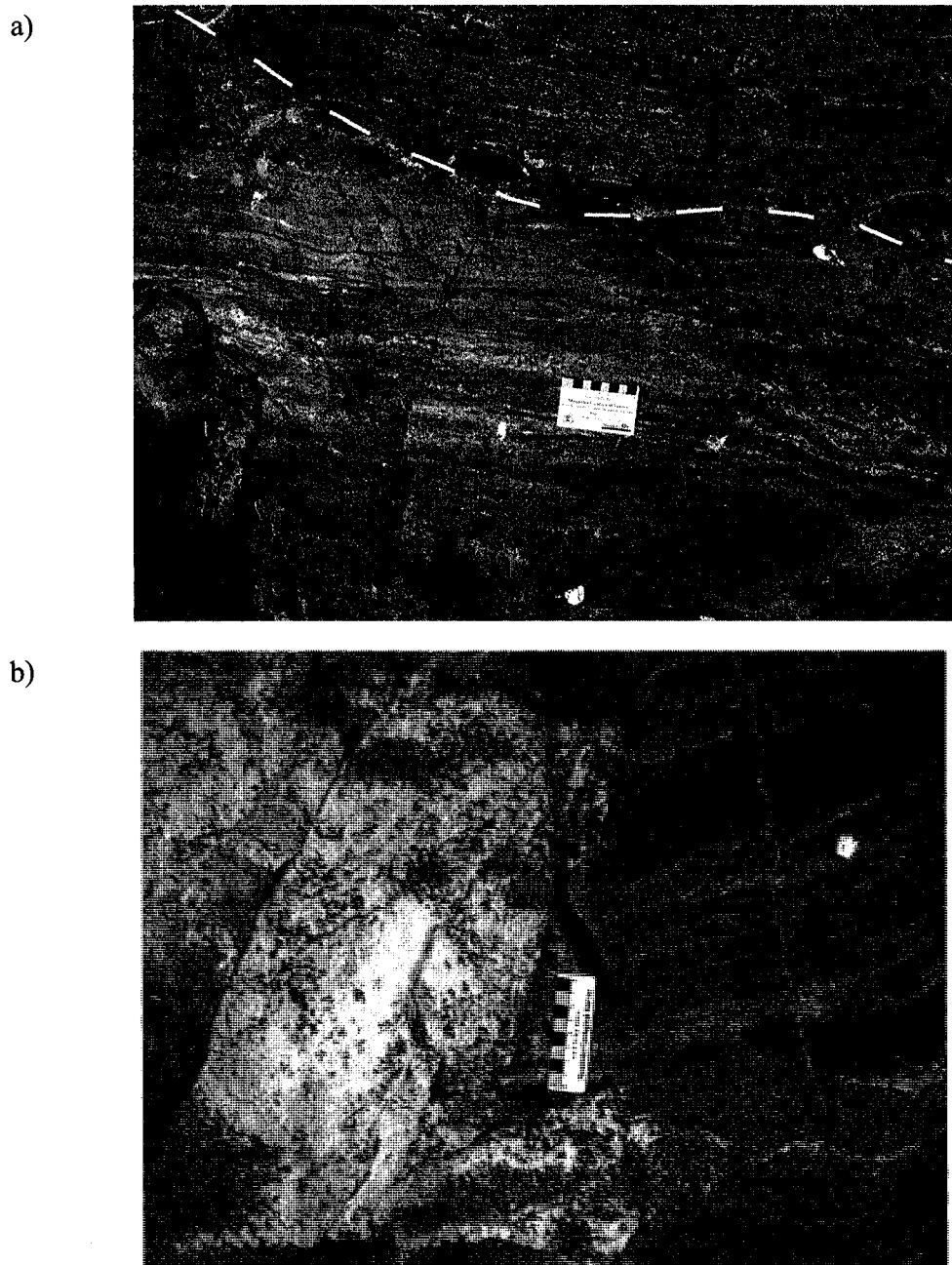


Figure 4: Photographs of the main lithologies present in the Split Lake Block and Gull Rapids. (a) A dashed line shows the contact between foliated mafic granulite in the lower half of the photo and aluminous garnet-bearing granulite in the top half of the photo. (b) Foliated mafic amphibolite in the right half of the photo is cross-cut by a pod of coarse partial melt to the left. Photographs are from sample location 9704-7054 in the central Split Lake Block.

MC-ICP-MS) (Hartlaub *et al.* 2005).

2.2.2 Amphibolite

Exposures of amphibolite and amphibolite rafts in orthogneiss are found throughout the Split Lake Block (e.g. Figure 4b). The major minerals present include amphibole + plagioclase ± clinopyroxene ± quartz and a strong foliation of these minerals is apparent. This foliation is crosscut by felsic orthogneiss.

2.2.3 Metasediment

Exposures of metasedimentary rocks within the Split Lake Block are rare. Alternating layers of psammite and pelite (major phases: quartz + feldspar + biotite ± garnet ± Fe-amphibole ± sulphides ± graphite), are most likely remnants of original compositional banding (Figures 5a and 5b). The metasediment is normally fine grained, with rare beds of conglomerate, mafic clasts, and calc-silicate. Layers of iron formation range from 1-2 m in thickness and are usually found as trains of boudins < 4 m in length within metasediment (Figure 6a). A strong compositional banding is a product of alternating layers of oxide, silicate, and sulphide iron formation facies (quartz-chert ± magnetite ± hematite ± garnet ± biotite ± amphibole ± sulphides). These metasediments are strongly folded and injected by multiple phases of granitoids. Layers of greywacke from the Split Lake Block contain detrital zircons that cover a wide span of ages from 2.65-3.8 Ga, while the depositional age for these metasediments is interpreted to be between 2.7-2.66 Ga (Hartlaub *et al.* 2005), based on the youngest detrital zircon age (2.7 Ga) and the approximate age of metamorphism (Hartlaub 2005, Downey 2005).

2.2.4 Aluminous Granulite

Occasionally rafts or small zones of aluminous granulite are found along the Nelson River in the Split Lake Block. These rocks are typically composed of garnet + ilmenite

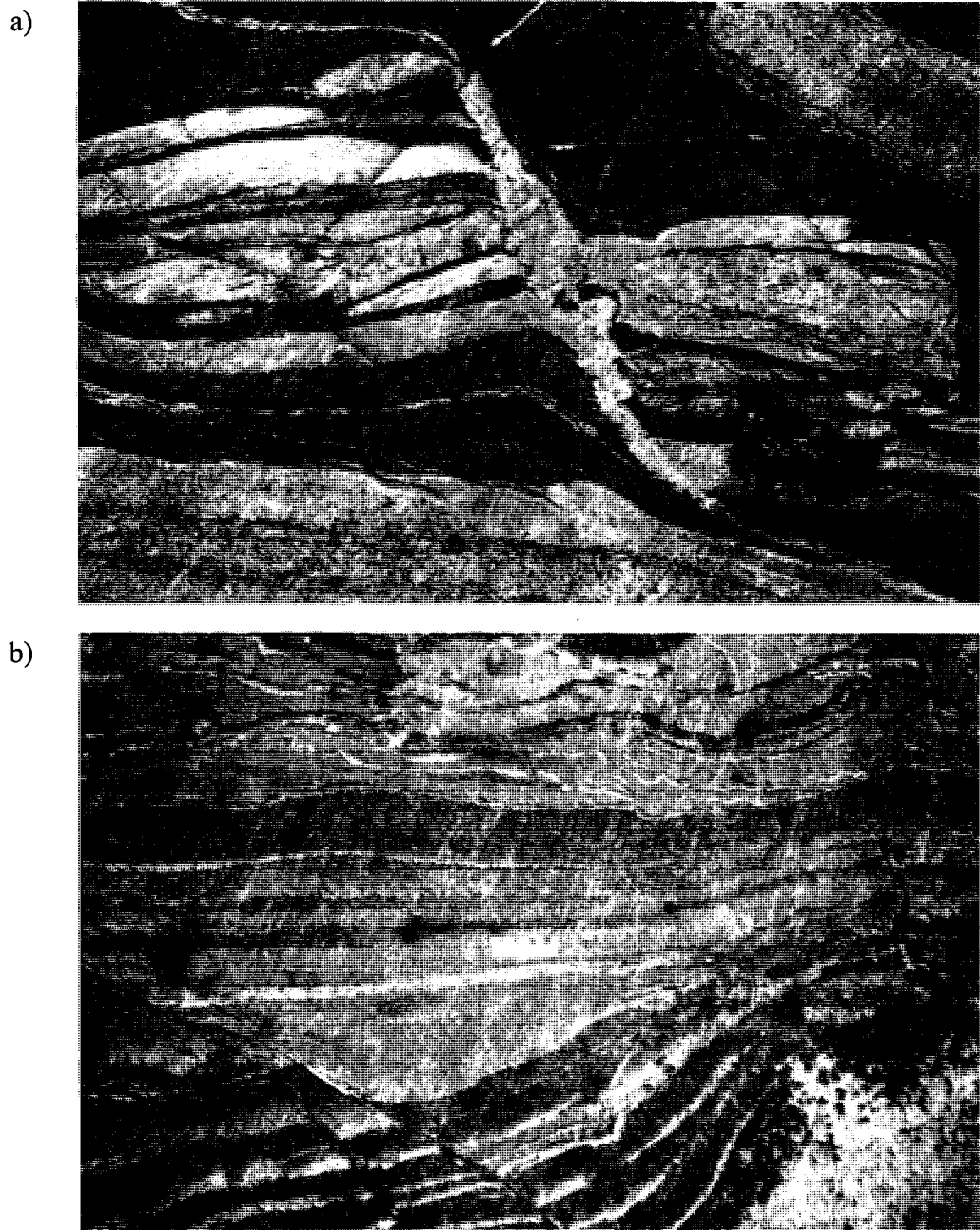
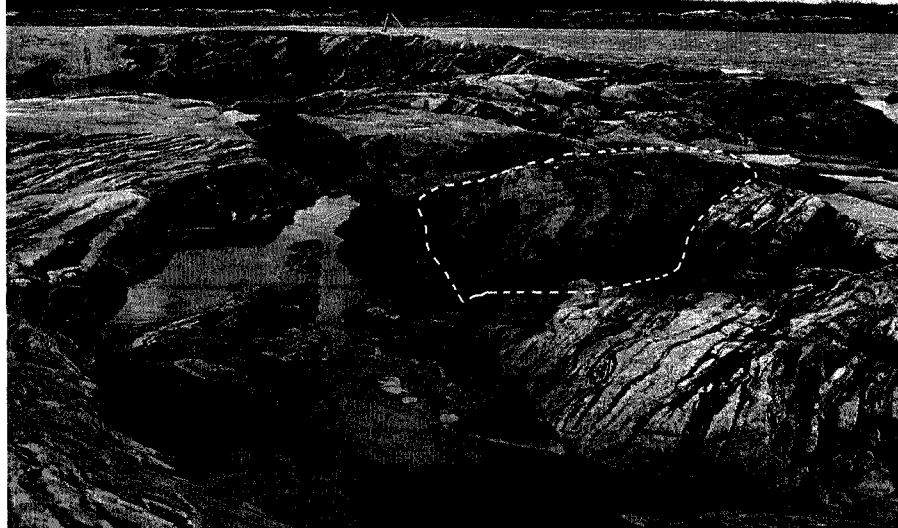


Figure 5: Photographs of the main lithologies present in the Split Lake Block and Gull Rapids. (a) Stringers of leucocratic granite cross cut dark grey metasediment. Pencil for scale. (b) Layered metasediment with leucocratic injection pod at lower right.

a)



b)

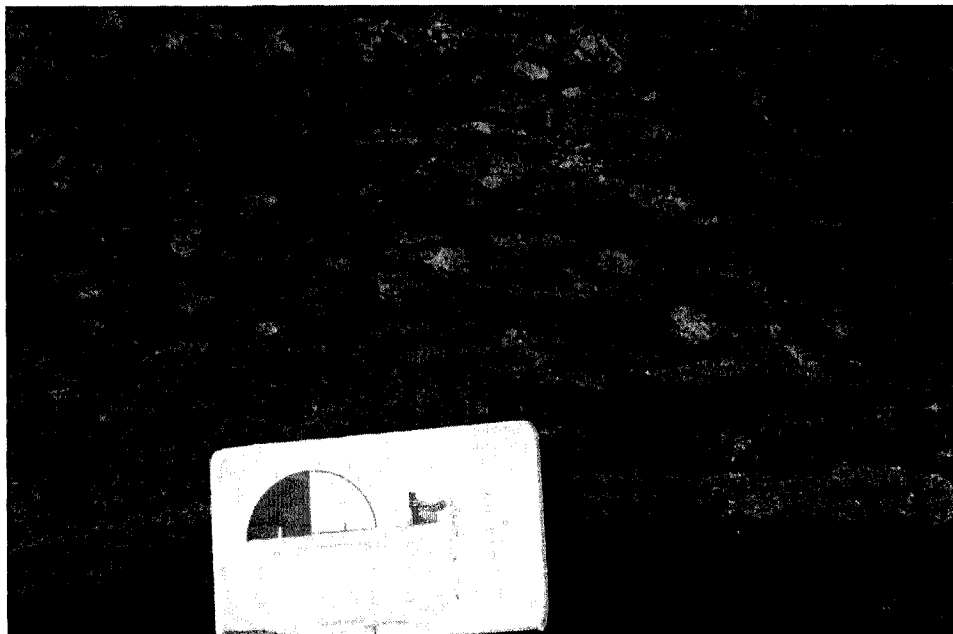


Figure 6: Photographs of the main lithologies present in the Split Lake Block and Gull Rapids. (a) A black mafic dyke cross-cuts metasediment with granitic injection. A dark boudin of iron formation is surrounded by a dashed white line. (b) Augen textured felsic gneiss with field book for scale. Photographs are from outcrop in the Gull Rapids Area. Photographs are from the Gull Rapids Area.

+ quartz + plagioclase + hercynite + sillimanite ± rutile ± titanite ± monazite. A strong compositional layering is exhibited by these granulites, which are often surrounded by felsic orthogneisses and crosscut by leucocratic granitoid injection. In one location, the relationship between mafic granulite and aluminous granulite is exposed and reveals a gradational contact between the two compositions (Figure 4a).

2.2.5 Felsic Intrusive Units

Orthogneiss is the most common lithology found within the Split Lake Block and commonly contains xenoliths and appears to crosscut metasedimentary, amphibolite, and mafic granulite lithologies in various locales. The basic mineralogy is consistent (plagioclase ± K-feldspar ± quartz ± biotite ± amphibole) and varies in no apparent systematic way. Units of orthogneiss are strongly deformed (e.g. Figure 6b) and often show a strong foliation defined by the orientation and segregation of mafic minerals. The deformed nature of the orthogneiss makes it difficult to discern crosscutting relationships in the field between the orthogneiss and other lithologies. Due to the complex metamorphic history of these orthogneisses, obtaining unequivocal crystallization ages has proven difficult, although model Nd ages of orthogneisses from the Split Lake Block are dominantly Mesoarchean (Böhm et al. 2000). The U-Pb geochronology data shows that the crystallization age of the protoliths of these gneisses are pre-2.8 Ga, and suggest emplacement ages of 2.95 Ga and older (Böhm *et al.* 1999).

Leucocratic granitoid injection and pods of granitic material are found throughout the Split Lake Block and crosscut all lithologies except mafic dykes. These granitoids are leucocratic (<10% mafic minerals) (Figure 5a) and feature a consistent mineralogy of plagioclase + quartz ± K-feldspar ± biotite ± amphibole ± garnet ± pyroxene. The separation of these granitoids has not been possible on the basis of field observation alone but geochronology is useful for separation of different phases based on age. A LA-MC-ICP-MS U-Pb zircon age for a granodiorite from Split Lake yielded an age of 2663 ± 11

Ma (Hartlaub *et al.* 2005), while a granite from Gull Lake in the central Split Lake Block yielded an ID-TIMS zircon age of 2708.0 ± 2.5 Ma (Böhm *et al.* 1999).

2.2.6 Mafic Dykes

Late stage, undeformed mafic dykes are present in the Split Lake Block and crosscut all lithologies (Figure 6a). The dominant orientation of these dykes are $080\text{--}110^\circ$ and they range from a few metres in width to >100 metres. The major minerals present are pyroxene \pm amphibole \pm plagioclase and grain size from aphanitic to coarse (4-6 mm elongate plagioclase phenocrysts). A mafic dyke from Birthday Rapids has a U-Pb zircon age of 2072 ± 3 Ma (Heaman and Corkery 1996), which is significantly different from the 1883 Ma northeast-trending Molson dyke swarm (Heaman *et al.* 1986) that is commonly found in the northwestern Superior Province.

2.3 Gull Rapids Study Area

The eastern margin of the Split Lake Block is marked by a large exposure of supracrustal rocks that is somewhat different than supracrustal rocks found in the rest of the block. Most of the lithologies are nearly identical to those exposed in the Split Lake Block; it is their relative proportions and a few unique characteristics of the Gull Rapids lithologies that set them apart. These supracrustal rocks consist mainly of layered amphibolite, greywacke and to a lesser extent iron formation. Throughout the map area, granitoid injection is common and crosscuts nearly every lithology. A band of orthogneisses in the western half of the map area separates these supracrustal rocks from the Split Lake Block. These felsic orthogneisses feature distinct units with strong foliations, lineations, and an augen texture. The youngest lithology in the Gull Rapids area is also a series of E-W trending, unmetamorphosed mafic dykes.

2.3.1 Metamorphic History

A complex history of metamorphism and deformation has affected the Split Lake Block. Field observations have supported the notion of multiple episodes of metamorphism (Corkery 1985) and subsequent studies have further expanded the knowledge of these tectonothermal events. Field and petrographic observations indicate the presence of at least three episodes of high-grade metamorphism (upper-amphibolite and higher) followed by a heterogeneous Paleoproterozoic greenschist-grade overprint (Corkery 1985). The earliest episode of metamorphism (termed M_{1a} by Corkery 1985) created the penetrative foliation present in the amphibolites and mafic granulites. This metamorphic event occurred at 2705 ± 2 Ma; the time of metamorphic zircon growth in an enderbite from the Split Lake Block as well as a similar emplacement age for the 2708.0 ± 2.5 Ma Gull Lake granite (Böhm *et al.* 1999). The gneissosity developed in the felsic gneisses is due to a granulite-grade event, M_{1b} (Corkery 1985). Partial melting of the mafic granulites during this episode of metamorphism produced patches of leucosome that cross-cuts the M_{1a} foliation and these leucosomes record zircon growth at $2695 +4/-1$ Ma (Böhm *et al.* 1999). The youngest Archean event, termed M_2 (Corkery 1985) is distinguished mostly by amphibole pseudomorphing clinopyroxene and orthopyroxene as well as the replacement of M_1 amphiboles by a second phase of coarse amphibole growth (Corkery 1985). Samples of tonalite and granodiorite gneiss yield concordant U-Pb ages of metamorphic zircon growth at ~ 2620 Ma, which could represent the timing of M_2 metamorphism in the Split Lake Block (Böhm *et al.* 1999). The M_3 event manifests itself as a fine coating of greenschist-grade minerals (epidote and chlorite) that is present in most samples (Corkery 1985). This event is attributed to effects from the nearby ~ 1.8 Ga Trans-Hudson Orogen.

2.3.2 Previous Research

Early investigations of the Gull Rapids field area delineated these supracrustal rocks as being part of the Paleoproterozoic Burntwood Group metasedimentary rocks that

are abundant just east of Gull Rapids in Stephens Lake (Corkery 1985). Preliminary Nd isotope information from Gull Rapids returned a depleted mantle model Nd age of 3.1 Ga for metasedimentary rocks (Bowerman *et al.* 2004) which is an indication of ancient detritus to these sediments.

The tectonothermal history of Gull Rapids has not been studied in detail until recently. Preliminary field observations of Gull Rapids distinguished that the supracrustal units are multiply deformed, based on the development of multiple cleavages and refolded folds (Böhm *et al.*, 2003; Downey 2004). Further examination by Downey (2006) delineated 5 generations of deformation. The first generation of structures (G1) formed the main foliation that is subparallel in the supracrustal assemblage and the nearby Split Lake Block. This first generation is closely followed by a second, dominant generation of structures. Structures formed during G2 are isoclinal F2 folds that are part of a dextral, southwest-side-up shearing event, that is followed by a weak deformation event (G3), characterized by open folding of pre-existing structures (Downey 2005). The final two generations of deformation (G4-G5) are difficult to distinguish from one another considering that they are both brittle-ductile structures in the form of mostly sinistral shear zones, G4 shearing pre-dates the emplacement of mafic dykes in the area while G5 deformation is post-dyke emplacement (Downey 2005).

Age data for granitoid intrusions have allowed some constraints on the timing of deformation at Gull Rapids to be determined. A U-Pb titanite age of 2689.0 ± 2.8 Ma for a granitic intrusion that truncates a boudin neck is interpreted to constrain the timing of late G1 to early G2 deformation (Downey 2005). A possible extension of the G2 event is defined by a U-Pb zircon age of ca. 2640 Ma from a granodiorite dyke that cross-cuts S1 and is folded by F2 (Downey 2005). The youngest age constraint is a U-Pb zircon age of 2614 ± 30 Ma representing the crystallization age for a granitoid stringer that is syn-tectonic with a G4 related shear zone (Downey 2005).

3.0 Analytical Techniques

A table summarizing all samples collected for this study, lithologic classifications, and UTM coordinates is presented in Appendix 1.

3.1 Geochemistry

A full suite of samples from various lithologies was selected for bulk-rock geochemical analysis for classification and to determine information about their origin. Samples of relatively unaltered lithologies were chosen and trimmed of any weathered edges prior to crushing. Powdered fractions were submitted to Activation Laboratories Ltd., Ancaster, Ontario for analysis. Major-element analyses were obtained by X-Ray Fluorescence (XRF) and trace-element analyses were obtained by Inductively Coupled Plasma-Mass Spectrometry (ICP-MS). The geochemical data are presented with corresponding analytical uncertainties in Appendix 2.

3.2 Mineral Chemistry, Imaging, and Chemical Ages

Both qualitative and quantitative mineral analyses were carried out using a JEOL 8900 Electron Microprobe (EMPA) located at the University of Alberta. Both energy-dispersive (EDS) and wavelength-dispersive (WDS) modes were used as well as backscatter electron imaging. Mineral analyses in WDS mode were performed with a beam diameter of $3\mu\text{m}$ and an accelerating voltage of 15kV and beam current of 15nA. EMPA monazite analyses were conducted using a $1\text{-}3\mu\text{m}$ beam diameter with 20 kV accelerating voltage. Natural mineral samples were used as standards in the analysis procedure. A ZAF correction routine was used to convert X-ray counts to concentrations. All mineral chemical data are reported in Appendix 3.

3.3 Thermobarometry

The quantitative thermobarometric results were obtained by the use of the mineral

Table - 1
Definition of Thermodynamic System for Mafic Granulite

Phases: **5** (Garnet, Orthopyroxene, Clinopyroxene, Plagioclase, Quartz)

System Components: **5** (CaO-FeO-MgO-Al₂O₃- SiO₂)

Thermodynamic end-members: **10**

Almandine	Alm	Fe ₃ Al ₂ Si ₃ O ₁₂
Pyrope	Py	Mg ₃ Al ₂ Si ₃ O ₁₂
Grossular	Gr	Ca ₃ Al ₂ Si ₃ O ₁₂
Ferrosilite	Fsl	FeSiO ₃
Enstatite	En	MgSiO ₃
Aluminum in	Opx	Al ₂ O ₃
Hedenbergite	Hed	CaMgSi ₂ O ₆
Diopside	Di	CaFeSi ₂ O ₆
Anorthite	An	CaAl ₂ Si ₂ O ₈
Alpha Quartz	Qtz	SiO ₂

Total Number of Equilibria: **6**

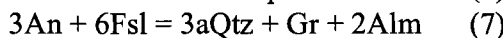
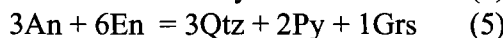
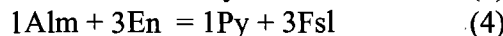
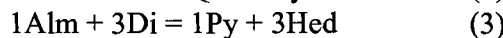
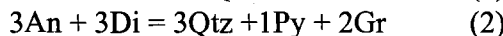
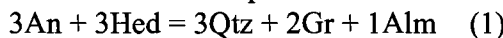


Table X: Definition of Thermodynamic System for Garnetite

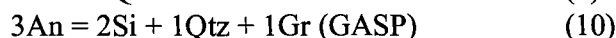
Phases: **7** (Garnet, Plagioclase, Quartz, Rutile, Sillimanite, Hercynite, Ilmenite)

System Components: **5** (CaO-FeO-Al₂O₃- SiO₂-TiO₂)

Thermodynamic end-members: **10**

Garnet	Alm	Fe ₃ Al ₂ Si ₃ O ₁₂
	Grs	Ca ₃ Al ₂ Si ₃ O ₁₂
Plagioclase	An	CaAl ₂ Si ₂ O ₈
Quartz	Qtz	SiO ₂
Sillimanite	Si	Al ₂ O ₃
Ilmenite	Ilm	FeTiO ₃
Hercynite	Hrc	FeAl ₂ O ₄
Rutile	Ru	TiO ₂

Total Number of Equilibria: **3**



compositions and thermodynamic data to determine the location of various reaction equilibria in P-T space. A number of different reactions were used for thermobarometry and are summarized in Table 1. The individual reactions are discussed in further detail below. Thermobarometric analyses were completed using an internally consistent thermobarometric technique, first described by Powell (1985) and then further developed by Powell & Holland (1988) and Berman (1988, 1991). An internally consistent data set is created by combining calorimetric measurements with the results from experimental studies and means that all relevant reactions between end-member phases can be used in the P-T calculations (Powell 1985). The program TWQ v.2.02 was used to perform the P-T calculations. This program is based on thermodynamic data for end-member phases and activity-composition models derived from a number of sources (Berman 1988, Berman and Aranovich 1996, Berman *et al.* 1995, Fuhrman and Lindsley 1998, and McMullin *et al.* 1991). This method calculates the positions of all possible equilibria relevant to a particular mineral assemblage within P-T space by a pressure-temperature window defined by the user.

3.4 Mineral Separation

The initial crushing and mineral separation was preformed at the University of Alberta, beginning with the sample being pulverized by a jaw crusher and then powdered by a Bico disk mill. Heavy mineral concentrates were obtained using a Wilfley Table; Methylene Iodide (MI) heavy-liquid separation; and a Frantz Isodynamic Separator for magnetic fractions. The remaining zircons were described and photographed before being prepared for either epoxy grain mounts (LA-MC-ICP-MS) or ID-TIMS chemistry.

3.5 Tracer Isotopes

A representative suite of lithologies were chosen for Nd isotopic compositions and were analysed at the Canadian Center for Innovative Geochronology, University of Alberta

following the method described in Hollings *et al.* (2007). The Sm-Nd isotopic system can be used for both sedimentary and igneous rocks to provide an estimate of their average provenance age. The Sm-Nd results are presented in Appendix 4. For the purposes of comparison, the ϵ_{Nd} values of all samples were calculated at a common age of 2.7 Ga. Depleted mantle model ages were calculated using the model of Goldstein *et al.* (1984).

3.6 U-Pb Laser Ablation MC-ICP-MS

The Canadian Center for Innovative Geochronology at the University of Alberta houses a Nu Plasma laser ablation multi-collector inductively coupled plasma mass spectrometer (LA-MC-ICP-MS) capable of analyzing minerals in grain mounts as well as in-situ analysis of minerals in thin sections. A full description of the exact techniques and procedures used for in-situ LA-MC-ICP-MS analyses are outlined in Simonetti *et al.* (2005; 2006). Depending on the size of zircon and the strength of the signal (evaluated by counts per second of ^{206}Pb), the diameter of the laser analysis spot was varied from 20 to 40 microns. All data is presented in Appendix 4. Precambrian zircons averaging Pb and U concentrations of ~100 and ~300 ppm, respectively normally produce ion beams of ~300,000-800,000 counts per second (cps) of ^{206}Pb when using a 40 μm spot size. On occasion, ^{206}Pb counts dip below 100,000 cps, which means the treatment of the data must be carefully evaluated so as to obtain meaningful and accurate results. Corrections for instrument drift were monitored by the analysis of an in-house Proterozoic zircon standard (LH94-15) of known age, a calc-alkaline enderbite with a precise ID-TIMS determined age of 1830 ± 1 Ma (Ashton *et al.* 1999). The data are treated for instrument drift by analyses of approximately 10 unknown zircons being bracketed by analyses the zircon standard.

The evaluation of the data for the purpose of correcting for the presence of common lead requires the consideration of many variables. For zircon analyses containing ^{204}Pb , a correction was made using the initial Pb isotopic composition calculated from the two-stage terrestrial evolution model of Stacey and Kramers (1975), and using the $^{207}\text{Pb}/^{206}\text{Pb}$

age of the zircon.

Although the U-Pb LA-MC-ICP-MS dating technique for magmatic zircons with high concentrations of U have been documented (Simonetti *et al.* 2005; 2006), the adaptation of these methods to low-U metamorphic zircons have not. The lower counts of radiogenic ^{206}Pb that typically occur in low-U metamorphic zircon are due to not only the low concentration of U and Pb, but also because of the small beam size ($<40\ \mu\text{m}$) required to analyse small metamorphic grains (any of the metamorphic zircon grains analysed in this study have diameters only slightly larger than 40 microns). In this case, careful evaluation of each grain analysis is exceedingly important. For example, the incorrect application of a common Pb correction could produce a spuriously old or young age. A number of factors are considered when deciding whether to apply a common Pb correction or not. The LA-MC-ICP-MS is configured in such a way that the counts returned at mass 204 could be the result of more than just ^{204}Pb coming from the zircon crystal itself. Distinguishing the source of this 204 signal is therefore imperative so as to not over- or under-correct the data and therefore create an erroneous result. A number of sources for interference at mass 204 have been proposed (Simonetti *et al.* 2005) and examining the relationship between how the $^{207}\text{Pb}/^{206}\text{Pb}$ ratio (common Pb corrected) changes with respect to ^{204}Pb over the ablation run can indicate whether the ^{204}Pb is indigenous to the zircon. If a plot of ^{204}Pb corrected $^{207}\text{Pb}/^{206}\text{Pb}$ versus ^{204}Pb defines a horizontal line, it implies that the common Pb correction procedure has been effective in improving the precision of the measured ^{207}Pb and ^{206}Pb ratios. In turn, this suggests that the measured ^{204}Pb counts are indigenous to the zircon (Simonetti *et al.* 2005). If the $^{207}\text{Pb}/^{206}\text{Pb}$ ratio does not vary in a systematic way with ^{204}Pb , creating a non-linear pattern when graphed, the source of ^{204}Pb is from something other than the zircon. In the case where a strong negative correlation is present on a plot of $^{207}\text{Pb}/^{206}\text{Pb}$ and ^{204}Pb , a systematic over-correction of the data is being made, resulting in an artificially young age. In this case, where an excess of ions measured at mass 204 are being included with common ^{204}Pb in the age calculations, there are means by which an

estimation of these excess ions can be made. By using the average amount of $^{207}\text{Pb}/^{206}\text{Pb}$ measured and the slope of the line created by the graph an estimate can be made on the amount of common ^{204}Pb originating from the zircon and that value is substituted for the amount of indigenous common ^{204}Pb .

3.7 Thermal Ionization Mass Spectrometry

Analyses of zircons by Isotope Dilution Thermal Ionization Mass Spectrometry (ID-TIMS) were carried out at the Canadian Center for Innovative Geochronology at the University of Alberta. Analytical procedures and data reporting techniques generally follow Heaman *et al.* (2002). Analyses were performed on a VG354 mass spectrometer operating in single Faraday or Daly (analogue) collector peak-hopping mode. Measured blanks yielded U and Pb concentrations of 0.5 and 1 pg, respectively. Analyses obtained with the Daly photomultiplier were corrected for detector bias (Pb, 0.13%/amu; U, 0.15%/amu). All measurements were corrected for mass discrimination (Pb, 0.088%/amu; U, 0.155%/amu) based on repeated analyses of the NBS981 and U500 standards. Analyses with common Pb composition in excess of the analytical blank were calculated using the two-stage evolution model of Stacey and Kramers (1975). Concordia diagrams were created using the ISOPLOT/Ex 3.0 computer program (Ludwig 2003) for all geochronology results in this publication. All errors reported in Appendix 4 as well as all concordia diagrams are displayed as 2σ and are calculated by propagating all known sources of analytical uncertainty.

4.0 Results

4.1 Geochemistry

4.1.1 Metasediment

The major- and trace-element compositions of metasedimentary rocks from the Split Lake Block ($n=2$) and Gull Rapids area ($n=11$) are presented in Appendix 2.1. The variability of composition from psammite to pelite in the metasedimentary rocks observed during

field analysis is also manifested in their whole-rock compositions. A wide range in SiO_2 content, from 48-70 wt % as well as a low abundance of Al_2O_3 (11-23 wt %) (Appendix 2.1). These geochemical characteristics are supported by the low abundance of aluminous metamorphic minerals (e.g. garnet). This observation, combined with the occurrence of mafic layers within the metasediment composed of amphibolite clasts suggest a mafic source contributed to these sediments. A discrimination diagram to further delineate the source area of these sediments uses two discriminant functions calculated using SiO_2 , Al_2O_3 , TiO_2 , Fe_2O_3 , MgO , CaO , Na_2O , K_2O (Roser and Korsch 1988) and is divided into a number of fields that show the lithologic provenance of sedimentary rocks. Samples of metasedimentary rocks from Gull Rapids and the Split Lake Block plot in the mafic-igneous field of the discrimination diagram save one sample from the Split Lake Block that plots well within the felsic-igneous protolith field (Figure 7a). These data indicate that the primary source for these metasedimentary rocks is dominantly a mafic igneous protolith. One sample (9704-7143) indicates detrital input from a felsic-igneous source. The rare-earth element (REE) pattern derived from metasedimentary samples from Gull Rapids and the Split Lake Block displays a flat pattern when normalized to the North American Shale Composition (NASC) (Gromet *et al.* 1984), and no systematic difference between samples from different areas is apparent (Figure 7b).

4.1.2 Mafic Igneous Units

Exposures of amphibolite in the form of rafts in felsic orthogneiss or limited exposures are common within the Split Lake Block and in the Gull Rapids field area. The chemical compositions of 15 amphibolite samples are presented in Appendix 2.2. These amphibolites range in composition from mafic to ultramafic, based on their MgO content (4-10 wt %) and their SiO_2 content (44-51 wt %) (Appendix 2.2). The trace-element composition of amphibolite units from Gull Rapids and the Split Lake Block are similar, both showing relatively flat N-MORB normalized (Sun and McDonough 1989) REE patterns with slight

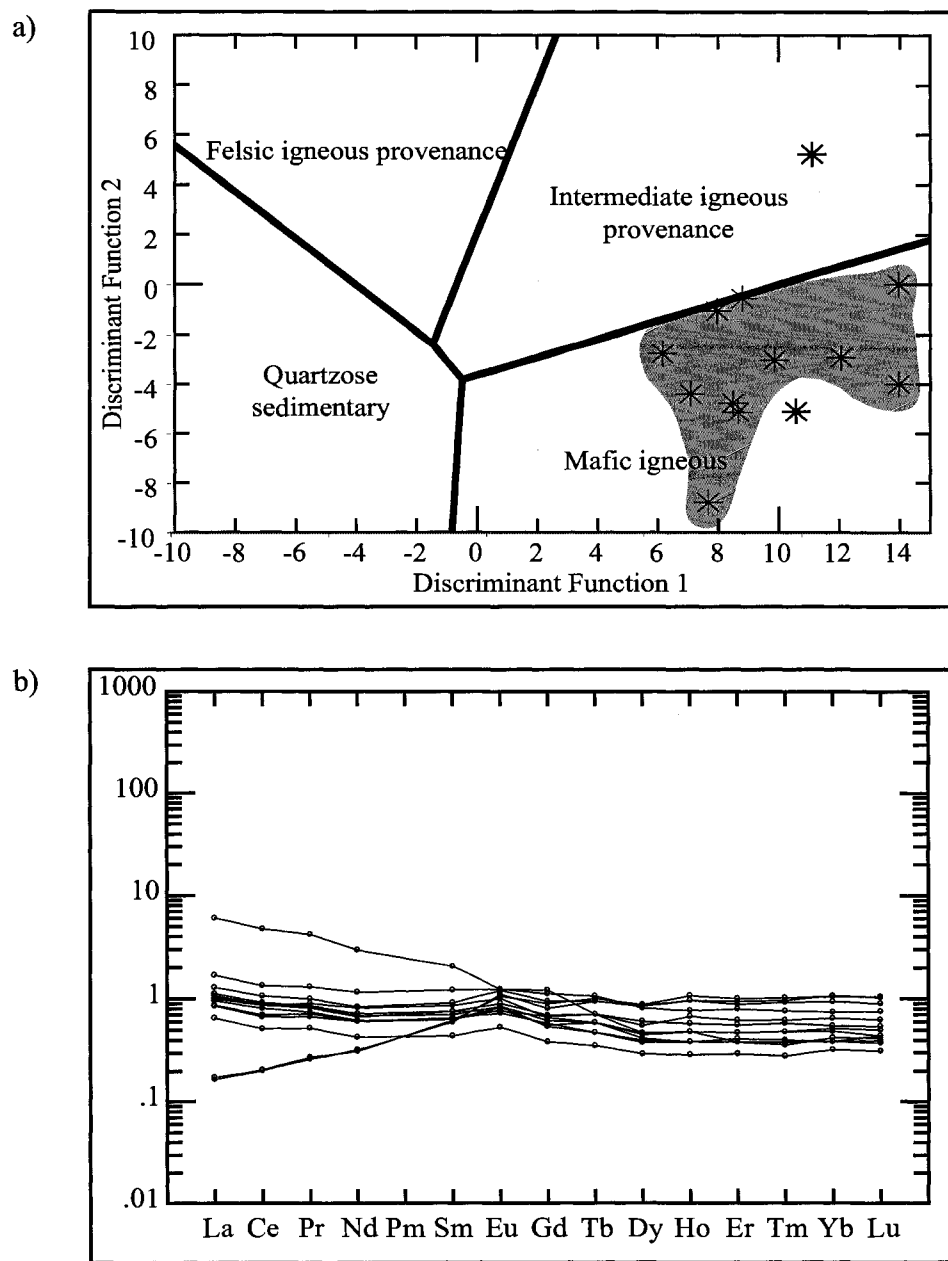


Figure 7: a) Discrimination diagram with metasediment analyses from Gull Rapids plotted in grey and two Split Lake Block analyses in white. Discriminant function 1: $-1.733\text{TiO}_2 + 0.607\text{Al}_2\text{O}_3 + 0.76\text{Fe}_2\text{O}_3 - 1.5\text{MgO} + 0.616\text{CaO} + 0.905\text{Na}_2\text{O} + 1.224\text{K}_2\text{O} - 9.09$. Discriminant function 2 = $0.445\text{TiO}_2 + 0.07\text{Al}_2\text{O}_3 - 0.25\text{Fe}_2\text{O}_3 - 1.142\text{MgO} + 0.438\text{CaO} + 1.475\text{Na}_2\text{O} + 1.426\text{K}_2\text{O} - 6.8612$. b) REE diagram of metasediment samples normalized to NASC (North American Shale Composition).

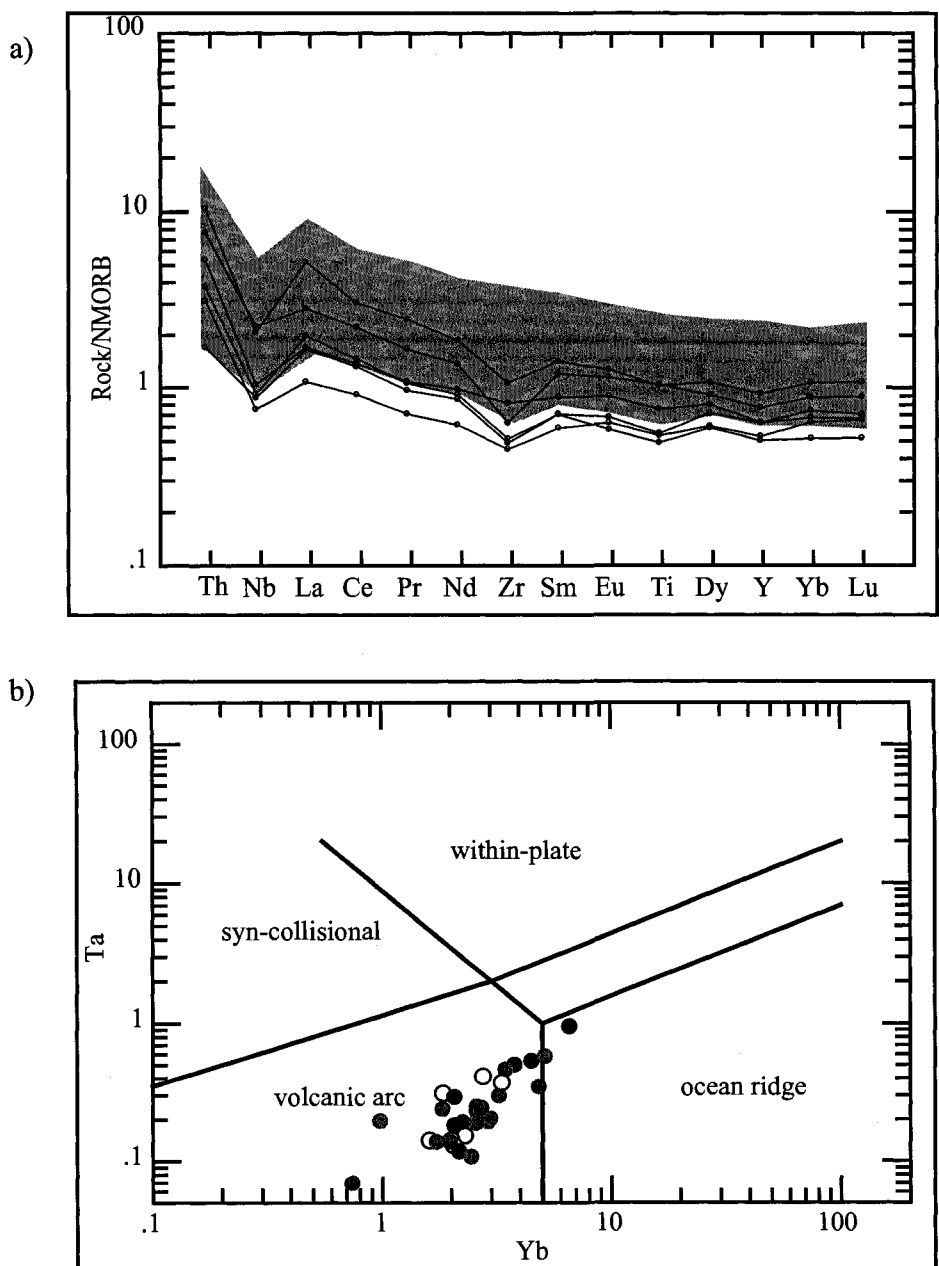


Figure 8: a) Multi-element diagram displaying samples of amphibolite from both the Split Lake Block (individual analyses) and Gull Rapids (grey area). b) Tectonic association diagram with samples of amphibolite from the Split Lake Block (open circles) and Gull Rapids (filled circles) as well as Mafic Granulites from the Split Lake Block (grey circles) Pearce *et al.* (1984).

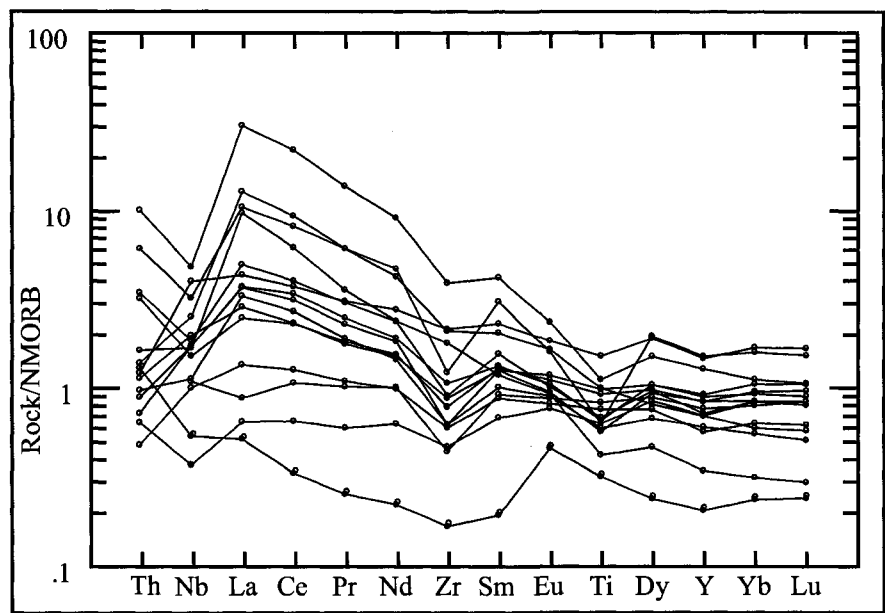


Figure 9: Multi-element diagram of mafic granulite samples from the Split Lake Block. Normalization of NMORB is from Sun and McDonough (1989).

enrichment in LREE relative to HREE (Figure 8a). A slight depletion in Nb is common in most samples and in general, the Split Lake Block samples are less enriched in REE than Gull Rapids amphibolite samples. A minor enrichment in Dy and depletion in Zr is also apparent in some samples. Amphibolite analyses plotted on a tectonic association diagram using the composition of Ta and Yb (Pearce *et al.* 1984) clearly plot within the volcanic arc field with one sample from Gull Rapids plotting in the ocean ridge field (Figure 8b).

Fifteen mafic granulite samples from the Split Lake Block contain relatively low SiO_2 (46-52 wt %), intermediate MgO contents (4-8 wt %), and a range in Fe_2O_3 of 5-18 wt % which overlaps the amphibolite compositions (Appendix 2.3). One sample, 9704-7066, has a distinctly higher SiO_2 content (62.95 wt%) and may indicate that this sample contains a significant proportion of felsic injection that has affected the geochemical analysis. The trace-element patterns of mafic granulite from the Split Lake Block show more enrichment of LREE relative to HREE compared to amphibolite samples (Figure 9). Other elements like La, Ce, and Dy show relative enrichments in the trace-element geochemistry while Nb, Zr, and Ti show relative depletions. The mafic granulite samples plot within the volcanic arc field on a Ta and Yb tectonic association diagram (Figure 8b) with one sample straddling the boundary between the volcanic arc and ocean ridge fields.

4.1.3 Aluminous Granulite

Closely associated with mafic granulite outcrops are zones of aluminous granulites. The chemical compositions for four aluminous granulite samples are presented in Appendix 2.4. In general, these layers have higher SiO_2 (51-55 wt %) and Fe_2O_3 (20-25 wt %) while the MgO content (2-3 wt %) is lower than the associated mafic granulite. One sample, 9704-7054B is distinctly different from the other aluminous granulite analyses with significantly higher SiO_2 , CaO , and K_2O and lower Fe_2O_3 and TiO_2 . This sample shares more characteristics with the metasediment analyses and suggests that sample 9704-7054B had an evolved sediment as a protolith in contrast to the other aluminous granulites.

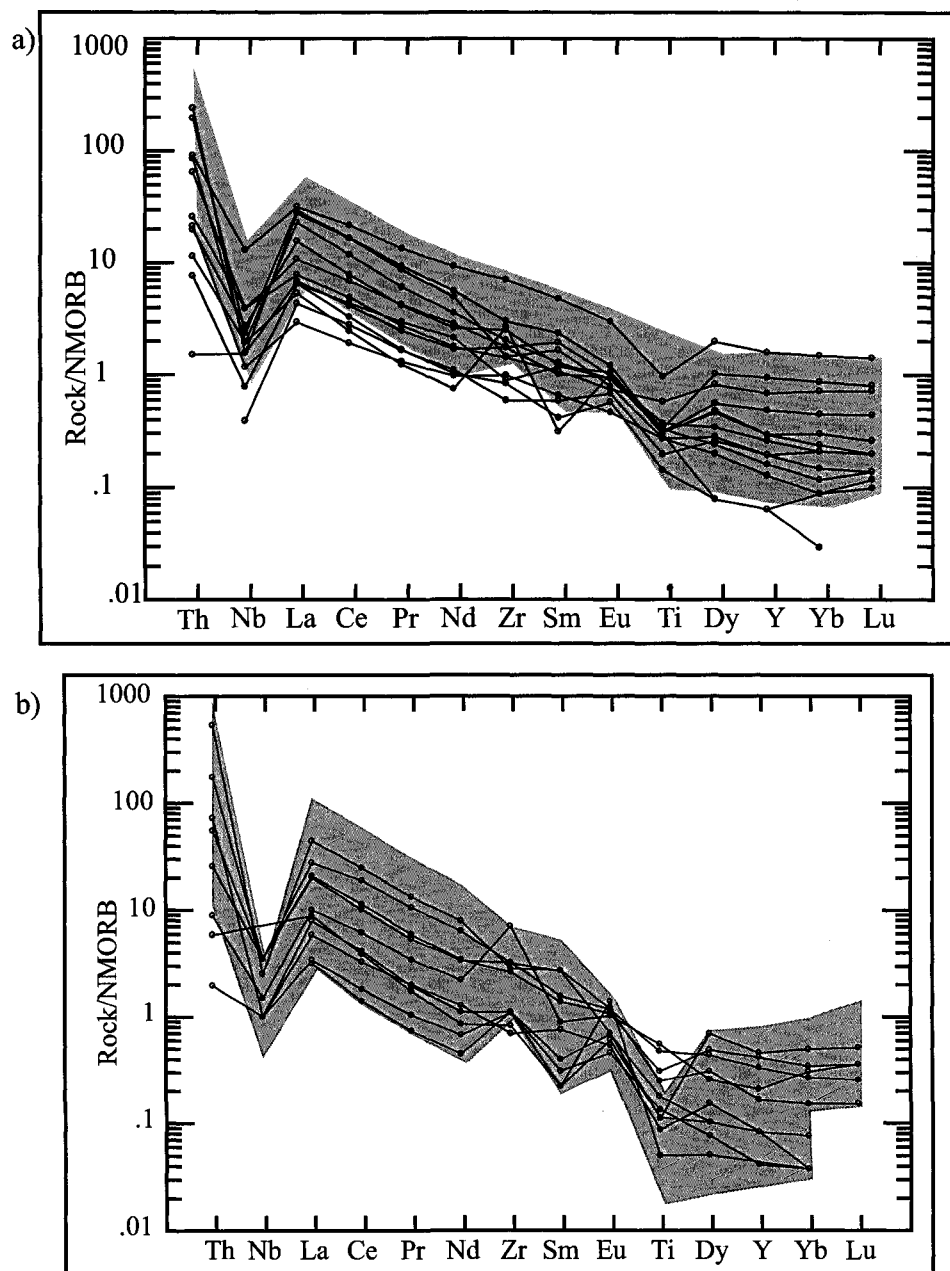


Figure 10: a) Multi-element diagram with samples of felsic orthogneisses from the Split Lake Block (individual analyses) and Gull Rapids (grey area). Modified spider diagram normalized by NMORB composition determined by Sun and McDonough (1989). b) Multi-element diagram of leucogranite geochemistry from the Split Lake Block (individual analyses) and Gull Rapids (grey filled area). Normalization of NMORB from Sun and McDonough (1989). Modified diagram uses fewer elements.

A few notable enrichments in trace-elements are present in samples of aluminous granulite: Zr (76-186 ppm), U (0.08-0.6 ppm), and Hf (3-6 ppm) are all higher than the average values obtained for most other lithologies in the Split Lake Block and Gull Rapids. This geochemical feature may be explained by the high abundance of zircon found in aluminous granulites.

4.1.4 Felsic Orthogneiss

The chemical compositions for 26 felsic orthogneiss samples are presented in Appendix 2.5. Felsic orthogneisses from both the Split Lake Block and Gull Rapids show a range of SiO_2 contents (62-74 wt %). The trace-element composition of samples of felsic orthogneiss are strongly fractionated from LREE to HREE (Figure 10a). Relative depletions in Nb and Ti are present and samples from the Split Lake Block are slightly more depleted in LREE than samples from the Gull Rapids area.

4.1.5 Granitoid Injection

The chemical compositions for leucocratic granite samples are presented in Appendix 2.6. The ubiquitous leucocratic granitoid injection found in the Split Lake Block and Gull Rapids is rich in SiO_2 (66-76 wt %; Appendix 2.6). The trace-element pattern defined by the granitoid injection is more fractionated between the enriched LREE and relatively depleted HREE (Figure 10b) than felsic orthogneiss. There are two notable depletions in Nb and Ti. There does not seem to be a systematic difference in the trace-element compositions of granitoid injection from the Split Lake Block and Gull Rapids.

4.2 Petrography

A wide range of lithologies were sampled and thin sections prepared for the purpose of finding metamorphic mineral assemblages appropriate for thermobarometric analysis as well as for evaluating metamorphic textures and finding zircon for *in-situ* analysis. Of the

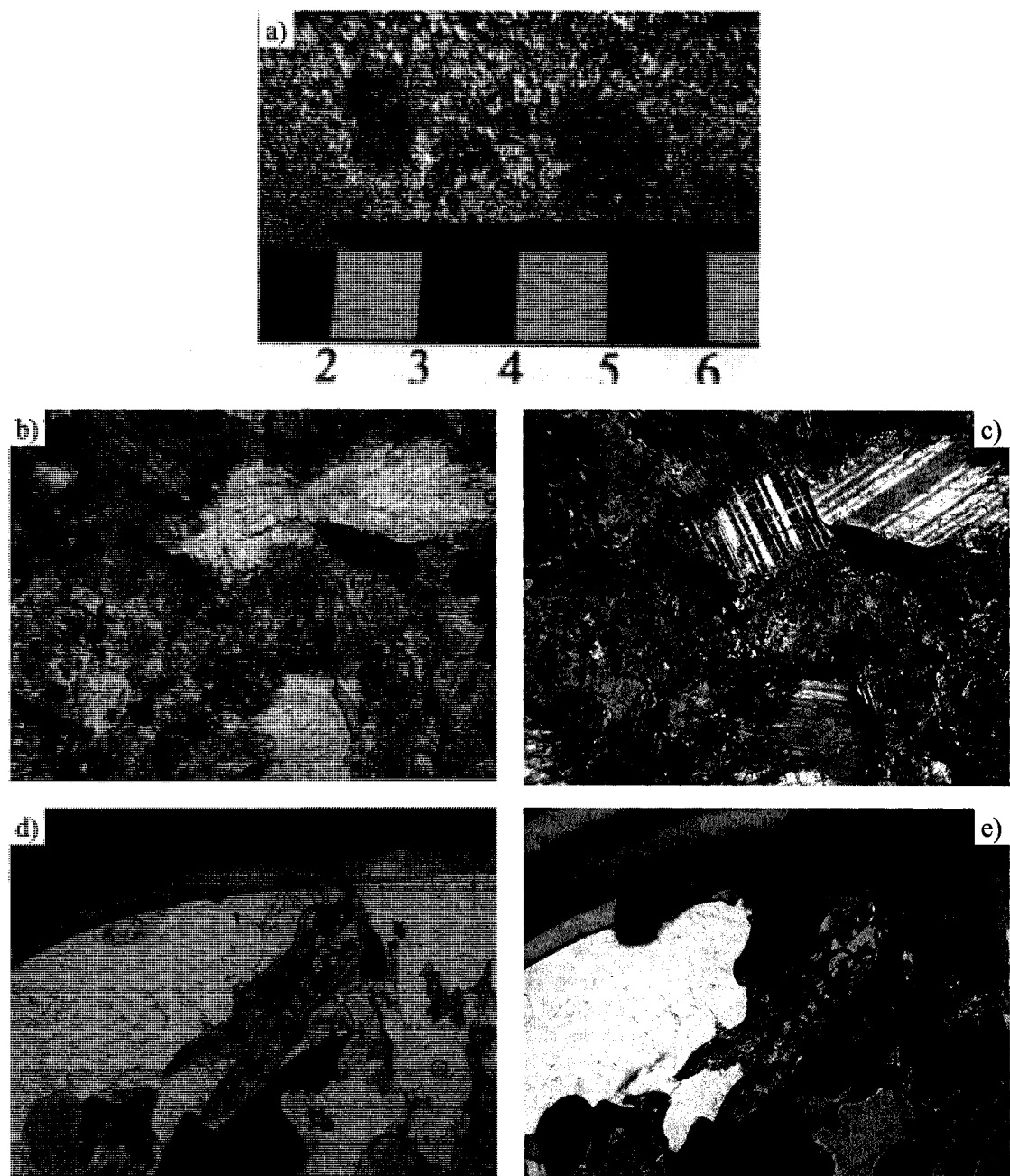


Figure 11a) Garnet porphyroblasts rimmed by clinopyroxene in a matrix of clinopyroxene and plagioclase. Centimetre card for scale. Photograph is from the central Split Lake Block. Figures b) through e) are photomicrographs of mafic granulite samples with 2.5mm field of views. Photomicrograph b) is a plane polarized view of a strongly retrogressed mafic granulite with clinopyroxene, amphibole, and plagioclase. c) is the same view in cross-polarized light of sample 9704-7134. Figure d) is a view of an orthopyroxene porphyroblast rimmed by amphibole. e) is a cross polarized view of the same porphyroblast in sample 9704-7069.

lithologies present in the Split Lake Block and Gull Rapids, the best candidates are garnet-bearing mafic granulites and aluminous granulite.

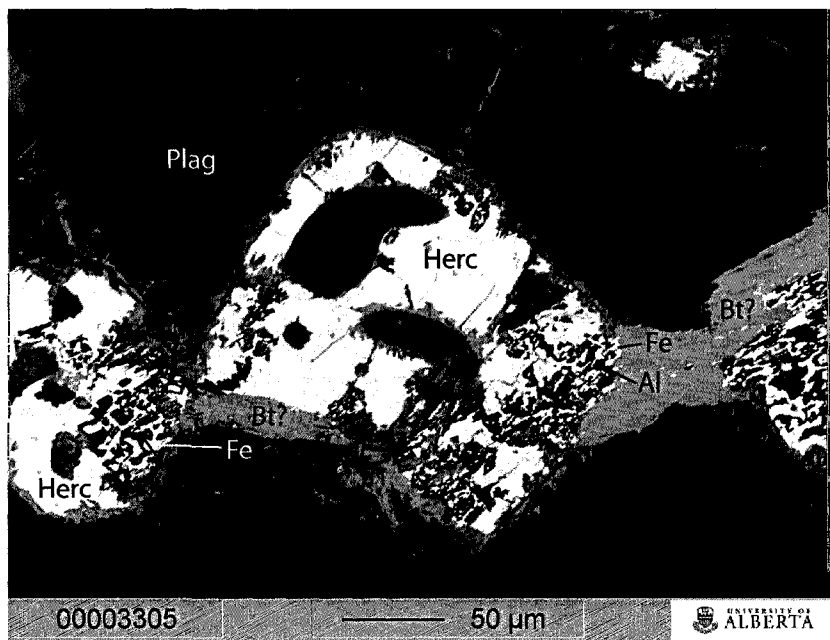
4.2.1 Mafic Granulite

The variably retrogressed nature of the samples is clear in thin section. Mafic granulites in the study area are granoblastic, consisting of a mosaic of plagioclase, clinopyroxene, and variable amounts of garnet, hornblende, orthopyroxene, and quartz. The protolith of this lithology is most likely mafic in nature, possibly gabbroic or basaltic. The modal abundance of garnet can range as high as 10% but is normally <10%. Garnet porphyroblasts with abundant mineral inclusions are typically subhedral to euhedral, with rims of clinopyroxene (Figure 11a). The abundance of pyroxene and hornblende varies according to the degree of retrogression. Some samples of mafic granulite have been completely retrogressed from pyroxene-bearing assemblages to hornblende and biotite (Figure 11b and c) being the principal mafic phases. Samples with pristine clinopyroxene are common but orthopyroxene-bearing samples are rare. In places, clinopyroxene has overgrowths of amphibole (Figure 11d and e).

4.2.2 Aluminous Garnet-bearing Granulite

A second garnet-bearing lithology is found in the field area but this rock unit is characterized by a distinctly different mineral assemblage than that present in typical mafic granulite. Besides abundant (20-80 modal %) garnet porphyroblasts, this unit comprises mainly plagioclase, quartz, hercynite, ilmenite, rutile, and sillimanite. The strongly peraluminous nature of this lithology suggests a sedimentary protolith, such as an aluminous iron formation or heavy mineral-rich sedimentary rock. Garnet porphyroblasts range in size from 0.3 to 1.2 cm and have a variety of mineral inclusions (e.g. quartz, plagioclase, monazite, and zircon). Clusters of hercynite and ilmenite occur throughout and range in modal abundance from 10-30%. The hercynite is rimmed by fine-grained biotite and features inclusions of

a)



b)

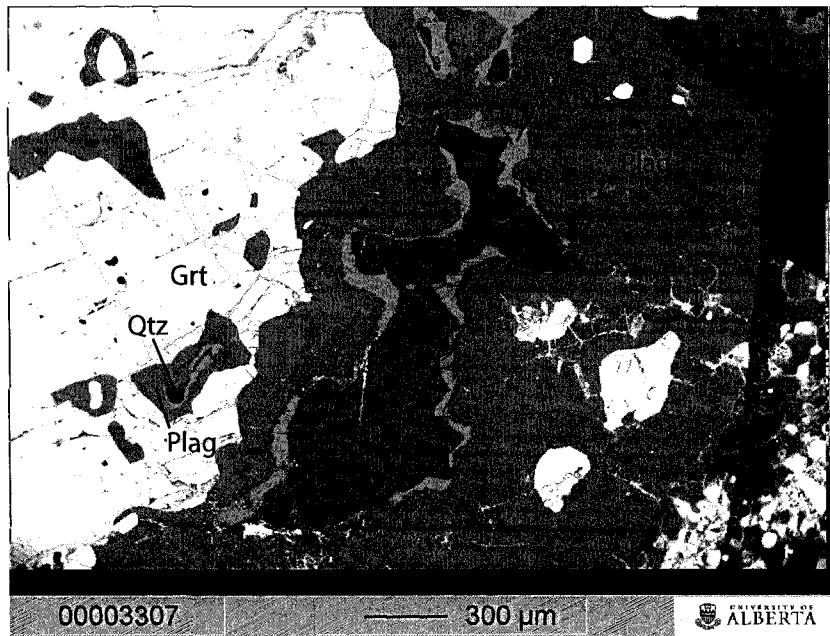


Figure 12 a) A backscattered electron image of a hercynite symplectite in sample GAR-03 b) A view of the relationship of quartz with other phases in an aluminous garnet-bearing granulite in sample GAR-03. Note how quartz is surrounded entirely by plagioclase.

Fe (Magnetite)-Al (Corundum) symplectite (Figure 12a). Fibrous to bladed sillimanite is also present, but comprises less than 5% of mineral mode. Accessory phases are also present as small blades of rutile, as well as monazite and zircon. The matrix is dominated by plagioclase and the <20% modal quartz occurs as inclusions within plagioclase meaning that quartz is generally isolated from almost all other phases including hercynite (Figure 12b).

4.3 Mineral Chemistry

A number of thin sections were selected for quantitative mineral analysis. These were chosen based on their mineral assemblage as well as the degree of preservation of primary phases through late-stage alteration. The complete analytical dataset is given in Appendix 3. Quantitative chemical analyses were preformed along transects from rim-to-rim of each grain in an attempt to assess the degree of compositional zonation. In general the analyses across garnet grains show a minor increase in grossular content and Fe/Fe+Mg from core to rim but many porphyroblasts show no distinguishable zonation trend. The plagioclase analyses also show a tendency for an increase in anorthite content from core to rim but all of the other phases analysed (orthopyroxene and clinopyroxene) show no discernable compositional zonation. Core compositions were used in the thermobarometric calculations in an effort to minimize the effect of retrograde Fe-Mg exchange on calculated temperatures.

4.3.1 Garnet

All of the garnets analysed are dominantly almandine (Alm_{63} to Alm_{78}) with appreciable amounts of pyrope (Pyr_{10-21}), grossular (Grs_{3-21}), and minor spessartine (Sp_{1-5}) (Appendix 3.2). Garnet compositions in the mafic granulite and aluminous garnet-bearing granulite are distinct in that mafic granulite garnets have higher pyrope and grossular and lower almandine contents than garnets from the aluminous granulite. These differences in garnet

composition reflect differences in the bulk composition of the two rock units.

4.3.2 Feldspar

Plagioclase from mafic granulite and aluminous garnet-bearing granulite display a range in anorthite content (An_{16-54}) (Appendix 3.3). The bimodality in mineral chemistry associated with lithology that is apparent in the garnet compositions is also present in the feldspar analyses. Plagioclase in the mafic granulite lithology is distinctly more anorthitic (An_{49-54}) than in the aluminous garnet-bearing granulite (An_{19-20}).

4.3.3 Clinopyroxene

In general, the abundance of Ca in clinopyroxene is constant, with the bulk of analyses having an atomic fraction of Ca ranging from ~0.86 to 0.91 calculated on a 6 oxygen basis. However, a small group of outlier analyses (8 of 61 analyses) of an approximate composition of 0.46 also exists and are most likely the product of clinopyroxene that is partially altered to amphibole as evidenced by their corresponding lower totals and higher aluminum content than other pyroxene analyses (Appendix 3.4).

4.3.4 Orthopyroxene

Only two samples of mafic granulite contained orthopyroxene. The analyses ranged in X_{Fe} from 0.56 to 0.59; otherwise all other elemental analyses were consistent (Appendix 3.5) and in particular show a low concentration of Al_2O_3 (0.6-0.7 wt %).

4.3.5 Accessory Minerals

A number of accessory minerals in the aluminous granulite were also analysed for use in thermobarometry. Rutile, ilmenite, hercynite, and sillimanite are close to end-member compositions which are all displayed in Appendix 3.6. Quartz is also present in both the mafic granulite and aluminous granulite samples.

4.4 Thermobarometry

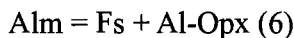
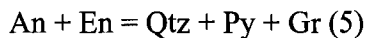
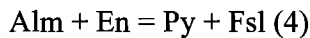
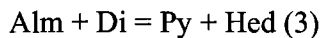
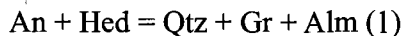
4.4.1 Thermodynamic System

The thermodynamic system used for thermobarometry is summarized in Table 1. Thermobarometric calculations were preformed with a software program TWQ v. 2.02 initially developed by Berman (1991) using an internally consistent set of thermodynamic data that includes end-member properties (Berman 1988, 1990) and the solid solution models of Berman (1990), Berman and Koziol (1991; garnet); Fuhrman and Lindsley (1988; plagioclase); Berman *et al.* (1995; clinopyroxene); and Berman and Aranovich (1996 a,b; orthopyroxene, hercynite, ilmenite). This program uses thermodynamic information calculated by experimental means combined with data input by the user (mineral chemistry and calculated activities) to calculate all possible mineral equilibria involving those phases. In an ideal situation, all calculated equilibria would converge at a single intersection, which would represent the temperature and pressure of equilibration of the mineral assemblage in the rock. In practice, however, equilibria intersect over a range of P-T conditions, which reflects a combination of uncertainties in the thermodynamic data and solution models, and in the choice of equilibrium mineral assemblages and compositions used in the calculations.

4.4.2 Mafic Granulite

Two samples of mafic granulite from the interior of the Split Lake Block (see Figure 3 for sample locations) were analysed for the purpose of thermobarometry. Many mafic granulites are the metamorphosed equivalent of mafic igneous rocks, either volcanic or intrusive in nature. The bulk mineralogy of mafic granulites is dominated by anhydrous mafic minerals such as clinopyroxene and orthopyroxene with plagioclase and quartz in the matrix and accessory minerals like garnet and zircon. Considering the co-existing mineral assemblage garnet + orthopyroxene + clinopyroxene + plagioclase + quartz, the following

reactions were used to estimate pressure and temperature:



Some of the equilibria used for geothermometry in mafic granulites are based on the distribution of ferrous iron and magnesium between clinopyroxene and garnet. Equation (3) uses Fe-Mg exchange between garnet and clinopyroxene while Equation (4) is concerned with the partitioning of Fe and Mg between garnet and co-existing orthopyroxene. The Fe-Mg exchange reactions are characterized by small volume changes with respect to the changes in entropy, which then creates a large dP/dT slope, amenable for thermometry (Harley 1984).

The barometers used for the garnet-bearing mafic granulite lithology were based on garnet-plagioclase-pyroxene net-transfer equilibria. These equilibria are much less susceptible than Fe-Mg exchange reactions to re-equilibration on cooling but the calculated position of these equilibria is affected to some degree by retrograde Fe-Mg exchange (Frost and Chacko, 1989).

The results of the thermobarometric analyses are plotted in Figure 13a and b and summarized in Table 2. The conditions of equilibration determined for sample 9704-7069 temperature determined for sample 9704-7069 indicate a range in temperature (700 to 750°C) and pressure (6.5 to 8.2 kbar). A second sample of mafic granulite, 9704-7142D yielded a range in equilibration temperatures from 810 to 850°C and pressures from 8.4 to 9.1 kbar.

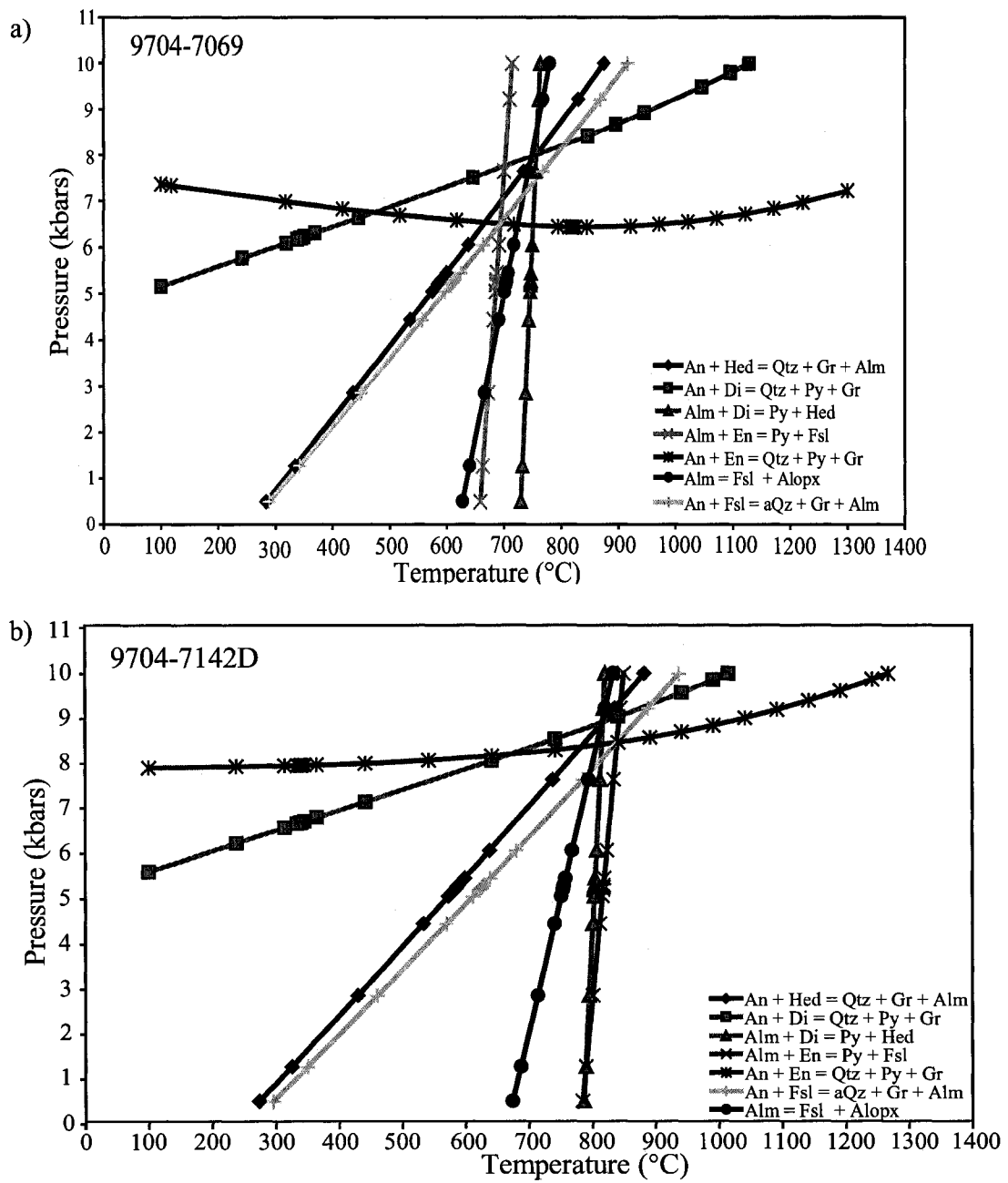


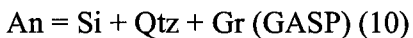
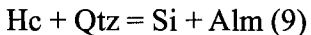
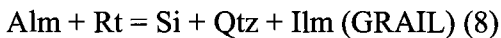
Figure 13: Metamorphic equilibria of mafic granulite samples 9704-7069 (a) and 9704-7142D (b) plotted in P-T space. Legend in (a) defines the symbols used for each reaction.

Table 2

Sample	Location	Lithology	P (kbar)	T (°C)
9704-7069	Nelson River	Mafic Granulite	6.5-8.2	700-750
9704-7142D	Nelson River	Mafic Granulite	8.4-9.1	810-850
9704-7086	Gull Rapids	Aluminous Granulite	9.2	920
Garnetite GR	Gull Rapids	Aluminous Granulite	7.5-9.5	690-950
GAR03	Gull Rapids	Aluminous Granulite	9 to 10	810 to 940
Authors	Location		P	T
Arima and Barnett (1984)	Sipiwek Lake	Metasediment, Mafic Granulite	9 ± 1	780-880
Pattison et al. (2003)	Sipiwek Lake	Recalculation of Arima and Barnett	9.7	908
Paktunc and Baer (1986)	TNB,Sipiwek.L., Wint. L. Cent.PGD	Orthogneisses, Metasediment	9-12.0	700-927
Vry and Brown (1992)	Cauchon Lake	opx-cord-Granulite, fsp-sill	730	
Mezger, Bohlen, and Hanson (1990)	Utik, Cauchon, Nataw. L.	Granulite	3 to 9	575-830

4.4.3 Aluminous Garnet-bearing Granulite

Three samples of aluminous garnet-bearing granulite were sampled across the Split Lake Block for thermobarometric analysis. Three linearly independent net-transfer equilibria were applicable to the mineral assemblage in the aluminous granulite.



A common geobarometer is garnet-sillimanite-rutile-ilmenite-quartz (GRAIL), shown as Equation (8) while Equation (10) is a geobarometer using garnet-sillimanite-plagioclase-quartz (GASP). These equilibria are frequently used for medium- to high-grade metapelitic rocks because this mineral assemblage is common over a wide range of pressures and temperatures (Koziol and Newton 1988). The third equilibria used for the aluminous garnet-bearing granulite (Equation 9) involves the reaction of hercynite with quartz to produce sillimanite and almandine. Although samples of aluminous garnet-bearing granulite have significant amounts of modal hercynite and quartz (>20 modal %), there was no petrographic evidence to clearly indicate the relationship between these two phases. Although it is likely that the two are in equilibrium considering their high abundance, in the event that they are not, the temperatures returned by this equilibrium would then be considered a maximum limit on temperature of equilibration, rather than the actual temperature.

Three samples of aluminous garnet-bearing granulite: GarnetiteGR, GAR03 and 9704-7086 from the Split Lake Block (Figure 3) were used for the purpose of thermobarometric calculations. A summary of these thermobarometric results can be found in Table 2 and each sample is plotted individually in Figure 14a, b, and c. These samples are consistent among themselves as well as yielding results comparable to those obtained for the mafic granulite lithology. The calculated range of equilibration temperatures for sample GarnetiteGR from the western Gull Rapids Area is from 690°C to 950°C and a

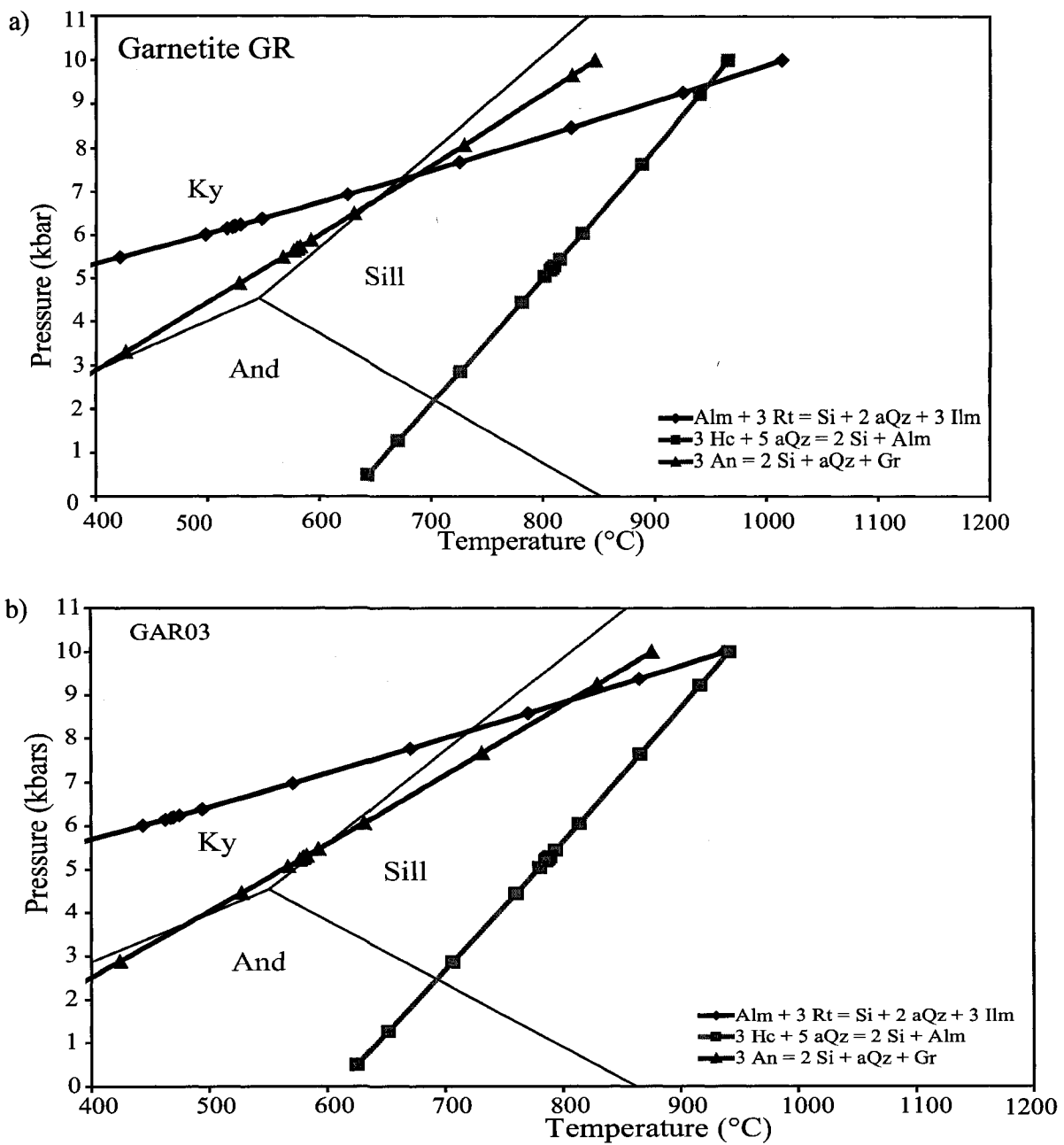


Figure 14 a-b: Metamorphic equilibria of aluminous garnet-bearing granulite samples Garnetite-GR (a), and GAR03 (b) vplotted in P-T space.

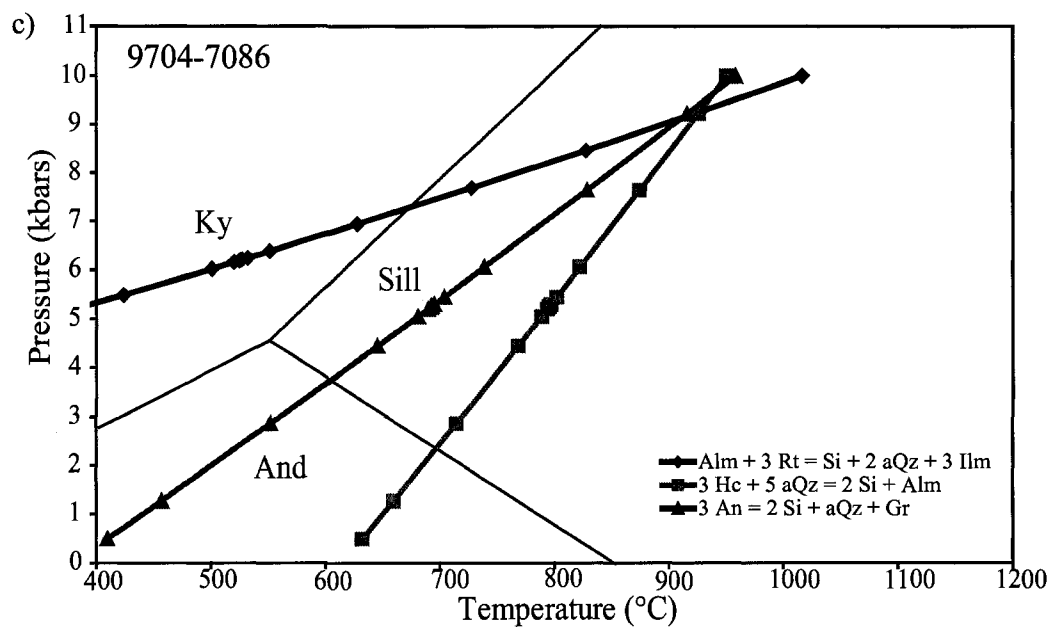


Figure 14 (continued) c: Metamorphic equilibria of aluminous garnet-bearing granulite sample 9704-7086 (c) plotted in P-T space.

range in pressure from 7.5 to 9.5 kbar. Sample GAR03 has a more restricted range of temperature of equilibrium from 810°C to 940°C and pressures from 9.0 to 10.0 kbar. Sample 9704-7086 has a clear intersection with all 3 equilibria at a temperature of 920°C and a pressure of 9.2 kbar.

4.5 Radiogenic Isotope Analyses

4.5.1 Samarium-Neodymium

A total of 6 samples from Gull Rapids were processed for Nd isotopic composition to evaluate the provenance of various granitoids and quartzo-feldspathic gneiss. The results of these analyses are listed in Appendix 4.1. Three samples of orthogneiss produced a small range of T_{DM} ages from 3.42-3.51 Ga with $\epsilon Nd_{2.7\text{ Ga}}$ values from -6.7 to -8.0. These values suggest that the orthogneiss samples are Mesoarchean in age or that significant Mesoarchean crust was involved in their generation. Two relatively undeformed granitoid samples yielded T_{DM} ages of 3.13 Ga and 3.32 Ga for a tonalite and leucogranite, respectively. These granitoids appear to be more juvenile in composition than the orthogneisses, with $\epsilon Nd_{2.7\text{ Ga}}$ of -3.2 and -4.5. Lastly, a sample of quartzo-feldspathic gneiss from Gull Rapids produced a T_{DM} age of 3.13 Ga, also indicating derivation or interaction with an older protolith. This sample has the most primitive $\epsilon Nd_{2.7\text{ Ga}}$ signature (-1.7) of the analysed samples. When plotted on an ϵNd versus Time diagram (Figure 15) the data from the Split Lake Block show a range in ages of removal from the depleted mantle that overlaps with that of the Pikwitonei Granulite Domain and not the Assean Lake Crustal Complex.

4.5.2 Uranium-Lead Geochronology

Although a wide range of lithologies were sampled in search of suitable samples for geochronology, mafic-granulite compositions proved to be the most useful for determining metamorphic age information. In addition, this lithology was an ideal candidate for both geochronological and thermobarometric study. Initial geochronological investigations

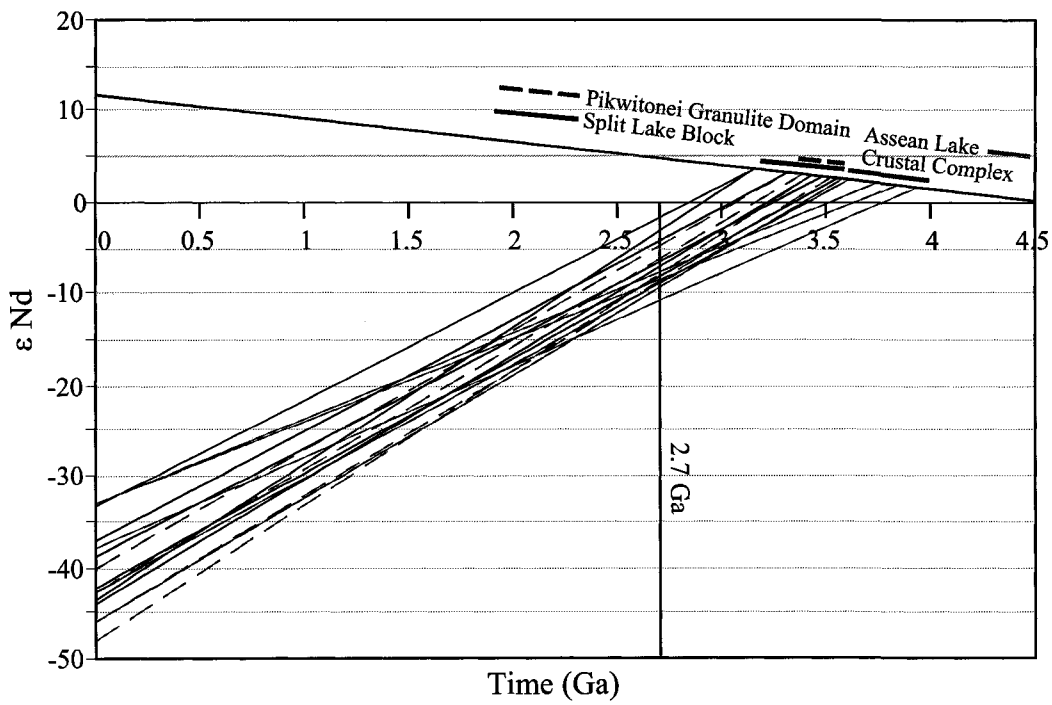


Figure 15: A plot of ε_{Nd} vs. Time for samples from the Pikwitonei Granulite Domain (green dashed), Split Lake Block (black), and the Assean Lake Crustal Complex (red). Data from the Pikwitonei Granulite Domain and Assean Lake Crustal Complex is from Böhm *et al.* 2000.

of the aluminous garnet-bearing granulite were carried out by determining chemical U-Th-Total Pb ages of monazite in thin section using the JEOL 8900 Electron Microprobe (Suzuki *et al.* 1991; Montel *et al.* 1996, Cocherie and Albarede 2001). Further mafic granulite samples were prepared for grain mount or in-situ thin section LA-MC-ICP-MS analysis. Most samples yielded an appreciable amount of zircon with a wide range of characteristics.

4.5.3 Electron Microprobe Analysis

Prior to in-depth U-Pb isotopic investigations, the chemical dating of monazite using the Electron Microprobe was used to obtain an estimate of the timing of metamorphism in the Gull Rapids mapping area. A sample from garnetite sample GAR 01 collected within the orthogneisses in the western half of Gull Rapids was selected due to the presence of large ($>100 \mu\text{m}$) and numerous monazite grains. The monazite grains had irregular, anhedral margins that suggest metamorphic monazite growth as opposed to detrital grains of monazite that would be more rounded and pitted by transport. The chemical composition of 117 spot analyses of 52 monazite grains are compiled in Appendix 4.2 and the results are displayed on a histogram diagram in Figure 16. Although multiple analyses were preformed on single grains, there was no correlation between age distribution and location within the monazite grains. The histogram displaying all analyses in Figure 16 indicate a range of ages from 2900 to 2400 Ma with a number of age peaks. The overall distribution of analyses is bell-shaped and shows a main peak at ~2700 Ma with subsidiary peaks at 2630, 2680, and 2720 Ma. In general, the bell curve is skewed toward older ages.

4.5.4 Uranium-Lead Laser Ablation Inductively Coupled Plasma Mass Spectrometry

4.5.4.1 Sample 9703-6365

Grain Mount LA-MC-ICP-MS

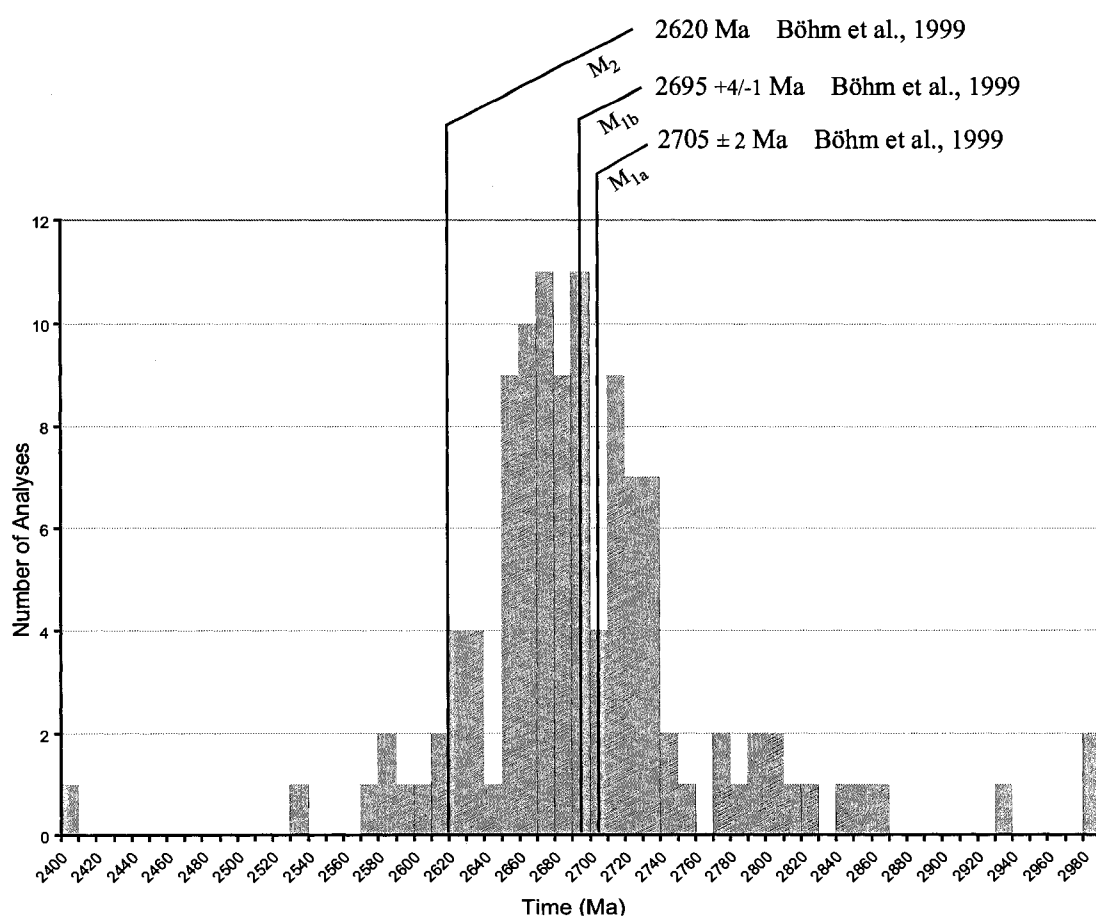


Figure 16: A histogram showing the distribution of ages obtained by EMPA of monazite in sample Garnetite GR. Note the roughly bell-shaped distribution that is slightly skewed to older vages. Plotted on this diagram are the ages of metamorphism reported in Bohm et al. 1999.

a)

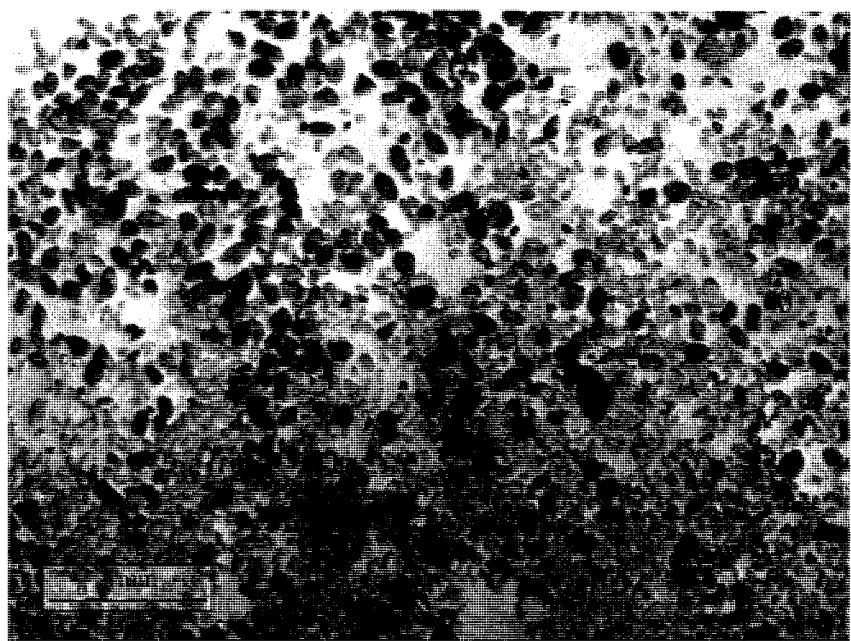


Figure 17: Photomicrograph of zircon separated from sample 9703-6365.

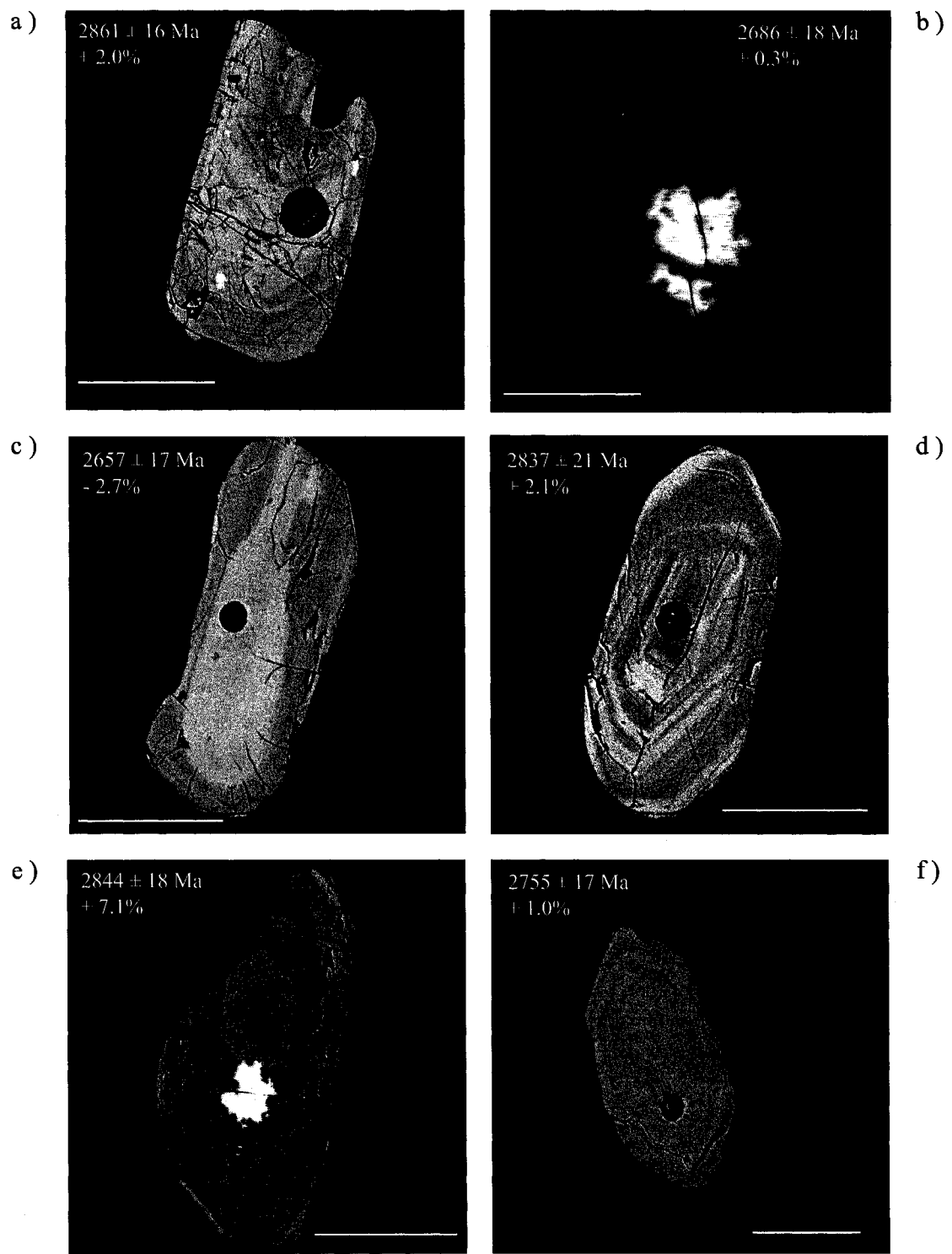


Figure 18: BSE images of zircons with $^{207}\text{Pb}/^{206}\text{Pb}$ age and discordance. Analysis number:
 a) 9703-6365-4 b) 9703-6365-65 c) 9703-6365-64 d) 9703-6365-11 e) 9703-6365-12 f)
 9703-6365-13b. Scale bar is $100\mu\text{m}$

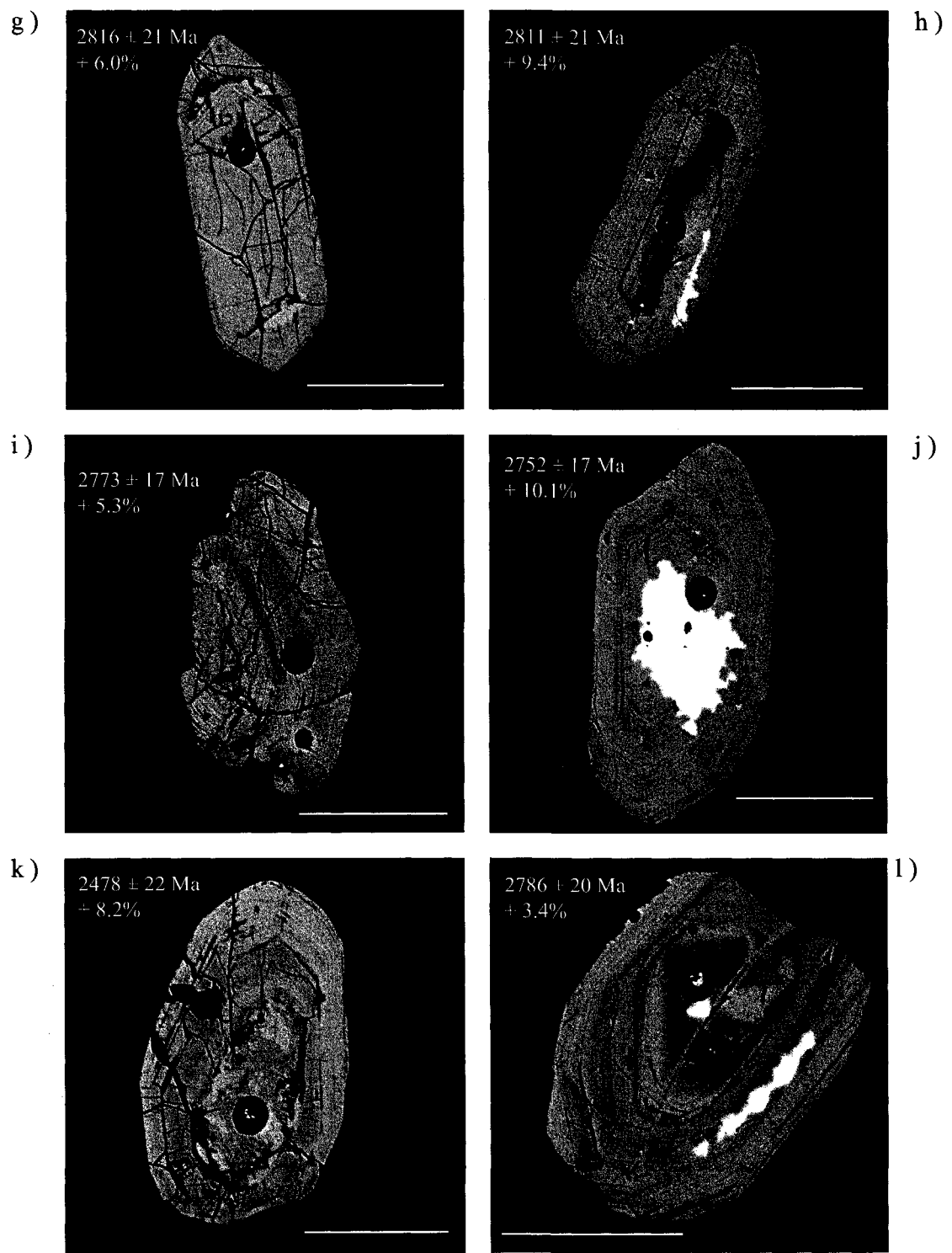


Figure 18: BSE images of zircon analyses with $^{207}\text{Pb}/^{206}\text{Pb}$ age and discordance. Analysis number: g) 9703-6365-14 h) 9703-6365-15 i) 9703-6365-17 j) 9703-6365-20 k) 9703-6365-23 l) 9703-6365-24

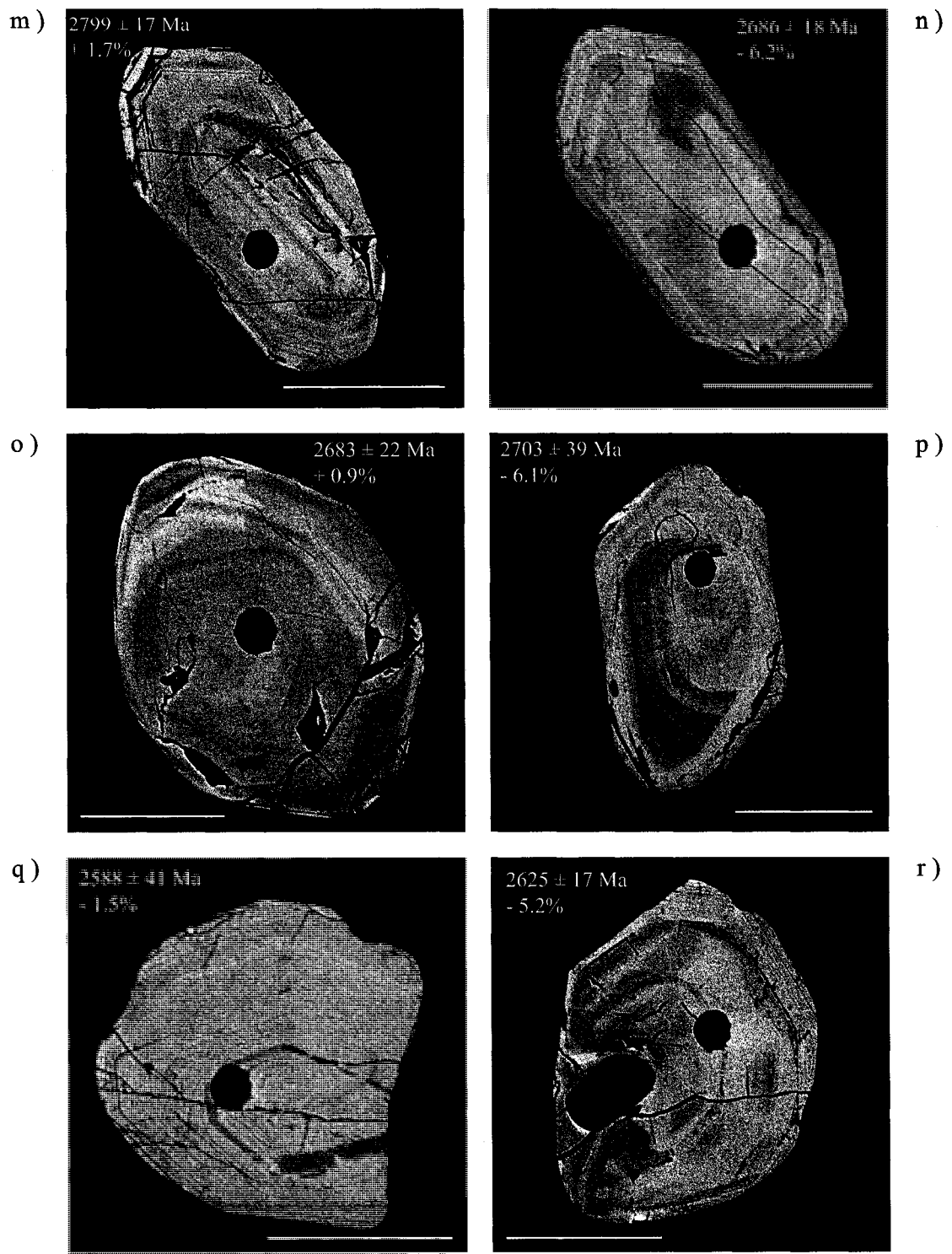


Figure 18: BSE images of zircon analyses with $^{207}\text{Pb}/^{206}\text{Pb}$ age and discordance. Analysis number: m) 9703-6365-25 n) 9703-6365-28 o) 9703-6365-34 p) 9703-6365-35 q) 9703-6365-40 r) 9703-6365-41

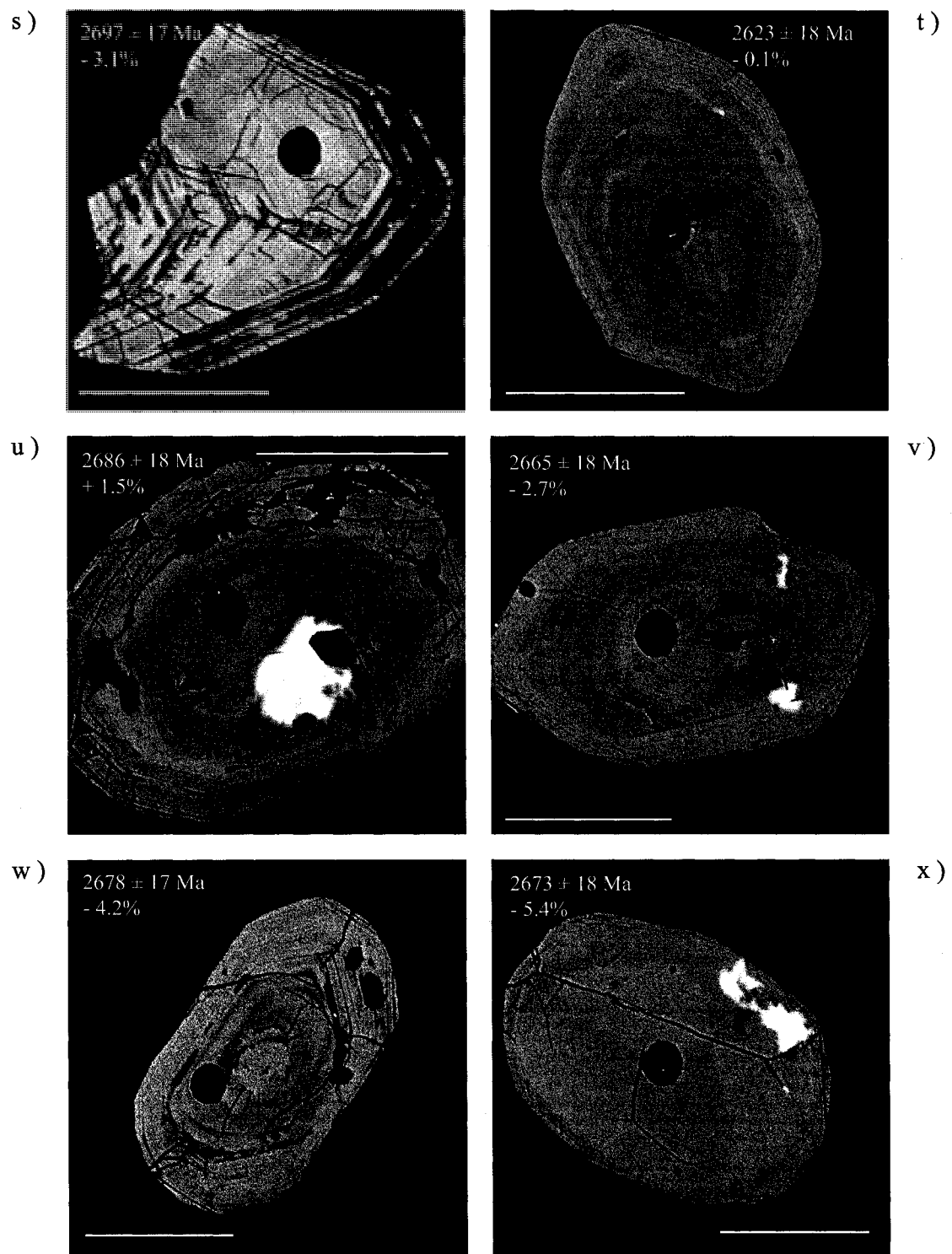


Figure 18: BSE images of zircon analyses with $^{207}\text{Pb}/^{206}\text{Pb}$ age and discordance. Analysis number: s) 9703-6365-42 t) 9703-6365-50 u) 9703-6365-51 v) 9703-6365-52 w) 9703-6365-53 x) 9703-6365-55

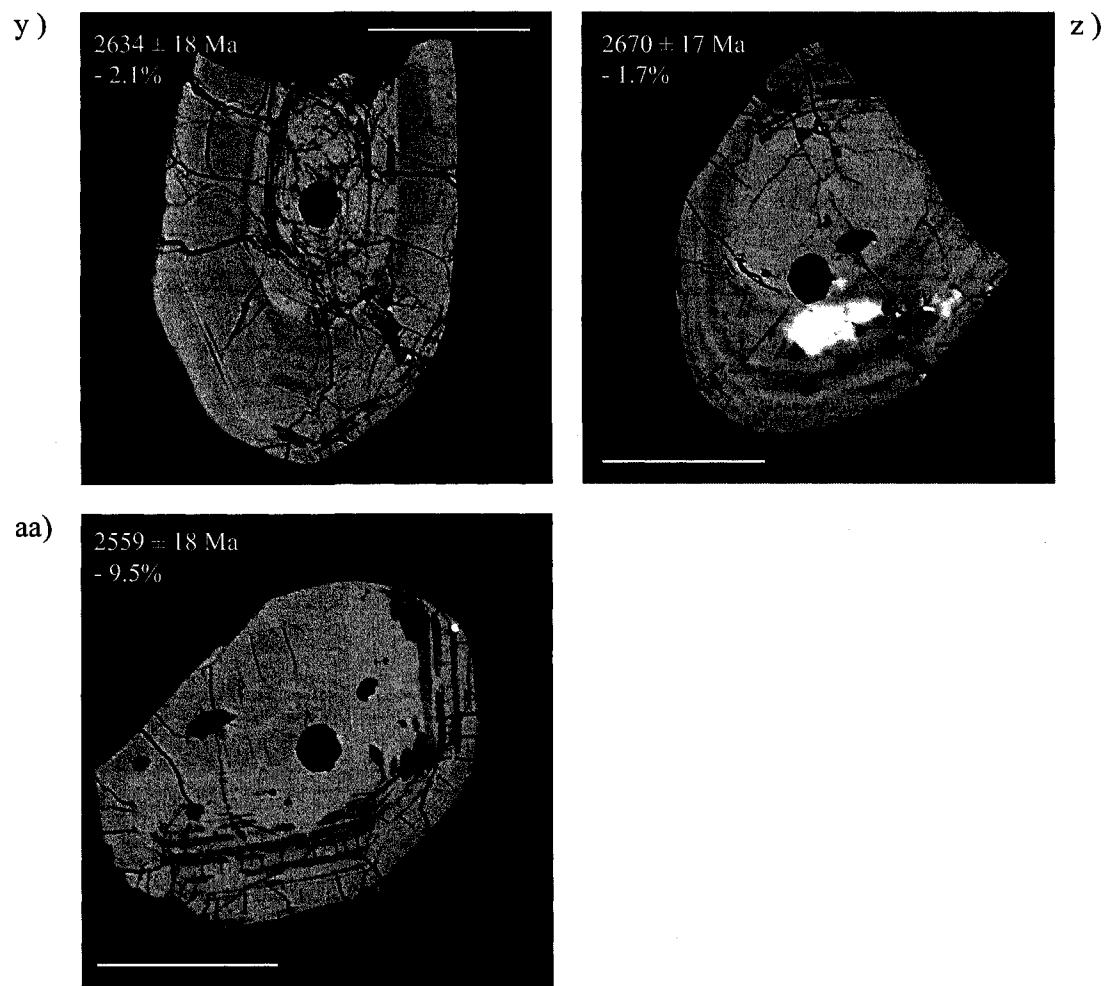
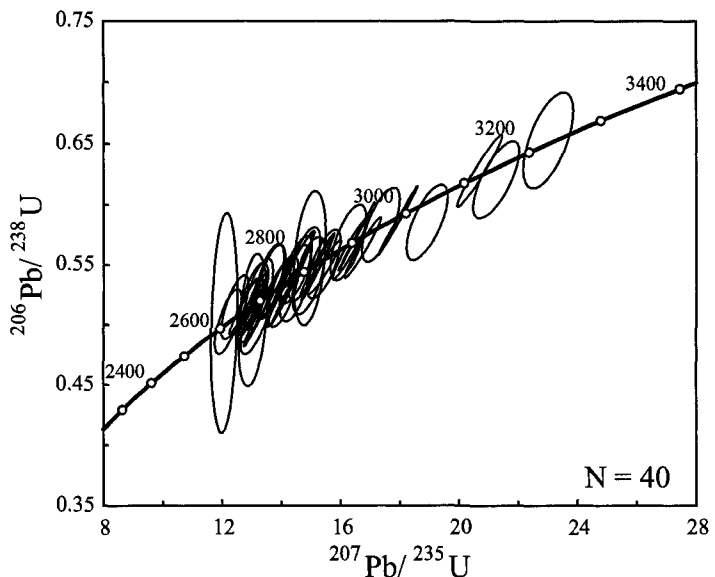


Figure 18: BSE images of zircon analyses with $^{207}\text{Pb}/^{206}\text{Pb}$ age and discordance. Analysis number: y) 9703-6365-57 z) 9703-6365-61 aa) 9703-6365-62

a)



b)

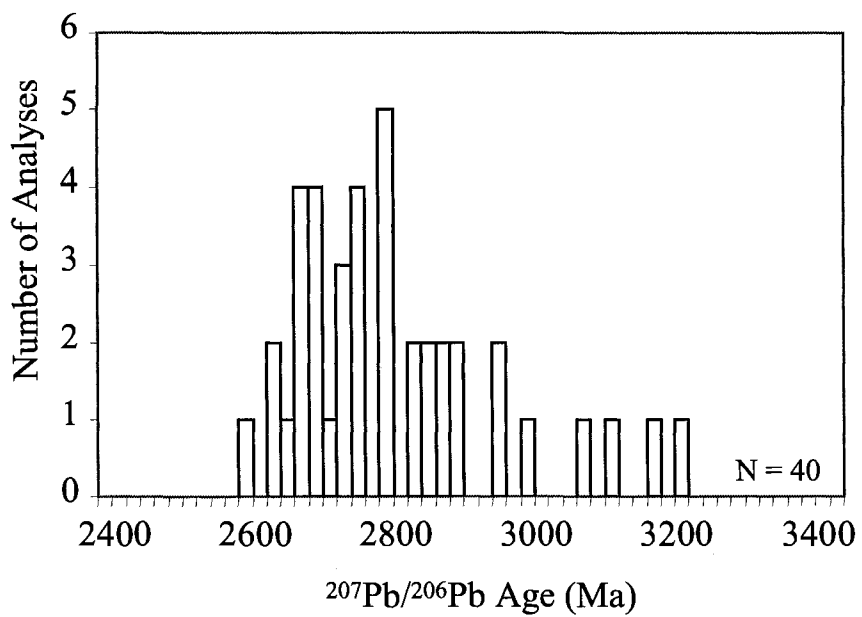


Figure 19 a) A concordia diagram displaying 40 LA-ICP-MS analyses that are less than 5% discordant from sample 9703-6365. Error ellipses are 2σ . Figure b) displays a histogram with the same data set.

Quartz-feldspathic gneiss

A sample of quartz-feldspathic gneiss relatively free of leucocratic injection was sampled at Gull Rapids for analysis by LA-MC-ICP-MS. The fine-grained nature and non-unique mineralogy of sample 9703-6365 precludes a straightforward classification of this sample as sedimentary or igneous in origin.

Zircons were separated from sample 9703-6365 and secured into a grain mount for U-Pb analysis by laser ablation. The zircons range in colour, from clear to pink to brown, and in size from < 20 µm to 200 µm in the longest direction (Figure 17a). The degree of rounding of the grains is quite variable from prismatic to spherical with the dominant habit being prismatic. Backscatter images of the grains (Figure 18) show a range of internal structures from homogeneous to zoned grains with sector (e.g. Figure 18x), and oscillatory (e.g. Figure 18y) zoning. Most of the grains show complex oscillatory zoning in backscattered electron images.

Analysis by laser ablation was completed using a laser spot diameter of 20 µm and the average ^{206}Pb beam intensity was approximately 300,000 cps (Appendix 4.3.1). A histogram of $^{207}\text{Pb}/^{206}\text{Pb}$ ages and a concordia plot for all analyses with less than 5% discordance are shown in Figures 19a and b, respectively. These analyses display a range of $^{207}\text{Pb}/^{206}\text{Pb}$ ages between 2588 and 3214 Ma, with one outlier at 955 Ma. A concordia diagram displaying analyses that are less than 5% discordant clearly shows that the bulk of the data lie between 2700-2800 Ma. The oldest nearly concordant grain is number 9703-6063-70 with a $^{207}\text{Pb}/^{206}\text{Pb}$ age of 3214 ± 17 Ma (+ 1.0% discordant). The youngest concordant grain, besides Proterozoic outliers, is zircon number 9703-6365-50 with an age of 2623 ± 18 Ma (- 0.1% discordant; Figure 19) with distinct oscillatory zoning visible (Figure 18t).

The significance of these results cannot be understood fully without knowing the protolith of this quartz-feldspathic gneiss. It is apparent in thin section that a foliation is present in sample 9703-6365 but is not as strongly developed as in most other samples

of metasediment collected from the Gull Rapids area. There is also a lack of garnet porphyroblasts in sample 9703-6365 which are occasionally present in metasediment. Unfortunately, the geochemical composition of the quartzo-feldspathic gneiss does not clearly distinguish whether it is more likely igneous or sedimentary in origin because the range of values for the major and trace-element compositions for sedimentary and igneous units in the Split Lake Block overlap (Appendix 2.6). The most distinct evidence for an igneous source for this quartzo-feldspathic gneiss is the presence of zircons younger than the predicted age of sedimentation that display oscillatory zoning, a feature normally attributed to zircons with an igneous provenance (Schaltegger *et al.* 1999; Vavra *et al.* 1996; Hanchar and Rudnick 1995; Vavra *et al.* 1996, Watson and Liang 1995). Many of the zircons from sample 9703-6365 are euhedral and retain their original prismatic shape suggesting that they are not likely detrital, considering that transport would have rounded or fragmented these zircons although it is possible they are detrital and from a proximal source.

If this quartzo-feldspathic gneiss has an igneous protolith, the spread of ages would represent the ages of crust sampled by the igneous body. The youngest igneous zircon grain at 2623 ± 18 Ma (-0.1% discordance, analysis number 9703-6365-50, Figure 18t) would represent the age of crystallization for this unit. The presence of this igneous unit within metasediment means that the age results place some constraint on the depositional age of the metasediment. The youngest age results from the quartzo-feldspathic gneiss, if volcanic in nature, represent an age of synchronous deposition with the volcanics. If this quartzo-feldspathic gneiss is an intrusive igneous unit that cross-cuts the metasediment, the youngest igneous zircons in the feldspathic gneiss represent a maximum age of deposition for the metasediment. Although this distinction between an intrusive and volcanic provenance is difficult to make, the less developed foliation in the feldspathic gneiss would suggest that it is an intrusive igneous phase that has not been deformed to the same extent than the metasediment.

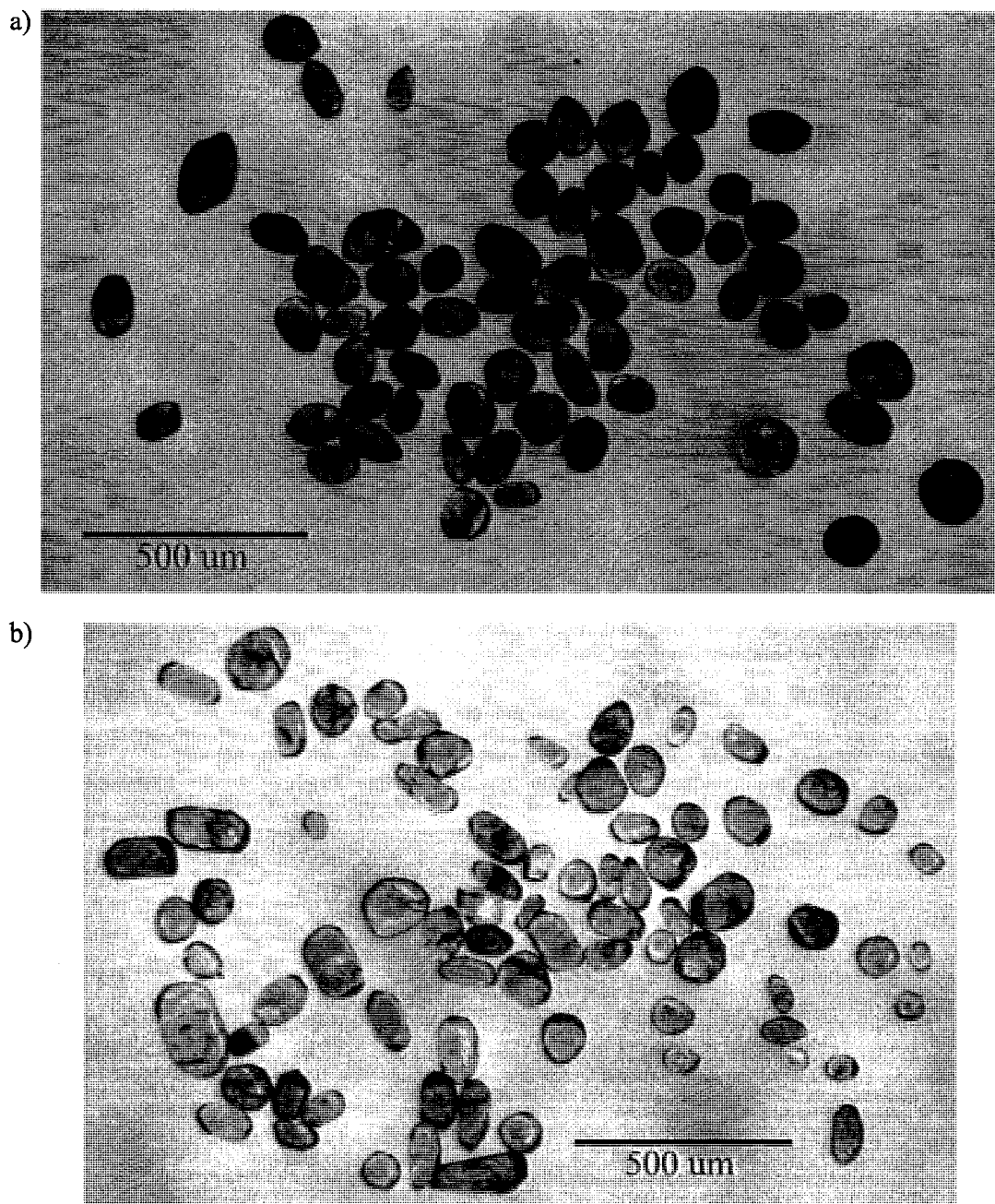


Figure 20: Photomicrographs of zircon separated from sample 9704-7069 (a) and (b).

9704-7069

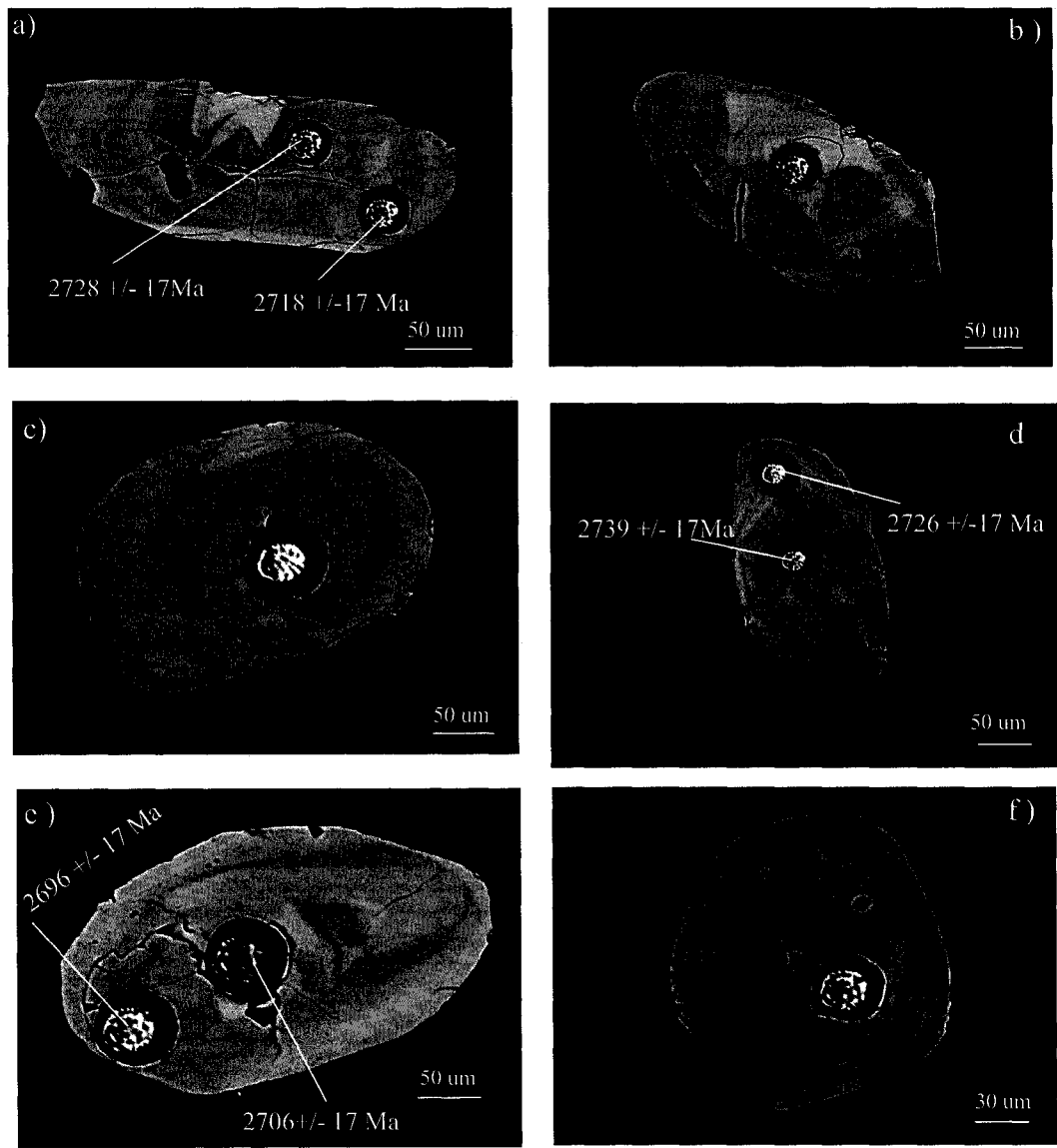


Figure 21: Backscattered Electron images of zircon separated from sample 9704-7069. $^{207}\text{Pb}/^{206}\text{Pb}$ ages are from LA-ICP-MS analyses. a) Zircon 9704-7069-1 and 2 b) 9704-7069-unknown c) 9704-7069-unknown d) 9704-7069-98 and 99 e) 9704-7069-72 and 73 f) 9704-7069-unknown

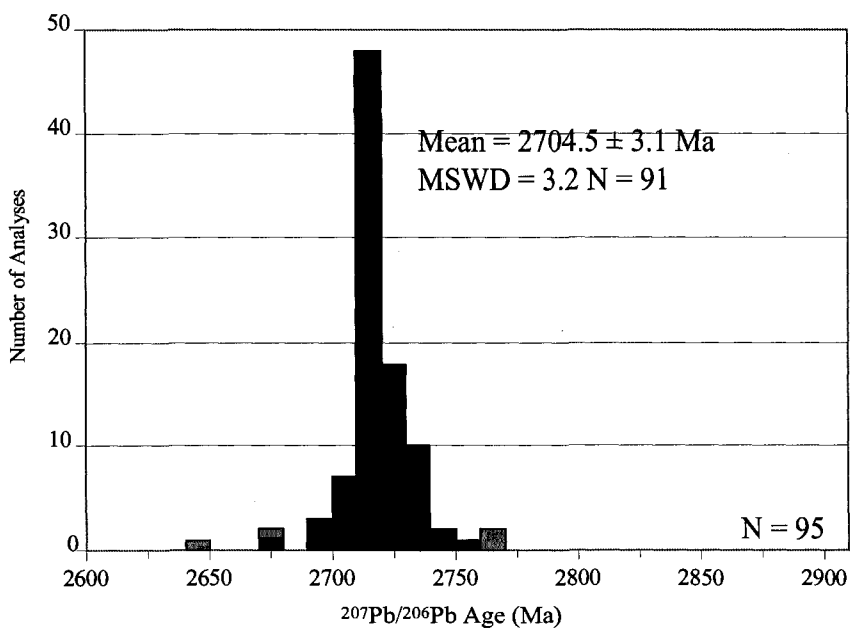
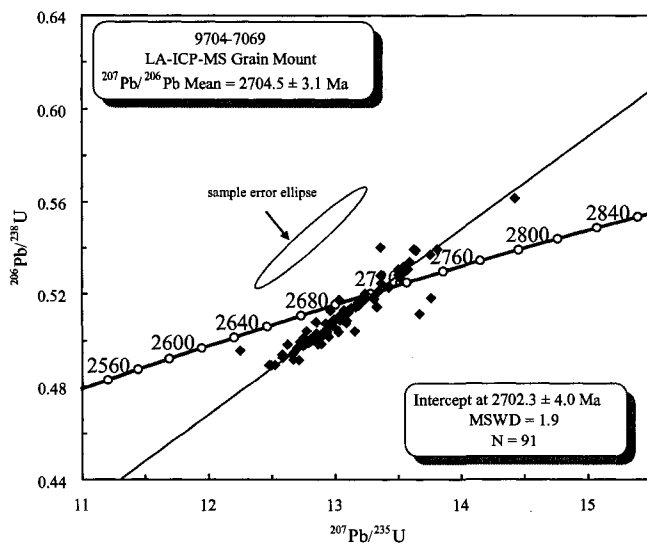


Figure 22: a) Concordia diagram with 91 LA-ICP-MS analyses plotted. Note, sample error ellipses for analyses not plotted to clarify diagram. Sample error ellipse plotted as an example. b) A histogram displaying ninety-five $^{207}\text{Pb}/^{206}\text{Pb}$ ages of zircons analyzed by LA-ICP-MS. The mean calculation excluded four analyses, these analyses are shown in grey.

4.5.4.2 Sample 9704-7069

Grain Mount – LA-MC-ICP-MS

Mafic Granulite

A seven-kilogram sample of garnet-bearing mafic granulite from the Nelson River (Sample 9704-7069, Figure 3) was processed and used for both grain mount and in-situ thin section analysis by LA-MC-ICP-MS. More than one thousand individual grains were liberated in the mineral separation process. This zircon population consists of a number of separate grain types, suggesting that there may be a complex history of zircon growth. The zircon colour varies from clear to pink to brown (Figure 20a and b) with the most common colour being light pink. The habit of the zircon grains ranges from nearly spherical, anhedral crystals to prismatic and euhedral specimens with the majority (>75%) near the anhedral end of the spectrum. The size of zircon covers a wide range, from grains less than twenty microns to the largest being nearly two hundred microns. The majority of zircon (>75%) are less than thirty microns in the longest dimension, precluding their analysis by LA-MC-ICP-MS. In backscatter electron images (Figure 21), the zircons from this sample show either a lack of internal structure or irregular zonation, typical of metamorphic zircon (Schaltegger *et al.* 1999; Vavra *et al.* 1996; Hanchar and Rudnick 1995; Vavra *et al.* 1996, Watson and Liang 1995).

An epoxy grain mount was prepared with ninety-nine zircons from this sample, representing the entire spectrum of zircon morphologies. The bulk of the LA-MC-ICP-MS analyses (ninety-one of ninety-nine) are presented in Appendix 4.3.2 and shown in the concordia diagram of Figure 22a. The average counts of ^{206}Pb for the zircons during analysis are $\sim 280,000$ cps using a $40\mu\text{m}$ diameter laser, indicating these zircons have relatively low uranium contents. By comparison, the ^{206}Pb signal for the zircon standard analyses at the same spot size range from 400,000 to 700,000 cps, which corresponds to an average Pb concentration of ~ 115 ppm and U content of ~ 300 ppm (Ashton *et al.* 1999). Other than

three grains younger than 2600 Ma, all analyses plot on the same discordia line that has an upper intercept age of 2702.3 ± 4.0 Ma (MSWD = 1.9). The lower intercept of the discordia line intersects the concordia curve within error of the origin (-107 ± 340 Ma), suggesting that the slight Pb-loss in these grains is a relatively recent effect. The discordance for these analyses is from – 7.5% to 6.3% with one outlier at -26.6%. The distribution of $^{207}\text{Pb}/^{206}\text{Pb}$ ages is shown in the histogram of Figure 22b and ranges from 1044 ± 23 Ma (-1.7% discordant) to 2774 ± 17 Ma (4.9% discordant) with the bulk of analyses (>90%) occurring between 2695 ± 17 Ma (0.2% discordant) and 2710 ± 17 Ma (concordant). The weighted mean $^{207}\text{Pb}/^{206}\text{Pb}$ age obtained for 91 zircon grains is 2704.5 ± 3.1 Ma (MSWD = 2.5) with a distribution that forms a bell-shaped curve that is slightly skewed to older ages (Figure 22b) and is identical within analytical uncertainty to the discordia line upper intercept age of 2702.3 ± 4.0 Ma (Figure 22a). A single analysis at 1832 ± 19 Ma (0.3% discordant) is an indication of Trans-Hudsonian aged zircon growth in the northwestern Superior Province. Considering the uniformity of the bulk of the ages obtained, the internal structure of their zircons, and low Pb counts (i.e. these are likely low-uranium zircons), it is likely that this age of 2702.3 ± 4.0 Ma records an episode of metamorphic zircon growth. There are concordant outliers that may represent other episodes of metamorphism, most notably at 2682 ± 17 Ma (- 0.2% discordant) and 2710 ± 17 Ma (0.0% discordant) but they are within error of the concordia age.

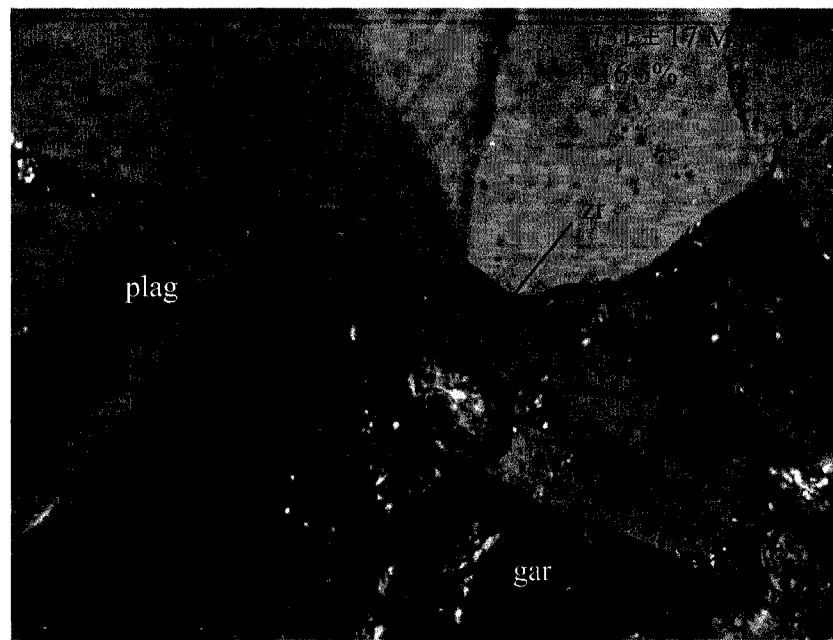
4.5.4.3 Sample 9704-7069

Thin Sections

Mafic Granulite – Upper Nelson River

Two thin sections were prepared from samples collected at the same outcrop as the 9704-7069 mafic granulite sample that was processed through crushing and mineral separation. The thin sections were used for in-situ LA-MC-ICP-MS analyses, a total of twenty-three zircons were analysed from both thin sections and the data is presented in Appendix 4.3.3.

a)



b)

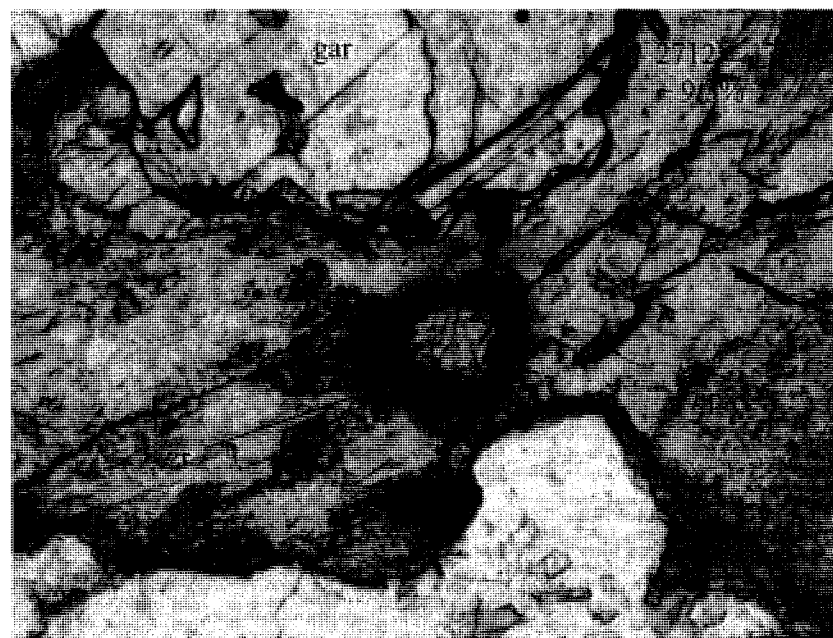


Figure 23: Photomicrographs of zircons analysed by LA-ICP-MS. a) Zircon number 9704-7069A-6a included within plagioclase in cross polarized light. b) Zircon number 9704-7069A-12 included in altered clinopyroxene in plane polarized light. All displayed ages are $^{207}\text{Pb}/^{206}\text{Pb}$ ages.

9704-7069a

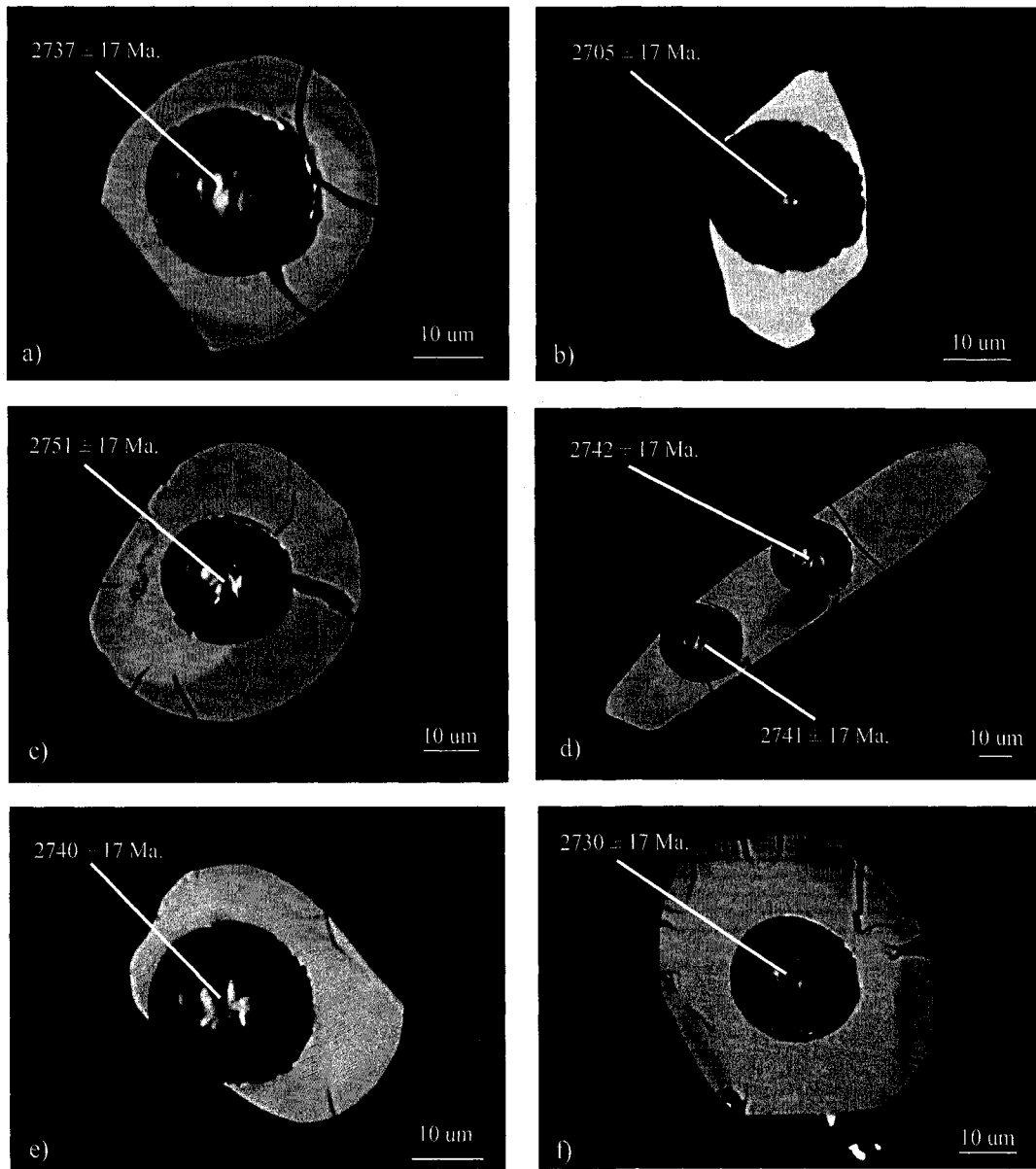


Figure 24: Backscattered electron images of zircons in thin section 9704-7069a with laser pits a) Zircon 9704-7069a-3 b) Zircon 9704-7069a-6c c) Zircon 9704-7069a-5 d) Zircon 9704-7069a-6b e) Zircon 9704-7069a-7 f) Zircon 9704-7069a-12.

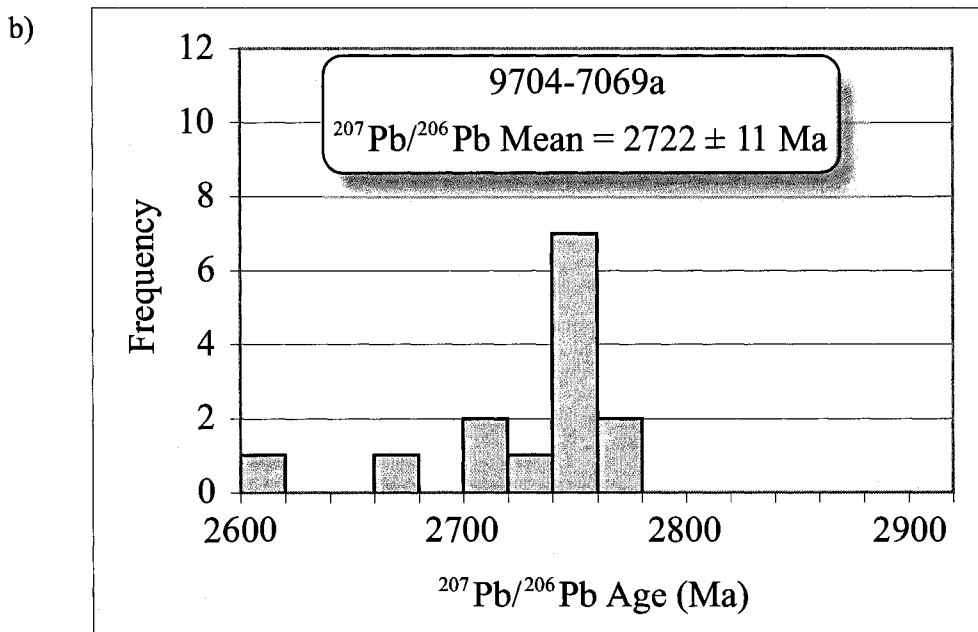
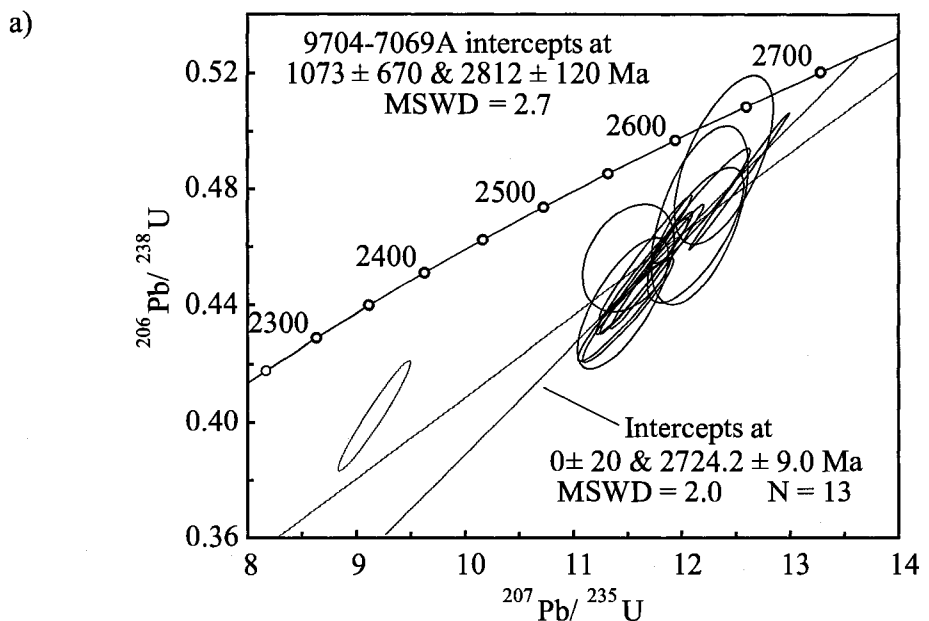


Figure 25: Figure a) is a concordia diagram of LA-ICP-MS analyses from sample 9704-7069a with a corresponding histogram of $^{207}\text{Pb}/^{206}\text{Pb}$ ages in figure b).

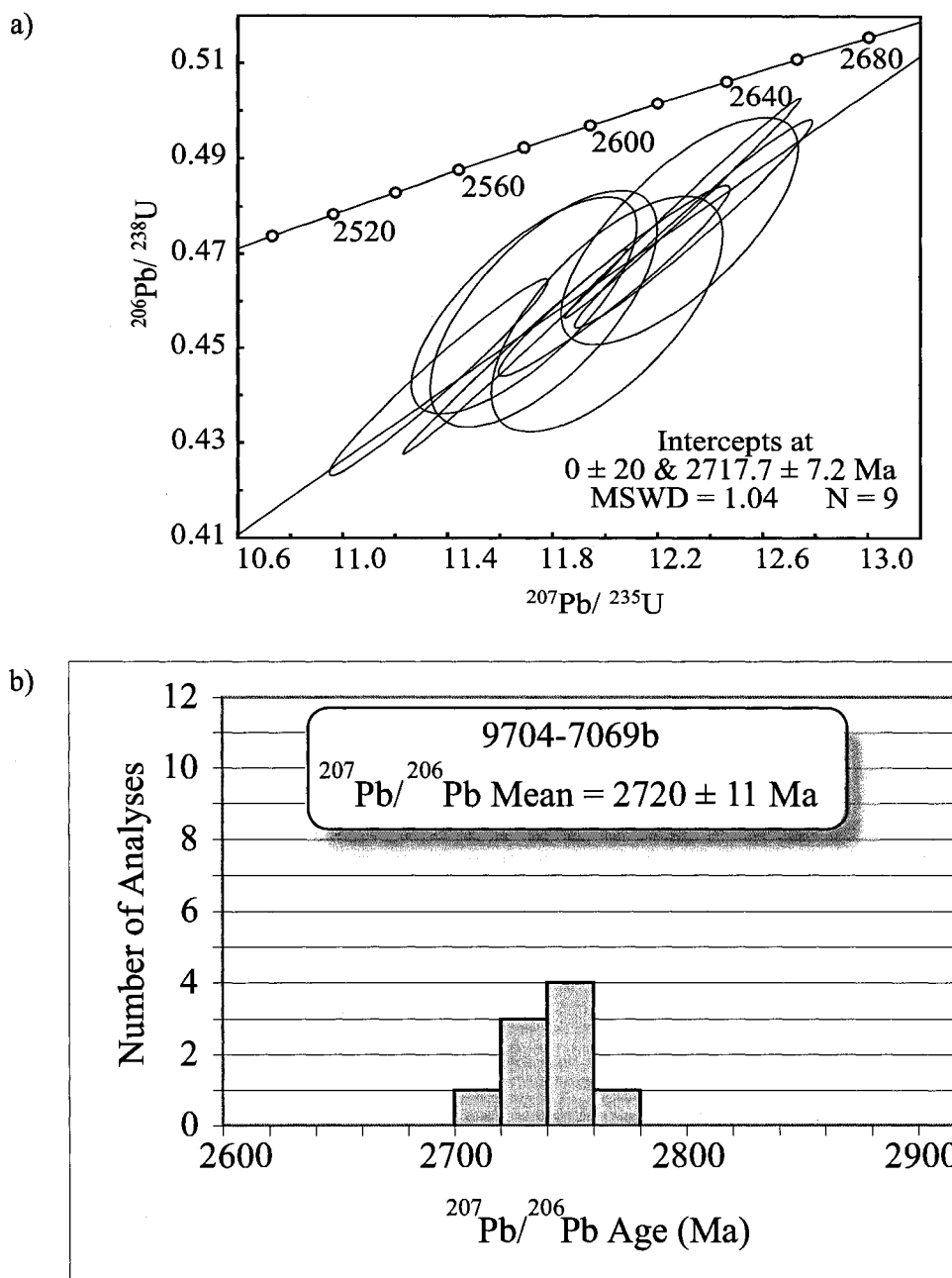


Figure 26: Figure a) is a concordia diagram of LA-ICP-MS analyses from sample 9704-7069b with a corresponding histogram of $^{207}\text{Pb}/^{206}\text{Pb}$ ages in figure b). Error ellipses are 2σ .

The size and shape of zircons in this sample are uniform, ranging in size from thirty to fifty microns in the longest direction and are round to subhedral prisms. Zircons are found as inclusions in mineral phases such as plagioclase (Figure 23a) and clinopyroxene (Figure 23b). Backscatter electron images of these zircons show that the zircons commonly lack internal structure, besides a few with irregular zonation or rims of slightly different composition (Figure 24). The analyses were preformed using a 30 μ m diameter laser and an average of ~300,000 ^{206}Pb cps was obtained for these zircons. Fourteen zircons from thin section 9704-7069a were analysed using LA-MC-ICP-MS and the U-Pb results are presented in Table 9 and plotted in a concordia diagram in Figure 25a. The analyses are slightly discordant (5.2% to 17.3%) and cluster along a discordia line anchored at 0 ± 20 Ma, with an upper intercept of 2724.2 ± 9.0 Ma (MSWD = 2.0). One analysis is significantly younger ($^{207}\text{Pb}/^{206}\text{Pb}$ age of 2508 ± 20 Ma) than the main population and is not included in the age calculation (Appendix 4.3.3). A histogram showing the distribution of $^{207}\text{Pb}/^{206}\text{Pb}$ ages (Figure 25b) shows the range of $^{207}\text{Pb}/^{206}\text{Pb}$ ages between 2508 ± 20 Ma and 2743 ± 17 Ma. The mean $^{207}\text{Pb}/^{206}\text{Pb}$ age, calculated from thirteen analyses is 2722 ± 11 Ma (MSWD = 4.4).

Nine zircons from a second thin section, number 9704-7069b, were analysed by LA-MC-ICP-MS using a thirty-micron diameter laser spot size and generated an average of 160,000 ^{206}Pb cps (Appendix 4.3.4). All nine zircon analyses cluster (discordance ranges from 8.1% to 15.1%) along an discordia line anchored through 0 ± 20 Ma with an upper intercept of 2717.7 ± 7.2 Ma and MSWD of 1.04 (Figure 26a). The mean $^{207}\text{Pb}/^{206}\text{Pb}$ age of these analyses is 2720 ± 11 Ma (MSWD = 2.8) with a roughly bell-shaped distribution that ranges from 2697 ± 17 Ma to 2746 ± 18 Ma (Figure 26b).

Both of these thin sections have small, rounded zircons that have low counts of Pb, which is consistent with a metamorphic origin for these zircons. The calculated ages of 2724.2 ± 9.0 Ma and 2717.7 ± 7.2 Ma for samples 9704-7069a and 9704-7069b, respectively, are interpreted to be ages of metamorphic zircon growth. The ages obtained

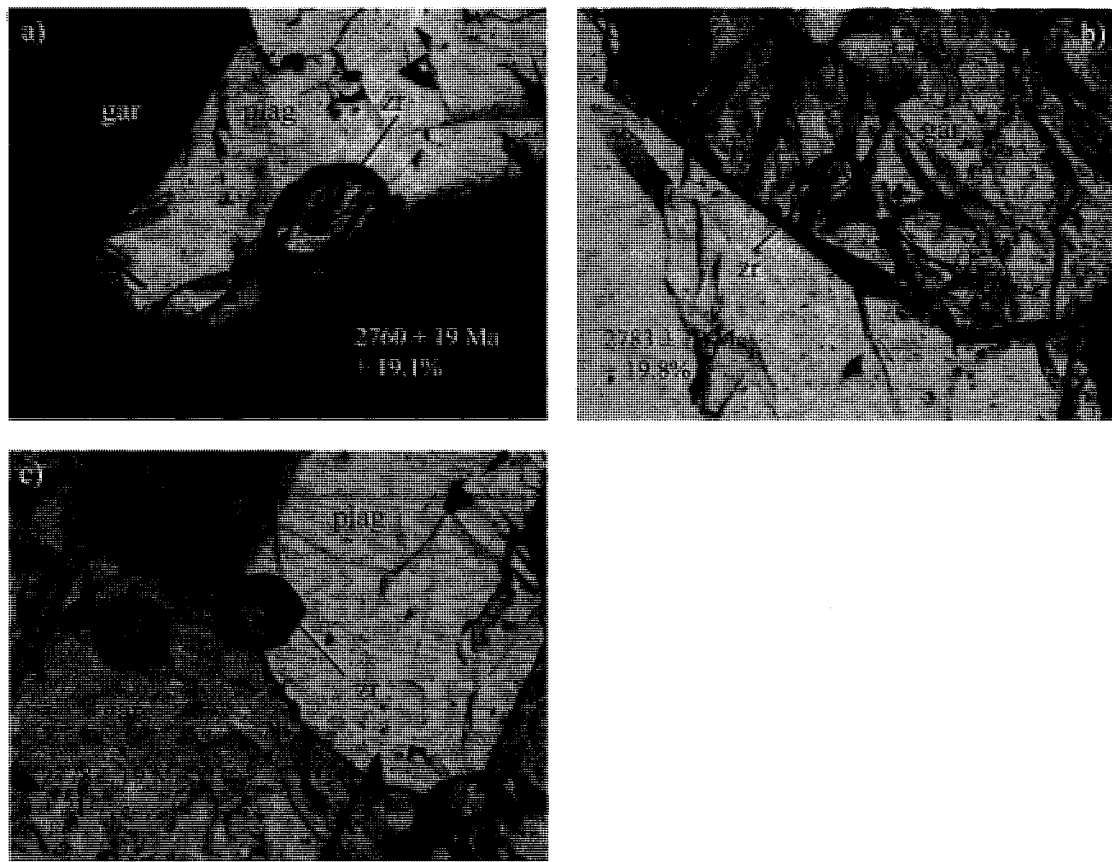


Figure 27: Photomicrographs of zircons analysed by LA-ICP-MS. a) Zircon number 9704-7054-11 included in plagioclase and in contact with garnet (black) in cross polarized light. b) Zircon number 9704-7054-16 included in garnet in plane polarized light. c) Zircon number 9704-7054-13 partially included in garnet in plane polarized light. All displayed ages are $^{207}\text{Pb}/^{206}\text{Pb}$ ages.

9704-7054

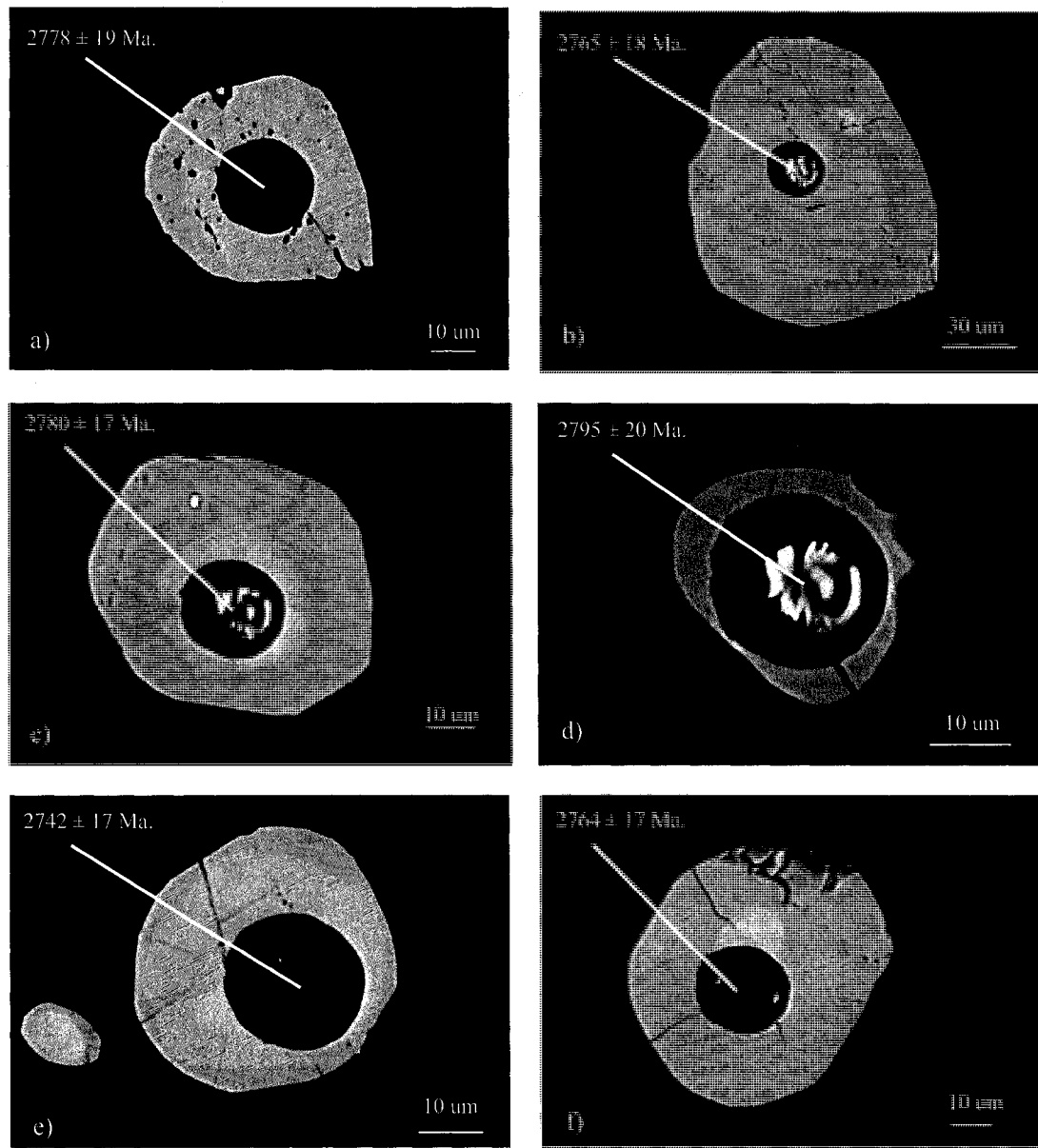


Figure 28: Backscattered electron images of zircons in thin section 9704-7069a with laser pits a) Zircon 9704-7054-22a b) Zircon 9704-7054-20a c) Zircon 9704-7054-17 d) Zircon 9704-7054-16 e) Zircon 9704-7054-3a f) Zircon 9704-7054-3b.

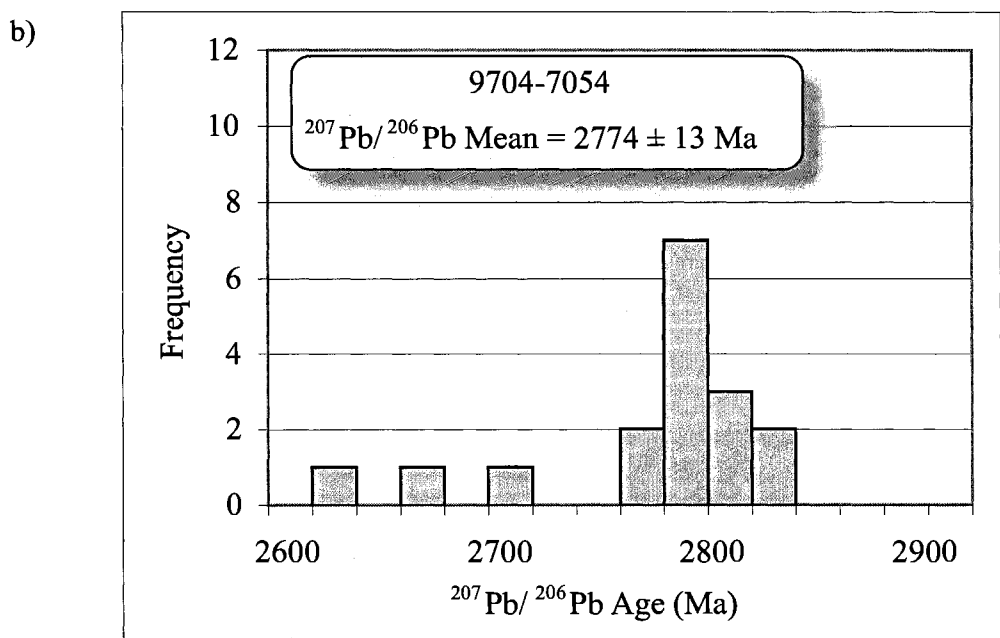
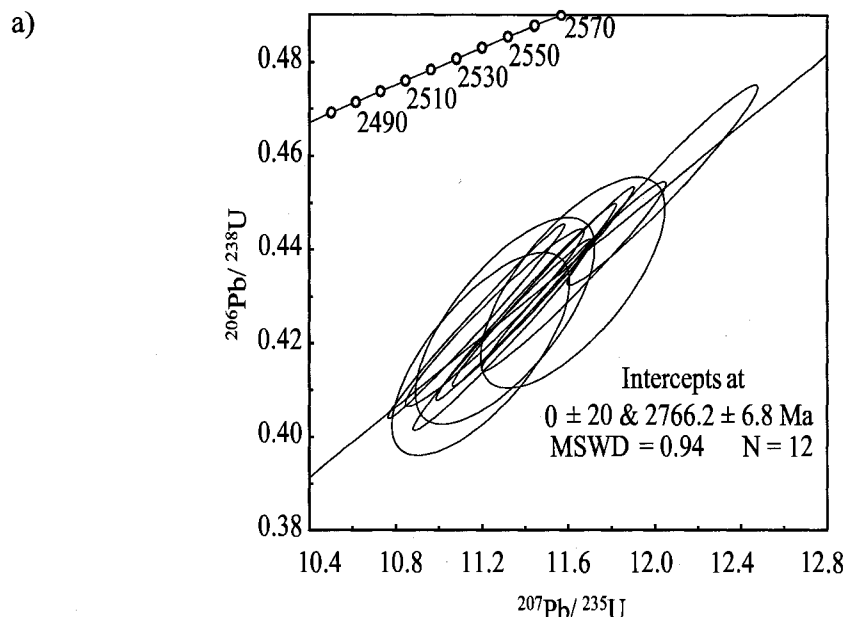


Figure 29: Figure a) is a concordia diagram of LA-ICP-MS analyses from sample 9704-7054 with a corresponding histogram of $^{207}\text{Pb}/^{206}\text{Pb}$ ages in figure b).

from these thin sections do not agree within error of the 2702.3 ± 4.0 Ma age obtained on separated zircon grains from a sample from the same location. This may be due to separate age populations of zircons being analyzed that would produce a scatter of ages not representative of a single event. The disagreement between the two thin sections may also be caused by inaccuracy as a result of the increased significance of the common Pb correction with low Pb samples.

4.5.4.4 Sample 9704-7054

Thin Section

Mafic Granulite –Upper Nelson River

A separate outcrop of mafic granulite (9704-7054) near Birthday Rapids on the Nelson River (Figure 3) was sectioned and seventeen zircons analysed by LA-MC-ICP-MS using a thirty-micron diameter laser beam (Appendix 4.3.5). The average ^{206}Pb signal during analysis was $\sim 45,000$ cps, significantly lower than the other samples analysed by laser ablation. The zircons range in size from thirty to fifty microns and the majority (>60%) are round in shape. Zircon crystals are found as inclusions in phases such as plagioclase (Figure 27a), garnet (Figure 27b), and often near the margins or half-included in garnet porphyroblasts (Figure 27c). Backscatter electron images of the zircons revealed slight irregular zoning but no distinctive internal structure or inclusions (Figure 28). The analyses, when plotted on a concordia diagram (Figure 29a), cluster along a discordia line anchored at a lower intercept of 0 ± 20 Ma with an upper intercept of 2766.2 ± 6.8 Ma (MSWD of 0.94), this is excluding five analyses (3a, 9, 18, 22b, and 22c) that fall outside of the main grouping. The analyses are fairly discordant and range from 14.9% to 22.3%. The distribution of $^{207}\text{Pb}/^{206}\text{Pb}$ ages is broad, with one central peak as shown in the histogram of Figure 29b with a mean $^{207}\text{Pb}/^{206}\text{Pb}$ age, excluding the five analyses from outside of the main cluster, of 2774 ± 13 Ma (MSWD = 5.0). Although these thin section analyses

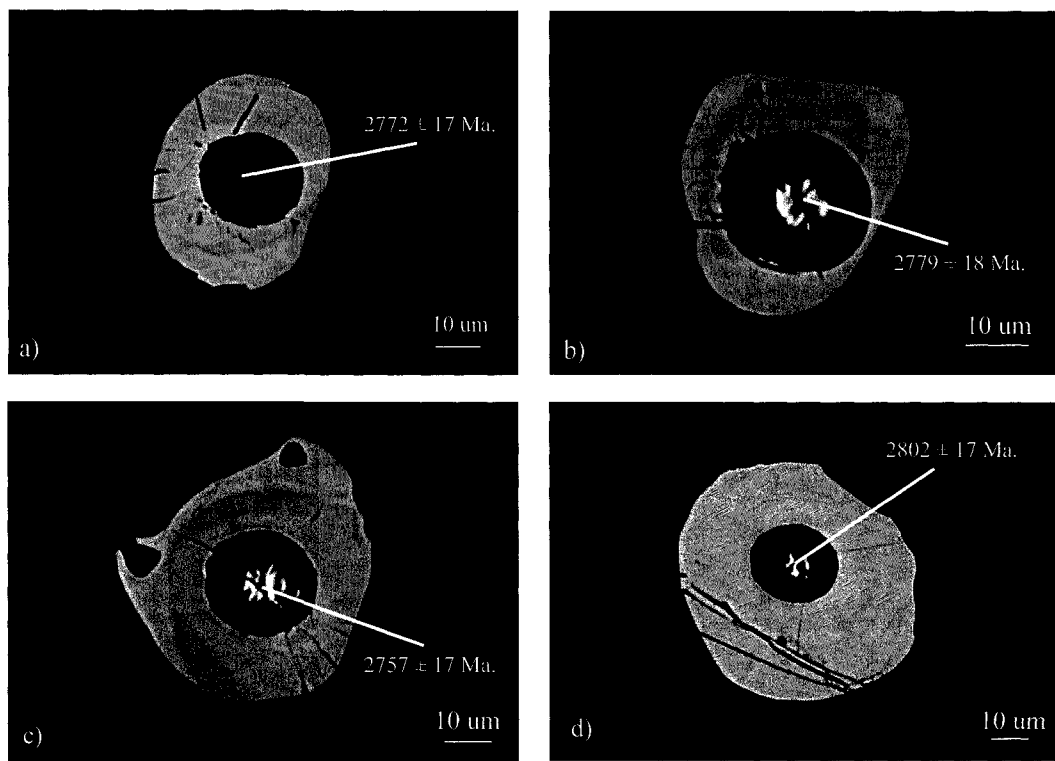


Figure 30: Backscatter electron images of zircons in thin section (GAR01) with laser ablation pits: a) Zircon GAR01-1, b) Zircon Gar01-6, c) Zircon GAR01-8, d) Zircon GAR01-9.

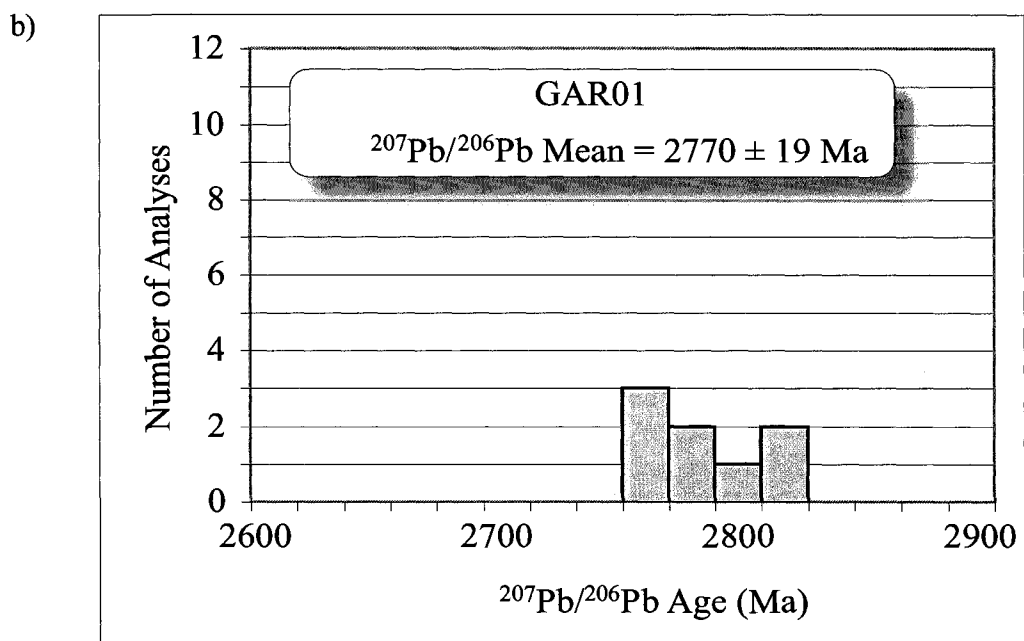
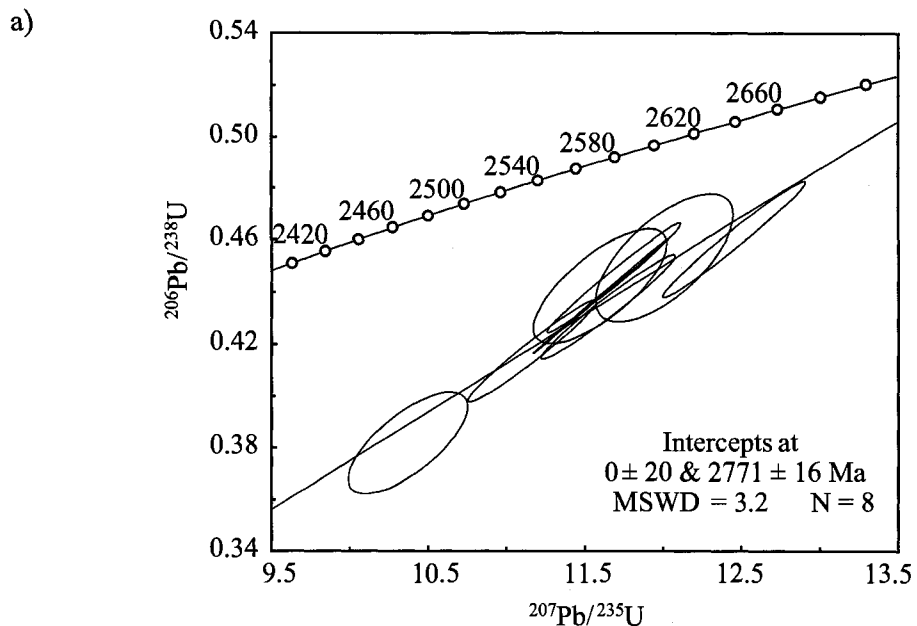


Figure 31: a) A concordia diagram displaying analyses from sample GAR01. All error ellipses are 2σ . b) A histogram displaying $^{207}\text{Pb}/^{206}\text{Pb}$ ages for the same data set in figure a).

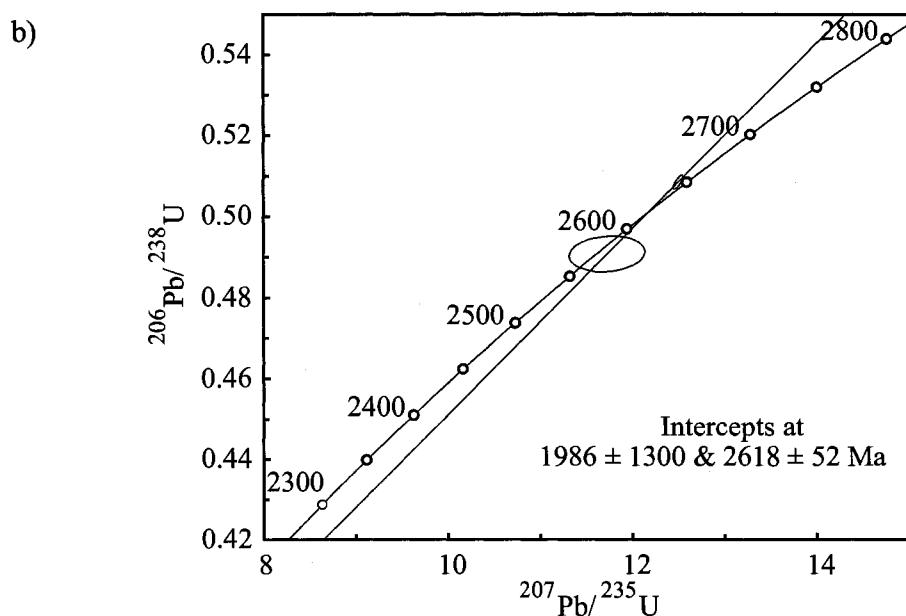
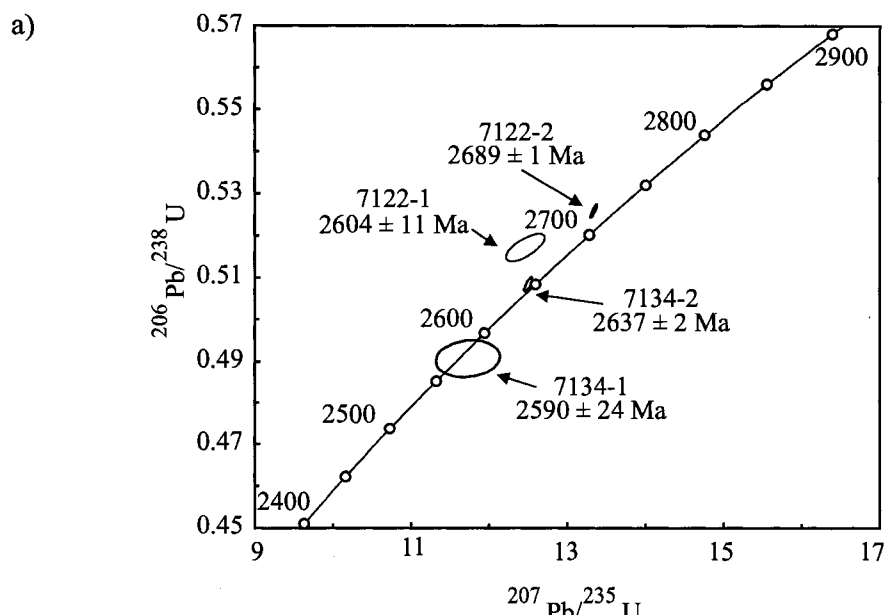


Figure 32: A concordia diagram with TIMS data from samples 9704-7122 and 9704-7134 plotted with corresponding $^{207}\text{Pb}/^{206}\text{Pb}$ ages for each fraction. b) A concordia diagram for fractions 9704-7134-1 and 9704-7134-2. All error ellipses are 2σ .

are highly discordant, the 2766 Ma anchored concordia age indicates the possibility of metamorphic zircon growth in this sample prior to the 2702.3 ± 4.0 Ma event recorded by the nearby sample 9704-7069.

4.5.4.5 Sample GAR01

Thin Sections

Mafic Granulite –Gull Rapids

A sample of mafic granulite from the Gull Rapids field area was selected for in-situ LA-MC-ICP-MS analyses. Eight zircons amenable for analysis by LA-MC-ICP-MS were found in thin section and were analysed with a 30 μm diameter laser (Appendix 4.3.6). The average counts of ^{206}Pb returned for these analyses were 175,000 cps. The morphology of zircons in this sample ranged from round to slightly prismatic and size ranged from thirty to forty microns in the longest direction. Backscattered electron images of the zircons show no oscillatory zonation, mostly weak or no internal structure was visible in the zircons used for analysis (Figure 30). The analyses range from 15.2% to 29.9% discordant and fall on a discordia line anchored at 0 ± 20 Ma that has an upper intercept of 2771 ± 16 Ma and an MSWD of 3.2 (Figure 31a). A histogram of the $^{207}\text{Pb}/^{206}\text{Pb}$ ages yields a roughly bell-shaped pattern with the average weighted $^{207}\text{Pb}/^{206}\text{Pb}$ age being 2770 ± 19 Ma (MSWD = 6.7) (Figure 31b). The zircon grains analysed from this thin section, like the 9704-7054 sample described above, have low Pb ion signals, but the ages for both thin sections agree within error. The concordia age of 2771 ± 16 Ma obtained for sample GAR01 also indicates the possibility of metamorphic zircon growth prior to the 2702.3 ± 4.0 Ma event defined above.

4.5.5. Thermal Ionization Mass Spectrometry

Two samples of mafic granulite, 9704-7134 and 9704-7122, were selected for TIMS analysis in order to obtain precise ages of metamorphism. The results from these

analyses are displayed in Appendix 4.4 and are plotted on a concordia diagram in Figure 32a. All of the zircons analysed had low concentrations of U (25-99 ppm) and radiogenic Pb (13-56 ppm) and the Th/U ratio of these fractions range from 0.231-0.348.

The zircon population of 9704-7134 was dominated by pink zircons that ranged from round to prismatic. Smaller fractions of brown anhedral zircons and clear prismatic zircons were also present. One coloured zircon displayed a pink core with brown tips. The zircons range in size from 50-100 μm in the smallest dimension. Two fractions of zircons were selected for TIMS analysis, the first batch consisting of three colourless abraded zircons (7134-1) and the second of two pink abraded zircons (7134-2). The first fraction yielded a nearly concordant (0.76%) grain with a $^{207}\text{Pb}/^{206}\text{Pb}$ age of 2590 ± 24 Ma. A second analysis from this sample gave a more precise $^{207}\text{Pb}/^{206}\text{Pb}$ age of 2637 ± 2 Ma with a discordance of -0.60%. Both analyses are plotted on the Concordia diagram in Figure 32a and no regression line was calculated due to the low number of data points.

The mineral separates that were obtained from sample 9704-7122 contained a significant amount of titanite, which contrasts sharply with the absence of titanite in sample 9704-7134. The zircon population was dominated by pink and colourless rounded zircons. Two zircons were found with pink cores and brown overgrowths. Two fractions of zircons were selected for TIMS analysis, the first batch containing four light pink abraded zircons and the second, three dark pink abraded zircons. A $^{207}\text{Pb}/^{206}\text{Pb}$ age of 2604 ± 11 Ma (-3.96% discordance) was obtained for the first fraction. The second analysis of sample 9704-7122 yielded a $^{207}\text{Pb}/^{206}\text{Pb}$ age of 2689 ± 1 Ma and was reversely concordant (-1.61%). The analyses for sample 7122 are displayed on the concordia diagram of Figure 32a. A discordia line plotted through these two fractions yields an isochron with an upper intercept of 2618 ± 52 Ma and a lower intercept of 1986 ± 1300 Ma (Figure 32b). This would suggest that the age of metamorphism for this sample is ca. 2618 Ma. These samples are from the central Split Lake Block and are most likely metamorphic zircon, considering their low U and Pb concentrations as well as their morphology. The ages returned by these

samples all suggest ages younger than the 2702.3 ± 4.0 Ma event defined by sample 9704-7069, also from the central Split Lake Block. No hint of an earlier event is suggested by these zircons.

5.0 Discussion

5.1 Tectonothermal History

Split Lake Block

Thermobarometry

The temperatures and pressures obtained for the mafic granulites were fairly consistent and range from 700 to 850°C and 6.5 to 9.1 kbar. The temperature given by the garnet-orthopyroxene Fe-Mg exchange reaction (4) is approximately 50°C less than the temperature given by the garnet-clinopyroxene reaction (3). The discrepancy between the temperatures between equations (3) and (4) is most likely related to the altered nature of the orthopyroxene which is apparent in thin section as well. Retrograde exchange between garnet and orthopyroxene means that equation (4) is not indicative of peak metamorphic conditions. Equation (3) that uses Fe-Mg exchange between garnet and more pristine clinopyroxene is closer to the peak temperatures attained.

Conditions of peak metamorphism recorded by the aluminous granulites gave a temperature estimate of 690 to 940°C and a pressure of 7.5 to 10 kbar. The calculated positions of the GASP equilibrium (equation 10) show some scatter between samples, which may be due to the low anorthite content of the plagioclase and low grossular content of the garnet. Such compositions require long extrapolations from the end-member and therefore provide somewhat less precise results (Koziol and Newton 1988).

The P-T conditions of metamorphism deduced from the thermobarometric calculations are consistent with the field and petrographic observations in the Split Lake Block. Ubiquitous evidence of the attainment of granulite-grade metamorphism in the form of partial melting as well as the presence of orthopyroxene is supported by the clearly

granulite-grade temperatures returned from the thermobarometric calculations.

Sample 9704-7069 returned a range in equilibration conditions from 700 to 750 °C and 6.5 to 8.2 kbar. A second sample of mafic granulite, 9704-7142D showed a range in equilibration temperatures from 810 to 850°C and pressures from 8.4 to 9.1 kbar. These ranges in temperature are reasonable considering that the minimum temperature of formation for orthopyroxene- + clinopyroxene- + plagioclase-bearing assemblages in metabasic rocks is between 800 and 850°C (fluid-absent conditions, Pattison *et al.* 2003).

The range in pressures and temperatures returned by both the mafic and aluminous granulite lithologies of the Split Lake Block are similar to the upper pressure and temperature conditions reported for the Pikwitonei Granulite Domain by other authors (Mezger *et al.* 1989; Patunc and Baer 1986, Arima and Barnett 1984, summarized in Table 2).

5.2 Timing of Events

Initial estimates of the ages of metamorphic events in the Split Lake Block were made using EMPA monazite and revealed four separate episodes of monazite growth with peaks at: 2630, 2680, 2720, and 2800 Ma, most likely representing ages of metamorphism, although the possibility exists that some of these monazite grains are detrital. There appears to be no systematic difference in the chemistry or appearance in backscatter imaging of the different age groups of monazite. Ages determined by EMPA are known to be imprecise and are usually a general guide for determining the age of monazite growth.

The EMPA monazite data suggests that an episode of monazite growth likely related to metamorphism occurred between 2620 and 2640 Ma. A TIMS zircon analysis of 2637 ± 2 Ma (-0.60 % discordant) from a mafic granulite is within the range defined by the EMPA monazite data. Zircon from a feldspathic gneiss feature a number of nearly concordant zircon crystallization ages in the 2620-2640 Ma range that represent an age or age range of intrusions likely related to these episodes of metamorphic zircon and monazite growth in other lithologies. The most similar age reported for the Split Lake Block is ca. 2620 Ma

(Böhm *et al.* 1999) determined from single zircon grains in a tonalite and a granodiorite in the Split Lake Block and is classified as the M₂ metamorphic event described by Corkery (1985). A similar age of 2637 ± 2 Ma is reported for an amphibolite-grade metamorphic event in the Pikwitonei Granulite Domain (Heaman *et al.* 1986b).

The $^{207}\text{Pb}/^{206}\text{Pb}$ ID-TIMS age for one zircon fraction from a sample of mafic granulite (9704-7122) from the Split Lake Block returned an age of 2689 ± 1 Ma (-1.61% discordance). This age falls within the EMPA monazite age range of 2650 to 2700 Ma and is also similar to the ca. 2680 Ma age reported by Downey (2005) as the timing of M_{1b} metamorphism in the Gull Rapids Area; the $2695 +4/-1$ Ma age of metamorphic zircon growth in the Split Lake Block (Böhm *et al.* 1999); and the metamorphic zircon age of 2684 ± 35 Ma (Hartlaub *et al.* 2004) from a metasediment in the Split Lake Block. This age of metamorphism has been classified as the M1b event, representing widespread granulite-grade metamorphism in the Split Lake Block (Böhm *et al.* 1999).

A well-constrained age for the timing of metamorphic zircon growth is the U-Pb LA-MC-ICP-MS zircon age (grain mount) obtained for sample 9704-7069 that returned an age of 2702.3 ± 4.0 Ma. A large number of zircons were analysed (N=97) and most had relatively high Pb signals with negligible common Pb corrections. This age agrees within error of a U-Pb zircon age of 2705 ± 2 Ma from a leucosome in mafic granulite from the central Split Lake Block (Böhm *et al.* 1999).

Two thin sections from the same sample (9704-7069) were analysed by in-situ LA-MC-ICP-MS to confirm this age as well as search for other phases of metamorphic zircon growth. The in situ U-Pb ages for these two sections yielded older upper intercept concordia ages of 2724.2 ± 9 Ma and 2717.7 ± 7.2 Ma that do not agree within error of the age obtained from the grain mount but fit into the range of 2710 to 2740 Ma suggested by the ages of monazite growth. Although the ages determined from the thin sections are nearly within error of the more accurate and precise age obtained from the grain mount, the older age returned from the thin sections may be the suggestion of an older age component

is present in these grains. Ages of metamorphism near 2720 Ma are not uncommon from the northwestern Superior Province. The initiation of the accretion events that brought together the Superior Province are thought to have began as early as 2720 Ma (Percival *et al.* 2006) and an age of metamorphism of 2725 ± 9 Ma reported from Pikwitonei basement exposed in the Thompson Nickel Belt also supports this notion (Machado *et al.* 1990).

Two other samples of aluminous granulite returned LA-MC-ICP-MS U-Pb ages that were significantly older than the metamorphic ages reported for the Northwestern Superior Province. The ages returned were 2766.2 ± 6.8 Ma for a sample from the Split Lake Block (9704-7054) and 2771 ± 16 Ma for a sample from western Gull Rapids (GAR01). Although these ages agree within error of each other, the low amount Pb ion signals measured during analysis may have created an overestimation of the age of these zircons. One way of verifying the treatment of the ^{204}Pb correction for this data set is to compare treated and untreated $^{207}\text{Pb}/^{206}\text{Pb}$ ratios for the standard analyses to the expected ratio returned from the TIMS analysis of the standard. The $^{207}\text{Pb}/^{206}\text{Pb}$ ratio for the standard when using measured ^{204}Pb is less than the expected TIMS $^{207}\text{Pb}/^{206}\text{Pb}$ value by 3.4%. When the appropriate ^{204}Pb correction is applied, the average $^{207}\text{Pb}/^{206}\text{Pb}$ value for the standard is within 1.6% of the expected value. It is also reassuring that there is some agreement in age between these two samples which adds some credibility to this older age of metamorphism.

These older ages may be explained by their location texturally within these samples. The zircons selected for the grain mount were some of the larger (>50 μm in the shortest dimension) crystals so that a larger diameter laser spot size could be used for LA-MC-ICP-MS analysis. The thin sections have a small number of zircons available for analysis so many of the zircons are smaller (<50 μm in the longest dimension) than would have been selected for grain mount analysis. Although the zircons may not have been significantly different in morphology, size may be a division between age populations in the samples from location 9704-7069. The location of these older zircons in relation to other mineral phases is also an important observation. Although these older zircons can be found in a

Table 3

Zircon	Mineral	Age	Error	Discordance
#	included in	(Ma)	(Ma)	(%)
9704-7054-16	Grt	2783	19	19.8
9704-7054-20a	Grt	2750	18	20.2
9704-7054-20b	Grt	2764	20	22.0
9704-7054-3b	Grt	2756	19	14.9
GAR01-2	Grt	2778	19	22.5
GAR01-6	Grt	2759	18	17.9
Average		2765	19	20
9704-7054-11	Half in Grt	2760	19	19.1
9704-7054-13	Half in Grt	2778	19	21.7
9704-7054-17	Half in Grt	2761	17	20.4
9704-7054-22a	Half in Grt	2769	19	20.8
9704-7054-22b	Half in Grt	2616	19	21.4
9704-7069b-1	Half in Grt	2719	17	12.6
Average		2734	18	19
9704-7054-14	Plag	2766	18	20.0
9704-7054-18	Plag	2655	39	15.9
9704-7054-22c	Plag	2796	21	12.0
9704-7054-3a	Plag	2792	22	13.2
9704-7054-5	Plag	2813	21	22.3
9704-7054-6	Plag	2819	18	20.6
9704-7054-9	Plag	2699	22	21.2
9704-7069a-13a	Plag	2508	20	15.4
9704-7069a-3	Plag	2720	17	10.3
9704-7069a-5a	Plag	2737	17	12.3
9704-7069a-5b	Plag	2657	60	10.6
9704-7069a-6a	Plag	2731	17	16.5
9704-7069a-7	Plag	2724	17	14.2
9704-7069a-8	Plag	2743	17	17.3
9704-7069b-3	Plag	2724	17	9.4
9704-7069b-5	Plag	2730	17	11.9
9704-7069b-6a	Plag	2697	17	11.6
9704-7069b-7	Plag	2721	17	9.6
GAR01-10	Plag	2745	17	16.7
GAR01-5	Plag	2803	19	15.5
GAR01-7	Plag	2802	19	29.9
GAR01-9	Plag	2781	17	19.5
Average		2745	21	16

Table 14 continued

Zircon		Mineral	Age included in	Error (Ma)	Discordance (%)
#					
9704-7069a-1		Cpx	2729	17	8.4
9704-7069a-12		Cpx	2712	17	9.3
9704-7069a-13b		Cpx	2695	17	12.0
9704-7069a-6c		Cpx	2685	17	5.2
9704-7069b-4		Cpx	2707	17	8.1
9704-7069b-8		Cpx	2712	18	15.1
9704-7069b-10		Cpx	2746	18	13.9
	Average		2712	17	10
9704-7069a-6b-core	Cpx and Plag		2730	17	14.0
9704-7069a-6b-rim	Cpx and Plag		2722	17	14.3
GAR01-1	Opaque		2760	17	15.2
GAR01-8	Opaque		2745	17	16.1
9704-7069b-6b	Opaque		2728	17	14.7
9704-7069a-10	Qtz		2741	17	17.3
9704-7054-4	Bt		2778	18	19.4

variety of phases, a high proportion of these older zircons are found as inclusions in garnet (Figure 27b, Table 3). On average, the zircon inclusions within garnet have an average $^{207}\text{Pb}/^{206}\text{Pb}$ age of 2765 Ma, while zircons only partially included in garnet or plagioclase have younger average ages of 2734 Ma and 2745 Ma, respectively. Grains included in garnet represent ages of metamorphic zircon growth prior to the granulite grade event that formed the garnet that protected the included zircon from equilibrating during subsequent events.

5.3 Origin of the Orthogneisses

Evidence from this study and others (Böhm *et al.* 1999, Hartlaub *et al.* 2005) has defined the Split Lake Block as a terrane with a basement of ~3.0 Ga granitoid gneisses that were significantly reworked at ~2.7 Ga. The ubiquitous granitoid gneisses of the Split Lake Block have model Nd ages that range from 3.09 to 3.6 Ga (Böhm *et al.* 2000, this study). The U-Pb crystallization ages of samples with Nd analyses (e.g. 9703-6372 and 9703-6247) have similar ages, from 2.85-3.18 Ga (Böhm unpubl. data, Bowerman *et al.* 2004) with evidence for crystallization ages as old as 3.3 Ga (Böhm *et al.* 1999). The range of $\epsilon\text{Nd}_{(2.7\text{Ga})}$ is broad, from -0.8 to -8.0 (Bohm *et al.* 2000, this study) with the majority of samples showing the incorporation of a more evolved component. The majority of the felsic orthogneisses in the Split Lake Block appear to have crystallization ages of 3.1 Ga or younger and likely intruded into even older crust as evidenced by the evolved ϵNd signature and numerous rounded mafic granulite xenoliths.

5.4 Origin of Supracrustal Assemblages

The supracrustal units that are found in the Split Lake Block have related origins and contain information about the crustal evolution of the northwestern Superior Province. Initially, with the lack of age constraints and the apparent cross cutting relationship of the felsic orthogneiss, these units (metasediment, aluminous garnet-bearing granulite, amphibolite,

and mafic granulite) were thought to be older than the felsic orthogneiss (Böhm *et al.* 2003, Bowerman *et al.* 2004). The ambiguous field relationship of the orthogneiss with these other lithologies formed the basis of this relative age determination. Further examination of the supracrustal units has challenged this assumption.

Information on the origin of the mafic units within the orthogneisses can be inferred from the geochemical data gathered. The silica and magnesium content of the mafic rocks classify these units as mafic, not ultramafic, and multi-element diagrams of the data show an evolved signature (Figure 8a and 9) for mafic rocks. The trace-element data are consistent with a volcanic arc tectonic setting and that, to some extent, they are derived from magmas that interacted with continental crust.

The growth of zircon (a silicate mineral) in the silica-poor mafic granulite units is likely controlled by the availability of Zr which can be liberated during the breakdown of amphibole (Fraser *et al.* 1997). Due to the metamorphic source for most of the zircon in the mafic granulites, the oldest age determined from zircon in a mafic granulite is 2766.2 ± 6.8 Ma, represents the oldest age of metamorphism for the Split Lake Block and a minimum age for mafic granulite. Metamorphic zircon ages at ca. 2720 and 2770 Ma have higher errors than the ages returned for the circa 2.7 Ga events but they do suggest unrecognized earlier episodes of metamorphism. All of the ages of metamorphism determined from mafic units are younger than crystallization ages reported for orthogneisses in the Split Lake Block (Böhm *et al.* 1999, Bohm unpubl. data, Bowerman *et al.* 2004, Hartlaub *et al.* 2005). If the intrusion of the orthogneisses occurred after the formation of the mafic lithologies, the thermal event produced by the intrusion of the orthogneisses would likely have been recorded in mafic lithologies by the growth of metamorphic zircon. No evidence for metamorphic zircon with an age similar to the intrusion of the orthogneiss protoliths has been discovered, suggesting that the large exposures of mafic granulite in the Split Lake Block post-date the intrusion of the orthogneisses.

Rare exposures of aluminous granulite are closely associated with mafic granulite in the Split Lake Block. The high proportion of ilmenite and other heavy minerals like garnet and rutile in association with quartz would suggest that the protolith for the aluminous granulite is heavy mineral rich sediment, proximal to a mafic source or iron formation. The zircon population from these aluminous granulites show internal structures and habit of metamorphic zircon ((Schaltegger *et al.* 1999; Vavra *et al.* 1996; Hanchar and Rudnick 1995; Vavra *et al.* 1996, Watson and Liang 1995)), meaning that most of the ages obtained from these zircons are metamorphic ages. The lack of detrital zircons in these aluminous granulites is due to the fact that the protolith of these granulites is sediment from a proximal mafic source that would have very little to no primary zircon. This notion is supported by the fact that interlayering between mafic and aluminous granulite has been observed.

The metasediment of the Split Lake Block ranges in composition from pelitic to psammitic which is a reflection of the range in composition of the sources for these metasediment. The range of SiO_2 , MgO , and FeO concentration in samples of metasediment from the Split Lake Block is a product of the contrasting geochemical composition of the sources of sediment. The paucity of aluminous metamorphic minerals in the metasediments is an indicator of low Al_2O_3 content caused by the large contribution of an Al-poor mafic source. Biotite is a common accessory mineral with the occasional layer of garnet-rich metasediment but no other aluminous metamorphic minerals are present in the metasediment samples. This dominance of mafic input for the metasediment requires a proximal mafic source for these metasediment units. The proximal nature of the mafic granulite and amphibolite units with metasediment in the Split Lake Block as well as the similar deformational history for these units (Downey *et al.* 2005) would suggest that these mafic units are a likely source for mafic component of these sediments.

Constraining the depositional age of metasediment relies on determining oldest crosscutting igneous phase and ages of deformation that have affected the metasediment and the age of the youngest detrital grain. A U-Pb titanite age of 2686.0 ± 2.8 Ma

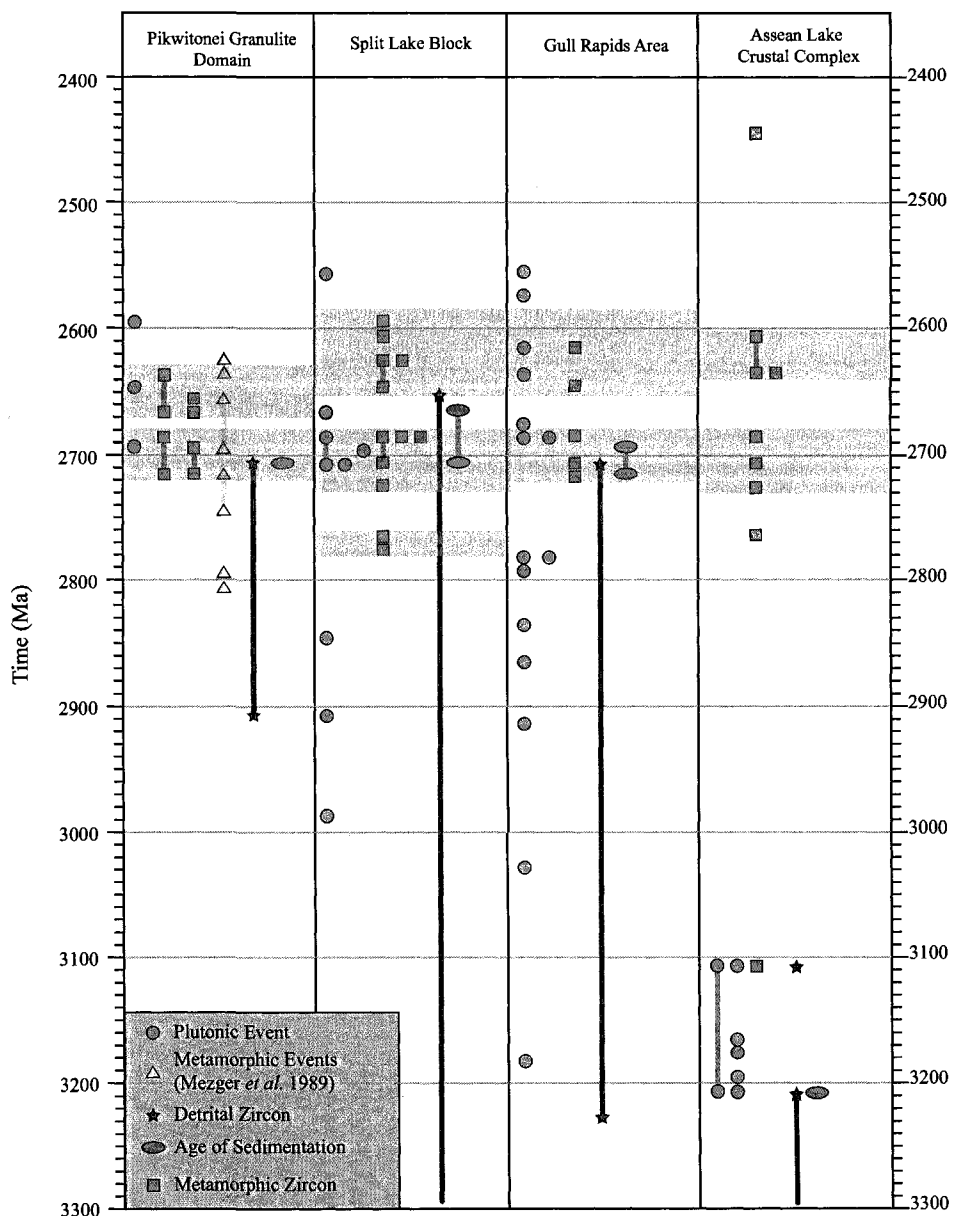


Figure 33: A compilation of known geochronological information from the northwestern Superior Province. Shaded areas span time of proposed metamorphic zircon growth. Data gathered from: Heaman *et al.* 1986, Mezger *et al.* 1989, Bohm *et al.* 1999, Bohm *et al.* 2000, Bohm *et al.* 2003, Bowerman *et al.* 2004, Downey 2005, and Hartlaub *et al.* 2005.

from a pegmatitic granitoid may be the oldest known magmatic phase to cross cut the metasediments in the Gull Rapids area (Downey, 2005). This titanite age post-dates the first phase of deformation (G1) that is known to have affected the metasediments and may represent either an age of magmatic or metamorphic titanite growth (Downey, 2005). The closure temperature of titanite is on average, 600°C (Cherniak 1993), which is below the temperatures predicted for peak metamorphism by this study. The 2686.0 ± 2.8 Ma age returned by these titanite grains is a minimum constraint on the age of peak metamorphism due to the low closure temperature of the titanite. This age of the crosscutting pegmatite is also an approximate minimum age for deposition of the metasediment. The youngest ages of zircon separated from metasediment samples from the Split Lake Block are as young as 2.66 Ga with the youngest concordant grain at ca. 2.70 Ga (Hartlaub *et al.* 2005). The morphology of these grains is not known and therefore the veracity of their detrital origin is suspect. These metasediments are deformed by a number of Neoarchean events (G1 through G5, Downey 2005) and the ages of this metamorphism and deformation are the most reliable constraints on the minimum depositional age of metasediment in the Split Lake Block.

Although it still remains to be proven whether the youngest zircon grains analysed from mafic metasedimentary rocks in the Split Lake Block are detrital or of metamorphic origin, there is an interesting correlation between the ages of older detrital zircons and the ages of igneous rocks in the region. Detrital zircon U-Pb age results from samples in the Birthday Rapids area, central Split Lake Block indicate a range of ages between ca. 2600 to 3800 Ma (Hartlaub *et al.* 2005). The detrital zircon ages between 2700 to 3200 Ma correspond to ages for magmatic events reported in the Gull Rapids area (Downey 2005, Bowerman *et al.* 2004, Böhm unpubl. data) and nearby Split Lake Block (Böhm *et al.* 1999, Hartlaub *et al.* 2005, Bowerman *et al.* 2004, Böhm unpubl. data, Downey 2005, Figure 33).

The geochronology and evidence from field observations suggests that these

mafic units are younger than the surrounding orthogneisses but predate the major episodes of metamorphism at circa 2700 Ma. These units appear to be cross cut by the orthogneiss but the true nature of these contacts is not clear. For example, the metasediment has layers of iron formation that are found as discontinuous boudins, and because of structural shortening are now 2-10 m apart. Knowing the sedimentary nature of the iron formation and the surrounding metasediment precludes the notion that these isolated blocks of iron formation formed prior to the formation of the metasediment. In the same way, these supracrustal units surrounded by orthogneiss may be disarticulated due to deformation after the intrusion of the orthogneiss protoliths rather than rafts in an orthogneiss matrix. These mafic igneous rocks and sediments most likely occurred in a primitive arc environment with limited input from distal sources although those distal sources are the likely origin of the ancient detritus found in the Split Lake Block metasediment.

5.5 Comparison with the Assean Lake Crustal Complex

Evidence for the existence of ancient crust related to the formation of the northwestern Superior Province is found in the form of detrital zircon in metasediment from the Split Lake Block. Detrital zircons from metasediment in the central Split Lake Block vary between 2.65 to 3.8 Ga (Hartlaub *et al* 2005). The source of this old detritus is not known, although the nearby Assean Lake Crustal Complex has detrital zircons as old as 3.9 Ga (Böhm *et al.* 2001) and may have a common source with the Split Lake Block sediment. An ancient source within the Superior Province has not yet been discovered. The oldest units identified in the Split Lake Block are felsic orthogneisses as old as 3.18 Ga (Gull Rapids Area, Bowerman *et al.* 2004, Böhm unpubl. data) while further south in the Winnipeg River and Wabigoon Subprovinces, 3.1-3.3 Ga felsic magmatism has been reported (Davis *et al.* 1988, Corfu 1988). The source of the oldest detritus is from a source that is no longer

exposed or from a terrane separate from the Superior Province.

Although sediment from the Assean Lake Crustal Complex and Split Lake Block features Paleoarchean detritus, the depositional age of Assean Lake sediment has been constrained to ~3.20 Ga (Böhm *et al.* 2003) which is considerably older than the ~2.70 Ga age of sedimentation for Split Lake Block sediment. Overall, the tectonic histories of the two terranes are not alike prior to 2.70 Ga as shown in a compilation of geochronological information for the areas in Figure 33. This contrast is also illustrated by the distinct difference between the predicted ages of crust extraction from the depleted mantle on an ϵ Nd versus Time diagram (Figure 15). The range of ages for the Split Lake Block crust do not overlap with the older ages of depleted mantle extraction for the Assean Lake Crustal Complex inferred from ϵ Nd values calculated for present day and 2.7 Ga. The Assean Lake Crustal Complex has only attained upper-amphibolite-grade metamorphism and therefore was not likely contiguous with the northwestern Superior Province during the ubiquitous episodes of granulite-grade metamorphism ca. 2.70 Ga although the timing of metamorphism between both areas is similar. There are also similarities in the timing of granitoid formation. The 3.1-3.2 Ga intrusion event reported for the Assean Lake Crustal Complex is similar to a crystallization age of 3.18 Ga for granitoids in the Gull Rapids Area. A distinct lack of plutonism in the Assean Lake Crustal Complex post-3.1 Ga contrasts with the abundant ~2.84-2.71 Ga granitoids of the Split Lake Block (Böhm *et al.* 1999). Although they share many characteristics, the Assean Lake Crustal Complex and the Split Lake Block were most likely joined post-2.62 Ga, after which both Assean Lake Crustal Complex and the Split Lake Block share a common tectonic history (Böhm *et al.* 2003).

5.6 Comparison with the Pikwitonei Granulite Domain

The striking physical and geochronological similarities between the Split Lake Block and Pikwitonei Granulite Domain suggest that these two terranes may have a common history or even part of the same terrane (Böhm *et al.* 1999). A compilation of results from this

research and other results from the Split Lake Block has allowed a comparison to be made with the Pikwitonei Granulite Domain (Figure 33). The characteristics of the units of the Split Lake Block and Pikwitonei Granulite Domain are similar, as are their relative proportions and crosscutting relationships.

The history of the formation and metamorphism of these two terranes is quite similar, which is apparent in Figure 33. The tectonothermal history of the Pikwitonei Granulite Domain is marked by a number of episodes of intrusion, sedimentation, and metamorphism in the Neoarchean, not unlike the neighboring Split Lake Block. The similar nature of the basement between these two domains is also illustrated by the overlap between the predicted ages of crust extraction from the depleted mantle on an ϵ Nd versus Time diagram (Figure 15).

A number of episodes of metamorphism have been reported in the Pikwitonei Granulite Domain (Hubregtse 1980; Mezger *et al.* 1989). Two ages of granitoid intrusions most likely related to metamorphism reported by Heaman *et al.* (1986b) at 2695 ± 2 Ma and 2637 ± 2 Ma.

The conditions attained during peak metamorphism in the Pikwitonei are comparable to the conditions attained in the Split Lake Block (Table 2). The narrow range of pressure and temperature of metamorphism defined by the Split Lake Block fits within the conditions of metamorphism reported for the Pikwitonei Granulite Domain, which are summarized in Table 2. Whereas the conditions of metamorphism in the Split Lake Block appear to be fairly consistent throughout, the Pikwitonei Granulite Domain is often referred to as a cross section through the crust (Mezger *et al.* 1990) meaning that the grade of metamorphism increases to the west near the edge of the Superior Province.

The metamorphic history of the Split Lake Block has been split into three discrete metamorphic events by previous researchers (Corkery 1985, Bohm *et al.* 1999) but subsequent studies, including this one, have shown that trying to assign ages to these events is problematic. Although some of the data agrees with the reported ages for metamorphic

events in the Split Lake Block, older and younger ages of metamorphism have been identified by this and other studies (Downey 2005). This abundance of metamorphic ages suggests that either the metamorphism was progressive or a more systematic approach to constraining the age of metamorphism must be applied. The Pikwitonei Granulite Domain faces a similar issue with multiple ages of metamorphism reported by various researchers (Heaman *et al.* 1986b, Heaman *et al.* unpubl. data).

In general, there is overlap between the 2680-2695 Ma and 2620-2640 Ma metamorphic ages reported for the Split Lake Block and Pikwitonei Granulite Domain. More data are needed to fully understand whether these are discrete events that are specific to these two terranes or if they are part of a long-lived metamorphic event.

6.0 Conclusions

- Detailed (1:5000) mapping in the Gull Rapids region identified more lithologic and structural complexity than was previously known.
- The Meso- to Neoarchean basement orthogneiss in the Split Lake Block are the oldest identified units thus far, with younger mafic and metasedimentary units.
- The mafic units from the Split Lake Block are evolved arc magmas and provided mafic detritus for the aluminous garnet-bearing granulites.
- Metasediment in the Split Lake Block is juvenile and most likely deposited in a restricted basin setting with the contemporaneous deposition of iron formation and very little input from distal sediment sources.
- The spread of ages from zircon in a quartz-feldspathic gneiss shows a distribution of ages from 3214 to 2623 Ma. This age distribution represents the age of Split Lake Crust sampled by the intrusion as well as the crystallization age of ~2623 Ma places a minimum constraint on the age of sedimentation of metasediment that it cross-cuts.

- The origin of the ancient detritus found in the Assean Lake Crustal Complex and the Split Lake Block metasediments is not from any currently known units within the Superior Province.
- The ages of metamorphic zircon growth determined from mafic and aluminous garnet-rich granulites in the Split Lake Block:
 - M_{1a} : 2702 Ma
 - M_{1b} : 2680-2695 Ma
 - M_2 : 2620-2640 Ma
- Metamorphic zircon in mafic granulites from the Split Lake Block have older ages that may represent the beginning of the amalgamation of the Superior Province or events prior to that:
 - 2720 Ma
 - 2770 Ma
- The first known pressure and temperature constraints for the Split Lake Block show granulite-grade metamorphic conditions of 8-10 kbar and 750-920°C and are supported by petrographic and field observations.
- Conditions of metamorphism in both the Split Lake Block and nearby Pikwitonei Granulite Domain are similar, although there is more variability in metamorphic grade across the Pikwitonei Granulite Domain.
- A comparison of the results from the Split Lake Block with the Pikwitonei Granulite Domain reveals similar ages of metamorphism at 2695 and 2640 Ma.
- The isotopic results (both U-Pb and Sm-Nd) for the Split Lake Block and the Pikwitonei Granulite Domain show many similarities in ages of crust formation between 2.8-3.1 Ga which contrasts with the Assean Lake Crustal Complex.
- These results suggest that the Split Lake Block and the Pikwitonei

Granulite Domain have a common origin whereas the Assean Lake Crustal Complex is a separate domain with a unique history.

7.0 Future Research

The research presented here has attempted to answer a number of important questions surrounding the formation of the Split Lake Block and its tectonic history. The level of knowledge of the Split Lake Block does allow some conclusions to be made, but many of these questions require further work. For example:

Are the metamorphic events in the Split Lake Block and Pikwitonei Granulite Domain discrete or continuous events?

What are the mechanisms behind the ca. 2700 Ma metamorphic events in Split Lake Block?

What are the timing and cause of exhumation of the Split Lake Block and Pikwitonei Granulite Domain?

Is there additional evidence to suggest that the accretion of the Superior Province began prior to 2.72 Ga?

Can the conditions of individual metamorphic events in the Split Lake Block be directly linked to specific ages of metamorphism?

The amount of geochronological information in the Split Lake Block does not clearly answer the question of whether or not these metamorphic events are discrete or continual. Resolving the timing of closely spaced (<10 Ma) metamorphic events is challenging and requires accurate and precise results. Although LA-MC-ICP-MS allows for fast in situ analyses, the uncertainty for most of the analyses for low-U zircon is greater than the age differences of the events that need to be resolved. The use of LA-MC-ICP-MS to identify separate populations of metamorphic zircon followed by detailed TIMS analyses would be one method to resolve these episodes of zircon growth.

Also, the nature of old metamorphic ages in the Split Lake Block should be investigated. Small zircons, in particular the ones included in garnet, in mafic granulite seem to be producing older ages. A larger sample of these zircons could be analysed by LA-MC-ICP-MS to identify older zircons and a separated fraction could be analysed by TIMS to further delineate this age of metamorphism.

The construction of an accurate P-T-t loop requires clearly linking the timing information with the conditions of metamorphism for multiple events. Petrographic examination alone has not proven an effective method for separating metamorphic episodes. Comparing the trace-element composition of the metamorphic phases and zircons from specific metamorphic events may be a way to link individual events to specific P-T values.

The northwestern Superior Province is a vast area with a complicated tectonothermal history. This complex history creates scientific challenges that make deciphering the nature of the Superior Province difficult but also preserves a number of secrets about the assembly of the Superior Province and Archean tectonics which have yet to be fully explored.

8.0 References

Aranovich, L.Y. and Berman R.G. (1997). A new garnet-orthopyroxene thermometer based on reversed Al_2O_3 solubility in $\text{FeO}-\text{Al}_2\text{O}_3-\text{SiO}_2$ orthopyroxene. *American Mineralogist* **82**, 345-353.

Anovitz, L.M. (1991). Al zoning in pyroxene and plagioclase: window on late prograde to early retrograde P-T paths in granulite terranes. *American Mineralogist* **76**, 1328-1343.

Arima, M and Barnett, R.L. (1984). Sapphirine bearing granulites from the Sipiweesk Lake area of the late Archean Pikwitonei granulite terrain, Manitoba, Canada. *Contributions to Mineralogy and Petrology* **88**, 102-112.

Ashton, K.E., Heaman, L.M., Lewry J.F., Hartlaub, R.P., Shi, R. (1999). Age and origin of the Jan Lake Complex: a glimpse at the buried Archean craton of the Trans Hudson Orogen. *Canadian Journal of Earth Sciences* **36**, 185-208.

Bedard, J.H., Brouillette, P., Madore, L., Berclaz, A. (2003). Archaean cratonization and deformation in the northern Superior Province, Canada; an evaluation of plate tectonic versus vertical tectonic models. *Precambrian Research* **127**, 61-87.

Bell, C.K. (1971). Boundary geology, upper Nelson River area, Manitoba and northwestern Ontario. In *Geoscience studies in Manitoba*. Edited by A.C. Turnock. *Geological Association of Canada, Special Paper* **9**, 11-39.

Berman, B.G. and Aranovich L.Y. (1996). Optimized standard state and solution properties of minerals. *Contributions to Mineralogy and Petrology* **126**, 1-24.
Berman, R.G. and Brown, T.H. (1985) The heat capacity of minerals in the system Na₂O-K₂O-CaO-MgO-FeO-Fe₂O₃-Al₂O₃-SiO₂-TiO₂-H₂O-CO₂: representation, estimation, and high temperature extrapolation. *Contributions to Mineralogy and Petrology* **89**, 168-183.

Berman, R.G. (1988). Internally-consistent thermodynamic data for minerals in the system Na₂O-K₂O-CaO-MgO-FeO-Fe₂O₃-Al₂O₃-SiO₂-TiO₂-H₂O-CO₂. *Journal of Petrology* **29**, 445-522.

Berman, R.G. (1991). Thermobarometry using multi-equilibrium calculations: A new technique, with petrological applications. *Canadian Mineralogist*, **29**, 833-855.

Berman R.G. and Koziol A.M. (1991). Ternary excess properties of grossular-pyrope-

almandine garnet and their influence in geothermobarometry. *American Mineralogist* **76**, 1223-1231

Bickford, M.E., Wooden, J.L., and Bauer R.L. (2006). SHRIMP study of zircons from Early Archean rocks in the Minnesota River Valley: Implications for the tectonic history of the Superior Province. *GSA Bulletin* **118**, 94-108.

Bohlen, S.R., Wall V.J., and Boettcher A.L., (1983) Experimental Investigation and Application of Garnet Granulite Equilibria. *Contributions to Mineralogy and Petrology* **83**, 52-61.

Bohlen, S.R., Wall V.J., and Boettcher A.L., (1983). Experimental investigations and geological applications of equilibria in the system FeO-TiO₂-Al₂O₃-SiO₂-H₂O. *American Mineralogist*, **68**, 1049-1058.

Böhm, C.O., Heaman L.M., and Corkery M.T. (1999). Archean crustal evolution of the northwestern Superior craton margin: U-Pb zircon results from the Split Lake Block. *Canadian Journal of Earth Science* **36**, 1973-1987.

Böhm, C.O., Heaman, L.M., Creaser R.A., Corkery, M.T. (2000). Discovery of pre-3.5 Ga exotic crust at the northwestern Superior Province margin, Manitoba. *Geology* **28**, 75-78.

Böhm, C.O., Heaman, L.M., Stern, R.A., Corkery, M.T., and Creaser, R.A. (2003). Nature of Assean lake ancient crust, Manitoba: a combined SHRIMP-ID-TIMS U-Pb geochronology and Sm-Nd isotope study. *Precambrian Research* **126**, 55-94.

Böhm, C.O., Hartlaub, R.P. and Heaman, L.M. (2007). The Assean Lake complex: ancient crust at the northwestern margin of the Superior craton, Manitoba, Canada. In *Earth's Oldest Rocks*, Edited by M.J. Van Krarkendonk, R.H. Smithies and V.C. Bennett, *Developments in Precambrian Geology*, Vol. 15 (K.C. Condie, Series Editor), Elsevier, Chapter 6.2, p. 751-773.

Bowerman, M.S., Böhm, C.O., Hartlaub R.P., Heaman, L.M., and Creaser, R.A. (2004). Preliminary Isotopic and Geochemical results from the Gull Rapids area of the eastern Split Lake Block, northwestern Superior Province, Manitoba (Parts of NTS 54D5 and 6). *Manitoba Industry, Economic Development, and Mines: Report of Activities*, 156-170.

Bowring, S.A., and Housh, T.B. (1995). The Earth's early evolution. *Science* **269**, 1535-1540.

Bowring, S.A., Williams, I.S., and Compston, W. (1989). 3.96 Ga gneisses from the Slave province, Northwest Territories, Canada. *Geology* **17**, 971-975.

Card, K.D. (1990). A review of the Superior Province of the Canadian Shield, a product of Archean accretion. *Precambrian Research* **48**, 99-156.

Carlson, R.W. and Irving, A.J. (1994). Depletion and Enrichment History of Subcontinental Lithospheric Mantle - an Os, Sr, Nd and Pb Isotopic Study of Ultramafic Xenoliths From the Northwestern Wyoming Craton. *Earth and Planetary Science Letters* **126**, 457-472.

Chacko, T., De, S.K., Creaser, R.A., and Muehlenbachs, K. (2000). Tectonic setting of the Taltson magmatic zone at 1.9-2.0 Ga: a granitoid-based perspective. *Canadian*

Journal of Earth Science **37**, 1597-1609.

Cherniak, D.J. (1993). Lead diffusion in titanite and preliminary results on the effects of radiation damage on Pb transport. *Chemical Geology* **110**, 177-194.

Cocherie, A. and Albarede, F. (2001). An improved U-Th-Pb age calculation for electron microprobe dating of monazite. *Geochimica et Cosmochimica Acta*, **65**, 4509-4522.

Corfu, F. and Stott, G.M. (1993). Age and petrogenesis of two late Archean magmatic suites, Northwestern Superior Province, Canada: Zircon U-Pb and Lu-Hf isotopic relations. *Journal of Petrology* **34**, 817-838.

Corkery, M.T. (1985) Geology of the Lower Nelson River Project Area. Winnipeg, Manitoba, Manitoba Energy and Mines: Geological Services. Geological Report GR82-1. 65p.

Corkery, M.T., Davis, D.W., and Lenton, P.G. (1992). Geochronological constraints on the development of the Cross Lake Greenstone-Belt, Northwest Superior Province, Manitoba: *Canadian Journal of Earth Sciences* **29**, 2171-2185.

Creaser, R.A., Erdmer, P., Stevens, R.A., and Grant, S.L. (1997). Tectonic Affinity of Nisutlin and Anvil Assemblage strata from the Teslin Tectonic Zone, Northern Canadian Cordillera: Constraints From neodymium isotope and geochemical evidence. *Tectonics* **16**, 107-121.

David, J., Parent, M., Stevenson, R., Nadeau, P., and Godin, L. (2003). The Porpoise Cove supracrustal sequence, Inukjuak area: a unique example of Paleoarchean crust

(ca. 3.8 Ga) in the Superior Province. *Geological Association of Canada Conference Proceedings; Vancouver.*

Davis, D.W., Sutcliffe, R.H., and Trowell, N.F. (1988). Geochronological constraints on the tectonic evolution of a late-Archean greenstone belt, Wabigoon subprovince, northwest Ontario, Canada. *Precambrian Research*, **39**, 171-191.

Davis, D., Amelin, Y., Nowell, G.M., and Parrish, R.R. (2005). Hf isotopes in zircon from the western Superior province, Canada: Implications for Archean crustal development and evolution of the depleted mantle reservoir. *Precambrian Research* **140**, 132-156.

de Wit, M.J. (1998). On Archean granites, greenstones, cratons and tectonics: does the evidence demand a verdict? *Precambrian Research* **91**, 181-226.

Downey, M.W. (2005). The Structural Geology, Kinematics and Timing of Deformation at the Superior craton margin, Gull Rapids, Manitoba. M.Sc. Thesis, University of Waterloo. 142 p.

Downey, M.W., Lin, S., and Böhm, C.O. (2004). New insights into the structural geology and timing of deformation at the Superior craton margin, Gull Rapids, Manitoba (NTS 54D6), *Manitoba Industry, Trades, and Mines*, 171-186

Droop, G.T.R. (1987). A general equation for estimating Fe³⁺ concentrations in ferromagnesian silicates and oxides from microprobe analyses, using stoichiometric criteria. *Mineralogical Magazine* **51**, 431-435.

Ermanovics, I.F. and Wanless, R.K. (1983). Isotopic Age studies and tectonic interpretation of Superior Province in Manitoba. *Geological Survey of Canada Paper* **82-**

12.

Fitzsimmons, I.C.W., and Harley, S.L. (1994). The influence of retrograde cation exchange on granulite P-T estimates and a convergence technique for the recovery of peak metamorphic conditions. *Journal of Petrology* **35**, 543-576.

Foster, G., P. Kinny, D. Vance, C. Prince, N., and Harris, (2000). The significance of monazite U-Th-Pb age data in metamorphic assemblages; a combined study of monazite and garnet chronometry. *Earth and Planetary Science Letters* **181**, 327-340.

Fountain, D.M. and Salisbury, M.H. (1996). Seismic properties of rock samples from the Pikwitonei Granulite Belt - God's Lake Domain crustal cross section, Manitoba. *Canadian Journal of Earth Sciences* **33**. 757-768.

Fountain, D.M., M. H. Salisbury, M.H., and Furlong, K.P. (1987). Heat-production and thermal-conductivity of rocks From the Pikwitonei Sachigo continental cross-section, Central Manitoba - implications for the thermal structure of Archean crust. *Canadian Journal of Earth Sciences* **24**, 1583-1594.

Fraser, G., Ellis, D., Eggins, S. (1997). Zirconium abundance in granulite-facies minerals, with implications for zircon geochronology in high-grade rocks. *Geology* **25**, 607-610.

Frost, D. and Chacko T. (1989). The granulite uncertainty principle: limitations on thermobarometry in granulites. *Journal of Geology* **97**, 435-450.

Fuhrman, M.L. and Lindsley, D.H. (1988). Ternary-feldspar modeling and thermometry. *American Mineralogist* **73**, 201-215.

Gromet, L.P., Dymek, R.F., Haskin, L.A., and Korotev, R.L. (1984). The “North American shale composite”; its compilation, major and trace-element characteristics. *Geochimica et Cosmochimica Acta* **48**, 12, 2469-2482.

Goldstein, S.L., O’Nions, R.K. and Hamilton, P.J. (1984) A Sm-Nd study of atmospheric dusts and particulates from major river systems. *Earth and Planetary Science Letters*, **70**, 221–236.

Hanchar J.M. and Rudnick R.L. (1995). Revealing hidden structures: the application of cathodoluminescence and back-scattered electron imaging to dating zircons from lower crustal xenoliths. *Lithos* **36**, 289-303.

Harley S.L. (1989). The origins of granulites: A metamorphic perspective. *Geological Magazine* **126**, 215-247.

Harley, S.L. (1984). An experimental study of the partitioning of Fe and Mg between garnet and orthopyroxene. *Contributions to Mineralogy and Petrology* **86**, 359-373.

Harley, S.L. and Green, D.H. (1982). Garnet-orthopyroxene barometry for granulites and peridotites. *Nature* **300**, 697-701.

Hartlaub, R.P., Böhm, C.O., Heaman, L.M., and Simonetti, A. (2005). Northwestern Superior craton margin, Manitoba: an overview of Archean and Proterozoic episodes of crustal growth, erosion and orogenesis (parts of NTS 54D 64A). *Report of Activities 2005: Manitoba Industry, Economic Development and Mines, Manitoba Geological Survey*, 54-60.

Hartlaub, R.P., Böhm, C.O., Kuiper, Y.D., Bowerman, M.S., and Heaman, L.M. (2004). Archean and Paleoproterozoic geology of the northwestern Split Lake Block, Superior Province, Manitoba (parts of NTS 54D4, 5, 6 and 64A1): *Report of Activities 2004: Manitoba Industry, Economic Development and Mines, Manitoba Geological Survey*, 187-194.

Hartlaub, R.P., Heaman, L.M., Böhm, C.O., and Corkery, M.T. (2003). Split Lake Block revisited: new geological constraints from the Birthday to Gull Rapids corridor of the Lower Nelson River (NTS 54D5 and 6): *Report of Activities 2003: Manitoba Industry, Economic Development and Mines, Manitoba Geological Survey*. 114-117.

Heaman, L.M., Erdmer, E., and Owen, J.V. (2002). U-Pb geochronologic constraints on the crustal evolution of the Long Range Inlier, Newfoundland. *Canadian Journal of Earth Sciences*. **39**, 845–865.

Heaman, L.M., and Corkery, M.T. (1996). U-Pb geochronology of the Split Lake Block, Manitoba; preliminary results. In *Trans-Hudson Orogen Lithoprobe Transect, Sixth Transect Meeting*. Edited by Z. Hajnal and J. F. Lewry. *Lithoprobe Report* **55**, 60-68.

Heaman, L., Machado, N., Krogh, T.E. and Weber, W. (1986). Preliminary U-Pb zircon results from the Pikwitonei granulite domain, Manitoba. In: *Geological Association of Canada-Mineralogical Association of Canada Joint Annual Meeting 1986, Ottawa, Ontario, Program and Abstracts* **11**, 79.

Hoffman, P.F. (1989). Precambrian geology and tectonic history of North America. In AW Bally and AR Palmer (eds), *The Geology of North America*. The Geological Society of

America. p. 447-512.

Hoffman, P.F. (1988). United Plates of America, The Birth of A Craton: Early Proterozoic Assembly and Growth of Laurentia. *Annual Review of Earth and Planetary Science Letters* **16**, 543-603.

Hollings, P., Richardson, A., Creaser, R.A., Franklin, J.M. (2007). Radiogenic isotope characteristics of the Mesoproterozoic intrusive rocks of the Nipigon embayment, northwestern Ontario. *Canadian Journal of Earth Sciences* **44**, 1111-1129.

Hubregtse, J.J.M.W. (1980). The Archean Pikwitonei granulite domain and its position at the margin of the northwestern Superior Province (central Manitoba). *Geological Paper* (Winnipeg), **80-3**, 16 p.

Iizuka, T., Horie, K., Komiya, T., Maruyama, S., Hirata, T., Hidaka, H., and Windley, B.F. (2006). 4.2 Ga zircon xenocryst in an Acasta gneiss from northwestern Canada; evidence for early continental crust. *Geology* **34**, 245-248.

Koziol, A.M. and Newton, R.C. (1988). Redetermination of the anorthite breakdown reaction and improvement of the plagioclase-garnet-Al₂SiO₅-quartz geobarometer. *American Mineralogist* **73**, 216-223.

Kuiper, Y.D., Böhm, C.O., and Lin, S. (2005). Structural geology of the Mystery-Apussigamasi lakes area, Manitoba (parts of NTS 63P13 and 14). *Report of Activities 2005: Manitoba Industry, Economic Development and Mines, Manitoba Geological Survey*, 61-68.

Kuiper, Y.D., Lin, S., Böhm, C.O., and Corkery, M.T. (2004). Structural geology of

Assean Lake, Manitoba (NTS 64A1, 2 and 8). *Report of Activities 2004: Manitoba Industry, Economic Development and Mines, Manitoba Geological Survey*, 95-200.

Kuiper, Y.D., Lin, S., Böhm, C.O., and Corkery, M.T. (2004). Structural geology of the Aiken River deformation zone, Manitoba (NTS 64A1 and 2). *Report of Activities 2004: Manitoba Industry, Economic Development and Mines, Manitoba Geological Survey*, 201-208.

Kuiper, Y.D., Lin, S., Böhm, C.O., and Corkery, M.T. (2003). Structural geology of the Assean Lake and Aiken River deformation zones, northern Manitoba (NTS 64A1,2 and 8). *Report of Activities 2003: Manitoba Industry, Economic Development and Mines, Manitoba Geological Survey*, 105-113.

Lee, H.Y. and Ganguly J. (1988). Equilibrium compositions of coexisting garnet and orthopyroxene: Experimental determinations in the system FeO-MgO-Al₂O₃-SiO₂, and applications. *Journal of Petrology* **29**, 93-113.

Ludwig, K. R. (2003). Isoplot/Ex, a geochronological toolkit for Microsoft Excel, Version 3.00. *Berkeley Geochronology Center Special Publication 4*, Berkeley, California.

Machado, N., Krogh, T.E., and Weber, W. (1990). U-Pb geochronology of basement gneisses in the Thompson Belt (Manitoba) - evidence for pre-Kenoran and Pikwitonei-type crust and early Proterozoic basement reactivation in the western margin of the Archean Superior Province. *Canadian Journal of Earth Sciences* **27**, 794-802.

Mezger, K., Bohlen, S.R., and Hanson, G.N. (1990). Metamorphic history of the Archean Pikwitonei Granulite Domain and the Cross Lake Subprovince, Superior Province,

Manitoba, Canada. *Journal of Petrology* **31**, 483-517.

Mezger, K., Hanson, G.N., and Bohlen S.R. (1989). U-Pb systematics of garnet: dating the growth of garnet in the Late Archean Pikwitonei granulite domain at Cauchon and Natawanhunan Lakes, Manitoba, Canada. *Contributions to Mineralogy and Petrology* **101**, 136-148.

McMullin, D., Berman, R.G., Greenwood, H.J. (1991). Calibration of the SGAM thermobarometer for pelitic rocks using data from phase equilibrium experiments and natural assemblages. *Canadian Mineralogist* **29**, 889-908.

Montel, J.M., Foret, S., Veschambre, M., Nicollat, C., and Provost, A. (1996). Electron microprobe dating of monazite. *Chemical Geology* **131**, 37-53.

Pactunc, A.D. and Baer, A.J. (1986). Geothermobarometry of the northwestern margin of the Superior province: implications for its tectonic evolution. *Journal of Geology* **94**, 381-394.

Pattison, D.R.M., Chacko, T., Farquhar, J., and McFarlane, C.R.M. (2003). Temperatures of granulite-facies metamorphism: Constraints from experimental phase equilibria and thermobarometry corrected for retrograde exchange. *Journal of Petrology* **44**, 867-900.

Pattison, D.R.M. and Newton, R.C. (1989). Reversed experimental calibration of the garnet-clinopyroxene Fe-Mg exchange thermometer. *Contributions to Mineralogy and Petrology* **101**, 87-103.

Pearce, J.A., Harris, N.B.W., and Tindle, A.G., (1984). Trace-element discrimination

diagrams for the tectonic interpretation of granitic rocks. *Journal of Petrology* **25**, 956-983.

Percival, J.A., Sanborn-Barrie, M., Skulski, T., Stott, G.M., Helmstaedt, H., and White, D.J. (2006). Teconic Evolution of the western Superior Province from NATMAP and Lithoprobe studies. *Canadian Journal of Earth Sciences* **43**, 1085-1117.

Perkins, D. (1990). Thermometry and barometry of mafic granulites based on garnet-clinopyroxene-plagioclase-quartz assemblages. *Granulites and Crustal Evolution*, 435-449.

Powell, R. (1985). Geothermometry and geobarometry: a discussion. *Journal of the Geological Society of London* **142**, 29-38.

Powell, R. and Holland, T.J.B. (1988). An internally consistent dataset with uncertainties and correlations: 3. Applications to geobarometry, worked examples and a computer program. *Journal of Metamorphic Geology* **6**, 173-204.

Roser, B.P. and Korsch, R.J. (1988). Provenance signatures of sandstone–mudstone suites determined using discriminant function analysis of major-element data. *Chemical Geology* **67**, 119–139.

Schaltegger, U., Fanning, C.M., Guènther, D., Maurin, J.C., Schulmann, K., and Gebauer, D. (1999). Growth, annealing and recrystallization of zircon and preservation of monazite in high-grade metamorphism: conventional and in-situ U-Pb isotope, cathodoluminescence and microchemical evidence. *Contributions to Mineralogy and Petrology* **134**, 186-201.

Simonetti, A., Heaman, L.M., Hartlaub, R.P., Creaser, R.A., MacHattie, T.G., and Böhm, C. (2005). U-Pb zircon dating by laser ablation-MC-ICP-MS using a new multiple ion counting Faraday collector array. *Journal Analytical Atomic Spectroscopy* **20**, 677-686.

Simonetti, A., Heaman, L. M., Chacko, T., Banerjee, N. R. (2006) In-situ petrographic thin section U-Pb dating of zircon, monazite, and titanite using laser ablation-MC-ICP-MS. *Geological Association of Canada Conference Proceedings; Montreal* **31**, p. 140

Stacey, J.S. and Kramers, J.D. (1975). Approximation of terrestrial lead isotope evolution by a two-stage model. *Earth and Planetary Science Letters* **26**, 207-221.

Sun, S. and McDonough, W.F. (1989). Chemical and isotopic systematics of oceanic basalts; implications for mantle composition and processes. *Geological Society Special Publications* **42**, 313-345.

Suzuki, K., Adachi, M., and Tanaka, T. (1991) Middle Precambrian provenance of Jurassic sandstone in the Mino Terrane, central Japan: Th-U-total Pb evidence from an electron microprobe monazite study. *Sedimentary Geology* **75**, 141-147.

Vry, J.K. and Brown, P.E. (1992). Evidence for early fluid channellization, Pikwitonei granulite domain, Manitoba, Canada. *Canadian Journal of Earth Science* **29**, 1701-1716.

Watson, E.B. and Liang, Y. (1995). A simple model for sector zoning in slowly grown crystals: implications for growth rate and lattice diffusion, with emphasis on accessory minerals in crustal rocks. *American Mineralogist* **80**, 1179-1187.

Weber, W. (1980). The Pikwitonei granulite domain, edge of the Superior Province craton. *EOS Transactions of the American Geophysical Union* **61**, 386-387.

White, D.J., Jones, A.G., Lucas, S.B., and Hajnal, Z. (1999). Tectonic evolution of the Superior boundary zone from coincident seismic reflection and magnetotelluric profiles. *Tectonics* **18**, 430-451.

White, D.J., Lucas, S.B., Hajnal, Z., Green, A.G., Lewry, J.F., Weber, W., Bailes, A.H., Syme, E.C., and Ashton, K. (1994) Paleo-Proterozoic thick-skinned tectonics - lithoprobe seismic- reflection results from the eastern Trans-Hudson Orogen. *Canadian Journal of Earth Sciences* **31**, 458-469.

Appendix 1 - Sample Descriptions and Locations

	97-03- Rock Type	Location	UTMmN northing	UTMmE eastling
6001	Iron Formation	Gull Rapids	6246874	362959
6002	Greywacke	Gull Rapids	6246874	362959
6004	Greywacke	Gull Rapids	6246569	363133
6006	Grey Orthogneiss	Gull Rapids	6246585	363119
6019	Grey Orthogneiss	Gull Rapids	6236689	362643
6020	Granodiorite Gneiss	Gull Rapids	6246689	362575
6027	Diabase	Gull Rapids	6247157	362473
6028	Granodiorite Gneiss	Gull Rapids	6247020	362423
6030	Granodiorite Gneiss	Gull Rapids	6246949	362303
6031	Granodiorite Gneiss	Gull Rapids	6246961	362278
6032	Granodiorite Gneiss	Gull Rapids	6246959	362266
6038	Layered Amphibolite	Gull Rapids	6247347	363387
6041	Granodiorite Gneiss	Gull Rapids	6245878	362121
6044	Granodiorite augen gneiss	Gull Rapids	6245721	362305
6045	Augen granodiorite gneiss	Gull Rapids	6245706	362327
6046	Granodiorite Gneiss	Gull Rapids	6245693	362426
6057	Ampt raft in granod gneiss	Gull Rapids	6245692	362613
6114	Amphibolite raft	Gull Rapids	6246295	360903
6117	Granodiorite Gneiss	Gull Rapids	6246252	361092
6122	Granodiorite Gneiss	Gull Rapids	6246061	361523
6126	Granodiorite Gneiss	Gull Rapids	6245993	361709
6141	Granodiorite Gneiss	Gull Rapids	6245360	362761
6146	Augen Gneiss	Gull Rapids	6245373	362468
6147	Augen Gneiss	Gull Rapids	6245371	362383
6149	Pegmatite	Gull Rapids	6245603	361955
6156	Garnetite	Gull Rapids	6245597	361582
6165	Granodiorite Gneiss	Gull Rapids	6245676	361045
6174	Amphibolite raft	Gull Rapids	6247104	361501
6176	Granodiorite Gneiss	Gull Rapids	6246995	361444
6180	Granodiorite Gneiss	Gull Rapids	6246999	361172
6198	Anorthosite	Gull Rapids	6245275	363819
6212	Greywacke	Gull Rapids	6245724	363158
6214	Straight Gneiss	Gull Rapids	6247063	362507
6219	Layered Amphibolite	Gull Rapids	6247221	362702
6240	Granodiorite Gneiss	Gull Rapids	6245643	360575
6245	Granodiorite Gneiss	Gull Rapids	6245737	360751
6246	Granodiorite Gneiss	Gull Rapids	6245742	360787

97-03- Rock Type		Location	UTMmN northing	UTMmE easting
6247	Hbl-bi granodiorite gneiss	Gull Rapids	6245726	360805
6262	Bi granodiorite gneiss	Gull Rapids	6245700	360823
6265	Granodiorite Gneiss	Gull Rapids	6245680	360907
6269	Leucogranodiorite	Gull Rapids	6245681	361055
6273	Granodiorite Gneiss	Gull Rapids	6245717	361133
6277	Metagreywacke/psammite	Gull Rapids	6247383	364866
6283	Greywacke	Gull Rapids	6246520	363555
6338	Lay tonalite-granodiorite gneiss	Gull Rapids	6245704	362530
6354	Greywacke	Gull Rapids	6245857	363673
6359	Greywacke	Gull Rapids	6245677	363674
6364	Granodiorite augen gneiss	Gull Rapids	6247305	363646
6365	Psammitic metagreywacke	Gull Rapids	6247325	364630
6367	Melt in layered amphibolite	Gull Rapids	6247358	363378
6368	Melt in layered amphibolite	Gull Rapids	6247341	363395
6369	Granodiorite augen gneiss	Gull Rapids	6247340	363676
6371	Biotite gneiss	Gull Rapids	6245453	362645
6372	Augen bi granodiorite gneiss	Gull Rapids	6245451	362665
6373	Grey tonalite	Gull Rapids	6245393	362602
6374	Pyroxene-bearing pegmatite	Gull Rapids	6245480	362660
6387	Young injection phase	Gull Rapids	6246882	362963
6389	Felsic Injection	Gull Rapids	6246893	362975
6390	Greywacke	Gull Rapids	6246891	362977
6391	Amphibolite (mafic volcanics)	Gull Rapids	6246958	362706
6392	Layered granodiorite gneiss	Gull Rapids	6246979	362555
6407	Layered hbl granodiorite gneiss	Gull Rapids	6245989	3617646
6415	Mafic dyke or fragmental	Gull Rapids	6246634	363868
6418	Ultramafic (dyke)	Gull Rapids	6246803	363507
6479	Granite-granodiorite gneiss	Gull Lake	6247789	355697
6590	Grey Tonalite	Gull Rapids	6245704	363008
6590	Grey Tonalite	Gull Rapids	6245704	363008
6591	Leucogranite	Gull Rapids	6245686	363023
6592	Greywacke	Gull Rapids	6245679	363116
8101	Leucogranite	Gull Rapids	6246403	363715
8102	Garnetite	Gull Rapids	6245609	361504
8103	Banded Iron Formation	Gull Rapids	6246884	362955

97-04-	Rock Type	Location	UTMmN	UTMmE
			northing	easting
7000	metagabbro	Ripley's Field	6247268	363240
7004	ultramafic	Ripley's Field	6247312	363199
7008	metagreywacke	Spitzbergen	6246887	362909
7009	greywacke	Spitzbergen	6246876	362966
7009	greywacke	Spitzbergen	6246876	362966
7021	mafic dyke (gabbro)	W end camp island	6246982	362557
7024	mafic dyke (gabbro)	W end camp island	6247123	362555
7038	mafic fragmental	SE camp island	6246663	363850
7044	banded IF	Greenland	6246598	363157
7052	garnet mafic granulite	Nelson River	6243671	333893
7054	garnetite	Nelson River	6244964	337568
7055	mafic xenolith in orthogneiss	Gull Lake	6248376	355166
7057	augen grandiorite gneiss	Gull Lake	6247067	354469
7058	garnet-rich gneiss	Gull Lake	6245725	353331
7066	garnet mafic granulite	Nelson River/Birthday Rapids	6242707	331101
7068	leucogranite	Nelson River	6244616	335263
7069	garnet mafic granulite	Nelson River	6244035	338887
7070	hbl-bearing enderbitite	Nelson River	6243257	339436
7071	greywacke	Maui	6246427	363574
7072	greywacke	Maui	6246394	363649
7074	greywacke	Maui	6246423	363763
7086	garnetite	S-shore	6245605	361569
7090	leucogranite	Nelson River	6244045	344597
7091	mafic granulite	Nelson River	6243915	343951
7092	charnockite	Nelson River	6243744	343338
7093	leucogranite		6243454	340272
7094	granodiorite gneiss	Gull Lake	6242888	352106
7095	tonalite gneiss	Gull Lake	6243497	353703
7109	greywacke	Greenland Is.	6246617	363474
7110	greywacke	Oahu	6245678	363621
7112	greywacke	S-shore	6245438	363831
7120	amphibolite	Nelson River	6248247	355050
7121	mafic Granulite	Nelson River	6244734	336060
7122	garnet mafic granulite	Nelson River	6244551	335051
7125	ultramafic	Ripley's Field	6247318	363202
7128	greywacke	Iceland	6245720	363172
7129	leucogranite	Iceland	6245705	363130
7131	leucosome in amphibolite	North Shore	6247306	363735
7132	amphibolite	North Shore	6247300	363729
7133	greywacke	Spitzbergen	6246856	363006
7134	garnet mafic granulite	Nelson River	6242282	330646

97-04-	Rock Type	Location	UTMmN northing	UTMmE easting
7135	garnet mafic granulite	Nelson River	6236248	316789
7136	greywacke	Nelson River	6236255	316784
7137	garnet mafic granulite	Nelson River	6234022	685470
7138	garnet mafic granulite	Nelson River	6238052	317445
7139	greywacke	Spitzbergen	6246867	363008
7140	mafic clastic	Spitzbergen	6246894	362905
7141	amphibolite Raft	Nelson River	6243575	353507
8153	garnet metapelite	Greenland	6246577	363127
7053A	garnet mafic granulite	Nelson River	6244291	335745
7053B	garnet mafic granulite	Nelson River	6244291	335746
7054B	garnetite	Nelson River	6244967	337625
7056A	banded iron formation	Gull Lake	6248233	355025
7074B	greywacke	Maui	6246423	363763
7088A	metasediment	S-shore, across Hawaii	6245358	363818
7088B	greywacke	S-shore	6245358	363818
7093B	mafic dyke (gabbro)	Nelson River	6243464	340239
7108B	garnetite	S-shore	6245605	361569
7142A	granodiorite gneiss	Nelson River	6245225	337281
7142B	greywacke	Nelson River	6245222	337270
7142C	greywacke	Nelson River	6245222	337270
7142D	garnet mafic granulite	Nelson River	6245222	337270
7143A	amphibolite leucosome	North Shore	6247290	363460
7143B	amphibolite	North Shore	6247304	363456
8151A	garnet metapelite	Greenland	6246581	363157
8151B	megacrystic garnet in quartzite	Greenland	6246581	363157

Appendix 2 - Whole Rock Geochemical Analyses

Appendix 2.1 - Metasediment Whole Rock Geochemistry

Sample	Location	SiO ₂	Al ₂ O ₃	Fe ₂ O ₃	MnO	MgO	CaO	Na ₂ O	K ₂ O	P ₂ O ₅	LOI	Total	Alumina Index
97-04-7060	Gull Rapids	48.34	16.53	15.94	0.20	3.40	9.65	2.56	0.44	1.94	0.13	0.27	99.40
97-04-7088A	Gull Rapids	61.58	15.33	10.56	0.12	3.51	2.84	2.10	1.91	0.58	0.13	1.25	99.91
97-04-7142CS	Split Lake Block	54.64	23.05	9.06	0.10	3.87	1.10	1.15	2.99	1.03	0.03	2.24	99.28
97-04-8151	Gull Rapids	57.97	14.96	13.10	0.14	3.66	2.00	2.77	3.60	0.61	0.11	0.75	99.68
97-04-8153	Gull Rapids	60.54	15.46	10.20	0.12	3.75	2.85	3.02	2.53	0.61	0.13	0.79	99.99
97-04-8167	Gull Rapids	49.48	12.81	15.61	0.23	6.48	10.18	1.92	0.44	1.42	0.12	1.00	99.69
97-04-7143CS	Split Lake Block	69.31	14.40	3.17	0.03	0.93	1.93	3.01	5.23	0.51	0.12	0.99	99.63
97-03-8100B	Gull Rapids	48.94	21.80	9.82	0.05	4.61	0.46	1.19	7.41	1.05	0.10	3.91	99.66
97-03-8100A	Gull Rapids	64.41	14.51	7.43	0.12	2.94	5.09	1.39	1.52	0.52	0.13	1.71	99.84
97-03-4404A2	Gull Rapids	67.68	14.62	6.43	0.07	2.43	2.30	3.34	2.17	0.49	0.09	0.35	100.08
97-03-6277	Gull Rapids	64.01	15.68	6.23	0.07	2.77	3.26	3.22	2.49	0.58	0.18	1.01	99.49
97-04-7008	Gull Rapids	64.23	13.83	10.89	0.11	2.94	2.19	2.39	1.70	0.53	0.09	1.18	100.07
97-03-6359	Gull Rapids	70.59	11.40	7.21	0.09	2.16	2.24	2.64	1.79	0.40	0.07	0.49	99.15
Average		60.13	15.72	9.67	0.11	3.34	3.55	2.36	2.63	0.79	0.11	1.23	99.68
Maximum		70.59	23.05	15.94	0.23	6.48	10.18	3.34	7.41	1.94	0.18	3.91	100.08
Minimum		48.34	11.40	3.17	0.03	0.93	0.46	1.15	0.44	0.40	0.03	0.27	99.15
													1.02

Appendix 2.1 (continued) - Metasediment Whole Rock Geochemistry

Sample	Sc	Be	V	Cr	Co	Ni	Cu	Zn	Ga	Ge	As	Rb	Sr	Y	Zr	Nb	Mo
97-04-7060	36.00	n.d.	368.23	n.d.	41.31	33.00	128.00	110.00	23.18	1.35	n.d.	5.33	139.68	24.76	83.63	4.94	n.d.
97-04-7088A	20.00	1.00	116.44	203.48	23.10	103.00	42.00	82.00	19.72	1.80	n.d.	93.08	198.28	16.78	104.37	7.01	2.00
97-04-7142CS	37.00	n.d.	238.51	241.27	43.09	117.62	108.58	107.21	32.08	1.37	n.d.	99.39	169.25	25.19	133.27	10.20	3.27
97-04-8151	18.00	n.d.	113.41	168.64	22.76	96.00	32.00	78.00	17.43	1.98	n.d.	122.29	170.79	13.11	102.28	5.83	3.00
97-04-8153	20.00	1.00	126.48	207.41	24.82	106.00	55.00	71.00	19.19	1.69	n.d.	111.78	221.61	16.48	113.19	6.94	4.00
97-04-8167	47.00	n.d.	354.52	197.72	48.68	80.00	130.00	102.00	17.37	1.50	n.d.	12.90	82.36	26.18	73.42	4.36	n.d.
97-04-7143CS	4.00	n.d.	39.15	n.d.	7.28	n.d.	22.00	n.d.	16.80	n.d.	n.d.	86.65	152.67	12.05	409.71	11.88	3.00
97-03-8100B	28.00	5.00	218.24	276.65	36.32	155.34	71.80	85.69	28.46	1.20	n.d.	312.92	106.88	25.96	173.92	10.31	n.d.
97-03-8100A	14.00	2.00	85.10	332.41	19.64	100.57	27.08	58.89	16.07	1.58	n.d.	81.70	336.69	13.85	154.82	5.91	3.12
97-03-4404A2	13.00	1.00	85.29	132.47	17.78	73.35	48.60	63.65	14.42	n.d.	n.d.	69.53	352.70	12.23	127.58	4.71	2.90
97-03-6277	15.00	2.00	101.51	179.01	24.67	65.75	51.63	78.31	17.59	n.d.	n.d.	140.20	538.14	11.09	118.34	4.55	n.d.
97-04-7008	15.00	1.00	101.27	185.89	21.86	82.00	41.00	80.00	20.16	n.d.	n.d.	86.74	172.69	13.39	107.33	6.42	3.00
97-03-6359	9.00	1.00	67.18	108.91	14.40	68.22	44.74	48.76	12.03	1.29	n.d.	64.97	167.13	9.96	104.39	3.92	10.74
	21.23	1.75	155.03	203.08	26.59	90.07	61.72	80.46	19.58	1.53	0.00	99.04	216.07	17.00	138.94	6.69	3.89
	47.00	5.00	368.23	332.41	48.68	155.34	130.00	110.00	32.08	1.98	0.00	312.92	538.14	26.18	409.71	11.88	10.74
	4.00	1.00	39.15	108.91	7.28	33.00	22.00	48.76	12.03	1.20	0.00	5.33	82.36	9.96	73.42	3.92	2.00

Appendix 2.1 (continued) - Metasediment Whole Rock Geochemistry

Sample	Ag	In	Sn	Sb	Cs	Ba	La	Ce	Pr	Nd	Sm	Eu	Gd	Tb	Dy	Ho	Er	Tm	Yb	Lu
97-04-7060	n.d.	n.d.	n.d.	n.d.	n.d.	32.13	5.33	14.77	2.08	10.61	3.36	1.37	4.18	0.78	5.04	1.01	3.00	0.46	2.86	0.43
97-04-7088A	n.d.	n.d.	n.d.	3.42	420.47	31.91	63.31	64.5	22.09	4.32	0.94	3.54	0.62	3.47	0.63	1.93	0.29	1.73	0.26	
97-04-7142CS	n.d.	n.d.	n.d.	n.d.	529.88	41.14	77.40	7.91	27.59	5.16	1.49	4.87	0.82	4.85	1.04	3.22	0.48	3.27	0.49	
97-04-8151	n.d.	n.d.	n.d.	1.33	511.72	34.21	64.19	6.59	22.45	4.02	1.05	3.18	0.49	2.57	0.53	1.58	0.24	1.58	0.24	
97-04-8153	n.d.	n.d.	n.d.	2.32	629.50	35.80	67.11	6.77	23.61	4.32	1.12	3.61	0.57	3.19	0.67	2.07	0.31	1.99	0.30	
97-04-8167	n.d.	n.d.	1.86	0.47	39.58	5.57	15.02	2.17	10.35	3.53	1.31	4.67	0.85	5.06	1.11	3.40	0.51	3.24	0.50	
97-04-7143CS	0.70	n.d.	n.d.	n.d.	2450.00	193.33	345.74	33.15	97.89	11.69	1.53	6.28	0.64	2.67	0.48	1.30	0.18	1.28	0.20	
97-03-8100B	0.91	n.d.	2.49	n.d.	5.14	1840.00	53.95	97.59	10.34	38.17	6.94	1.53	5.78	0.91	4.70	0.84	2.67	0.38	2.27	0.36
97-03-8100A	0.69	n.d.	3.32	n.d.	1.18	463.86	27.25	48.86	5.31	20.00	3.69	0.90	2.97	0.44	2.26	0.42	1.36	0.20	1.23	0.21
97-03-4404A2	0.86	n.d.	n.d.	n.d.	1.08	651.24	27.73	50.86	5.64	20.05	3.61	1.03	2.77	0.40	2.19	0.42	1.28	0.19	1.20	0.19
97-03-6277	n.d.	n.d.	n.d.	n.d.	3.21	481.49	32.75	63.63	7.13	26.91	4.90	1.25	3.40	0.47	2.39	0.45	1.35	0.19	1.19	0.18
97-04-7008	n.d.	n.d.	n.d.	n.d.	1.95	301.22	30.68	59.00	5.88	20.36	3.56	0.97	2.92	0.47	2.70	0.53	1.58	0.24	1.46	0.21
97-03-6359	0.58	n.d.	n.d.	n.d.	0.81	392.26	20.91	37.48	4.10	14.14	2.49	0.66	1.99	0.31	1.69	0.34	1.02	0.14	0.97	0.15
	0.75	0.00	2.56	0.00	2.09	672.57	41.58	77.31	7.96	27.25	4.74	1.16	3.86	0.60	3.29	0.65	1.98	0.29	1.87	0.29
	0.91	0.00	3.32	0.00	5.14	2450.00	193.33	345.74	33.15	97.89	11.69	1.53	6.28	0.91	5.06	1.11	3.40	0.51	3.27	0.50
	0.58	0.00	1.86	0.00	0.47	32.13	5.33	14.77	2.08	10.35	2.49	0.66	1.99	0.31	1.69	0.34	1.02	0.14	0.97	0.15

Appendix 2.1 (continued) - Metasediment Whole Rock Geochemistry

Sample	Hf	Ta	W	Tl	Pb	Bi	Th	U
97-04-7060	2.61	0.33	4.47	n.d.	7.00	n.d.	0.40	0.12
97-04-7088A	3.17	0.64	n.d.	0.76	21.00	0.54	12.75	3.63
97-04-7142CS	4.18	0.56	n.d.	0.51	21.13	n.d.	8.67	0.96
97-04-8151	3.17	0.50	n.d.	0.85	31.00	0.45	9.58	1.43
97-04-8153	3.58	0.59	n.d.	0.91	25.00	n.d.	11.79	1.80
97-04-8167	2.44	0.26	n.d.	0.10	5.00	0.18	0.45	0.11
97-04-7143CS	11.11	0.20	n.d.	0.42	17.00	3.52	26.53	0.97
97-03-8100B	4.35	1.10	n.d.	2.16	25.15	n.d.	17.64	4.09
97-03-8100A	3.50	0.44	n.d.	0.63	9.36	n.d.	8.30	2.27
97-03-4404A2	3.29	0.35	n.d.	0.55	20.23	n.d.	10.47	2.00
97-03-6277	3.44	0.33	n.d.	1.73	8.03	n.d.	8.59	2.84
97-04-7008	3.17	0.65	15.54	0.40	23.00	0.41	9.58	2.42
97-03-6359	2.94	0.35	n.d.	0.58	12.59	n.d.	9.10	1.91
	3.92	0.48	10.00	0.80	17.35	1.02	10.30	1.89
	11.11	1.10	15.54	2.16	31.00	3.52	26.53	4.09
	2.44	0.20	4.47	0.10	5.00	0.18	0.40	0.11

Appendix 2.2 - Amphibolite

Sample	Location	SiO ₂	Al ₂ O ₃	Fe ₂ O ₃	MnO	MgO	CaO	Na ₂ O	K ₂ O	P ₂ O ₅	LOI	Total	
97-04-7120	Split Lake Block	47.94	14.53	13.77	0.18	7.34	9.22	3.04	0.71	1.34	0.13	1.77	99.95
97-04-7132	Gull Rapids	47.76	11.64	16.40	0.24	10.03	8.21	2.14	0.84	1.06	0.08	1.68	100.08
97-04-7143B	Split Lake Block	48.92	14.31	12.45	0.19	8.28	10.41	2.57	0.70	0.70	0.06	0.84	99.43
97-03-6391	Gull Rapids	49.62	13.84	13.09	0.18	8.96	7.33	2.37	1.30	0.92	0.09	1.72	99.45
97-04-7141	Split Lake Block	45.62	14.98	13.81	0.21	7.65	11.22	2.67	1.06	1.36	0.11	0.65	99.32
97-03-4499B	Gull Rapids	51.39	12.62	17.10	0.24	3.94	7.92	2.91	1.07	2.11	0.22	0.27	99.80
97-04-2019	Split Lake Block	48.32	13.88	12.97	0.21	8.25	10.80	2.46	0.97	0.72	0.07	1.32	99.97
97-04-2104	Split Lake Block	48.19	16.14	11.39	0.16	7.49	9.60	3.30	1.01	0.63	0.06	1.95	99.91
97-03-6057	Gull Rapids	47.60	14.37	13.73	0.22	7.29	9.42	2.77	1.33	0.96	0.08	1.04	98.83
97-03-4504	Gull Rapids	44.33	11.97	21.60	0.28	4.42	9.49	2.45	0.63	3.24	0.70	0.16	99.30
97-03-2124a	Split Lake Block	48.20	14.29	12.64	0.17	5.95	12.37	2.64	0.17	0.98	0.09	1.51	99.00
97-03-6038	Gull Rapids	47.93	13.22	12.17	0.32	7.57	13.20	2.07	0.61	0.80	0.08	0.74	98.72
97-03-4509B	Gull Rapids	50.16	13.27	11.50	0.22	7.68	10.79	2.78	0.64	0.83	0.08	0.95	98.92
97-03-4274	Gull Rapids	47.77	13.79	16.21	0.23	6.71	9.81	2.60	0.41	1.13	0.10	0.40	99.17
97-04-7000	Gull Rapids	49.50	13.38	15.29	0.21	6.47	9.96	2.81	0.67	1.19	0.12	0.42	100.02
Average		48.22	13.75	14.27	0.22	7.20	9.98	2.64	0.81	1.20	0.14	1.03	99.46
Maximum		51.39	16.14	21.60	0.32	10.03	13.20	3.30	1.33	3.24	0.70	1.95	100.08
Minimum		44.33	11.64	11.39	0.16	3.94	7.33	2.07	0.17	0.63	0.06	0.16	98.72

Appendix 2.2 (continued) - Amphibolite

Sample	Sc	Be	V	Cr	Co	Ni	Cu	Zn	Ga	Ge	As	Rb	Sr	Y	Zr
97-04-7120	40	1.00	319.99	174.34	49.73	104.00	16.00	103.00	20.28	1.68	n.d.	11.22	185.53	26.56	81.00
97-04-7132	30	2.00	237.03	60.62	67.51	135.00	13.00	108.00	15.96	1.66	n.d.	26.81	50.34	16.98	51.85
97-04-7143B	47	n.d.	245.75	240.17	45.35	121.00	54.00	60.00	13.67	1.47	n.d.	15.80	79.84	15.21	34.08
97-03-6391	42	n.d.	280.86	99.03	41.32	42.16	40.76	80.74	14.86	1.31	n.d.	45.42	75.73	25.40	77.02
97-04-7141	44	1.00	339.77	209.33	48.20	111.00	19.00	90.00	19.17	1.89	n.d.	9.56	118.95	22.07	48.31
97-03-4499B	35	1.00	359.19	n.d.	38.93	32.00	51.56	112.98	19.62	1.57	n.d.	10.99	144.00	42.35	184.16
97-04-2019	43	n.d.	253.51	204.04	49.48	90.00	21.00	99.00	15.64	1.85	n.d.	9.11	158.64	18.06	37.19
97-04-2104	35	n.d.	195.07	254.96	42.12	98.00	27.00	88.00	16.00	1.36	n.d.	8.12	279.04	14.38	39.16
97-03-6057	38	3.00	247.85	111.88	48.80	101.15	21.25	106.37	15.77	1.71	n.d.	55.79	123.81	21.36	70.90
97-03-4504	43	2.00	314.51	36.20	42.79	40.12	64.43	138.51	22.50	1.37	n.d.	13.21	136.27	66.93	278.76
97-03-2124a	39	1.00	249.72	241.32	46.62	120.42	16.37	73.55	17.71	2.00	n.d.	1.67	294.56	18.23	62.31
97-03-6038	47	n.d.	244.73	189.91	44.54	49.69	27.08	122.13	14.34	1.46	n.d.	6.78	127.16	17.09	47.17
97-03-4509B	44	n.d.	269.74	129.89	40.51	41.30	32.08	75.42	14.79	1.29	n.d.	14.84	112.88	20.60	64.50
97-03-4274	46	1.00	322.28	146.35	47.01	66.65	80.44	98.51	16.06	1.47	n.d.	6.80	116.34	25.25	63.30
97-04-7000	33	1.00	284.85	111.28	60.69	79.00	85.00	98.00	22.11	1.58	n.d.	9.25	130.28	19.46	74.48
Average	40	1.44	277.66	157.81	47.57	82.10	37.93	96.95	17.23	1.58	0.00	16.36	142.23	24.66	80.95
Maximum	47	3.00	359.19	254.96	67.51	135.00	85.00	138.51	22.50	2.00	0.00	55.79	294.56	66.93	278.76
Minimum	30	1.00	195.07	36.20	38.93	32.00	13.00	60.00	13.67	1.29	0.00	1.67	50.34	14.38	34.08

Appendix 2.2 (continued) - Amphibolite

Sample	Nb	Mo	Ag	In	Sn	Sb	Cs	Ba	La	Ce	Pr	Nd	Sm	Eu	Gd	Tb	Dy
97-04-7120	4.97	n.d.	n.d.	n.d.	3.04	n.d.	95.48	13.64	23.69	3.36	14.13	3.83	1.33	4.69	0.83	5.02	
97-04-7132	3.58	n.d.	n.d.	n.d.	2.69	n.d.	0.78	63.09	6.52	16.16	2.08	9.50	2.74	0.99	3.36	0.56	
97-04-7143B	1.83	n.d.	n.d.	n.d.	1.57	n.d.	0.23	64.78	2.78	7.05	0.96	4.61	1.59	0.66	2.38	0.43	
97-03-6391	3.93	2.84	0.82	n.d.	3.63	n.d.	1.32	170.19	7.04	14.87	1.92	8.84	2.64	0.85	3.39	0.68	
97-04-7141	5.38	n.d.	n.d.	n.d.	2.96	n.d.	n.d.	55.92	7.33	17.22	2.26	10.34	3.26	1.20	4.04	0.71	
97-03-4499B	8.56	n.d.	2.09	n.d.	2.33	3.49	n.d.	157.95	15.60	35.01	4.82	21.04	5.67	1.89	6.82	1.25	
97-04-2019	2.06	n.d.	n.d.	n.d.	n.d.	n.d.	0.24	209.91	4.27	10.16	1.31	6.46	1.91	0.71	2.39	0.48	
97-04-2104	2.18	n.d.	n.d.	n.d.	n.d.	n.d.	n.d.	223.90	5.11	11.26	1.44	6.87	1.90	0.60	2.23	0.43	
97-03-6057	3.31	n.d.	0.83	n.d.	0.91	n.d.	2.05	140.59	4.99	11.75	1.69	7.74	2.42	0.88	3.01	0.57	
97-03-4504	12.49	2.05	2.43	n.d.	1.24	n.d.	0.35	130.44	19.42	46.05	6.67	30.42	8.99	2.97	10.52	1.91	
97-03-2124a	2.45	n.d.	n.d.	n.d.	n.d.	n.d.	n.d.	29.95	4.39	10.59	1.47	7.38	2.39	0.94	2.98	0.57	
97-03-6038	2.25	n.d.	n.d.	n.d.	1.31	n.d.	0.21	39.45	4.52	10.62	1.43	7.04	2.07	0.76	2.57	0.50	
97-03-4509B	3.18	2.45	0.78	n.d.	n.d.	n.d.	0.12	103.57	4.73	10.75	1.51	6.85	2.12	0.75	2.66	0.51	
97-03-4274	3.95	n.d.	1.06	n.d.	1.06	n.d.	0.13	42.59	4.00	10.35	1.58	7.70	2.58	0.93	3.40	0.67	
97-04-7000	4.12	n.d.	n.d.	n.d.	n.d.	n.d.	0.14	125.07	12.48	28.03	3.28	14.60	3.79	1.26	4.13	0.72	
Average	4.28	2.45	1.34	0.00	2.97	3.49	0.56	110.19	7.79	17.57	2.39	10.90	3.19	1.12	3.91	0.72	
Maximum	12.49	2.84	2.43	0.00	9.91	3.49	2.05	223.90	19.42	46.05	6.67	30.42	8.99	2.97	10.52	1.91	
Minimum	1.83	2.05	0.78	0.00	1.06	3.49	0.12	29.95	2.78	7.05	0.96	4.61	1.59	0.60	2.23	0.43	
																2.76	

Appendix 2.2 (continued) - Amphibolite

Sample	Ho	Er	Tm	Yb	Lu	Hf	Ta	W	Tl	Pb	Bi	Th	U
97-04-7120	1.10	3.34	0.52	3.34	0.51	2.55	0.37	n.d.	0.11	12.00	1.81	1.31	0.58
97-04-7132	0.68	1.99	0.28	1.85	0.27	1.69	0.31	0.76	0.22	12.00	6.59	1.36	1.14
97-04-7143B	0.65	1.98	0.30	1.99	0.31	1.21	0.14	1.20	0.17	5.00	8.50	0.39	0.45
97-03-6391	0.80	2.69	0.41	2.58	0.41	2.19	0.23	n.d.	0.38	n.d.	n.d.	1.23	0.42
97-04-7141	0.93	2.79	0.43	2.76	0.42	1.79	0.41	1.16	0.12	9.00	4.22	0.96	0.96
97-03-4499B	1.51	4.73	0.69	4.46	0.69	4.79	0.53	1.83	0.11	n.d.	n.d.	2.03	0.68
97-04-2019	0.71	2.17	0.33	2.11	0.31	1.20	0.13	n.d.	0.08	10.54	0.45	0.21	0.09
97-04-2104	0.58	1.75	0.26	1.61	0.24	1.21	0.14	n.d.	n.d.	6.00	1.14	0.47	0.18
97-03-6057	0.72	2.42	0.37	2.23	0.36	1.92	0.19	1.40	0.44	n.d.	1.27	1.11	0.71
97-03-4504	2.34	7.19	1.06	6.56	1.06	6.74	0.93	0.53	0.11	n.d.	n.d.	1.04	0.49
97-03-2124a	0.78	2.43	0.37	2.31	0.33	1.92	0.15	n.d.	n.d.	9.06	n.d.	0.67	0.26
97-03-6038	0.72	2.25	0.33	2.17	0.33	1.53	0.12	n.d.	0.12	6.00	0.67	0.32	0.10
97-03-4509B	0.67	2.17	0.34	2.08	0.33	1.82	0.18	n.d.	0.13	6.66	n.d.	0.89	0.28
97-03-4274	0.85	2.78	0.42	2.69	0.43	1.84	0.24	n.d.	0.06	n.d.	0.41	0.21	0.18
97-04-7000	0.85	2.45	0.34	2.10	0.30	2.40	0.29	n.d.	0.13	8.00	2.82	1.10	0.35
Average	0.93	2.88	0.43	2.72	0.42	2.32	0.29	1.15	0.17	8.43	2.79	0.89	0.46
Maximum	2.34	7.19	1.06	6.56	1.06	6.74	0.93	1.83	0.44	12.00	8.50	2.03	1.14
Minimum	0.58	1.75	0.26	1.61	0.24	1.20	0.12	0.53	0.06	5.00	0.41	0.21	0.09

Appendix 2.3 - Mafic Granulite

Sample	Location	SiO ₂	Al ₂ O ₃	Fe ₂ O ₃	MnO	MgO	CaO	Na ₂ O	K ₂ O	P ₂ O ₅	LOI	Total	
97-04-7053A	Split Lake Block	49.16	14.35	13.16	0.29	5.19	12.92	2.71	0.37	0.83	0.08	0.54	99.61
97-04-7066	Split Lake Block	62.95	16.18	5.22	0.06	2.46	4.76	1.38	0.56	0.15	1.63	99.90	
97-04-7134	Split Lake Block	48.53	15.67	12.10	0.25	5.49	13.27	2.04	0.49	1.28	0.11	0.67	99.89
97-04-7135	Split Lake Block	45.99	15.23	14.08	0.23	8.63	11.12	1.69	0.63	1.20	0.07	1.17	100.04
97-04-2163	Split Lake Block	48.41	13.67	14.81	0.22	7.80	10.09	2.04	0.40	1.08	0.10	0.80	99.41
97-03-2056	Split Lake Block	50.97	13.85	13.99	0.21	6.17	10.06	2.69	0.35	0.90	0.13	0.80	100.12
97-03-2114a	Split Lake Block	49.36	13.20	13.73	0.22	7.84	12.02	1.97	0.10	0.99	0.09	0.52	100.05
97-03-2151	Split Lake Block	52.45	11.67	18.29	0.29	4.25	5.64	2.46	0.26	1.95	0.23	1.05	98.55
97-03-2159	Split Lake Block	50.64	14.41	12.17	0.19	6.66	8.66	3.16	0.92	0.83	0.09	1.13	98.86
97-04-2172	Split Lake Block	51.72	14.21	12.11	0.20	5.93	11.25	2.17	0.56	0.75	0.13	0.91	99.93
97-04-2253	Split Lake Block	48.58	12.43	13.32	0.21	8.63	12.14	1.76	0.29	0.78	0.08	1.11	99.33
97-04-2378	Split Lake Block	48.07	15.51	13.91	0.18	5.94	8.98	3.11	0.86	1.45	0.67	1.29	99.96
97-04-2416	Split Lake Block	47.46	16.11	13.99	0.16	6.23	9.79	3.01	0.63	1.30	0.27	0.88	99.81
97-04-2224	Split Lake Block	46.07	25.66	6.33	0.08	4.44	14.42	1.87	0.22	0.42	n.d.	0.58	100.10
97-04-7091	Split Lake Block	48.92	14.23	13.99	0.22	6.67	11.13	2.20	0.39	0.87	0.13	1.22	99.95
Average		49.95	15.09	12.75	0.20	6.16	10.42	2.50	0.52	1.01	0.17	0.95	99.70
Maximum		62.95	25.66	18.29	0.29	8.63	14.42	4.56	1.38	1.95	0.67	1.63	100.12
Minimum		45.99	11.67	5.22	0.06	2.46	4.76	1.69	0.10	0.42	0.07	0.52	98.55

Appendix 2.3 - Mafic Granulite (continued)

Sample	Sc	Be	V	Cr	Co	Ni	Cu	Zn	Ga	Ge	As	Rb	Sr	Y	Zr
97-04-7053A	46.00	n.d.	283.58	251.30	52.53	101.00	90.00	86.00	18.24	1.71	n.d.	1.17	90.59	20.30	36.35
97-04-7066	10.00	1.00	87.46	59.30	12.93	42.00	49.00	64.00	19.83	n.d.	8.43	556.40	10.29	134.55	
97-04-7134	45.00	n.d.	320.35	301.00	54.52	197.00	54.00	95.00	18.90	1.41	n.d.	5.82	187.78	26.36	67.18
97-04-7135	45.00	n.d.	310.68	218.05	51.37	119.00	23.00	113.00	18.41	1.64	n.d.	5.47	104.08	24.13	59.69
97-04-2163	50.00	n.d.	309.10	114.81	49.18	45.00	101.00	112.00	17.32	1.61	n.d.	4.46	120.16	22.09	34.39
97-03-2056	43.00	1.00	249.99	0.00	57.12	61.73	234.11	119.82	18.36	1.58	n.d.	2.50	208.77	20.94	69.29
97-03-2114a	46.00	n.d.	254.27	455.82	57.23	105.27	51.39	125.75	15.79	1.39	n.d.	n.d.	120.14	16.53	45.52
97-03-2151	42.00	1.00	317.53	n.d.	40.41	n.d.	49.99	142.65	21.65	1.73	n.d.	1.21	170.04	41.89	161.90
97-03-2159	48.00	2.00	198.78	190.92	44.37	124.29	45.34	102.50	19.65	1.61	n.d.	7.44	187.78	43.02	93.25
97-04-2172	41.00	1.00	239.93	61.07	45.50	59.00	30.00	115.00	19.46	1.58	n.d.	4.73	223.47	24.35	47.78
97-04-2253	34.00	n.d.	216.97	538.01	59.44	123.00	72.00	99.00	18.74	1.84	n.d.	1.30	146.79	17.48	48.09
97-04-2378	25.00	2.00	211.46	134.14	45.14	111.00	86.00	113.00	26.12	1.35	n.d.	4.54	462.53	36.63	291.52
97-04-2416	25.00	1.00	247.20	128.83	49.35	117.00	87.00	104.00	24.73	1.24	n.d.	2.77	601.20	20.19	157.86
97-04-2224	19.00	n.d.	98.10	72.96	25.09	72.00	n.d.	n.d.	17.70	0.82	n.d.	1.29	128.71	6.02	12.61
97-04-7091	43.00	n.d.	274.56	151.26	53.41	106.00	115.00	91.00	18.75	1.20	n.d.	1.57	177.81	25.65	80.83
Average	37.47	1.29	241.33	191.25	46.51	98.81	77.70	105.91	19.58	1.48	0.00	3.76	232.41	23.72	89.39
Maximum	50.00	2.00	320.35	538.01	59.44	197.00	234.11	142.65	26.12	1.84	0.00	8.43	601.20	43.02	291.52
Minimum	10.00	1.00	87.46	0.00	12.93	42.00	23.00	64.00	15.79	0.82	0.00	1.17	90.59	6.02	12.61

Appendix 2.3 - Mafic Granulite (continued)

Sample	Nb	Mo	Ag	In	Sn	Sb	Cs	Ba	La	Ce	Pr	Nd	Sm	Eu	Gd	Tb	Dy	
97-04-7053A	0.91	n.d.	n.d.	n.d.	n.d.	n.d.	n.d.	81.30	1.68	5.08	0.82	4.77	1.86	0.81	2.84	0.58	3.96	
97-04-7066	4.29	n.d.	n.d.	n.d.	n.d.	n.d.	n.d.	435.40	24.51	46.78	4.77	17.77	3.22	0.97	2.66	0.42	2.25	
97-04-7134	4.65	n.d.	n.d.	n.d.	n.d.	n.d.	n.d.	91.60	7.26	17.79	2.38	11.15	3.41	1.23	4.34	0.77	4.85	
97-04-7135	3.61	n.d.	n.d.	n.d.	n.d.	n.d.	n.d.	60.48	6.32	17.59	2.46	11.48	3.49	1.16	4.32	0.76	4.55	
97-04-2163	2.56	n.d.	n.d.	n.d.	n.d.	n.d.	n.d.	0.11	42.78	2.26	8.23	1.38	7.57	2.49	0.92	3.24	0.63	4.14
97-03-2056	4.41	n.d.	n.d.	n.d.	n.d.	n.d.	n.d.	84.70	12.48	30.37	4.06	17.74	4.17	1.06	4.30	0.76	4.48	
97-03-2114a	2.44	n.d.	n.d.	n.d.	1.19	n.d.	0.11	47.22	3.45	9.74	1.48	7.42	2.37	0.86	2.87	0.57	3.56	
97-03-2151	9.39	n.d.	n.d.	n.d.	1.29	n.d.	n.d.	81.30	10.92	28.37	4.13	20.49	6.17	1.91	7.27	1.44	8.81	
97-03-2159	7.57	n.d.	n.d.	1.59	n.d.	n.d.	n.d.	230.43	26.36	61.83	8.11	34.46	8.18	1.66	8.20	1.54	9.04	
97-04-2172	4.06	n.d.	n.d.	n.d.	n.d.	n.d.	n.d.	0.13	96.92	9.31	23.91	3.08	13.61	3.40	0.99	3.63	0.69	4.37
97-04-2253	2.66	n.d.	n.d.	n.d.	n.d.	n.d.	n.d.	75.26	8.37	20.62	2.56	10.78	2.72	0.94	3.13	0.53	3.17	
97-04-2378	11.33	n.d.	n.d.	1.66	n.d.	0.23	340.69	75.53	165.95	18.28	67.17	11.07	2.44	9.18	1.41	6.97		
97-04-2416	6.02	2.00	n.d.	1.15	n.d.	n.d.	n.d.	277.06	32.32	70.83	8.12	31.20	5.46	1.71	4.67	0.74	3.79	
97-04-2224	1.35	n.d.	n.d.	n.d.	n.d.	n.d.	n.d.	14.95	1.34	2.61	0.35	1.69	0.53	0.49	0.75	0.17	1.13	
97-04-7091	4.13	n.d.	n.d.	n.d.	n.d.	n.d.	n.d.	66.72	9.43	25.90	3.34	14.19	3.58	1.10	4.06	0.80	4.86	
Average	4.63	2.00	0.00	1.38	0.00	0.15	135.12	15.44	35.71	4.35	18.10	4.14	1.22	4.36	0.79	4.66		
Maximum	11.33	2.00	0.00	1.66	0.00	0.23	435.40	75.53	165.95	18.28	67.17	11.07	2.44	9.18	1.54	9.04		
Minimum	0.91	2.00	0.00	1.15	0.00	0.11	14.95	1.34	2.61	0.35	1.69	0.53	0.49	0.75	0.17	1.13		

Appendix 2.3 - Mafic Granulite (continued)

Sample	Ho	Er	Tm	Yb	Lu	Hf	Ta	W	Tl	Pb	Bi	Th	U
97-04-7053A	0.83	2.62	0.42	2.62	0.38	1.27	0.03	n.d.	7.00	0.46	0.08	0.04	
97-04-7066	0.42	1.23	0.17	1.02	0.14	3.51	0.17	n.d.	0.12	13.00	0.61	0.21	0.14
97-04-7134	1.07	3.27	0.50	3.28	0.49	2.12	0.30	n.d.	0.08	6.00	n.d.	0.14	0.05
97-04-7135	1.00	3.05	0.47	2.98	0.45	2.06	0.21	n.d.	0.06	8.00	0.44	0.39	0.13
97-04-2163	0.89	2.70	0.39	2.50	0.39	1.30	0.11	n.d.	n.d.	0.97	n.d.	0.05	
97-03-2056	0.91	2.80	0.42	2.62	0.38	2.17	0.19	n.d.	8.99	n.d.	0.42	0.08	
97-03-2114a	0.72	2.19	0.32	2.00	0.29	1.57	0.14	n.d.	n.d.	n.d.	0.06	0.02	
97-03-2151	1.83	5.57	0.82	5.23	0.77	4.78	0.58	n.d.	n.d.	6.17	n.d.	0.15	0.11
97-03-2159	1.85	5.62	0.82	4.93	0.71	2.76	0.35	n.d.	0.07	6.42	n.d.	0.74	0.27
97-04-2172	0.92	2.81	0.41	2.64	0.39	1.74	0.25	n.d.	0.07	n.d.	1.58	0.09	0.42
97-04-2253	0.66	1.90	0.28	1.75	0.24	1.67	0.14	n.d.	n.d.	0.34	0.12	0.02	
97-04-2378	1.33	4.04	0.57	3.49	0.50	7.42	0.47	0.51	n.d.	5.00	n.d.	1.22	0.14
97-04-2416	0.74	2.14	0.29	1.88	0.27	3.91	0.24	n.d.	n.d.	n.d.	0.17	0.04	
97-04-2224	0.24	0.74	0.11	0.75	0.11	0.36	0.07	1.21	n.d.	n.d.	0.16	0.04	
97-04-7091	0.98	3.11	0.48	2.90	0.42	2.36	0.20	0.53	n.d.	6.00	0.23	0.11	0.05
Average	0.96	2.92	0.43	2.71	0.40	2.60	0.23	0.75	0.08	7.40	0.66	0.29	0.11
Maximum	1.85	5.62	0.82	5.23	0.77	7.42	0.58	1.21	0.12	13.00	1.58	1.22	0.42
Minimum	0.24	0.74	0.11	0.75	0.11	0.36	0.03	0.51	0.06	5.00	0.23	0.06	0.02

Appendix 2.4- Aluminous Garnet-bearing Granulite

Sample	Location	SiO ₂	Al ₂ O ₃	Fe ₂ O ₃	MnO	MgO	CaO	Na ₂ O	K ₂ O	TiO ₂	P ₂ O ₅	LOI	Total	Alumina Index
97-04-7054	Split Lake Block	55.67	10.91	25.31	0.36	2.56	3.73	0.15	0.11	2.10	0.30	n.d.	99.96	2.73
97-04-7054B	Split Lake Block	72.50	15.48	1.45	0.01	0.46	2.58	5.07	2.04	0.14	0.06	0.21	100.00	1.60
97-04-7086	Gull Rapids	51.59	18.11	22.42	0.32	3.04	2.30	1.46	0.49	1.76	0.24	1.58	100.16	4.26
97-03-4098A	Gull Rapids	53.60	17.25	20.99	0.30	2.98	2.37	1.65	0.50	1.61	0.22	n.d.	100.10	3.82
Average		58.34	15.44	17.54	0.25	2.26	2.75	2.08	0.79	1.40	0.21	0.89	100.06	3.10
Maximum		72.50	18.11	25.31	0.36	3.04	3.73	5.07	2.04	2.10	0.30	1.58	100.16	4.26
Minimum		51.59	10.91	1.45	0.01	0.46	2.30	0.15	0.11	0.14	0.06	0.21	99.96	1.60

Appendix 2.4 - Aluminous Garnet-bearing Granulite (continued)

Sample	Sc	Be	V	Cr	Co	Ni	Cu	Zn	Ga	Ge	As	Rb	Sr	Y
97-04-7054	45.00	n.d.	26.95	25.66	38.25	n.d.	11.00	115.00	22.55	1.81	n.d.	n.d.	4.26	71.10
97-04-7054B	n.d.	n.d.	11.77	n.d.	3.02	n.d.	23.00	n.d.	20.36	n.d.	n.d.	29.47	514.17	n.d.
97-04-7086	42.00	n.d.	347.30	161.95	61.32	108.00	75.00	123.00	16.37	0.84	n.d.	7.52	33.69	24.88
97-03-4098A	37.00	n.d.	288.86	132.61	57.56	97.31	66.17	118.87	14.20	n.d.	n.d.	8.70	49.19	24.76
Average	41.33	0.00	168.72	106.74	40.04	102.66	43.79	118.96	18.37	1.32	0.00	15.23	150.33	40.25
Maximum	45.00	0.00	347.30	161.95	61.32	108.00	75.00	123.00	22.55	1.81	0.00	29.47	514.17	71.10
Minimum	37.00	0.00	11.77	25.66	3.02	97.31	11.00	115.00	14.20	0.84	0.00	7.52	4.26	24.76

Appendix 2.4- Aluminous Garnet-bearing Granulite (continued)

Sample	Zr	Nb	Mo	Ag	In	Sn	Sb	Cs	Ba	La	Ce	Pr	Nd	Sm	Eu	Gd	Tb
97-04-7054	186.33	11.99	n.d.	0.12	n.d.	n.d.	8.64	5.79	19.75	3.28	20.62	8.28	2.79	11.87	2.32		
97-04-7054B	75.65	n.d.	2.00	n.d.	n.d.	n.d.	n.d.	1220.00	10.14	14.65	1.23	3.98	0.54	0.47	0.27	n.d.	
97-04-7086	110.45	8.96	2.00	n.d.	n.d.	n.d.	0.16	92.91	20.94	45.83	5.20	21.20	4.69	1.80	5.16	0.92	
97-03-4098A	112.60	7.77	n.d.	1.66	n.d.	1.24	n.d.	n.d.	107.83	19.93	40.86	5.07	20.15	4.52	1.66	4.69	0.79
Average	121.26	9.58	2.00	1.66	0.12	1.24	0.00	0.16	357.35	14.20	30.27	3.70	16.48	4.51	1.68	5.50	1.34
Maximum	186.33	11.99	2.00	1.66	0.12	1.24	0.00	0.16	1220.00	20.94	45.83	5.20	21.20	8.28	2.79	11.87	2.32
Minimum	75.65	7.77	2.00	1.66	0.12	1.24	0.00	0.16	8.64	5.79	14.65	1.23	3.98	0.54	0.47	0.27	0.79

Appendix 2.4- Aluminous Garnet-bearing Granulite (continued)

Sample	Dy	Ho	Er	Tm	Yb	Lu	Hf	Ta	W	Tl	Pb	Bi	Th	U
97-04-7054	14.79	3.06	9.50	1.44	8.96	1.32	6.01	0.64	0.65	n.d.	6.00	0.24	0.09	0.08
97-04-7054B	0.15	n.d.	n.d.	n.d.	n.d.	n.d.	2.05	n.d.	1.19	0.17	18.00	n.d.	n.d.	0.14
97-04-7086	5.22	1.01	2.99	0.45	2.64	0.38	3.22	0.61	0.00	0.08	9.00	0.37	2.45	0.60
97-03-4098A	4.61	0.91	2.78	0.40	2.49	0.38	2.96	0.54	0.00	0.15	n.d.	n.d.	2.57	0.56
Average	6.19	1.66	5.09	0.76	4.70	0.70	3.56	0.59	0.46	0.13	11.00	0.31	1.70	0.35
Maximum	14.79	3.06	9.50	1.44	8.96	1.32	6.01	0.64	1.19	0.17	18.00	0.37	2.57	0.60
Minimum	0.15	0.91	2.78	0.40	2.49	0.38	2.05	0.54	0.00	0.08	6.00	0.24	0.09	0.08

Appendix 2.5 - Orthogneiss

Sample	Location	SiO ₂	Al ₂ O ₃	Fe ₂ O ₃	MnO	CaO	Na ₂ O	K ₂ O	P ₂ O ₅	LOI	Total
97-03-6372	Gull Rapids	68.10	13.62	5.20	0.10	1.10	3.09	2.97	3.76	0.78	0.27
97-04-7057	Split Lake Block	61.25	14.71	8.47	0.15	1.87	5.32	3.60	2.58	1.34	0.50
97-03-6262	Gull Rapids	71.11	14.64	2.58	0.03	0.75	2.88	4.01	2.68	0.28	0.09
97-03-6371	Gull Rapids	47.88	11.90	17.98	0.24	4.92	9.04	2.78	0.96	2.77	0.44
97-03-2057	Split Lake Block	73.76	13.67	1.63	0.02	0.38	1.76	2.65	4.94	0.41	0.11
97-04-7092	Split Lake Block	72.24	16.43	0.32	n.d.	0.03	3.00	4.61	2.86	0.02	0.02
97-03-6479	Split Lake Block	68.03	15.44	4.40	0.05	1.29	3.71	4.02	1.71	0.52	0.19
97-03-2033	Split Lake Block	69.55	14.94	3.71	0.04	0.99	2.81	3.37	3.31	0.43	0.15
97-03-2053	Split Lake Block	62.61	16.17	5.59	0.07	2.91	6.53	4.37	0.60	0.43	0.12
97-04-7070	Split Lake Block	53.47	23.05	4.41	0.05	2.92	9.61	4.06	0.85	0.28	0.03
97-04-7058	Split Lake Block	62.73	13.88	10.07	0.25	3.96	1.60	2.29	2.03	0.80	0.03
97-03-2121	Split Lake Block	69.71	14.86	3.86	0.04	1.00	3.41	3.77	2.12	0.45	0.15
97-03-2169	Split Lake Block	65.44	14.62	4.86	0.10	2.72	3.71	3.54	1.00	0.38	0.08
97-04-2302	Split Lake Block	62.46	16.98	5.43	0.08	2.95	6.62	3.59	0.67	0.43	0.13
97-03-6044	Gull Rapids	71.82	14.11	2.16	0.02	0.71	1.60	3.66	4.22	0.26	0.09
97-03-6369	Gull Rapids	66.11	15.57	5.26	0.07	1.39	3.48	4.27	1.69	0.56	0.11
97-03-4041	Gull Rapids	72.66	13.63	1.90	0.02	0.55	1.72	3.17	4.38	0.27	0.06
97-03-6247	Gull Rapids	72.09	14.03	2.02	0.02	0.55	2.37	3.69	3.33	0.26	0.08
97-03-6338	Gull Rapids	74.66	13.37	1.30	0.02	0.36	1.20	4.06	3.80	0.12	0.04
97-03-4499A	Gull Rapids	68.95	13.55	5.04	0.07	1.09	2.74	3.14	3.41	0.69	0.21
97-03-6392	Gull Rapids	73.27	14.07	1.65	0.02	0.38	1.53	3.44	4.67	0.15	0.04
97-03-6407	Gull Rapids	66.75	15.31	4.39	0.05	1.26	3.41	3.89	2.72	0.50	0.16
97-03-4043	Gull Rapids	68.81	14.72	3.78	0.05	1.04	3.04	3.83	2.40	0.39	0.13
97-04-7094	Split Lake Block	69.39	15.09	3.59	0.03	1.01	2.90	3.83	3.01	0.38	0.12
97-04-7142A	Split Lake Block	69.92	16.24	1.98	0.02	0.68	2.76	5.54	1.83	0.20	0.11
97-04-7095	Split Lake Block	63.39	17.25	5.04	0.08	2.29	5.33	4.50	1.19	0.47	0.11
Average		67.16	15.07	4.49	0.07	1.50	3.66	3.72	2.57	0.52	0.14
Maximum		74.66	23.05	17.98	0.25	4.92	9.61	5.54	4.94	2.77	0.50
Minimum		47.88	11.90	0.32	0.02	0.03	1.20	2.29	0.60	0.02	0.22

Appendix 2.5 - Orthogneiss (continued)

Sample	Alumina Index	Sc	Be	V	Cr	Co	Ni	Cu	Zn	Ga	Ge	As	Rb
97-03-6372G	1.39	8.00	2.00	44.84	n.d.	6.43	n.d.	17.97	58.05	15.62	1.02	n.d.	67.79
97-04-7057S	1.28	15.00	2.00	85.75	n.d.	13.46	n.d.	22.00	109.00	22.31	1.27	n.d.	33.94
97-03-6262G	1.53	3.00	2.00	21.77	n.d.	3.94	n.d.	10.34	44.64	15.32	n.d.	n.d.	42.03
97-03-6371G	0.93	43.00	2.00	422.95	55.13	43.19	53.79	53.75	108.61	19.35	1.48	n.d.	13.37
97-03-2057S	1.46	1.00	1.00	53.72	n.d.	2.84	n.d.	n.d.	n.d.	14.52	n.d.	n.d.	84.59
97-04-7092S	1.57	n.d.	1.00	n.d.	n.d.	n.d.	n.d.	n.d.	n.d.	19.24	n.d.	n.d.	22.96
97-03-6479S	1.64	9.00	2.00	43.42	n.d.	7.37	n.d.	n.d.	64.09	16.90	n.d.	n.d.	37.71
97-03-2033S	1.57	6.00	1.00	32.32	n.d.	6.98	n.d.	n.d.	52.62	19.47	n.d.	n.d.	73.33
97-03-2053S	1.41	17.00	1.00	103.88	85.53	24.84	56.34	76.61	60.44	19.82	n.d.	n.d.	2.33
97-04-7070S	1.59	10.00	n.d.	74.21	37.62	13.97	84.00	22.52	35.59	20.93	n.d.	n.d.	6.16
97-04-7058S	2.34	24.00	n.d.	163.63	459.00	40.33	245.00	49.00	91.00	17.61	1.93	n.d.	35.61
97-03-2121S	1.60	4.00	2.00	39.99	n.d.	7.63	n.d.	n.d.	63.55	18.13	n.d.	n.d.	50.46
97-03-2169S	1.77	17.00	2.00	69.47	77.26	14.30	47.49	44.79	63.88	20.13	n.d.	n.d.	16.40
97-04-2302S	1.56	11.00	1.00	67.60	55.07	18.97	53.00	29.00	63.00	21.74	n.d.	n.d.	4.24
97-03-6044G	1.49	2.00	2.00	14.55	n.d.	3.33	n.d.	17.07	n.d.	15.44	n.d.	n.d.	51.12
97-03-6369G	1.65	10.00	2.00	61.21	n.d.	8.38	n.d.	n.d.	77.65	20.24	n.d.	n.d.	101.02
97-03-4041G	1.47	2.00	1.00	14.81	n.d.	3.09	n.d.	n.d.	n.d.	14.77	n.d.	n.d.	81.30
97-03-6247G	1.49	2.00	1.00	18.09	n.d.	3.01	n.d.	n.d.	38.87	14.71	n.d.	n.d.	44.63
97-03-6338G	1.48	n.d.	2.00	n.d.	n.d.	1.60	n.d.	n.d.	n.d.	15.96	n.d.	n.d.	89.54
97-03-4499AG	1.46	8.00	3.00	48.79	n.d.	7.13	n.d.	19.61	42.51	17.49	1.36	n.d.	100.54
97-03-6392G	1.46	2.00	2.00	8.14	n.d.	1.61	n.d.	12.90	n.d.	15.26	n.d.	n.d.	84.27
97-03-6407G	1.53	7.00	2.00	40.91	n.d.	7.19	n.d.	16.38	68.73	18.96	n.d.	n.d.	80.71
97-03-4043G	1.59	6.00	2.00	31.30	n.d.	6.14	n.d.	n.d.	71.40	18.65	n.d.	n.d.	45.97
97-04-7094S	1.55	2.00	1.00	51.65	n.d.	6.08	n.d.	12.00	34.00	20.28	n.d.	n.d.	56.47
97-04-7142AS	1.60	n.d.	n.d.	19.16	n.d.	3.72	n.d.	16.00	39.00	19.81	n.d.	n.d.	17.00
97-04-7095S	1.57	10.00	2.00	56.81	35.08	14.86	49.00	n.d.	68.00	21.38	1.35	n.d.	24.56
	1.54	9.52	1.70	66.21	114.95	10.82	84.09	28.00	62.73	18.23	1.40	0.00	48.77
	2.34	43.00	3.00	422.95	459.00	43.19	245.00	76.61	109.00	22.31	1.93	0.00	101.02
	0.93	1.00	1.00	8.14	35.08	1.60	47.49	10.34	34.00	14.52	1.02	0.00	2.33

Appendix 2.5 - Orthogneiss (continued)

Sample	Sr	Y	Zr	Nb	Mo	Ag	In	Sn	Sb	Cs	Ba	La	Ce	Pr	Nd	Sm		
97-03-6372G	282.58	33.10	319.65	13.69	n.d.	n.d.	4.18	n.d.	1540.00	103.67	175.22	18.02	64.66	10.46				
97-04-7057S	404.18	49.10	565.68	33.46	n.d.	n.d.	2.70	n.d.	2030.00	86.55	179.26	19.42	73.58	13.69				
97-03-6262G	248.73	3.62	144.38	3.43	n.d.	0.53	n.d.	0.00	n.d.	1160.00	24.02	35.92	3.42	10.83	1.68			
97-03-6371G	249.54	40.48	191.42	8.09	2.86	2.03	n.d.	4.07	n.d.	219.23	22.53	44.74	5.49	23.85	5.99			
97-03-2057S	303.81	1.79	216.43	4.55	n.d.	n.d.	0.00	n.d.	2050.00	14.58	20.38	1.80	6.02	0.85				
97-04-7092S	653.28	n.d.	32.25	n.d.	n.d.	n.d.	0.00	n.d.	2170.00	6.63	8.73	0.63	1.62	0.15				
97-03-6479S	229.39	8.38	204.46	7.23	n.d.	0.87	n.d.	3.74	n.d.	613.27	42.44	63.98	6.02	20.97	3.48			
97-03-2033S	259.16	8.69	242.93	5.84	n.d.	0.54	n.d.	0.00	n.d.	905.85	80.63	137.21	13.37	44.57	6.78			
97-03-2053S	888.95	9.42	72.28	1.92	n.d.	n.d.	0.00	n.d.	n.d.	364.20	17.71	35.70	4.31	17.05	3.42			
97-04-7070S	567.05	6.20	47.97	1.21	n.d.	n.d.	0.00	n.d.	n.d.	492.75	11.77	23.09	2.42	8.78	1.75			
97-04-7058S	75.43	21.36	115.23	9.89	2.00	n.d.	n.d.	0.00	n.d.	224.53	21.33	40.30	4.01	14.20	3.10			
97-03-2121S	278.53	4.53	164.05	4.64	n.d.	n.d.	0.00	n.d.	n.d.	931.43	62.59	96.92	8.78	28.36	3.65			
97-03-2169S	350.55	3.94	79.53	2.64	n.d.	n.d.	0.14	n.d.	n.d.	257.19	8.13	15.87	1.91	7.80	1.93			
97-04-2302S	255.06	15.25	141.94	3.93	n.d.	n.d.	1.23	n.d.	n.d.	276.28	18.68	34.20	3.60	13.56	2.90			
97-03-6044G	206.00	6.94	141.11	4.93	n.d.	n.d.	0.00	n.d.	n.d.	1120.00	48.24	79.12	7.77	24.74	3.86			
97-03-6369G	184.06	11.13	138.95	9.27	n.d.	0.80	n.d.	2.59	n.d.	2.07	328.16	26.05	41.82	4.09	13.38	2.48		
97-03-4041G	189.19	3.93	174.62	4.31	n.d.	0.62	n.d.	0.00	n.d.	n.d.	993.96	64.10	107.77	10.54	31.36	4.46		
97-03-6247G	255.99	3.01	117.53	2.44	n.d.	0.50	n.d.	1.14	n.d.	n.d.	1430.00	17.22	24.39	2.28	7.11	1.24		
97-03-6338G	147.15	7.42	95.40	3.89	n.d.	n.d.	1.50	n.d.	n.d.	605.44	19.89	32.76	3.27	10.93	2.05			
97-03-4499AG	244.30	38.30	367.13	18.27	11.01	0.84	n.d.	2.99	n.d.	0.57	1170.00	132.12	225.81	22.57	71.88	10.97		
97-03-6392G	276.26	3.39	92.20	3.21	n.d.	n.d.	3.42	n.d.	0.98	788.73	20.00	30.02	2.84	9.96	1.71			
97-03-6407G	265.30	27.02	261.07	14.34	n.d.	0.73	n.d.	3.87	n.d.	n.d.	798.58	73.28	119.34	11.69	40.29	7.23		
97-03-4043G	228.83	26.28	207.12	12.19	n.d.	n.d.	0.00	n.d.	n.d.	627.12	50.17	90.18	9.45	31.77	6.27			
97-04-7094S	410.89	6.19	117.72	4.10	2.00	n.d.	1.64	n.d.	n.d.	1450.00	76.00	136.10	12.50	39.27	4.78			
97-04-7142AS	634.38	1.74	67.87	n.d.	n.d.	n.d.	1.30	n.d.	n.d.	816.60	17.87	27.06	2.45	8.22	1.16			
97-04-7095S	210.67	28.51	144.36	10.40	n.d.	n.d.	2.04	n.d.	n.d.	251.14	29.20	56.28	6.13	22.68	5.57			
	319.20	14.79	171.66	7.83	4.47	0.83	0.00	1.44	0.00	1.20	908.25	42.13	72.39	7.26	24.90	4.29		
	888.95	49.10	565.68	33.46	11.01	2.03	0.00	4.18	0.00	2.07	2170.00	132.12	225.81	22.57	73.58	13.69		
	75.43	1.74	32.25	1.21	2.00	0.50	0.00	0.00	0.00	0.57	219.23	6.63	8.73	0.63	1.62	0.15		

Appendix 2.5 - Orthogneiss (continued)

Sample	Eu	Gd	Tb	Dy	Ho	Er	Tm	Yb	Lu	Hf	Ta	W	Tl	Pb	Bi	Th	U
97-03-6372G	2.28	8.15	1.20	6.23	1.13	3.46	0.47	2.87	0.44	7.39	0.81	n.d.	0.51	27.30	n.d.	16.92	1.23
97-04-7057S	3.33	11.56	1.86	9.93	1.88	5.60	0.82	5.03	0.71	14.24	1.66	n.d.	0.22	25.00	0.47	11.80	1.50
97-03-6262G	0.82	1.07	0.15	0.71	0.13	0.35	n.d.	0.31	0.05	3.68	0.10	n.d.	0.31	16.00	n.d.	5.24	0.55
97-03-6371G	2.02	6.72	1.19	6.77	1.32	4.33	0.63	3.82	0.62	4.44	0.52	n.d.	0.14	n.d.	n.d.	1.87	0.53
97-03-2057S	1.15	0.62	n.d.	0.38	n.d.	0.20	n.d.	0.32	0.06	6.88	0.18	n.d.	0.69	14.01	n.d.	1.48	0.50
97-04-7092S	0.62	n.d.	n.d.	n.d.	n.d.	n.d.	n.d.	n.d.	n.d.	1.26	n.d.	n.d.	0.17	22.00	n.d.	n.d.	0.10
97-03-6479S	1.02	2.71	0.36	1.74	0.28	0.77	0.10	0.65	0.10	4.61	0.22	4.27	0.31	10.06	n.d.	2.61	0.66
97-03-2033S	1.34	5.05	0.58	2.41	0.38	0.98	0.13	0.78	0.10	6.76	0.15	n.d.	0.38	20.85	n.d.	25.50	1.09
97-03-2053S	1.18	3.06	0.45	2.26	0.41	1.13	0.16	0.95	0.13	2.07	n.d.	n.d.	n.d.	9.07	n.d.	0.95	0.11
97-04-7070S	0.76	1.54	0.24	1.32	0.25	0.73	0.11	0.67	0.10	1.24	n.d.	n.d.	n.d.	12.85	n.d.	n.d.	n.d.
97-04-7058S	0.83	3.37	0.66	4.13	0.81	2.50	0.40	2.43	0.36	3.48	1.03	n.d.	0.24	18.00	0.78	8.38	1.04
97-03-2121S	1.02	2.12	0.25	1.19	0.19	0.47	0.07	0.42	0.07	4.47	0.12	n.d.	0.47	17.08	n.d.	11.09	0.63
97-03-2169S	0.52	1.48	0.22	1.02	0.17	0.44	0.06	0.34	0.05	2.42	0.18	n.d.	0.13	5.61	n.d.	2.83	0.74
97-04-2302S	1.05	2.88	0.50	2.80	0.54	1.56	0.22	1.50	0.22	3.80	0.18	n.d.	n.d.	n.d.	n.d.	0.18	n.d.
97-03-6044G	0.72	2.56	0.34	1.46	0.24	0.57	0.07	0.39	0.06	3.84	0.17	n.d.	0.33	15.44	n.d.	31.43	2.10
97-03-6369G	0.59	1.99	0.34	1.81	0.34	1.10	0.16	0.98	0.16	3.65	1.10	n.d.	0.96	18.81	n.d.	17.50	3.64
97-03-4041G	1.11	2.31	0.23	0.95	0.14	0.42	n.d.	0.31	0.05	4.74	n.d.	n.d.	0.53	22.86	n.d.	34.48	2.62
97-03-6247G	0.83	0.87	0.13	0.59	n.d.	0.28	n.d.	0.24	0.04	2.86	0.13	n.d.	0.27	11.64	n.d.	2.29	0.43
97-03-6338G	0.42	1.49	0.25	1.31	0.25	0.74	0.11	0.67	0.11	3.02	0.25	n.d.	0.52	25.90	n.d.	12.01	4.23
97-03-4499AG	1.93	8.10	1.24	6.56	1.24	3.91	0.55	3.33	0.51	9.32	1.14	n.d.	0.67	21.44	n.d.	44.90	4.42
97-03-6392G	0.46	1.24	0.14	0.66	0.11	0.31	n.d.	0.29	0.05	2.69	0.16	n.d.	0.58	25.18	n.d.	11.54	2.25
97-03-6407G	1.14	6.25	0.99	5.06	0.89	2.58	0.35	1.94	0.30	5.96	0.44	n.d.	0.58	12.91	n.d.	15.02	1.02
97-03-4043G	0.94	5.46	0.90	4.82	0.91	2.65	0.35	1.90	0.26	5.42	0.35	n.d.	0.23	8.36	n.d.	18.16	1.54
97-04-7094S	0.88	2.54	0.30	1.42	0.23	0.60	0.08	0.48	0.07	3.33	0.28	n.d.	0.44	27.00	0.57	31.39	0.98
97-04-7142AS	0.64	0.76	n.d.	0.38	n.d.	0.18	n.d.	0.13	n.d.	1.91	n.d.	n.d.	0.11	18.00	n.d.	n.d.	0.13
97-04-7095S	1.09	5.52	0.95	5.10	1.06	3.16	0.47	2.89	0.40	3.71	0.53	n.d.	0.19	16.00	n.d.	3.37	0.24
	1.10	3.58	0.58	2.84	0.59	1.56	0.28	1.35	0.21	4.51	0.46	4.27	0.39	17.56	0.61	13.52	1.34
	3.33	11.56	1.86	9.93	1.88	5.60	0.82	5.03	0.71	14.24	1.66	4.27	0.96	27.30	0.78	44.90	4.42
	0.42	0.62	0.13	0.38	0.11	0.18	0.06	0.13	0.04	1.24	0.10	4.27	0.11	5.61	0.47	0.18	0.10

Appendix 2.6 - Leucogranite

Sample	Location	SiO ₂	Al ₂ O ₃	Fe ₂ O ₃	MnO	MgO	CaO	K ₂ O	P ₂ O ₅	LOI	Total	Alumina Index		
97-03-2077	Split Lake Block	72.43	15.68	1.26	0.01	0.21	1.79	5.15	2.86	0.12	0.04	0.23	99.78	1.60
97-03-2079	Split Lake Block	73.28	14.92	0.81	0.01	0.19	1.28	4.74	4.30	0.10	0.05	0.39	100.17	1.45
97-03-2160	Split Lake Block	72.24	15.05	1.38	0.02	0.46	2.25	4.77	2.38	0.15	0.06	0.37	99.13	1.60
97-03-6591	Gull Rapids	71.97	14.77	0.81	n.d.	0.24	1.56	3.31	5.35	0.10	0.03	0.57	98.72	1.45
97-03-8101	Gull Rapids	75.25	13.45	1.03	0.04	0.16	0.58	2.88	5.93	0.01	0.03	0.43	99.88	1.43
97-04-7068	Split Lake Block	75.32	11.93	3.66	0.03	0.18	0.74	3.54	4.25	0.12	0.03	0.28	100.08	1.40
97-04-7090	Split Lake Block	70.94	15.93	1.76	0.03	0.62	2.89	5.04	2.20	0.19	0.07	0.26	99.93	1.57
97-04-7093	Split Lake Block	69.77	13.81	4.43	0.05	1.80	3.71	4.00	0.81	0.60	0.17	1.14	100.28	1.62
97-03-2054	Split Lake Block	72.43	15.38	1.06	0.02	0.44	3.66	4.07	1.40	0.06	0.02	0.51	99.03	1.68
97-03-2129	Split Lake Block	73.92	14.06	1.79	0.02	0.57	3.02	3.76	1.58	0.27	0.04	0.70	99.72	1.68
97-03-6387A	Gull Rapids	71.77	14.33	1.82	0.02	0.60	1.61	3.02	4.99	0.19	0.05	0.76	99.38	1.49
97-03-4022	Gull Rapids	75.05	13.30	0.88	0.03	0.19	0.74	2.85	6.14	0.05	0.03	0.70	100.03	1.37
97-03-8001B	Gull Rapids	72.56	14.67	1.35	0.01	0.53	1.54	3.34	5.19	0.17	0.05	0.62	100.02	1.46
97-03-6387C	Gull Rapids	72.05	14.63	1.36	0.01	0.50	1.67	3.29	4.98	0.15	0.04	0.70	99.56	1.47
97-03-6389	Gull Rapids	72.36	14.83	0.97	0.01	0.35	1.37	3.46	5.69	0.14	0.04	0.59	100.06	1.41
97-03-8001C	Gull Rapids	73.89	13.27	1.48	0.02	0.39	0.76	2.24	6.91	0.22	0.06	0.77	100.19	1.34
97-03-4029	Gull Rapids	76.07	13.07	1.41	0.03	0.43	2.07	4.67	1.06	0.08	0.02	1.09	100.03	1.68
97-03-4058	Gull Rapids	66.34	19.20	1.16	0.02	0.34	0.23	8.81	3.02	0.02	0.02	0.52	99.74	1.59
97-03-4364A	Gull Rapids	73.82	13.89	1.61	0.01	0.47	1.67	3.14	4.26	0.24	0.03	0.90	100.16	1.53
97-03-6365	Gull Rapids	64.16	14.74	7.84	0.09	3.28	2.05	2.96	2.56	0.53	0.12	2.00	100.30	1.95
97-04-2395	Split Lake Block	70.29	15.51	2.62	0.03	0.73	2.96	4.22	2.41	0.33	0.10	0.71	99.91	1.62
Average		72.19	14.59	1.93	0.03	0.60	1.82	3.96	3.73	0.18	0.05	0.68	99.81	1.54
Maximum		76.07	19.20	7.84	0.09	3.28	3.71	8.81	6.91	0.60	0.17	2.00	100.30	1.95
Minimum		64.16	11.93	0.81	0.01	0.16	0.23	2.24	0.81	0.01	0.02	0.23	98.72	1.34

Appendix 2.6 - Leucogranite (continued)

Sample	Sc	Be	V	Cr	Co	Ni	Cu	Zn	Ga	Ge	As	Rb	Sr	Y	Zr
97-03-2077	3.00	1.00	11.51	n.d.	1.55	n.d.	n.d.	18.96	n.d.	n.d.	22.95	874.30	1.58	70.23	
97-03-2079	n.d.	2.00	5.06	n.d.	n.d.	n.d.	n.d.	23.10	n.d.	n.d.	111.13	319.99	2.49	44.05	
97-03-2160	1.00	1.00	6.74	n.d.	2.41	n.d.	n.d.	34.80	19.29	n.d.	39.84	473.32	1.40	69.29	
97-03-6591	n.d.	1.00	5.49	n.d.	1.56	n.d.	n.d.	16.76	n.d.	n.d.	110.99	726.69	n.d.	71.52	
97-03-8101	5.00	n.d.	n.d.	n.d.	n.d.	n.d.	n.d.	12.56	n.d.	n.d.	108.61	118.93	21.84	52.68	
97-04-7068	n.d.	1.00	7.39	n.d.	1.99	n.d.	n.d.	16.50	1.20	n.d.	77.02	103.00	11.13	202.05	
97-04-7090	1.00	1.00	15.88	n.d.	3.34	n.d.	11.00	33.00	19.88	n.d.	20.18	589.42	1.74	70.48	
97-04-7093	4.00	n.d.	64.73	28.58	11.92	23.00	27.00	53.00	17.37	n.d.	3.94	520.85	5.28	443.00	
97-03-2054	n.d.	1.00	6.40	n.d.	2.01	n.d.	n.d.	17.81	n.d.	n.d.	8.04	459.52	n.d.	52.24	
97-03-2129	2.00	2.00	18.57	n.d.	2.69	n.d.	n.d.	17.67	n.d.	n.d.	25.27	254.16	4.43	179.08	
97-03-6387A	3.00	1.00	13.31	n.d.	2.67	n.d.	12.58	30.67	15.47	n.d.	n.d.	100.91	305.19	10.44	257.20
97-03-4022	2.00	n.d.	n.d.	n.d.	n.d.	n.d.	n.d.	12.48	n.d.	n.d.	122.91	103.40	22.31	69.10	
97-03-8001B	n.d.	1.00	6.34	n.d.	2.00	n.d.	n.d.	17.20	n.d.	n.d.	98.04	413.49	2.79	73.93	
97-03-6387C	1.00	1.00	15.90	n.d.	2.04	n.d.	n.d.	44.41	16.51	n.d.	95.63	380.33	1.88	84.05	
97-03-6389	2.00	1.00	8.73	n.d.	1.53	n.d.	n.d.	17.11	n.d.	n.d.	112.45	467.17	1.79	87.61	
97-03-8001C	3.00	1.00	6.41	n.d.	1.68	n.d.	n.d.	14.33	n.d.	n.d.	130.01	162.63	11.33	497.79	
97-03-4029	2.00	1.00	11.11	n.d.	2.23	n.d.	n.d.	14.78	n.d.	n.d.	20.68	122.70	3.74	116.23	
97-03-4058	6.00	2.00	n.d.	n.d.	1.39	n.d.	n.d.	12.29	n.d.	n.d.	36.49	94.97	7.73	131.20	
97-03-4364A	3.00	1.00	14.98	n.d.	2.42	n.d.	10.56	n.d.	16.51	n.d.	n.d.	94.00	164.87	6.87	181.69
97-03-6365	14.00	2.00	95.00	180.00	117.00	90.00	40.00	100.00	19.00	2.00	n.d.	167.00	874.30	22.31	497.79
97-04-2395	3.00	2.00	25.11	n.d.	5.25	n.d.	n.d.	46.00	22.56	n.d.	n.d.	46.81	292.95	9.95	163.73
Average	3.44	1.28	18.81	104.29	9.20	56.50	20.23	48.84	17.05	1.60	0.00	73.95	341.23	7.51	144.15
Maximum	14.00	2.00	95.00	180.00	117.00	90.00	40.00	100.00	23.10	2.00	0.00	167.00	874.30	22.31	497.79
Minimum	1.00	1.00	5.06	28.58	1.39	23.00	10.56	30.67	12.29	1.20	0.00	3.94	94.97	1.40	44.05

Appendix 2.6 - Leucogranite (continued)

Sample	Nb	Mo	Ag	In	Sn	Sb	Cs	Ba	La	Ce	Pr	Nd	Sm	Eu	Gd	Tb	Dy
97-03-2077	n.d.	1760.00	6.80	8.97	0.83	2.79	0.53	0.53	0.46	n.d.	0.38						
97-03-2079	1.95	n.d.	n.d.	n.d.	1.65	n.d.	0.55	678.48	12.52	20.91	2.24	7.94	1.69	0.47	1.17	0.15	0.56
97-03-2160	1.64	n.d.	n.d.	n.d.	n.d.	n.d.	n.d.	842.22	7.26	11.61	1.17	4.17	0.72	0.40	0.52	n.d.	0.28
97-03-6591	3.00	n.d.	n.d.	n.d.	n.d.	n.d.	n.d.	1550.00	6.96	9.82	0.87	2.75	0.48	1.02	0.27	n.d.	0.15
97-03-8101	1.18	n.d.	n.d.	n.d.	2.90	n.d.	n.d.	461.70	11.82	17.47	1.62	5.29	0.99	0.54	1.01	0.30	2.69
97-04-7068	6.93	2.00	0.60	n.d.	1.94	n.d.	n.d.	597.11	58.59	119.71	11.83	39.21	6.04	0.61	4.10	0.53	2.68
97-04-7090	1.90	n.d.	n.d.	n.d.	n.d.	n.d.	n.d.	1150.00	16.82	26.40	2.18	6.88	0.91	0.60	0.55	n.d.	0.37
97-04-7093	3.04	2.00	0.80	n.d.	n.d.	n.d.	n.d.	434.28	21.16	39.38	3.87	13.71	2.04	0.89	1.47	0.19	1.03
97-03-2054	n.d.	705.96	18.82	24.80	1.95	5.26	0.54	1.21	0.34	n.d.	0.21						
97-03-2129	5.00	n.d.	n.d.	n.d.	0.56	n.d.	413.28	94.24	157.42	14.81	48.47	6.10	1.03	3.29	0.29	1.25	
97-03-6387A	7.40	4.65	0.55	n.d.	3.45	n.d.	n.d.	1180.00	95.47	158.68	15.57	52.87	7.98	1.11	5.14	0.53	2.08
97-03-4022	1.20	n.d.	n.d.	n.d.	n.d.	n.d.	n.d.	485.91	17.69	31.59	3.42	11.28	2.54	0.44	2.37	0.49	3.27
97-03-8001B	7.10	n.d.	n.d.	n.d.	3.23	n.d.	n.d.	1350.00	16.08	27.34	2.89	9.56	1.77	0.91	1.14	0.14	0.58
97-03-6387C	4.12	n.d.	n.d.	n.d.	3.32	n.d.	n.d.	1070.00	13.65	21.91	2.17	7.82	1.44	0.93	0.99	0.12	0.41
97-03-6389	5.94	n.d.	n.d.	n.d.	2.66	n.d.	n.d.	1380.00	13.91	21.45	2.11	7.81	1.31	0.94	0.86	n.d.	0.34
97-03-8001C	6.97	n.d.	0.84	n.d.	4.25	n.d.	n.d.	1050.00	262.57	424.16	38.71	120.23	13.50	1.44	7.27	0.66	2.57
97-03-4029	1.40	n.d.	n.d.	n.d.	1.12	n.d.	n.d.	127.65	11.20	17.68	1.67	4.90	0.88	0.41	0.64	0.11	0.60
97-03-4058	2.48	n.d.	0.51	n.d.	n.d.	n.d.	n.d.	250.44	15.59	32.66	3.02	9.20	1.46	0.32	1.02	0.22	1.46
97-03-4364A	6.24	n.d.	n.d.	n.d.	1.24	n.d.	n.d.	683.05	70.45	128.99	13.12	42.65	6.66	0.80	4.16	0.42	1.68
97-03-6365	6.00	3.00	n.d.	n.d.	2.00	0.70	5.10	499.00	29.50	54.10	5.72	20.60	3.50	1.03	2.70	0.40	2.50
97-04-2395	6.99	2.00	n.d.	n.d.	n.d.	n.d.	n.d.	777.85	43.99	72.35	6.63	21.32	3.14	0.93	2.24	0.34	1.87
Average	4.24	2.73	0.66	0.00	2.52	0.63	2.83	830.81	40.24	67.97	6.50	21.18	3.06	0.79	1.99	0.33	1.28
Maximum	7.40	4.65	0.84	0.00	4.25	0.70	5.10	1760.00	262.57	424.16	38.71	120.23	13.50	1.44	7.27	0.66	3.27
Minimum	1.18	2.00	0.51	0.00	1.12	0.56	0.55	127.65	6.80	8.97	0.83	2.75	0.48	0.32	0.27	0.11	0.15

Appendix 2.6 - Leucogranite (continued)

Sample	Ho	Er	Tm	Yb	Lu	Hf	Ta	W	Tl	Pb	Bi	Th	U
97-03-2077	n.d.	0.19	n.d.	0.17	n.d.	2.17	n.d.	n.d.	0.18	26.51	n.d.	n.d.	0.14
97-03-2079	n.d.	0.22	n.d.	0.13	n.d.	1.61	n.d.	n.d.	1.08	38.30	n.d.	7.26	3.41
97-03-2160	n.d.	0.13	n.d.	0.12	n.d.	2.26	n.d.	n.d.	0.43	16.66	n.d.	n.d.	0.12
97-03-6591	n.d.	n.d.	0.12	n.d.	2.51	0.11	n.d.	0.92	45.71	n.d.	1.31	1.00	
97-03-8101	0.70	2.96	0.57	3.86	0.60	2.09	n.d.	n.d.	0.91	55.45	n.d.	6.33	7.58
97-04-7068	0.47	1.39	0.21	1.27	0.20	6.98	0.26	2.05	0.40	13.00	n.d.	17.46	1.14
97-04-7090	n.d.	0.20	n.d.	0.17	n.d.	1.89	n.d.	n.d.	0.17	22.00	n.d.	0.20	0.15
97-04-7093	0.19	0.66	0.10	0.77	0.14	11.68	0.13	n.d.	n.d.	12.00	0.41	0.91	0.70
97-03-2054	n.d.	0.14	n.d.	0.15	n.d.	1.51	n.d.	n.d.	n.d.	8.07	n.d.	0.62	0.10
97-03-2129	0.17	0.41	0.06	0.38	0.06	5.29	0.22	n.d.	0.35	18.24	n.d.	53.26	0.74
97-03-6387A	0.31	0.94	0.13	0.90	0.15	5.93	0.21	n.d.	0.71	53.04	n.d.	87.23	3.21
97-03-4022	0.78	2.86	0.46	2.85	0.42	2.65	n.d.	2.84	0.93	60.26	n.d.	13.19	9.19
97-03-8001B	n.d.	0.23	n.d.	0.20	n.d.	2.13	0.32	n.d.	0.57	46.10	n.d.	11.32	1.33
97-03-6387C	n.d.	0.17	n.d.	0.13	n.d.	2.30	0.17	n.d.	0.64	47.69	n.d.	6.31	1.29
97-03-6389	n.d.	0.18	n.d.	0.16	n.d.	2.59	0.13	n.d.	0.76	61.75	n.d.	5.66	2.22
97-03-8001C	0.36	0.98	0.12	0.78	0.13	11.75	0.25	n.d.	0.79	36.27	n.d.	60.52	1.41
97-03-4029	0.12	0.39	0.06	0.48	0.08	3.42	n.d.	n.d.	0.14	26.77	n.d.	2.26	3.02
97-03-4058	0.30	1.02	0.19	1.41	0.22	4.92	0.16	n.d.	0.23	12.14	n.d.	5.23	1.39
97-03-4364A	0.23	0.54	0.06	0.40	0.07	4.99	0.20	2.97	0.62	44.24	n.d.	44.63	1.81
97-03-6365	0.50	1.50	0.22	1.40	0.21	3.10	2.60	988.00	1.10	33.00	0.40	11.20	3.00
97-04-2395	0.36	1.06	0.15	0.89	0.14	4.66	0.20	n.d.	0.23	19.00	n.d.	5.63	0.40
Average	0.37	0.81	0.19	0.80	0.20	4.12	0.38	248.97	0.59	33.15	0.41	17.92	2.06
Maximum	0.78	2.96	0.57	3.86	0.60	11.75	2.60	988.00	1.10	61.75	0.41	87.23	9.19
Minimum	0.12	0.13	0.06	0.12	0.06	1.51	0.11	2.05	0.14	8.07	0.40	0.20	0.10

Appendix 3 - Mineral Chemistry

Appendix 3.1 - Summary of Mineral Chemistry

Mafic Granulite

Feldspar	Cation	Weight %																		
		Si	Al	Fe	Ca	Na	K	Total	SiO ₂	Al ₂ O ₃	FeO	CaO	Na ₂ O	K ₂ O	Total					
9704-7069		2.49	1.50	0.00	0.49	0.52	0.01	5.02	54.77	28.02	0.09	10.10	5.88	0.19	99.05					
9704-7142D		2.52	1.48	0.00	0.48	0.52	0.01	5.01	55.31	27.46	0.08	9.79	5.87	0.22	98.73					
Garnet	Cation	Weight %																		
Sample	Si	Ti	Al	Fe	Mn	Mg	Ca	Total	SiO ₂	TiO ₂	Al ₂ O ₃	FeO	MnO	MgO	Total					
9704-7069	2.98	0.00	1.98	2.05	0.09	0.34	0.59	8.03	37.49	0.03	21.22	30.74	1.21	2.69	7.24	100.62				
9704-7142D	2.97	0.00	2.00	1.91	0.12	0.44	0.59	8.03	37.51	0.00	21.50	29.16	2.02	3.52	6.80	100.51				
Clinopyroxene	Cation	Weight %																		
Sample	Si	Ti	Al	Cr	Fe	Mn	Mg	Ca	Na	Total	SiO ₂	TiO ₂	Al ₂ O ₃	Cr ₂ O ₃	FeO	MnO	MgO	CaO	Na ₂ O	Total
9704-7069	1.95	0.01	0.10	0.00	0.52	0.01	0.55	0.84	0.03	4.01	50.56	0.29	2.22	0.02	16.09	0.18	9.52	20.37	0.40	99.66
9704-7142D	1.94	0.01	0.11	0.00	0.48	0.01	0.54	0.90	0.03	4.01	50.66	0.23	2.48	0.02	14.86	0.15	9.41	21.92	0.44	100.17
Orthopyroxene	Cation	Weight %																		
Sample	Si	Ti	Al	Cr	Fe	Mn	Mg	Ca	Total	SiO ₂	TiO ₂	Al ₂ O ₃	Cr ₂ O ₃	FeO	MnO	MgO	CaO	Na ₂ O	Total	
9704-7069	1.98	0.00	0.04	0.00	1.15	0.01	0.80	0.03	4.00	49.66	0.00	0.86	0.02	34.54	0.40	13.45	0.61	99.53		
9704-7142D	1.98	0.00	0.05	0.00	1.09	0.01	0.81	0.03	3.99	50.33	0.14	1.12	0.06	33.22	0.97	13.85	0.68	100.36		

Appendix 3.1 (continued) - Summary of Mineral Chemistry

Aluminous Granulite

Feldspar	Cations (8 O)								Weight %											
	Si	Al	Fe	Ca	Na	K	Total	SiO ₂	Al ₂ O ₃	FeO	CaO	Na ₂ O	K ₂ O	Total						
9704-7086	2.72	1.29	0.00	0.27	0.72	0.01	5.00	60.63	24.36	0.05	5.67	8.26	0.10	99.06						
Garnetite GR	2.76	1.24	0.00	0.21	0.82	0.00	5.03	61.10	23.19	0.01	4.31	9.29	0.08	97.97						
GAR03	2.79	1.22	0.00	0.19	0.81	0.01	5.01	62.61	23.27	0.02	3.96	9.41	0.10	99.37						
Garnet	Cation (12 O)								Weight %											
Sample	Si	Ti	Al	Fe	Mn	Mg	Ca	Total	SiO ₂	TiO ₂	Al ₂ O ₃	FeO	MnO	MgO	CaO	Total				
9704-7086	2.98	0.01	2.03	2.21	0.04	0.63	0.10	8.00	38.05	0.12	21.99	33.82	0.67	5.38	1.15	101.17				
Garnetite GR	2.95	0.00	2.04	2.30	0.05	0.60	0.09	8.03	37.14	0.05	21.75	34.69	0.67	5.10	1.11	100.51				
GAR03	2.96	0.00	2.03	2.37	0.05	0.53	0.08	8.02	37.16	0.07	21.71	35.60	0.77	4.46	0.95	100.73				
Hercynite	Cation (4 O)								Weight %											
Sample	Si	Ti	Al	Cr	V	Fe	Mn	Zn	Mg	Total	SiO ₂	TiO ₂	Al ₂ O ₃	Cr ₂ O ₃	V ₂ O ₃	Total				
9704-7086	0.00	0.00	1.90	0.01	0.01	0.98	0.00	0.01	0.14	3.04	0.04	0.02	53.58	0.26	0.23	38.76	0.07	0.25	3.12	96.32
Garnetite GR	0.00	0.00	1.88	0.00	0.00	1.08	0.00	0.01	0.08	3.06	0.01	0.02	52.28	0.15	0.20	42.20	0.06	0.37	1.87	97.16
GAR03	0.00	0.00	1.87	0.00	0.01	1.09	0.00	0.01	0.08	3.06	0.05	0.03	51.53	0.13	0.21	42.60	0.11	0.24	1.75	96.65
Ilmenite	Cation (3 O)								Weight %											
Sample	TiO ₂	SiO ₂	Nb ₂ O ₅	FeO	MnO	MgO	Total	TiO ₂	SiO ₂	Nb ₂ O ₅	FeO	MnO	MgO	Total						
Garnetite GR	1.00	0.00	0.00	1.00	0.00	0.01	2.00	52.43	0.02	0.00	47.31	0.12	0.15	100.02						
GAR03	0.99	0.00	0.00	1.01	0.00	0.00	2.01	51.96	0.04	0.02	47.61	0.14	0.10	99.86						
9704-7086	1.00	0.00	0.00	0.99	0.00	0.01	2.00	52.06	0.02	0.02	46.73	0.18	0.24	99.24						

Appendix 3.2 - Garnet Mineral Chemistry

No.	Distance μm	Weight Percent						Cation Total O = 12.0									
		SiO ₂	TiO ₂	Al ₂ O ₃	FeO	MnO	MgO	CaO	Total	Si	Ti	Al	Fe	Mn	Mg	Ca	Total
Garnetite GR - Garnet 1																	
8	0	37.61	0.04	21.65	34.60	0.65	5.15	1.08	100.79	2.97	0.00	2.02	2.29	0.04	0.61	0.09	8.02
9	242	37.72	0.00	21.58	34.80	0.68	5.15	1.16	101.09	2.97	0.00	2.01	2.30	0.05	0.61	0.10	8.02
10	484	35.29	0.06	21.39	34.45	0.62	5.17	1.07	98.05	2.89	0.00	2.06	2.36	0.04	0.63	0.09	8.08
11	726	37.13	0.05	21.75	34.69	0.67	5.10	1.11	100.51	2.95	0.00	2.04	2.30	0.05	0.60	0.09	8.03
12	968	37.66	0.00	22.01	34.57	0.68	5.14	1.02	101.09	2.96	0.00	2.04	2.28	0.05	0.60	0.09	8.02
13	1210	37.55	0.06	22.00	34.51	0.67	5.24	1.14	101.17	2.95	0.00	2.04	2.27	0.04	0.61	0.10	8.02
14	1452	37.41	0.00	21.66	34.38	0.63	5.00	1.58	100.66	2.96	0.00	2.02	2.28	0.04	0.59	0.13	8.03
15	1694	37.12	0.00	21.61	34.15	0.63	5.11	1.50	100.11	2.95	0.00	2.03	2.27	0.04	0.61	0.13	8.03
16	1936	37.70	0.01	21.93	34.78	0.67	5.16	1.08	101.32	2.96	0.00	2.03	2.29	0.04	0.60	0.09	8.02
17	2178	37.63	0.01	21.83	34.77	0.70	4.99	1.08	101.00	2.97	0.00	2.03	2.29	0.05	0.59	0.09	8.02
Garnetite GR - Garnet 2																	
18	0	37.38	0.04	21.79	35.27	0.66	4.81	1.05	100.98	2.96	0.00	2.03	2.33	0.04	0.57	0.09	8.02
19	100	37.28	0.01	21.88	35.30	0.60	4.83	1.31	101.22	2.94	0.00	2.04	2.33	0.04	0.57	0.11	8.04
20	200	37.55	0.06	21.70	34.99	0.64	4.85	1.48	101.27	2.96	0.00	2.02	2.31	0.04	0.57	0.13	8.03
21	300	37.57	0.04	21.82	34.52	0.62	4.89	1.32	100.77	2.97	0.00	2.03	2.28	0.04	0.58	0.11	8.01
22	400	37.07	0.00	21.90	35.03	0.58	5.01	1.24	100.82	2.94	0.00	2.05	2.32	0.04	0.59	0.11	8.04
23	500	37.47	0.00	21.74	35.05	0.58	4.97	1.25	101.06	2.96	0.00	2.02	2.32	0.04	0.59	0.11	8.03
24	600	36.96	0.03	21.90	34.78	0.63	4.75	1.37	100.42	2.94	0.00	2.05	2.31	0.04	0.56	0.12	8.03
25	700	37.36	0.00	21.83	34.84	0.62	4.81	1.54	101.00	2.95	0.00	2.03	2.30	0.04	0.57	0.13	8.03
26	800	37.30	0.00	21.83	34.94	0.61	4.68	1.30	100.66	2.96	0.00	2.04	2.32	0.04	0.55	0.11	8.02
27	900	37.52	0.04	21.85	34.97	0.67	4.90	1.12	101.07	2.96	0.00	2.03	2.31	0.04	0.58	0.09	8.02

Appendix 3.2 (continued) - Garnet Mineral Chemistry

No.	Distance μm	Weight Percent						Cation Total O = 12.0									
		SiO ₂	TiO ₂	Al ₂ O ₃	FeO	MnO	MgO	CaO	Total	Si	Ti	Al	Fe	Mn	Mg	Ca	Total
Garnet GR - Garnet 3																	
28	0	37.13	0.00	21.82	34.91	0.62	5.05	0.99	100.53	2.95	0.00	2.04	2.32	0.04	0.60	0.08	8.03
29	115	37.34	0.00	21.81	34.77	0.63	5.14	1.06	100.76	2.95	0.00	2.03	2.30	0.04	0.61	0.09	8.03
30	230	37.34	0.00	21.83	35.13	0.68	5.19	1.10	101.27	2.94	0.00	2.03	2.32	0.05	0.61	0.09	8.04
31	345	37.61	0.03	21.87	35.02	0.68	5.19	1.11	101.51	2.96	0.00	2.03	2.30	0.05	0.61	0.09	8.03
32	460	37.55	0.01	21.66	34.70	0.68	5.31	1.03	100.94	2.96	0.00	2.02	2.29	0.05	0.63	0.09	8.03
33	575	37.26	0.00	21.33	37.62	0.82	3.07	1.02	101.13	2.98	0.00	2.01	2.52	0.06	0.37	0.09	8.02
34	690	37.67	0.00	21.74	34.55	0.62	5.25	1.11	100.94	2.97	0.00	2.02	2.28	0.04	0.62	0.09	8.02
35	805	37.48	0.00	21.80	34.53	0.68	5.09	1.07	100.65	2.96	0.00	2.03	2.28	0.05	0.60	0.09	8.02
36	920	37.50	0.03	21.82	34.72	0.70	5.23	1.02	101.01	2.96	0.00	2.03	2.29	0.05	0.62	0.09	8.03
37	1035	37.61	0.01	21.79	34.36	0.60	5.25	1.13	100.74	2.97	0.00	2.03	2.27	0.04	0.62	0.10	8.02
9704-7069 - Garnet 1																	
38	0	37.58	0.04	21.11	30.73	1.16	2.64	7.66	100.91	2.98	0.00	1.97	2.04	0.08	0.31	0.65	8.03
39	87	37.46	0.04	21.19	30.63	1.23	2.68	7.26	100.48	2.98	0.00	1.99	2.04	0.08	0.32	0.62	8.02
40	174	37.71	0.02	21.29	30.74	1.25	2.75	7.21	100.98	2.98	0.00	1.99	2.03	0.08	0.32	0.61	8.02
41	261	37.38	0.03	21.32	30.79	1.22	2.68	7.43	100.85	2.97	0.00	1.99	2.04	0.08	0.32	0.63	8.04
42	348	37.49	0.03	21.22	30.74	1.21	2.69	7.24	100.62	2.98	0.00	1.99	2.04	0.08	0.32	0.62	8.03
43	435	37.43	0.03	21.04	30.89	1.23	2.63	7.23	100.47	2.98	0.00	1.98	2.06	0.08	0.31	0.62	8.03
44	522	37.46	0.07	21.26	31.01	1.20	2.67	7.38	101.05	2.97	0.00	1.99	2.06	0.08	0.32	0.63	8.04
45	609	37.47	0.08	21.03	30.91	1.19	2.72	7.32	100.72	2.98	0.00	1.97	2.05	0.08	0.32	0.62	8.03
46	696	37.51	0.04	21.04	30.65	1.18	2.66	7.35	100.43	2.99	0.00	1.97	2.04	0.08	0.32	0.63	8.03
47	783	37.16	0.00	21.61	29.74	1.13	2.54	7.96	100.14	2.96	0.00	2.03	1.98	0.08	0.30	0.68	8.03

Appendix 3.2 (continued) - Garnet Mineral Chemistry

No.	Distance μm	SiO ₂	TiO ₂	Al ₂ O ₃	Weight Percent				Cation Total O = 12.0	Si	Ti	Al	Fe	Mn	Mg	Ca	Total
					FeO	MnO	MgO	CaO									
9704-7069 - Garnet 2																	
48	0	37.29	0.02	21.03	30.51	1.09	2.63	7.68	100.25	2.98	0.00	1.98	2.04	0.07	0.31	0.66	8.03
49	112	37.65	0.04	21.13	30.71	1.16	2.69	7.53	100.90	2.98	0.00	1.97	2.03	0.08	0.32	0.64	8.03
50	224	37.41	0.05	21.35	30.68	1.25	2.65	7.41	100.81	2.97	0.00	2.00	2.04	0.08	0.31	0.63	8.03
51	336	37.18	0.04	20.84	30.51	1.16	2.61	7.47	99.80	2.98	0.00	1.97	2.05	0.08	0.31	0.64	8.03
52	448	37.45	0.00	21.15	30.61	1.25	2.52	7.57	100.54	2.98	0.00	1.98	2.04	0.08	0.30	0.65	8.03
53	560	37.35	0.03	21.02	30.60	1.22	2.60	7.42	100.24	2.98	0.00	1.98	2.04	0.08	0.31	0.63	8.03
54	672	37.41	0.00	20.90	30.85	1.27	2.60	7.29	100.32	2.99	0.00	1.97	2.06	0.09	0.31	0.62	8.03
55	784	37.52	0.00	21.01	30.87	1.26	2.63	7.38	100.67	2.98	0.00	1.97	2.05	0.08	0.31	0.63	8.03
56	896	37.17	0.13	21.12	30.85	1.29	2.58	7.46	100.59	2.96	0.01	1.98	2.06	0.09	0.31	0.64	8.04
57	1008	36.42	0.06	20.99	30.72	1.18	2.41	7.56	99.35	2.94	0.00	2.00	2.08	0.08	0.29	0.66	8.05
9704-7069 - Garnet 3																	
58	0	37.49	0.05	21.46	29.98	1.14	2.54	8.06	100.72	2.97	0.00	2.00	1.99	0.08	0.30	0.68	8.02
59	158	37.40	0.04	21.09	30.85	1.15	2.60	7.13	100.26	2.98	0.00	1.98	2.06	0.08	0.31	0.61	8.02
60	316	37.54	0.00	21.23	31.16	1.18	2.66	7.27	101.04	2.98	0.00	1.98	2.06	0.08	0.31	0.62	8.03
61	474	37.40	0.08	21.20	30.87	1.12	2.61	7.17	100.43	2.98	0.00	1.99	2.06	0.08	0.31	0.61	8.02
62	632	37.63	0.00	21.16	30.93	1.16	2.63	7.26	100.77	2.99	0.00	1.98	2.05	0.08	0.31	0.62	8.02
63	790	37.55	0.07	21.22	30.89	1.29	2.86	7.01	100.89	2.98	0.00	1.98	2.05	0.09	0.34	0.59	8.03
64	948	37.42	0.05	21.32	30.98	1.26	2.65	6.83	100.51	2.98	0.00	2.00	2.06	0.08	0.31	0.58	8.02
65	1106	37.43	0.17	21.18	30.92	1.22	2.70	7.07	100.69	2.97	0.01	1.98	2.05	0.08	0.32	0.60	8.03
66	1264	37.47	0.12	21.13	31.15	1.25	2.62	7.12	100.85	2.98	0.01	1.98	2.07	0.08	0.31	0.61	8.03
67	1422	37.41	0.01	21.04	30.74	1.18	2.52	7.65	100.54	2.98	0.00	1.97	2.05	0.08	0.30	0.65	8.03

Appendix 3.2 (continued) - Garnet Mineral Chemistry

No.	Distance μm	Weight Percent						Cation Total O = 12.0									
		SiO ₂	TiO ₂	Al ₂ O ₃	FeO	MnO	MgO	CaO	Total	Si	Ti	Al	Fe	Mn	Mg	Ca	Total
9704-7142D - Garnet 1																	
68	0	37.16	0.04	21.11	29.07	2.43	2.72	7.12	99.66	2.98	0.00	1.99	1.95	0.16	0.33	0.61	8.02
69	54	37.66	0.00	21.18	28.84	2.27	2.94	7.40	100.30	2.99	0.00	1.98	1.91	0.15	0.35	0.63	8.02
70	108	36.92	0.00	21.26	29.10	2.36	2.89	7.06	99.59	2.96	0.00	2.01	1.95	0.16	0.35	0.61	8.03
71	162	37.60	0.00	21.11	29.08	2.29	3.11	6.99	100.17	2.99	0.00	1.98	1.93	0.15	0.37	0.60	8.02
72	216	37.52	0.08	21.39	29.27	2.41	3.13	7.03	100.84	2.97	0.00	1.99	1.94	0.16	0.37	0.60	8.03
73	270	37.27	0.05	21.39	29.06	2.37	3.11	6.99	100.23	2.96	0.00	2.01	1.93	0.16	0.37	0.60	8.03
74	324	37.52	0.00	21.34	29.17	2.45	3.16	6.97	100.62	2.97	0.00	1.99	1.93	0.16	0.37	0.59	8.03
75	378	37.53	0.08	21.26	28.98	2.46	3.06	6.90	100.27	2.98	0.00	1.99	1.93	0.17	0.36	0.59	8.02
76	432	37.53	0.00	21.25	29.24	2.35	3.13	7.09	100.58	2.98	0.00	1.99	1.94	0.16	0.37	0.60	8.03
77	486	37.78	0.02	21.20	29.05	2.32	3.11	7.07	100.55	2.99	0.00	1.98	1.92	0.16	0.37	0.60	8.02
9704-7142D - Garnet 2																	
78	0	37.57	0.07	21.26	28.64	2.12	2.70	7.85	100.21	2.99	0.00	1.99	1.90	0.14	0.32	0.67	8.02
79	42	37.63	0.04	21.46	28.59	2.10	2.99	7.66	100.47	2.98	0.00	2.00	1.89	0.14	0.35	0.65	8.02
80	84	37.64	0.00	21.13	28.91	2.24	3.14	6.93	99.98	2.99	0.00	1.98	1.92	0.15	0.37	0.59	8.01
81	126	37.58	0.00	21.19	29.07	2.19	3.10	6.96	100.10	2.99	0.00	1.99	1.93	0.15	0.37	0.59	8.02
82	168	37.60	0.09	21.48	29.23	2.31	3.09	6.94	100.75	2.97	0.01	2.00	1.93	0.15	0.36	0.59	8.02
83	210	37.41	0.03	21.05	29.24	2.24	3.11	6.96	100.04	2.98	0.00	1.98	1.95	0.15	0.37	0.59	8.03
84	252	37.30	0.02	21.11	29.41	2.28	3.17	7.03	100.31	2.97	0.00	1.98	1.96	0.15	0.38	0.60	8.04
85	294	37.56	0.00	21.06	29.20	2.29	3.17	7.01	100.29	2.99	0.00	1.97	1.94	0.15	0.38	0.60	8.03
86	336	37.30	0.05	21.38	28.30	2.16	2.77	8.08	100.03	2.97	0.00	2.01	1.88	0.15	0.33	0.69	8.03

Appendix 3.2 (continued) - Garnet Mineral Chemistry

No.	Distance μm	Weight Percent						Cation Total O = 12.0									
		SiO ₂	TiO ₂	Al ₂ O ₃	FeO	MnO	MgO	CaO	Total	Si	Ti	Al	Fe	Mn	Mg	Ca	Total
9704-7142D - Garnet 3																	
88	0	37.75	0.04	21.40	29.16	1.92	3.28	7.16	100.71	2.98	0.00	1.99	1.93	0.13	0.39	0.61	8.02
89	80	37.34	0.08	21.21	29.45	1.95	3.37	6.99	100.39	2.97	0.00	1.99	1.96	0.13	0.40	0.59	8.04
90	160	37.61	0.03	21.27	29.53	1.99	3.54	6.82	100.78	2.97	0.00	1.98	1.95	0.13	0.42	0.58	8.03
91	240	37.52	0.00	21.49	28.93	1.83	3.70	6.96	100.43	2.97	0.00	2.00	1.91	0.12	0.44	0.59	8.03
92	320	37.56	0.09	21.25	28.91	2.00	3.53	6.77	100.12	2.98	0.01	1.99	1.92	0.13	0.42	0.58	8.02
93	400	37.51	0.00	21.50	29.16	2.02	3.52	6.80	100.51	2.97	0.00	2.01	1.93	0.14	0.41	0.58	8.03
94	480	37.61	0.07	21.41	29.29	2.00	3.56	6.74	100.68	2.97	0.00	1.99	1.94	0.13	0.42	0.57	8.03
95	560	37.33	0.08	21.37	29.50	1.90	3.46	6.71	100.35	2.96	0.00	2.00	1.96	0.13	0.41	0.57	8.03
96	640	37.44	0.07	21.21	29.28	1.98	3.50	6.70	100.18	2.97	0.00	1.99	1.95	0.13	0.41	0.57	8.03
97	720	37.60	0.00	21.36	29.12	1.91	3.28	6.92	100.18	2.98	0.00	2.00	1.93	0.13	0.39	0.59	8.02
9704-7134 - Garnet 1																	
98	0	38.08	0.07	21.59	29.11	1.00	4.00	7.07	100.92	2.98	0.00	1.99	1.91	0.07	0.47	0.59	8.02
99	153	37.88	0.07	21.50	29.15	1.09	4.01	6.88	100.58	2.98	0.00	1.99	1.92	0.07	0.47	0.58	8.02
100	306	37.81	0.00	21.49	28.88	1.01	3.98	7.03	100.18	2.98	0.00	2.00	1.91	0.07	0.47	0.59	8.02
101	459	38.01	0.10	21.38	28.92	1.08	3.99	6.92	100.39	2.99	0.01	1.98	1.90	0.07	0.47	0.58	8.01
102	612	37.92	0.00	21.48	28.77	1.10	3.99	6.82	100.09	2.99	0.00	2.00	1.90	0.07	0.47	0.58	8.01
103	765	37.84	0.00	21.67	28.90	1.03	3.83	7.29	100.55	2.98	0.00	2.01	1.90	0.07	0.45	0.61	8.02
104	918	37.86	0.09	21.37	29.19	1.06	3.79	7.24	100.59	2.98	0.01	1.98	1.92	0.07	0.44	0.61	8.02
105	1071	37.54	0.02	21.27	29.01	1.06	3.87	6.99	99.76	2.98	0.00	1.99	1.93	0.07	0.46	0.59	8.02
106	1224	37.42	0.09	21.19	28.92	1.08	3.86	7.14	99.70	2.97	0.01	1.99	1.92	0.07	0.46	0.61	8.03
107	1377	37.67	0.03	21.29	29.18	1.04	3.63	7.05	99.90	2.99	0.00	1.99	1.94	0.07	0.43	0.60	8.01

Appendix 3.2 (continued) - Garnet Mineral Chemistry

No.	Distance μm	Weight Percent						Cation Total O = 12.0									
		SiO ₂	TiO ₂	Al ₂ O ₃	FeO	MnO	MgO	CaO	Total	Si	Ti	Al	Fe	Mn	Mg	Ca	Total
9704-7134 - Garnet 2																	
108	0	37.95	0.01	21.72	29.32	1.03	3.61	7.38	101.02	2.98	0.00	2.01	1.92	0.07	0.42	0.62	8.02
109	76	37.33	0.07	21.66	29.39	1.09	3.65	7.11	100.31	2.95	0.00	2.02	1.95	0.07	0.43	0.60	8.03
110	152	37.48	0.03	21.33	29.28	1.12	3.74	7.21	100.18	2.97	0.00	1.99	1.94	0.08	0.44	0.61	8.03
111	228	37.49	0.01	21.41	29.81	1.06	3.74	7.12	100.64	2.96	0.00	1.99	1.97	0.07	0.44	0.60	8.04
112	304	37.90	0.06	21.41	29.41	1.09	3.70	7.21	100.79	2.98	0.00	1.99	1.94	0.07	0.43	0.61	8.02
113	380	37.64	0.02	21.30	29.30	1.15	3.64	7.21	100.27	2.98	0.00	1.99	1.94	0.08	0.43	0.61	8.03
114	456	36.81	0.10	21.32	29.27	1.08	3.75	7.16	99.49	2.94	0.01	2.01	1.96	0.07	0.45	0.61	8.05
115	532	37.92	0.04	21.11	29.50	1.09	3.84	7.37	100.87	2.98	0.00	1.96	1.94	0.07	0.45	0.62	8.03
116	608	37.54	0.13	21.45	29.54	1.10	3.81	7.09	100.66	2.96	0.01	1.99	1.95	0.07	0.45	0.60	8.03
117	684	37.53	0.09	21.48	29.05	1.04	3.63	7.32	100.14	2.97	0.01	2.00	1.92	0.07	0.43	0.62	8.02
9704-7134 - Garnet 3																	
118	0	37.72	0.00	21.64	29.55	1.10	3.85	7.26	101.11	2.96	0.00	2.00	1.94	0.07	0.45	0.61	8.04
119	108	37.64	0.03	21.56	29.17	1.14	3.84	7.09	100.47	2.97	0.00	2.00	1.92	0.08	0.45	0.60	8.03
120	216	37.43	0.10	21.59	29.54	1.05	3.83	6.92	100.46	2.96	0.01	2.01	1.95	0.07	0.45	0.59	8.03
121	324	37.81	0.12	21.45	29.27	1.12	3.76	7.10	100.62	2.98	0.01	1.99	1.93	0.07	0.44	0.60	8.02
122	432	37.54	0.16	21.29	29.22	1.14	3.73	7.49	100.58	2.96	0.01	1.98	1.93	0.08	0.44	0.63	8.04
123	540	37.34	0.26	21.34	29.07	1.08	3.68	7.52	100.29	2.96	0.02	1.99	1.92	0.07	0.43	0.64	8.03
124	648	37.60	0.13	21.50	29.07	1.08	3.71	7.46	100.55	2.97	0.01	2.00	1.92	0.07	0.44	0.63	8.03
125	756	37.47	0.14	21.50	29.49	1.05	3.79	7.24	100.68	2.96	0.01	2.00	1.95	0.07	0.45	0.61	8.04
126	864	37.64	0.14	21.27	29.55	1.05	3.71	7.17	100.52	2.97	0.01	1.98	1.95	0.07	0.44	0.61	8.03
127	972	37.41	0.02	21.41	29.46	1.00	3.72	7.23	100.25	2.96	0.00	2.00	1.95	0.07	0.44	0.61	8.04

Appendix 3.2 (continued) - Garnet Mineral Chemistry

No.	Distance μm	Weight Percent						Cation Total O = 12.0								
		SiO ₂	TiO ₂	Al ₂ O ₃	FeO	MnO	MgO	CaO	Total	Si	Ti	Al	Fe	Mn	Mg	Ca
9704-7086 - Garnet 1																
128	0	37.91	0.07	21.93	33.62	0.64	5.19	1.76	101.11	2.97	0.00	2.03	2.21	0.04	0.61	0.15
129	166	37.70	0.01	21.73	32.89	0.62	4.76	2.99	100.70	2.97	0.00	2.02	2.17	0.04	0.56	0.25
130	332	37.80	0.05	21.67	32.37	0.63	4.68	3.72	100.92	2.97	0.00	2.01	2.13	0.04	0.55	0.31
131	498	38.05	0.08	21.76	32.16	0.61	4.63	3.96	101.24	2.98	0.00	2.01	2.11	0.04	0.54	0.33
132	664	38.19	0.02	21.57	32.00	0.62	4.52	3.93	100.85	3.00	0.00	2.00	2.10	0.04	0.53	0.33
133	830	37.69	0.02	21.82	32.20	0.63	4.71	3.38	100.45	2.97	0.00	2.03	2.12	0.04	0.55	0.29
134	996	38.06	0.00	21.68	32.40	0.66	4.61	3.72	101.13	2.99	0.00	2.00	2.13	0.04	0.54	0.31
135	1162	37.94	0.04	21.70	32.87	0.60	4.73	3.11	100.97	2.98	0.00	2.01	2.16	0.04	0.55	0.26
136	1328	37.91	0.02	21.78	33.53	0.70	4.99	2.13	101.06	2.98	0.00	2.02	2.20	0.05	0.58	0.18
137	1494	37.71	0.07	21.59	34.23	0.68	5.18	1.48	100.92	2.97	0.00	2.01	2.26	0.05	0.61	0.12
9704-7086 - Garnet 2																
138	0	37.88	0.03	21.89	34.17	0.66	5.43	1.19	101.24	2.97	0.00	2.02	2.24	0.04	0.63	0.10
139	173	37.69	0.00	21.69	33.70	0.63	5.34	1.32	100.37	2.98	0.00	2.02	2.23	0.04	0.63	0.11
140	346	37.90	0.01	21.79	33.52	0.68	5.30	1.41	100.61	2.99	0.00	2.02	2.21	0.05	0.62	0.12
141	519	37.96	0.02	21.87	33.81	0.71	5.20	1.34	100.91	2.98	0.00	2.03	2.22	0.05	0.61	0.11
142	692	37.69	0.12	21.82	34.18	0.63	5.38	1.23	101.05	2.96	0.01	2.02	2.25	0.04	0.63	0.10
143	865	37.69	0.00	21.58	34.26	0.67	5.21	1.18	100.59	2.98	0.00	2.01	2.27	0.04	0.61	0.10
144	1038	37.81	0.00	21.71	34.18	0.65	5.35	1.16	100.85	2.98	0.00	2.02	2.25	0.04	0.63	0.10
145	1211	38.04	0.08	21.75	33.97	0.65	5.23	1.13	100.84	2.99	0.00	2.02	2.23	0.04	0.61	0.09
146	1384	37.72	0.00	21.78	34.11	0.65	5.32	1.14	100.72	2.97	0.00	2.02	2.25	0.04	0.62	0.10
147	1557	36.86	0.03	21.90	34.15	0.63	5.37	1.11	100.05	2.93	0.00	2.05	2.27	0.04	0.64	0.09

Appendix 3.2 (continued) - Garnet Mineral Chemistry

No.	Distance μm	SiO ₂	TiO ₂	Al ₂ O ₃	Weight Percent				Total	Cation Total O = 12.0				Total
					FeO	MnO	MgO	CaO		Si	Ti	Al	Fe	
9704-7086 - Garnet 3														
148	0	37.59	0.06	21.69	33.70	0.79	5.43	1.25	100.50	2.97	0.00	2.02	2.23	0.05
149	93	37.76	0.00	21.55	33.86	0.72	5.38	1.32	100.58	2.98	0.00	2.01	2.24	0.05
150	186	38.06	0.00	21.82	34.05	0.73	5.55	1.21	101.42	2.98	0.00	2.01	2.23	0.05
151	279	38.00	0.00	21.79	34.01	0.78	5.54	1.13	101.24	2.98	0.00	2.01	2.23	0.05
152	372	37.71	0.00	21.96	33.92	0.76	5.46	1.23	101.04	2.96	0.00	2.03	2.23	0.05
153	465	38.05	0.12	21.99	33.82	0.67	5.38	1.15	101.17	2.98	0.01	2.03	2.21	0.04
154	558	37.74	0.02	21.85	34.70	0.73	4.96	1.21	101.22	2.97	0.00	2.03	2.28	0.05
155	651	37.36	0.02	22.00	34.02	0.72	5.37	1.15	100.63	2.95	0.00	2.05	2.25	0.05
156	744	37.87	0.02	21.85	34.01	0.78	5.41	1.20	101.13	2.97	0.00	2.02	2.23	0.05
157	837	38.00	0.01	21.87	34.36	0.72	5.22	1.26	101.43	2.98	0.00	2.02	2.25	0.05
GAR03 - Garnet 1														
158	0	37.52	0.00	21.70	35.23	0.78	4.28	0.90	100.41	2.98	0.00	2.03	2.34	0.05
159	143	37.41	0.05	21.76	35.73	0.83	4.40	0.85	101.02	2.96	0.00	2.03	2.37	0.06
160	286	37.25	0.00	21.69	35.76	0.88	4.21	0.96	100.75	2.96	0.00	2.03	2.38	0.06
161	429	36.88	0.09	21.72	35.55	0.82	4.37	0.96	100.37	2.95	0.01	2.04	2.37	0.06
163	715	37.25	0.00	21.68	35.04	0.87	4.55	0.95	100.35	2.97	0.00	2.03	2.33	0.06
164	858	37.34	0.00	21.37	35.18	0.82	4.64	0.99	100.34	2.98	0.00	2.01	2.35	0.06
165	1001	37.58	0.07	21.53	34.97	0.84	4.58	0.88	100.45	2.99	0.00	2.02	2.32	0.06
166	1144	37.37	0.18	21.65	35.10	0.82	4.60	0.84	100.56	2.97	0.01	2.03	2.33	0.06
167	1287	37.77	0.00	21.59	35.10	0.85	4.70	0.92	100.93	2.99	0.00	2.01	2.32	0.06

Appendix 3.2 (continued) - Garnet Mineral Chemistry

No.	Distance μm	Weight Percent						Cation Total O = 12.0									
		SiO ₂	TiO ₂	Al ₂ O ₃	FeO	MnO	MgO	CaO	Total	Si	Ti	Al	Fe	Mn	Mg	Ca	Total
GAR03 - Garnet 2																	
168	0	36.63	0.04	21.76	36.15	0.75	4.04	0.98	100.34	2.94	0.00	2.06	2.42	0.05	0.48	0.08	8.03
169	147	37.89	0.07	21.58	35.95	0.78	4.27	0.91	101.44	2.99	0.00	2.01	2.37	0.05	0.50	0.08	8.00
170	294	37.44	0.11	21.59	35.40	0.78	4.38	0.93	100.63	2.98	0.01	2.02	2.35	0.05	0.52	0.08	8.01
171	441	37.18	0.04	21.57	35.88	0.73	4.20	0.98	100.57	2.96	0.00	2.03	2.39	0.05	0.50	0.08	8.02
172	588	37.47	0.03	21.65	36.21	0.76	4.16	0.96	101.23	2.97	0.00	2.02	2.40	0.05	0.49	0.08	8.02
173	735	37.16	0.07	21.71	35.60	0.77	4.46	0.95	100.73	2.96	0.00	2.03	2.37	0.05	0.53	0.08	8.02
174	882	37.62	0.12	21.82	35.87	0.75	4.37	0.98	101.53	2.97	0.01	2.03	2.37	0.05	0.51	0.08	8.01
175	1029	37.48	0.05	21.76	35.62	0.79	4.30	1.04	101.04	2.97	0.00	2.03	2.36	0.05	0.51	0.09	8.01
176	1176	37.58	0.00	21.71	35.64	0.79	4.41	1.02	101.14	2.97	0.00	2.02	2.36	0.05	0.52	0.09	8.01
177	1323	37.42	0.02	21.48	35.65	0.73	4.44	1.03	100.77	2.97	0.00	2.01	2.37	0.05	0.53	0.09	8.02
GAR03 - Garnet 3																	
178	0	37.50	0.02	21.78	35.87	0.70	4.30	0.98	101.14	2.97	0.00	2.03	2.37	0.05	0.51	0.08	8.01
179	143	37.37	0.04	21.53	35.82	0.70	4.16	1.23	100.83	2.97	0.00	2.02	2.38	0.05	0.49	0.10	8.02
180	286	37.15	0.02	21.64	35.97	0.66	4.24	1.35	101.02	2.95	0.00	2.03	2.39	0.04	0.50	0.11	8.03
181	429	37.82	0.03	21.61	35.79	0.68	4.13	1.48	101.56	2.98	0.00	2.01	2.36	0.05	0.49	0.13	8.01
182	572	37.40	0.04	21.76	35.82	0.70	4.13	1.40	101.25	2.96	0.00	2.03	2.37	0.05	0.49	0.12	8.02
183	715	37.47	0.00	21.56	35.65	0.65	4.22	1.36	100.90	2.97	0.00	2.02	2.37	0.04	0.50	0.12	8.02
184	858	37.52	0.01	21.58	35.74	0.67	4.30	1.21	101.02	2.97	0.00	2.02	2.37	0.04	0.51	0.10	8.02
185	1001	37.30	0.00	21.67	35.89	0.66	4.26	1.04	100.83	2.97	0.00	2.03	2.39	0.04	0.50	0.09	8.02
186	1144	37.42	0.00	21.69	36.32	0.69	4.24	1.10	101.46	2.96	0.00	2.02	2.40	0.05	0.50	0.09	8.03
187	1287	37.44	0.00	21.50	36.16	0.68	4.15	0.95	100.88	2.98	0.00	2.02	2.40	0.05	0.49	0.08	8.02

Appendix 3.2 (continued) - Garnet Mineral Chemistry

No.	Distance μm	Weight Percent						Cation Total O = 12.0								
		SiO ₂	TiO ₂	Al ₂ O ₃	FeO	MnO	CaO	Total	Si	Ti	Al	Fe	Mn	Mg	Ca	Total
9704-7054 - Garnet 1																
188	0	37.56	0.02	21.18	32.40	0.70	3.55	5.18	100.59	2.98	0.00	1.98	2.15	0.05	0.42	0.44
189	188	37.33	0.03	21.22	33.69	0.83	2.53	5.11	100.75	2.98	0.00	2.00	2.25	0.06	0.30	0.44
190	376	37.65	0.02	21.31	32.25	0.68	3.41	5.18	100.51	2.99	0.00	1.99	2.14	0.05	0.40	0.44
191	564	37.56	0.06	21.24	32.15	0.72	3.48	5.20	100.41	2.98	0.00	1.99	2.14	0.05	0.41	0.44
192	752	37.79	0.08	20.99	32.58	0.72	3.36	5.11	100.63	3.00	0.00	1.96	2.16	0.05	0.40	0.43
193	940	37.56	0.00	21.12	32.39	0.70	3.45	5.15	100.38	2.99	0.00	1.98	2.16	0.05	0.41	0.44
194	1128	37.54	0.05	21.39	32.34	0.63	3.55	5.18	100.67	2.98	0.00	2.00	2.14	0.04	0.42	0.44
195	1316	37.55	0.04	21.14	32.89	0.73	3.16	5.05	100.56	2.99	0.00	1.98	2.19	0.05	0.38	0.43
196	1504	37.46	0.00	21.34	32.42	0.76	3.48	5.10	100.56	2.98	0.00	2.00	2.15	0.05	0.41	0.43
197	1692	37.24	0.00	21.14	32.70	0.70	3.43	5.20	100.41	2.97	0.00	1.99	2.18	0.05	0.41	0.44
9704-7054 - Garnet 2																
198	0	37.39	0.05	21.18	32.18	0.69	3.49	5.12	100.12	2.98	0.00	1.99	2.15	0.05	0.42	0.44
199	170	37.51	0.00	21.17	32.36	0.72	3.43	5.15	100.34	2.99	0.00	1.99	2.15	0.05	0.41	0.44
200	340	37.64	0.06	21.25	32.32	0.71	3.61	5.17	100.76	2.98	0.00	1.98	2.14	0.05	0.43	0.44
201	510	37.55	0.03	21.42	32.61	0.75	3.21	5.06	100.62	2.98	0.00	2.00	2.17	0.05	0.38	0.43
202	680	37.63	0.00	21.29	32.17	0.71	3.58	5.16	100.53	2.99	0.00	1.99	2.13	0.05	0.42	0.44
203	850	37.48	0.00	21.28	32.60	0.72	3.41	5.12	100.62	2.98	0.00	1.99	2.17	0.05	0.40	0.44
204	1020	37.42	0.00	21.29	32.13	0.71	3.41	5.11	100.06	2.98	0.00	2.00	2.14	0.05	0.41	0.44
205	1190	37.56	0.00	21.18	31.82	0.76	3.58	4.99	99.89	2.99	0.00	1.99	2.12	0.05	0.43	0.43
206	1360	37.45	0.02	20.98	33.02	0.75	2.96	5.13	100.30	2.99	0.00	1.98	2.21	0.05	0.35	0.44
207	1530	37.62	0.02	21.36	32.61	0.69	3.42	5.15	100.86	2.98	0.00	1.99	2.16	0.05	0.40	0.44

Appendix 3.2 (continued) - Garnet Mineral Chemistry

No.	Distance μm	Weight Percent						Total	Cation Total O = 12.0								
		SiO ₂	TiO ₂	Al ₂ O ₃	FeO	MnO	MgO		Si	Ti	Al	Fe	Mn	Mg	Ca		
9704-7054 - Garnet 3																	
208	0	37.44	0.00	21.18	32.24	0.65	3.58	5.44	100.54	2.98	0.00	1.98	2.14	0.04	0.42	0.46	8.03
209	128	37.43	0.00	20.96	32.12	0.71	3.44	5.43	100.09	2.99	0.00	1.97	2.14	0.05	0.41	0.46	8.03
210	256	37.15	0.04	21.13	32.33	0.71	3.26	5.43	100.04	2.97	0.00	1.99	2.16	0.05	0.39	0.47	8.03
211	384	37.24	0.09	21.15	32.30	0.71	3.56	5.40	100.45	2.96	0.01	1.99	2.15	0.05	0.42	0.46	8.04
212	512	37.45	0.05	21.09	32.11	0.72	3.52	5.48	100.42	2.98	0.00	1.98	2.14	0.05	0.42	0.47	8.03
213	640	37.60	0.03	21.08	32.00	0.72	3.51	5.40	100.33	2.99	0.00	1.98	2.13	0.05	0.42	0.46	8.02
214	768	37.39	0.01	21.27	31.77	0.70	3.53	5.35	100.00	2.98	0.00	2.00	2.12	0.05	0.42	0.46	8.02
215	896	37.58	0.06	21.22	31.96	0.69	3.42	5.58	100.50	2.98	0.00	1.99	2.12	0.05	0.41	0.47	8.02
216	1024	37.52	0.00	21.23	32.04	0.71	3.64	5.48	100.63	2.98	0.00	1.99	2.13	0.05	0.43	0.47	8.03
217	1152	37.31	0.05	21.02	31.44	0.71	3.62	5.46	99.62	2.98	0.00	1.98	2.10	0.05	0.43	0.47	8.02
Minimum		10.44	0.00	8.62	10.37	0.31	1.50	0.40	52.26	1.90	0.00	1.85	0.63	0.02	0.29	0.04	7.97
Maximum		41.74	0.43	23.31	37.62	2.46	18.40	15.18	101.56	3.01	0.02	2.06	3.84	0.32	1.98	1.24	9.17
Average		37.43	0.05	21.43	31.71	1.02	4.17	4.52	100.31	2.97	0.00	2.00	2.11	0.07	0.49	0.38	8.03
Sigma		2.02	0.06	0.96	3.75	0.51	1.82	2.93	3.40	0.08	0.00	0.02	0.28	0.04	0.20	0.25	0.08
No. of data		217															

Appendix 3.3 - Plagioclase Mineral Chemistry

No.	Distance μm	SiO ₂	Al ₂ O ₃	Weight Percent				K ₂ O Total	Si Total	Cation Total O = 8.0					
				FeO	CaO	Na ₂ O	K ₂ O Total			Al	Fe	Ca	Na	K	
9704-7069 - Plagioclase 1															
3	0	53.41	28.90	0.12	11.38	5.05	0.20	99.05	2.44	1.56	0.00	0.56	0.45	0.01	5.01
4	94	54.17	28.68	0.10	10.90	5.27	0.20	99.33	2.46	1.54	0.00	0.53	0.46	0.01	5.01
5	188	54.02	27.64	0.61	10.20	5.33	0.21	98.02	2.49	1.50	0.02	0.50	0.48	0.01	5.01
6	282	54.95	28.27	0.08	10.32	5.52	0.21	99.35	2.49	1.51	0.00	0.50	0.49	0.01	5.00
7	376	54.99	28.05	0.07	10.30	5.69	0.24	99.34	2.49	1.50	0.00	0.50	0.50	0.01	5.01
8	470	55.24	28.25	0.06	10.04	5.77	0.22	99.59	2.50	1.51	0.00	0.49	0.51	0.01	5.01
9	564	54.77	28.02	0.09	10.10	5.88	0.19	99.05	2.49	1.50	0.00	0.49	0.52	0.01	5.02
10	658	54.84	28.34	0.10	10.34	5.63	0.18	99.43	2.49	1.51	0.00	0.50	0.49	0.01	5.01
12	846	53.93	28.70	0.05	10.99	5.51	0.10	99.28	2.45	1.54	0.00	0.54	0.49	0.01	5.02
9704-7069 - Plagioclase 2															
14	79	53.63	29.26	0.07	11.37	5.00	0.13	99.46	2.44	1.57	0.00	0.55	0.44	0.01	5.01
15	158	53.87	28.79	0.08	11.00	5.40	0.13	99.27	2.45	1.54	0.00	0.54	0.48	0.01	5.02
16	237	54.15	28.66	0.09	10.74	5.37	0.09	99.10	2.46	1.54	0.00	0.52	0.47	0.01	5.01
17	316	54.31	29.07	0.07	11.12	5.14	0.12	99.83	2.45	1.55	0.00	0.54	0.45	0.01	5.00
18	395	53.91	29.20	0.06	11.39	5.19	0.12	99.86	2.44	1.56	0.00	0.55	0.46	0.01	5.01
19	474	53.34	29.00	0.07	11.56	4.96	0.11	99.05	2.43	1.56	0.00	0.57	0.44	0.01	5.01
20	553	53.16	29.13	0.08	11.60	4.82	0.13	98.91	2.43	1.57	0.00	0.57	0.43	0.01	5.00
21	632	53.36	29.30	0.12	11.41	4.86	0.14	99.18	2.43	1.57	0.00	0.56	0.43	0.01	5.00
22	711	51.91	29.73	0.30	12.20	4.51	0.07	98.71	2.39	1.61	0.01	0.60	0.40	0.00	5.01

Appendix 3.3 (continued) - Plagioclase Mineral Chemistry

No.	Distance μm	Plagioclase 3				Weight Percent				Cation Total O = 8.0					
		SiO ₂	Al ₂ O ₃	FeO	CaO	Na ₂ O	K ₂ O	Total	Si	Al	Fe	Ca	Na	K	
9704-7069 - Plagioclase 3															
23	0	53.32	29.46	0.48	11.54	4.64	0.26	99.70	2.42	1.58	0.02	0.56	0.41	0.02	5.00
24	93	52.96	29.55	0.13	11.67	4.66	0.15	99.11	2.42	1.59	0.00	0.57	0.41	0.01	5.00
25	186	53.81	29.00	0.11	11.21	5.11	0.15	99.40	2.45	1.55	0.00	0.55	0.45	0.01	5.01
26	279	54.05	29.01	0.09	11.19	5.33	0.16	99.83	2.45	1.55	0.00	0.54	0.47	0.01	5.02
27	372	54.09	28.96	0.06	11.00	5.18	0.15	99.45	2.45	1.55	0.00	0.53	0.46	0.01	5.00
28	465	54.28	28.57	0.06	10.71	5.40	0.19	99.21	2.47	1.53	0.00	0.52	0.48	0.01	5.01
29	558	54.56	28.64	0.09	10.90	5.34	0.14	99.67	2.47	1.53	0.00	0.53	0.47	0.01	5.01
30	651	54.17	28.78	0.07	11.07	5.19	0.17	99.44	2.46	1.54	0.00	0.54	0.46	0.01	5.01
31	744	53.69	28.99	0.05	11.35	4.98	0.15	99.21	2.44	1.56	0.00	0.55	0.44	0.01	5.00
32	837	53.00	29.12	0.27	11.67	4.72	0.10	98.89	2.42	1.57	0.01	0.57	0.42	0.01	5.00
9704-7142D - Plagioclase 1															
33	0	56.84	27.02	0.31	8.64	6.69	0.16	99.64	2.56	1.44	0.01	0.42	0.58	0.01	5.02
34	26	56.83	26.67	0.19	8.69	6.48	0.21	99.07	2.57	1.42	0.01	0.42	0.57	0.01	5.01
35	52	55.93	27.27	0.12	9.24	6.24	0.19	98.98	2.54	1.46	0.00	0.45	0.55	0.01	5.01
36	78	55.30	27.36	0.11	9.65	5.86	0.18	98.46	2.53	1.47	0.00	0.47	0.52	0.01	5.00
37	104	55.31	27.46	0.08	9.79	5.87	0.22	98.73	2.52	1.48	0.00	0.48	0.52	0.01	5.01
38	130	54.89	26.62	0.11	6.94	4.59	2.94	96.08	2.57	1.47	0.00	0.35	0.42	0.18	4.99
40	182	55.13	27.52	0.07	9.64	5.76	0.20	98.33	2.52	1.48	0.00	0.47	0.51	0.01	5.00
41	208	55.57	27.51	0.08	9.69	5.90	0.25	99.01	2.52	1.47	0.00	0.47	0.52	0.01	5.01
42	234	55.92	26.98	0.29	8.11	6.21	0.85	98.36	2.56	1.45	0.01	0.40	0.55	0.05	5.02

Appendix 3.3 (continued) - Plagioclase Mineral Chemistry

No.	Distance μm	SiO ₂	Al ₂ O ₃	Weight Percent				Cation Total O = 8.0				9704-7142D - Plagioclase 2			
				FeO	CaO	Na ₂ O	K ₂ O	Total	Si	Al	Fe	Ca			
43	0	52.70	29.09	0.16	11.67	4.71	0.17	98.50	2.42	1.58	0.01	0.57	0.42	0.01	5.01
45	128	53.38	28.42	0.08	11.22	4.97	0.25	98.31	2.45	1.54	0.00	0.55	0.44	0.01	5.01
46	192	53.06	28.46	0.07	11.03	5.21	0.22	98.04	2.45	1.55	0.00	0.55	0.47	0.01	5.02
47	256	53.98	28.45	0.08	10.75	5.22	0.20	98.68	2.47	1.53	0.00	0.53	0.46	0.01	5.00
48	320	53.71	28.48	0.08	10.94	5.02	0.21	98.43	2.46	1.54	0.00	0.54	0.45	0.01	5.00
49	384	53.63	28.51	0.06	10.96	4.97	0.20	98.33	2.46	1.54	0.00	0.54	0.44	0.01	5.00
50	448	53.22	28.84	0.06	11.33	4.91	0.21	98.56	2.44	1.56	0.00	0.56	0.44	0.01	5.01
51	512	53.02	29.30	0.08	11.48	4.78	0.19	98.85	2.42	1.58	0.00	0.56	0.42	0.01	5.00
52	576	52.99	29.14	0.05	11.61	4.70	0.20	98.68	2.43	1.57	0.00	0.57	0.42	0.01	5.00
9704-7142D - Plagioclase 3															
53	0	52.69	29.41	0.23	11.93	4.57	0.19	99.02	2.41	1.59	0.01	0.58	0.41	0.01	5.01
54	71	53.16	28.54	0.15	11.17	4.90	0.30	98.22	2.45	1.55	0.01	0.55	0.44	0.02	5.01
58	355	52.39	28.78	0.07	11.29	4.75	0.28	97.55	2.43	1.57	0.00	0.56	0.43	0.02	5.01
59	426	54.23	28.27	0.09	10.25	5.04	1.00	98.88	2.48	1.52	0.00	0.50	0.45	0.06	5.01
60	497	54.41	28.98	0.09	10.92	5.27	0.15	99.81	2.46	1.54	0.00	0.53	0.46	0.01	5.00
61	568	55.94	26.11	0.36	8.60	6.36	0.14	97.52	2.57	1.42	0.01	0.42	0.57	0.01	5.01
62	639	56.85	26.53	0.29	8.33	6.70	0.17	98.86	2.58	1.42	0.01	0.40	0.59	0.01	5.01

Appendix 3.3 (continued) - Plagioclase Mineral Chemistry

No.	Distance μm	Weight Percent						Cation Total O = 8.0						
		SiO ₂	Al ₂ O ₃	FeO	CaO	Na ₂ O	K ₂ O	Total	Si	Al	Fe	Ca	Na	K
Garnetite GR - Plagioclase 1														
63	0	61.01	24.05	0.29	3.99	8.40	0.94	98.69	2.75	1.28	0.01	0.19	0.73	0.05
64	56	60.96	23.13	0.04	4.33	8.30	1.17	97.93	2.77	1.24	0.00	0.21	0.73	0.07
65	112	61.41	23.63	0.06	4.85	9.04	0.15	99.14	2.75	1.25	0.00	0.23	0.78	0.01
66	168	61.76	23.31	0.02	4.47	9.41	0.10	99.06	2.76	1.23	0.00	0.21	0.82	0.01
67	224	61.10	23.19	0.01	4.31	9.29	0.08	97.97	2.76	1.24	0.00	0.21	0.82	0.00
68	280	62.08	23.40	0.00	4.25	9.33	0.07	99.14	2.77	1.23	0.00	0.20	0.81	0.00
69	336	61.97	23.78	0.01	4.19	9.21	0.16	99.32	2.76	1.25	0.00	0.20	0.80	0.01
70	392	62.35	23.26	0.02	4.30	9.34	0.10	99.37	2.78	1.22	0.00	0.21	0.81	0.01
71	448	62.06	23.36	0.04	4.07	9.27	0.11	98.91	2.78	1.23	0.00	0.20	0.80	0.01
72	504	62.78	23.13	0.00	3.90	9.26	0.12	99.19	2.80	1.21	0.00	0.19	0.80	0.01
Garnetite GR - Plagioclase 2														
73	0	62.23	22.99	0.03	4.20	9.36	0.08	98.88	2.79	1.21	0.00	0.20	0.81	0.00
74	95	60.67	24.29	0.02	5.63	8.24	0.33	99.19	2.72	1.28	0.00	0.27	0.72	0.02
75	190	60.31	24.50	0.03	5.74	8.17	0.31	99.06	2.71	1.30	0.00	0.28	0.71	0.02
76	285	60.86	24.09	0.00	5.35	8.52	0.22	99.05	2.73	1.27	0.00	0.26	0.74	0.01
77	380	60.88	23.92	0.01	5.28	8.55	0.17	98.81	2.73	1.27	0.00	0.25	0.74	0.01
78	475	60.83	24.13	0.01	5.45	8.41	0.19	99.00	2.73	1.28	0.00	0.26	0.73	0.01
79	570	61.43	24.03	0.01	5.14	8.61	0.11	99.31	2.74	1.26	0.00	0.25	0.74	0.01
80	665	62.21	23.17	0.01	4.18	9.25	0.11	98.93	2.78	1.22	0.00	0.20	0.80	0.01
81	760	61.06	24.13	0.00	5.17	8.70	0.12	99.17	2.73	1.27	0.00	0.25	0.75	0.01
82	855	61.94	23.48	0.04	4.46	9.07	0.23	99.22	2.77	1.24	0.00	0.21	0.79	0.01

Appendix 3.3 (continued) - Plagioclase Mineral Chemistry

No.	Distance μm	Weight Percent						Cation Total O = 8.0						
		SiO ₂	Al ₂ O ₃	FeO	CaO	Na ₂ O	K ₂ O	Total	Si	Al	Fe	Ca	Na	K
Garnetite GR - Plagioclase 3														
83	0	59.26	24.90	0.07	6.37	7.95	0.14	98.68	2.68	1.32	0.00	0.31	0.70	0.01
84	84	58.96	24.15	0.04	5.94	8.02	0.25	97.35	2.70	1.30	0.00	0.29	0.71	0.01
85	168	60.07	24.44	0.04	5.75	8.23	0.17	98.70	2.71	1.30	0.00	0.28	0.72	0.01
86	252	59.81	23.86	0.07	5.71	8.33	0.29	98.06	2.72	1.28	0.00	0.28	0.73	0.02
87	336	60.70	23.79	0.02	5.10	8.54	0.36	98.51	2.74	1.26	0.00	0.25	0.75	0.02
88	420	61.70	23.52	0.06	4.64	8.76	0.37	99.04	2.76	1.24	0.00	0.22	0.76	0.02
89	504	61.12	23.51	0.03	5.04	8.68	0.31	98.69	2.75	1.25	0.00	0.24	0.76	0.02
90	588	61.40	23.68	0.02	4.97	8.83	0.23	99.14	2.75	1.25	0.00	0.24	0.77	0.01
91	672	61.79	23.63	0.03	4.73	9.09	0.13	99.40	2.76	1.24	0.00	0.23	0.79	0.01
92	756	61.40	23.68	0.06	4.66	9.00	0.10	98.90	2.75	1.25	0.00	0.22	0.78	0.01
9704-7134 - Plagioclase 1														
93	0	56.15	27.77	0.17	4.91	6.02	2.61	97.62	2.58	1.50	0.01	0.24	0.54	0.15
94	145	53.66	28.97	0.03	11.37	4.99	0.15	99.16	2.44	1.56	0.00	0.55	0.44	0.01
95	290	54.09	28.45	0.00	10.82	5.46	0.09	98.92	2.47	1.53	0.00	0.53	0.48	0.01
96	435	54.50	28.50	0.02	10.47	5.56	0.10	99.14	2.48	1.53	0.00	0.51	0.49	0.01
97	580	53.94	29.02	0.02	11.09	5.08	0.17	99.31	2.45	1.55	0.00	0.54	0.45	0.01
98	725	55.41	26.75	0.43	7.95	5.59	1.33	97.45	2.56	1.46	0.02	0.39	0.50	0.08
99	870	55.69	25.81	0.14	7.44	4.48	3.73	97.30	2.59	1.42	0.01	0.37	0.40	0.22
101	1160	53.49	28.93	0.01	11.26	5.02	0.10	98.81	2.44	1.56	0.00	0.55	0.45	0.01
102	1305	53.17	28.94	0.01	10.86	4.87	0.43	98.29	2.44	1.57	0.00	0.53	0.43	0.03

Appendix 3.3 (continued) - Plagioclase Mineral Chemistry

No.	Distance μm	SiO ₂	Al ₂ O ₃	Weight Percent				K ₂ O	Total	Si	Cation Total O = 8.0				
				FeO	CaO	Na ₂ O	K ₂ O				Al	Fe	Ca	Na	K
9704-7134 - Plagioclase 2															
103	0	56.09	27.67	0.10	8.00	6.07	1.00	98.92	2.55	1.48	0.00	0.39	0.53	0.06	5.01
104	0	53.65	29.04	0.05	11.22	4.93	0.15	99.04	2.44	1.56	0.00	0.55	0.44	0.01	5.00
105	0	53.72	29.16	0.00	11.39	5.05	0.12	99.43	2.44	1.56	0.00	0.55	0.44	0.01	5.01
106	0	53.23	28.93	0.01	11.28	5.08	0.19	98.73	2.44	1.56	0.00	0.55	0.45	0.01	5.01
107	0	53.20	29.00	0.03	11.44	5.07	0.17	98.90	2.43	1.56	0.00	0.56	0.45	0.01	5.02
108	0	53.44	29.24	0.03	11.25	5.04	0.12	99.12	2.43	1.57	0.00	0.55	0.45	0.01	5.01
112	0	53.24	28.84	0.08	11.08	4.94	0.26	98.44	2.44	1.56	0.00	0.54	0.44	0.02	5.00
9704-7086 - Plagioclase 1															
113	0	59.75	25.18	0.02	6.64	7.80	0.23	99.62	2.67	1.33	0.00	0.32	0.68	0.01	5.01
114	127	59.93	24.50	0.01	5.98	8.21	0.16	98.80	2.70	1.30	0.00	0.29	0.72	0.01	5.01
115	254	61.04	24.10	0.00	5.38	8.67	0.15	99.35	2.73	1.27	0.00	0.26	0.75	0.01	5.02
116	381	61.16	24.00	0.06	5.18	8.73	0.18	99.30	2.73	1.26	0.00	0.25	0.76	0.01	5.02
117	508	61.24	23.95	0.04	5.13	8.84	0.19	99.38	2.74	1.26	0.00	0.25	0.77	0.01	5.02
118	635	62.16	22.98	0.25	3.23	5.81	5.32	99.75	2.80	1.22	0.01	0.16	0.51	0.31	5.00
119	762	60.97	23.92	0.17	5.03	8.82	0.18	99.08	2.73	1.26	0.01	0.24	0.77	0.01	5.02
120	889	61.33	23.77	0.04	5.10	8.69	0.09	99.00	2.75	1.25	0.00	0.24	0.75	0.01	5.01
121	1016	61.47	23.77	0.05	5.09	8.77	0.10	99.25	2.75	1.25	0.00	0.24	0.76	0.01	5.01
122	1143	60.13	24.61	0.33	5.87	8.41	0.09	99.44	2.69	1.30	0.01	0.28	0.73	0.01	5.02

Appendix 3.3 (continued) - Plagioclase Mineral Chemistry

No.	Distance μm	SiO ₂	Al ₂ O ₃	Weight Percent				K ₂ O	Total	Cation Total O = 8.0			
				FeO	CaO	Na ₂ O	K ₂ O			Si	Al	Fe	Ca
9704-7086 - Plagioclase 2													
123	0	60.81	23.98	0.03	5.24	8.62	0.10	98.78	2.73	1.27	0.00	0.25	0.75
124	80	60.44	24.41	0.00	5.89	8.23	0.11	99.08	2.71	1.29	0.00	0.28	0.72
125	160	61.35	24.03	0.01	5.15	8.80	0.13	99.47	2.74	1.26	0.00	0.25	0.76
126	240	61.58	23.99	0.04	5.12	8.53	0.29	99.54	2.74	1.26	0.00	0.24	0.74
127	320	61.48	23.94	0.02	5.12	8.67	0.18	99.39	2.74	1.26	0.00	0.24	0.75
128	400	61.21	23.82	0.05	4.94	8.97	0.14	99.12	2.74	1.26	0.00	0.24	0.78
129	480	61.38	23.92	0.07	4.99	8.83	0.08	99.26	2.74	1.26	0.00	0.24	0.76
130	560	60.90	24.11	0.13	4.94	8.68	0.19	98.96	2.73	1.27	0.00	0.24	0.76
131	640	61.45	24.26	0.09	5.42	8.44	0.14	99.80	2.73	1.27	0.00	0.26	0.73
132	720	60.83	24.21	0.16	5.52	8.34	0.08	99.14	2.72	1.28	0.01	0.26	0.72
9704-7086 - Plagioclase 3													
133	0	60.27	24.67	0.33	5.85	8.41	0.10	99.61	2.70	1.30	0.01	0.28	0.73
134	56	61.13	25.22	0.07	5.65	8.24	0.30	100.62	2.70	1.31	0.00	0.27	0.71
135	112	60.75	24.28	0.04	5.70	8.52	0.12	99.40	2.72	1.28	0.00	0.27	0.74
136	168	60.63	24.36	0.05	5.67	8.26	0.10	99.06	2.72	1.29	0.00	0.27	0.72
137	224	60.37	24.50	0.02	5.80	8.27	0.21	99.17	2.71	1.29	0.00	0.28	0.72
138	280	60.38	24.51	0.03	5.93	8.24	0.18	99.28	2.70	1.29	0.00	0.28	0.72
139	336	60.86	24.28	0.05	5.53	8.50	0.15	99.37	2.72	1.28	0.00	0.27	0.74
140	392	67.40	20.23	0.15	4.29	6.76	1.03	99.86	2.95	1.05	0.01	0.20	0.57
141	448	60.25	23.95	0.24	4.03	5.68	4.74	98.89	2.74	1.28	0.01	0.20	0.50
142	504	60.14	24.67	0.31	5.80	8.60	0.13	99.64	2.69	1.30	0.01	0.28	0.75

Appendix 3.3 (continued) - Plagioclase Mineral Chemistry

No.	Distance μm	SiO ₂	Al ₂ O ₃	Weight Percent				K ₂ O Total	Si Total	Cation Total O = 8.0					
				FeO	CaO	Na ₂ O	Al			Fe	Ca	Na	K		
<i>GAR03 - Plagioclase 1</i>															
143	0	60.65	23.80	0.10	4.75	8.81	0.15	98.26	2.74	1.27	0.00	0.23	0.77	0.01	5.02
144	61	62.47	23.08	0.02	4.02	9.33	0.11	99.03	2.79	1.21	0.00	0.19	0.81	0.01	5.01
145	122	62.27	23.01	0.02	4.19	9.15	0.11	98.74	2.79	1.21	0.00	0.20	0.79	0.01	5.00
146	183	59.86	25.85	0.02	4.29	8.51	0.18	98.70	2.68	1.37	0.00	0.21	0.74	0.01	5.01
147	244	62.52	23.27	0.00	3.92	9.30	0.09	99.10	2.79	1.22	0.00	0.19	0.80	0.01	5.01
148	305	62.61	23.27	0.02	3.96	9.41	0.10	99.37	2.79	1.22	0.00	0.19	0.81	0.01	5.01
149	366	62.38	23.42	0.09	4.26	9.44	0.09	99.68	2.77	1.23	0.00	0.20	0.81	0.01	5.02
150	427	62.07	23.50	0.12	4.65	8.97	0.06	99.37	2.77	1.23	0.00	0.22	0.78	0.00	5.01
151	488	61.60	23.67	0.30	4.81	8.93	0.09	99.39	2.75	1.25	0.01	0.23	0.77	0.00	5.02
152	549	61.22	23.91	0.61	4.99	8.85	0.07	99.67	2.73	1.26	0.02	0.24	0.77	0.00	5.02
<i>GAR03 - Plagioclase 2</i>															
153	0	62.28	23.54	0.04	4.19	9.28	0.07	99.39	2.77	1.23	0.00	0.20	0.80	0.00	5.01
154	69	62.17	23.08	0.06	4.21	9.03	0.16	98.70	2.79	1.22	0.00	0.20	0.78	0.01	5.00
155	138	62.64	23.03	0.01	4.14	9.33	0.17	99.31	2.79	1.21	0.00	0.20	0.81	0.01	5.01
156	207	63.02	22.48	0.04	3.55	9.82	0.09	99.00	2.81	1.18	0.00	0.17	0.85	0.01	5.02
157	276	62.65	22.96	0.01	3.88	9.53	0.16	99.19	2.79	1.21	0.00	0.19	0.82	0.01	5.02
158	345	62.19	23.01	0.04	3.80	8.42	1.45	98.90	2.79	1.22	0.00	0.18	0.73	0.08	5.01
159	414	62.82	22.98	0.02	4.03	9.45	0.08	99.38	2.80	1.20	0.00	0.19	0.81	0.00	5.01
160	483	61.83	22.96	0.04	4.28	9.20	0.13	98.44	2.78	1.22	0.00	0.21	0.80	0.01	5.02
161	552	62.18	23.75	0.02	4.62	8.86	0.24	99.67	2.76	1.24	0.00	0.22	0.76	0.01	5.00
162	621	61.56	24.03	0.14	5.16	8.62	0.12	99.63	2.74	1.26	0.01	0.25	0.74	0.01	5.00

Appendix 3.3 (continued) - Plagioclase Mineral Chemistry

No.	Distance μm	Weight Percent						Cation Total O = 8.0						
		SiO ₂	Al ₂ O ₃	FeO	CaO	Na ₂ O	K ₂ O	Total	Si	Al	Fe	Ca	Na	K
GAR03 - Plagioclase 3														
163	0	62.56	23.85	0.00	4.41	9.17	0.09	100.08	2.77	1.24	0.00	0.21	0.79	0.01
164	92	61.80	23.67	0.01	4.43	9.00	0.16	99.06	2.76	1.25	0.00	0.21	0.78	0.01
165	184	61.95	23.55	0.00	4.50	8.91	0.09	99.00	2.77	1.24	0.00	0.22	0.77	0.01
166	276	64.68	21.86	0.01	2.67	10.26	0.05	99.53	2.86	1.14	0.00	0.13	0.88	0.00
167	368	60.59	24.26	0.08	5.62	8.47	0.09	99.11	2.72	1.28	0.00	0.27	0.74	0.01
168	460	60.31	24.50	0.03	5.70	8.49	0.15	99.17	2.70	1.29	0.00	0.27	0.74	0.01
169	552	58.90	26.13	0.10	2.18	6.99	3.42	97.72	2.69	1.40	0.00	0.11	0.62	0.20
170	644	61.93	23.74	0.00	4.75	8.89	0.07	99.37	2.76	1.25	0.00	0.23	0.77	0.00
171	736	61.36	23.72	0.03	4.74	8.88	0.16	98.89	2.75	1.25	0.00	0.23	0.77	0.01
172	828	62.20	23.20	0.07	4.39	8.96	0.07	98.88	2.78	1.22	0.00	0.21	0.78	0.00
Minimum		0.00	0.00	0.00	0.00	0.00	0.00	0.00	0.00	0.00	0.00	0.00	0.00	4.77
Maximum		67.40	29.73	12.39	12.56	10.26	9.34	100.62	3.18	4.66	0.65	0.80	1.83	2.25
Average		57.24	25.39	0.20	7.28	6.92	0.45	97.48	2.61	1.38	0.01	0.36	0.62	0.05
Sigma		7.37	4.11	1.01	3.12	2.10	1.04	10.81	0.25	0.32	0.05	0.16	0.20	0.24
No. of data		172												

Appendix 3.4 - Clinopyroxene Mineral Chemistry

No.	μ_m	Distance	Weight Percent						Cation Total O = 6.0												
			SiO ₂	TiO ₂	Al ₂ O ₃	Cr ₂ O ₃	FeO	MnO	MgO	CaO	Na ₂ O	Total	Si	Ti	Al	Cr	Fe	Mn	Mg	Ca	Na
9704-7069 - Clinopyroxene 1																					
13	0	51.97	0.05	1.63	0.03	13.44	0.13	10.93	21.47	0.37	100.01	1.97	0.00	0.07	0.00	0.43	0.00	0.62	0.87	0.03	4.00
14	114	50.87	0.31	2.19	0.00	14.95	0.13	9.74	21.40	0.46	100.06	1.95	0.01	0.10	0.00	0.48	0.00	0.56	0.88	0.03	4.01
15	228	50.49	0.20	2.35	0.03	15.14	0.17	9.55	21.28	0.45	99.66	1.95	0.01	0.11	0.00	0.49	0.01	0.55	0.88	0.03	4.01
16	342	50.66	0.23	2.48	0.02	14.86	0.15	9.41	21.92	0.44	100.17	1.94	0.01	0.11	0.00	0.48	0.01	0.54	0.90	0.03	4.01
17	456	50.49	0.22	2.37	0.02	15.08	0.18	9.34	21.66	0.48	99.84	1.94	0.01	0.11	0.00	0.49	0.01	0.54	0.89	0.04	4.01
18	570	50.56	0.29	2.22	0.02	16.09	0.18	9.52	20.37	0.40	99.66	1.95	0.01	0.10	0.00	0.52	0.01	0.55	0.84	0.03	4.01
19	684	51.19	0.12	1.62	0.03	14.18	0.16	10.15	21.68	0.39	99.51	1.97	0.00	0.07	0.00	0.46	0.01	0.58	0.89	0.03	4.01
20	798	50.54	0.25	2.19	0.00	15.24	0.17	9.44	21.65	0.41	99.89	1.95	0.01	0.10	0.00	0.49	0.01	0.54	0.89	0.03	4.01
21	912	50.40	0.26	2.35	0.03	15.66	0.20	9.28	21.54	0.39	100.12	1.94	0.01	0.11	0.00	0.50	0.01	0.53	0.89	0.03	4.01
22	1026	51.18	0.17	1.68	0.02	14.49	0.18	9.96	21.62	0.43	99.71	1.96	0.00	0.08	0.00	0.47	0.01	0.57	0.89	0.03	4.01
9704-7069-Clinopyroxene 2																					
23	0	51.63	0.02	1.29	0.02	13.62	0.14	10.64	22.02	0.43	99.80	1.97	0.00	0.06	0.00	0.44	0.00	0.61	0.90	0.03	4.01
24	134	51.24	0.14	1.95	0.00	14.74	0.15	10.06	21.40	0.48	100.14	1.96	0.00	0.09	0.00	0.47	0.00	0.57	0.88	0.04	4.01
25	268	50.55	0.17	2.20	0.00	15.10	0.22	9.52	21.56	0.44	99.74	1.95	0.00	0.10	0.00	0.49	0.01	0.55	0.89	0.03	4.01
27	536	49.95	0.28	2.45	0.04	15.35	0.17	9.38	21.83	0.41	99.86	1.93	0.01	0.11	0.00	0.50	0.01	0.54	0.90	0.03	4.02
29	804	52.11	0.06	1.05	0.01	12.90	0.16	11.10	21.70	0.22	99.30	1.99	0.00	0.05	0.00	0.41	0.01	0.63	0.89	0.02	3.99
30	938	50.58	0.31	2.17	0.03	14.57	0.17	9.66	21.85	0.47	99.79	1.94	0.01	0.10	0.00	0.47	0.01	0.55	0.90	0.03	4.01
31	1072	50.77	0.18	2.05	0.01	14.89	0.19	9.48	21.87	0.41	99.86	1.95	0.01	0.09	0.00	0.48	0.01	0.54	0.90	0.03	4.01
32	1206	50.47	0.03	2.06	0.02	13.46	0.15	10.48	21.76	0.37	98.80	1.95	0.00	0.09	0.00	0.43	0.00	0.60	0.90	0.03	4.02

Appendix 3.4 (continued) - Clinopyroxene Mineral Chemistry

No.	μ_m	Distance	Weight Percent						Cation Total O = 6.0												
			SiO ₂	TiO ₂	Al ₂ O ₃	Cr ₂ O ₃	FeO	MnO	MgO	CaO	Na ₂ O	Total	Si	Ti	Al	Cr	Fe	Mn	Mg	Ca	Na
9704-7142D-Clinopyroxene 1																					
33	0	49.59	0.21	2.54	0.05	15.02	0.37	10.10	19.97	0.39	98.24	1.94	0.01	0.12	0.00	0.49	0.01	0.59	0.84	0.03	4.01
34	136	49.97	0.20	2.59	0.03	14.30	0.43	9.90	21.25	0.52	99.19	1.93	0.01	0.12	0.00	0.46	0.01	0.57	0.88	0.04	4.02
35	272	50.68	0.22	2.29	0.06	14.07	0.38	10.15	21.52	0.46	99.84	1.94	0.01	0.10	0.00	0.45	0.01	0.58	0.88	0.03	4.02
36	408	50.22	0.17	2.39	0.02	14.30	0.44	9.91	21.58	0.48	99.50	1.94	0.00	0.11	0.00	0.46	0.01	0.57	0.89	0.04	4.02
38	680	50.34	0.23	2.12	0.07	13.79	0.39	10.08	21.74	0.46	99.22	1.94	0.01	0.10	0.00	0.45	0.01	0.58	0.90	0.03	4.02
39	816	50.08	0.23	1.95	0.05	14.72	0.41	10.11	20.87	0.43	98.85	1.94	0.01	0.09	0.00	0.48	0.01	0.59	0.87	0.03	4.02
40	952	50.39	0.18	2.11	0.02	13.91	0.39	10.13	21.51	0.47	99.11	1.95	0.01	0.10	0.00	0.45	0.01	0.58	0.89	0.03	4.02
41	1088	50.68	0.25	2.16	0.07	13.81	0.40	10.09	21.41	0.47	99.34	1.95	0.01	0.10	0.00	0.44	0.01	0.58	0.88	0.03	4.01
42	1224	50.40	0.08	1.89	0.07	13.58	0.30	10.87	20.85	0.39	98.44	1.95	0.00	0.09	0.00	0.44	0.01	0.63	0.87	0.03	4.02
9704-7142D-Clinopyroxene 2																					
43	0	50.86	0.21	2.09	0.07	12.99	0.45	10.42	21.71	0.49	99.27	1.95	0.01	0.09	0.00	0.42	0.01	0.60	0.89	0.04	4.01
44	156	50.54	0.23	2.51	0.05	13.59	0.52	10.16	21.45	0.45	99.50	1.94	0.01	0.11	0.00	0.44	0.02	0.58	0.88	0.03	4.01
45	312	50.78	0.20	2.00	0.10	13.72	0.48	10.46	21.38	0.45	99.56	1.95	0.01	0.09	0.00	0.44	0.02	0.60	0.88	0.03	4.02
46	468	50.88	0.20	2.19	0.05	13.85	0.45	10.24	21.20	0.42	99.48	1.95	0.01	0.10	0.00	0.44	0.01	0.59	0.87	0.03	4.01
47	624	50.54	0.16	2.25	0.06	13.08	0.36	10.72	20.69	0.44	98.31	1.95	0.00	0.10	0.00	0.42	0.01	0.62	0.86	0.03	4.01
49	936	51.06	0.13	1.88	0.06	13.32	0.40	10.72	21.34	0.44	99.34	1.96	0.00	0.09	0.00	0.43	0.01	0.61	0.88	0.03	4.01
50	1092	50.81	0.26	2.42	0.02	15.85	0.35	10.62	17.37	0.38	98.09	1.97	0.01	0.11	0.00	0.51	0.01	0.61	0.72	0.03	3.98
51	1248	49.76	0.24	3.92	0.05	13.76	0.42	9.75	20.88	0.50	99.28	1.91	0.01	0.18	0.00	0.44	0.01	0.56	0.86	0.04	4.01
52	1404	50.89	0.18	2.11	0.07	13.21	0.40	10.28	21.85	0.41	99.40	1.95	0.01	0.10	0.00	0.42	0.01	0.59	0.90	0.03	4.01

Appendix 3.4 (continued) - Clinopyroxene Mineral Chemistry

No.	Distance μ_m	Weight Percent						Cation Total O = 6.0													
		SiO ₂	TiO ₂	Al ₂ O ₃	Cr ₂ O ₃	FeO	MnO	MgO	CaO	Na ₂ O	Total	Si	Ti	Al	Cr	Fe	Mn	Mg	Ca	Na	Total
9704-7142D-Clinopyroxene 3																					
53	0	48.66	0.19	3.19	0.05	15.67	0.43	10.79	17.87	0.37	97.22	1.92	0.01	0.15	0.00	0.52	0.01	0.63	0.75	0.03	4.02
54	164	50.35	0.44	2.70	0.03	14.15	0.40	9.86	21.16	0.47	99.56	1.93	0.01	0.12	0.00	0.45	0.01	0.57	0.87	0.04	4.01
55	328	49.88	0.34	2.84	0.05	14.06	0.46	9.80	20.81	0.51	98.74	1.93	0.01	0.13	0.00	0.46	0.02	0.57	0.86	0.04	4.01
56	492	50.56	0.18	2.28	0.06	13.91	0.42	9.97	21.65	0.48	99.52	1.94	0.01	0.10	0.00	0.45	0.01	0.57	0.89	0.04	4.02
57	656	50.62	0.24	2.69	0.02	14.04	0.39	9.94	21.44	0.50	99.88	1.94	0.01	0.12	0.00	0.45	0.01	0.57	0.88	0.04	4.01
58	820	49.29	0.31	2.99	0.04	14.22	0.40	9.52	21.27	0.50	98.53	1.92	0.01	0.14	0.00	0.46	0.01	0.55	0.89	0.04	4.02
59	984	50.65	0.22	1.88	0.01	14.11	0.49	9.78	21.84	0.21	99.19	1.96	0.01	0.09	0.00	0.46	0.02	0.56	0.90	0.02	4.00
60	1148	50.21	0.26	2.68	0.03	14.17	0.42	9.99	20.96	0.42	99.13	1.94	0.01	0.12	0.00	0.46	0.01	0.57	0.87	0.03	4.01
61	1312	44.38	0.11	13.26	0.04	13.45	0.32	9.80	16.92	0.32	98.61	1.70	0.00	0.60	0.00	0.43	0.01	0.56	0.69	0.02	4.01
9704-7134-Clinopyroxene 1																					
74	84	48.20	0.11	7.39	0.10	17.01	0.26	10.88	12.36	0.54	96.85	1.88	0.00	0.34	0.00	0.55	0.01	0.63	0.52	0.04	3.97
76	252	51.04	0.22	2.09	0.08	10.81	0.22	12.34	21.28	0.26	98.34	1.95	0.01	0.09	0.00	0.35	0.01	0.70	0.87	0.02	4.00
77	336	50.19	0.24	1.89	0.07	11.77	0.13	11.73	22.06	0.39	98.48	1.93	0.01	0.09	0.00	0.38	0.00	0.67	0.91	0.03	4.03
78	420	50.94	0.18	2.17	0.07	11.68	0.20	11.21	21.73	0.40	98.57	1.95	0.01	0.10	0.00	0.37	0.01	0.64	0.89	0.03	4.01
79	504	48.50	0.30	2.75	0.08	11.94	0.20	11.50	21.27	0.41	96.95	1.90	0.01	0.13	0.00	0.39	0.01	0.67	0.89	0.03	4.04
81	672	50.98	0.14	2.00	0.02	11.36	0.17	11.06	21.93	0.26	97.91	1.97	0.00	0.09	0.00	0.37	0.01	0.64	0.91	0.02	3.99
82	756	42.60	0.07	21.34	0.04	9.14	0.07	4.54	20.26	0.09	98.15	1.60	0.00	0.95	0.00	0.29	0.00	0.25	0.82	0.01	3.92

Appendix 3.4 (continued) - Clinopyroxene Mineral Chemistry

No.	μ_m	Distance	Weight Percent						Cation Total O = 6.0												
			SiO ₂	TiO ₂	Al ₂ O ₃	Cr ₂ O ₃	FeO	MnO	MgO	CaO	Na ₂ O	Total	Si	Ti	Al	Cr	Fe	Mn	Mg	Ca	Na
9704-7134-Clinopyroxene 2																					
83	0	50.78	0.22	4.87	0.15	17.90	0.36	10.83	11.85	0.47	97.42	1.96	0.01	0.22	0.00	0.58	0.01	0.62	0.49	0.03	3.94
85	180	49.17	0.19	5.57	0.09	17.93	0.30	10.38	11.98	0.53	96.14	1.93	0.01	0.26	0.00	0.59	0.01	0.61	0.50	0.04	3.95
86	270	49.91	0.17	5.26	0.08	17.65	0.38	10.88	11.80	0.55	96.66	1.95	0.00	0.24	0.00	0.58	0.01	0.63	0.49	0.04	3.95
87	360	50.55	0.09	4.81	0.00	18.25	0.45	10.79	11.89	0.48	97.31	1.96	0.00	0.22	0.00	0.59	0.01	0.62	0.49	0.04	3.94
88	450	50.33	0.25	5.46	0.05	17.79	0.38	11.08	11.66	0.48	97.47	1.94	0.01	0.25	0.00	0.57	0.01	0.64	0.48	0.04	3.94
91	720	50.39	0.21	5.54	0.11	17.63	0.43	11.26	11.67	0.62	97.85	1.94	0.01	0.25	0.00	0.57	0.01	0.65	0.48	0.05	3.95
92	810	49.70	0.40	5.77	0.11	17.89	0.44	10.94	11.55	0.62	97.42	1.92	0.01	0.26	0.00	0.58	0.01	0.63	0.48	0.05	3.95
Minimum		0.00	0.00	0.00	0.00	0.01	0.02	0.00	0.00	0.00	1.60	0.00	0.05	0.00	0.29	0.00	0.25	0.48	0.01	3.92	
Maximum		88.14	1.33	22.91	0.15	18.25	0.52	14.54	49.91	2.18	100.27	1.99	0.01	0.95	0.00	0.59	0.02	0.70	0.91	0.05	4.04
Average		48.70	0.19	3.30	0.04	13.74	0.27	9.63	18.89	0.40	95.16	1.93	0.01	0.15	0.00	0.47	0.01	0.59	0.82	0.03	4.00
Sigma		10.38	0.16	3.63	0.03	3.52	0.13	2.82	6.48	0.24	15.24	0.06	0.00	0.14	0.00	0.06	0.00	0.06	0.14	0.01	0.03
No. of data		92																			

Appendix 3.5 - Orthopyroxene Mineral Chemistry

No.	μ_m	Distance	Weight percent						Cation Total O = 6.0										
			SiO ₂	TiO ₂	Al ₂ O ₃	Cr ₂ O ₃	FeO	MnO	MgO	CaO	Total	Si	Ti	Al	Cr	Fe	Mn	Mg	Ca
9704-7069 - Orthopyroxene 1																			
3	0	49.84	0.03	0.64	0.00	33.31	0.29	14.31	0.41	98.83	1.98	0.00	0.03	0.00	1.11	0.01	0.85	0.02	4.00
4	98	49.48	0.00	0.70	0.00	33.24	0.34	14.50	0.56	98.81	1.97	0.00	0.03	0.00	1.11	0.01	0.86	0.02	4.01
5	196	49.65	0.03	0.77	0.01	33.94	0.39	13.90	0.52	99.20	1.98	0.00	0.04	0.00	1.13	0.01	0.82	0.02	4.00
6	294	49.10	0.06	0.73	0.02	34.29	0.34	13.75	0.57	98.86	1.97	0.00	0.03	0.00	1.15	0.01	0.82	0.02	4.01
7	392	49.24	0.04	0.72	0.00	33.81	0.40	13.68	0.47	98.36	1.98	0.00	0.03	0.00	1.14	0.01	0.82	0.02	4.00
8	490	49.27	0.00	1.59	0.03	33.45	0.35	13.57	0.52	98.78	1.96	0.00	0.07	0.00	1.12	0.01	0.81	0.02	4.00
9	588	49.44	0.02	0.64	0.02	34.06	0.37	13.79	0.51	98.84	1.98	0.00	0.03	0.00	1.14	0.01	0.82	0.02	4.01
10	686	49.65	0.06	0.70	0.00	33.05	0.35	14.20	0.58	98.57	1.98	0.00	0.03	0.00	1.10	0.01	0.84	0.02	4.00
11	784	49.31	0.03	0.73	0.03	33.23	0.46	14.31	0.49	98.59	1.97	0.00	0.03	0.00	1.11	0.02	0.85	0.02	4.01
12	882	49.30	0.02	0.73	0.03	33.61	0.43	13.85	0.48	98.47	1.98	0.00	0.03	0.00	1.13	0.01	0.83	0.02	4.00
9704-7069 - Orthopyroxene 2																			
13	0	49.61	0.13	0.73	0.00	34.18	0.43	13.25	0.65	98.98	1.98	0.00	0.03	0.00	1.14	0.01	0.79	0.03	4.00
14	48	49.75	0.00	0.82	0.02	34.38	0.40	13.31	0.65	99.32	1.98	0.00	0.04	0.00	1.15	0.01	0.79	0.03	4.00
15	96	49.66	0.00	0.86	0.02	34.54	0.40	13.45	0.61	99.53	1.98	0.00	0.04	0.00	1.15	0.01	0.80	0.03	4.00
16	144	49.60	0.07	0.74	0.01	34.21	0.38	13.47	0.66	99.14	1.98	0.00	0.04	0.00	1.14	0.01	0.80	0.03	4.00
17	192	50.14	0.04	0.69	0.00	34.20	0.36	13.54	0.55	99.51	1.99	0.00	0.03	0.00	1.13	0.01	0.80	0.02	3.99
18	240	48.37	0.04	0.63	0.03	34.07	0.42	13.42	0.67	97.64	1.97	0.00	0.03	0.00	1.16	0.01	0.81	0.03	4.02
19	288	50.52	0.01	0.73	0.03	32.55	0.40	13.47	2.34	100.04	1.99	0.00	0.03	0.00	1.07	0.01	0.79	0.10	4.00
20	336	50.11	0.11	0.72	0.01	33.70	0.38	13.89	0.63	99.54	1.98	0.00	0.03	0.00	1.12	0.01	0.82	0.03	4.00
21	384	50.42	0.07	0.66	0.00	34.40	0.38	13.74	0.64	100.30	1.99	0.00	0.03	0.00	1.13	0.01	0.81	0.03	4.00
22	432	50.35	0.00	0.68	0.01	34.16	0.40	13.75	0.63	99.99	1.99	0.00	0.03	0.00	1.13	0.01	0.81	0.03	4.00

Appendix 3.5 (continued) - Orthopyroxene Mineral Chemistry

No.	μ_m	Distance	Weight percent						Cation Total O = 6.0										
			SiO ₂	TiO ₂	Al ₂ O ₃	Cr ₂ O ₃	FeO	MnO	MgO	CaO	Total	Si	Ti	Al	Cr	Fe	Mn	Mg	Ca
9704-7069 - Orthopyroxene 3																			
23	0	49.97	0.00	0.60	0.00	33.76	0.38	13.70	0.48	98.90	1.99	0.00	0.03	0.00	1.13	0.01	0.81	0.02	3.99
24	62	49.95	0.02	0.89	0.00	33.78	0.35	13.77	0.64	99.40	1.98	0.00	0.04	0.00	1.12	0.01	0.81	0.03	4.00
25	124	49.97	0.05	0.70	0.02	34.17	0.41	13.61	0.65	99.58	1.98	0.00	0.03	0.00	1.13	0.01	0.80	0.03	4.00
26	186	50.59	0.00	0.66	0.00	33.49	0.37	13.77	1.28	100.16	1.99	0.00	0.03	0.00	1.10	0.01	0.81	0.05	4.00
27	248	50.38	0.08	0.74	0.00	34.16	0.37	13.71	0.54	99.97	1.99	0.00	0.03	0.00	1.13	0.01	0.81	0.02	3.99
28	310	50.11	0.02	0.65	0.00	34.45	0.38	13.60	0.58	99.80	1.99	0.00	0.03	0.00	1.14	0.01	0.80	0.02	4.00
29	372	50.48	0.08	0.56	0.00	34.17	0.39	13.66	0.56	99.90	1.99	0.00	0.03	0.00	1.13	0.01	0.80	0.02	3.99
30	434	49.59	0.07	0.66	0.04	33.92	0.44	13.98	0.58	99.28	1.97	0.00	0.03	0.00	1.13	0.01	0.83	0.02	4.01
31	496	50.07	0.05	0.70	0.01	33.68	0.39	13.86	0.63	99.39	1.99	0.00	0.03	0.00	1.12	0.01	0.82	0.03	4.00
32	558	50.60	0.03	0.79	0.00	33.96	0.41	13.77	0.54	100.09	1.99	0.00	0.04	0.00	1.12	0.01	0.81	0.02	3.99
9704-7142D - Orthopyroxene 1																			
33	0	49.72	0.06	1.01	0.02	33.03	0.89	13.68	0.66	99.05	1.98	0.00	0.05	0.00	1.10	0.03	0.81	0.03	4.00
34	60	50.34	0.05	1.03	0.01	33.17	0.89	14.01	0.63	100.12	1.98	0.00	0.05	0.00	1.09	0.03	0.82	0.03	4.00
35	120	49.26	0.14	0.99	0.02	32.72	0.97	14.20	0.57	98.87	1.96	0.00	0.05	0.00	1.09	0.03	0.84	0.02	4.01
36	180	50.18	0.03	0.87	0.03	32.91	0.90	14.50	0.50	99.93	1.98	0.00	0.04	0.00	1.08	0.03	0.85	0.02	4.00
37	240	50.70	0.00	0.60	0.04	33.29	0.87	14.28	0.57	100.35	1.99	0.00	0.03	0.00	1.09	0.03	0.83	0.02	4.00
38	300	51.04	0.12	0.79	0.02	32.87	0.91	14.23	0.69	100.66	1.99	0.00	0.04	0.00	1.07	0.03	0.83	0.03	3.99
39	360	50.33	0.14	1.12	0.06	33.22	0.97	13.85	0.68	100.36	1.98	0.00	0.05	0.00	1.09	0.03	0.81	0.03	3.99
40	420	50.59	0.05	1.12	0.03	32.81	0.94	14.14	0.71	100.39	1.98	0.00	0.05	0.00	1.07	0.03	0.82	0.03	3.99
41	480	50.29	0.03	1.08	0.00	33.07	0.91	14.09	0.59	100.06	1.98	0.00	0.05	0.00	1.09	0.03	0.83	0.02	4.00
42	540	49.81	0.02	1.09	0.00	32.87	0.95	14.04	0.61	99.39	1.97	0.00	0.05	0.00	1.09	0.03	0.83	0.03	4.00

Appendix 3.5 (continued) - Orthopyroxene Mineral Chemistry

No.	μ_m	Distance	Weight percent						Si	Ti	Al	Cr	Fe	Mn	Mg	Ca	Total	Cation Total O = 6.0	
			SiO ₂	TiO ₂	Al ₂ O ₃	Cr ₂ O ₃	FeO	MnO											
9704-7142D - Orthopyroxene 2																			
43	0	50.25	0.06	0.89	0.01	33.59	1.01	13.83	0.54	100.17	1.98	0.00	0.04	0.00	1.11	0.03	0.81	0.02	4.00
44	131	50.05	0.01	0.95	0.01	33.60	0.95	13.58	0.56	99.71	1.98	0.00	0.04	0.00	1.11	0.03	0.80	0.02	4.00
45	262	49.85	0.12	0.84	0.01	33.46	1.01	13.66	0.57	99.53	1.98	0.00	0.04	0.00	1.11	0.03	0.81	0.02	4.00
46	393	50.25	0.07	0.86	0.01	33.51	1.00	13.69	0.64	100.04	1.98	0.00	0.04	0.00	1.11	0.03	0.81	0.03	4.00
47	524	50.00	0.06	0.70	0.01	33.81	1.01	13.47	0.53	99.57	1.99	0.00	0.03	0.00	1.12	0.03	0.80	0.02	4.00
48	655	50.29	0.14	0.85	0.02	33.80	1.00	13.68	0.55	100.31	1.98	0.00	0.04	0.00	1.11	0.03	0.80	0.02	4.00
49	786	49.95	0.02	0.84	0.02	34.13	1.04	13.95	0.57	100.51	1.97	0.00	0.04	0.00	1.12	0.03	0.82	0.02	4.01
50	917	49.58	0.03	0.92	0.04	34.00	1.04	13.35	0.57	99.51	1.97	0.00	0.04	0.00	1.13	0.04	0.79	0.02	4.00
51	1048	49.16	0.00	0.89	0.02	34.02	0.96	13.35	0.51	98.92	1.97	0.00	0.04	0.00	1.14	0.03	0.80	0.02	4.01
52	1179	49.84	0.06	0.98	0.02	33.96	1.11	13.52	0.63	100.12	1.97	0.00	0.05	0.00	1.12	0.04	0.80	0.03	4.00
9704-7142D - Orthopyroxene 3																			
53	0	50.06	0.04	0.86	0.06	32.90	0.99	13.82	0.57	99.29	1.98	0.00	0.04	0.00	1.09	0.03	0.82	0.02	3.99
54	100	50.10	0.04	0.94	0.03	33.26	0.98	13.65	0.59	99.58	1.98	0.00	0.04	0.00	1.10	0.03	0.81	0.02	3.99
55	200	50.03	0.00	0.65	0.00	33.29	1.04	13.65	1.07	99.72	1.98	0.00	0.03	0.00	1.10	0.03	0.81	0.05	4.00
56	300	49.65	0.12	0.86	0.00	33.21	0.96	13.79	0.76	99.34	1.97	0.00	0.04	0.00	1.10	0.03	0.82	0.03	4.00
57	400	49.37	0.05	0.84	0.02	33.57	1.00	13.49	0.64	98.99	1.97	0.00	0.04	0.00	1.12	0.03	0.80	0.03	4.00
58	500	50.19	0.07	0.74	0.00	33.61	1.07	13.75	0.56	99.98	1.98	0.00	0.03	0.00	1.11	0.04	0.81	0.02	4.00
59	600	49.65	0.10	0.83	0.03	33.64	0.98	13.55	0.61	99.37	1.98	0.00	0.04	0.00	1.12	0.03	0.80	0.03	4.00
60	700	49.53	0.10	0.97	0.01	33.54	1.07	13.48	0.67	99.36	1.97	0.00	0.05	0.00	1.12	0.04	0.80	0.03	4.00
61	800	49.18	0.05	0.96	0.01	33.71	0.99	13.39	0.71	99.00	1.97	0.00	0.05	0.00	1.13	0.03	0.80	0.03	4.01
62	900	49.34	0.12	0.95	0.02	33.45	0.98	13.56	0.59	99.00	1.97	0.00	0.04	0.00	1.12	0.03	0.81	0.03	4.00

Appendix 3.5 (continued) - Orthopyroxene Mineral Chemistry

	Weight percent										Cation Total O = 6.0							
	SiO ₂	TiO ₂	Al ₂ O ₃	Cr ₂ O ₃	FeO	MnO	MgO	CaO	Total	Si	Ti	Al	Cr	Fe	Mn	Mg	Ca	Total
Minimum	48.37	0.00	0.56	0.00	14.61	0.29	13.25	0.41	97.64	1.96	0.00	0.03	0.00	0.44	0.01	0.79	0.02	3.98
Maximum	55.04	0.14	1.59	0.76	34.54	1.11	26.75	2.34	100.66	1.99	0.00	0.07	0.02	1.16	0.04	1.44	0.10	4.02
Average	50.05	0.05	0.83	0.04	33.02	0.68	14.18	0.65	99.49	1.98	0.00	0.04	0.00	1.09	0.02	0.83	0.03	4.00
Sigma	1.02	0.04	0.18	0.13	3.41	0.30	2.32	0.27	0.61	0.01	0.00	0.01	0.00	0.12	0.01	0.11	0.01	0.01
No. of data	62																	

Appendix 3.6 - Accessory Mineral Chemistry

No.	Weight percent						Cation Total O = 3.0						
	TiO ₂	SiO ₂	Nb ₂ O ₅	FeO	MnO	MgO	Total	Ti	Si	Nb	Fe	Mn	Mg
9704-7134-Ilmenite													
1	53.61	0.00	0.03	42.26	4.18	0.16	100.23	1.010	0.000	0.885	0.089	0.006	1.990
2	53.63	0.02	0.00	42.40	4.06	0.13	100.23	1.010	0.000	0.888	0.086	0.005	1.990
3	53.50	0.03	0.02	41.97	4.12	0.10	99.74	1.012	0.001	0.883	0.088	0.004	1.987
4	53.41	0.02	0.00	42.70	4.03	0.10	100.26	1.007	0.001	0.890	0.086	0.004	1.992
5	53.55	0.05	0.05	42.51	4.21	0.11	100.48	1.007	0.001	0.889	0.089	0.004	1.991
GarnetiteGR-Ilmenite													
6	52.43	0.02	0.00	47.31	0.12	0.15	100.02	0.996	0.001	0.000	0.999	0.003	0.006
7	52.30	0.00	0.13	47.38	0.14	0.16	100.10	0.993	0.000	0.001	1.001	0.003	0.006
8	51.63	0.00	0.00	47.29	0.23	0.12	99.27	0.991	0.000	0.000	1.009	0.005	0.005
9	51.76	0.05	0.03	47.05	0.42	0.05	99.36	0.992	0.001	0.000	1.003	0.009	0.002
10	51.71	0.06	0.00	47.45	0.25	0.05	99.51	0.990	0.002	0.000	1.010	0.005	0.002
GarnetiteGR - Rutile													
11	98.58	0.00	0.00	0.85	0.04	0.02	99.49	1.492	0.000	0.000	0.014	0.001	1.508
12	97.71	0.03	0.00	0.92	0.01	0.04	98.71	1.491	0.001	0.000	0.016	0.000	0.001

Appendix 3.6 (continued) - Accessory Mineral Chemistry

No.	TiO ₂	SiO ₂	Nb ₂ O ₅	FeO	MnO	MgO	Total	Ti	Si	Cation Total O = 3.0				
										Nb	Fe	Mn	Mg	Total
9704-7086-Ilmenite														
13	52.25	0.00	0.05	46.85	0.13	0.30	99.58	0.996	0.000	0.001	0.993	0.003	0.011	2.003
14	51.53	0.00	0.00	46.73	0.17	0.19	98.62	0.994	0.000	0.000	1.002	0.004	0.007	2.007
15	52.41	0.04	0.00	46.62	0.22	0.23	99.53	0.998	0.001	0.000	0.988	0.005	0.009	2.001
9704-7054-Ilmenite														
16	51.08	0.01	0.02	47.30	0.42	0.11	98.94	0.985	0.000	0.000	1.015	0.009	0.004	2.014
17	51.34	0.02	0.00	46.67	0.49	0.08	98.61	0.992	0.001	0.000	1.002	0.011	0.003	2.008
18	50.79	0.04	0.00	48.26	0.43	0.08	99.59	0.977	0.001	0.000	1.032	0.009	0.003	2.022
GAR03-Ilmenite														
19	52.83	0.04	0.00	47.41	0.14	0.07	100.48	0.998	0.001	0.000	0.996	0.003	0.003	2.001
20	51.68	0.04	0.05	47.77	0.12	0.11	99.77	0.987	0.001	0.001	1.015	0.003	0.004	2.011

Appendix 4 - Geochronologic Data

Appendix 4.1 - Sm-Nd Analyses

Sample Number	Rock Type	Sm ppm	Nd ppm	$^{147}\text{Sm}/^{144}\text{Nd}$	$^{143}\text{Nd}/^{144}\text{Nd}$	uncert. $2\sigma_{\text{sm}} +/-$	T_{DM}	$\sim T(\text{Ma})$	ε_{NdT} (2.7 Ga)
97-03-6365	quartzofeldspathic gneiss	3.09	17.69	0.1055	0.510925	0.000008	3.13	2700	-1.7
97-03-6372	augen gneiss	8.48	56.01	0.0915	0.510396	0.000005	3.42	2700	-7.2
97-03-6392	layered granodiorite gneiss	0.78	4.49	0.1045	0.510654	0.000005	3.47	2700	-6.7
97-03-6247	granodiorite gneiss	1.17	7.29	0.0971	0.510457	0.000008	3.51	2700	-8.0
97-03-8101	leucogranite	2.37	13.87	0.1032	0.510741	0.000005	3.32	2700	-4.5
97-03-6590	tonalite	7.35	56.49	0.0786	0.510374	0.000004	3.13	2700	-3.2

Appendix 4.2 - Monazite Analyses

Sample Garnetite GR

No.	L _a 2O ₃ (wt %)	Ce ₂ O ₃ (wt %)	Pr ₂ O ₃ (wt %)	Nd ₂ O ₃ (wt %)	Sm ₂ O ₃ (wt %)	Gd ₂ O ₃ (wt %)	Y ₂ O ₃ (wt %)	SiO ₂ (wt %)	CaO (wt %)	P ₂ O ₅ (wt %)	ThO ₂ (wt %)
3	17.4	33.1	3.4	12.2	1.8	0.3	0.1	0.1	0.8	29.8	1.4
4	13.9	28.3	3.0	12.8	2.1	0.7	0.1	0.3	1.8	29.7	7.2
5	13.8	28.7	3.0	12.9	2.1	0.7	0.2	0.2	1.6	29.5	6.1
6	17.8	29.1	2.6	9.8	1.4	0.2	0.0	0.4	2.0	29.4	6.3
8	16.0	28.4	2.7	10.6	1.7	0.3	0.1	0.5	2.0	28.7	6.7
9	14.6	31.7	3.5	15.0	2.4	0.6	0.1	0.1	0.6	29.6	2.3
10	14.7	31.6	3.8	14.9	2.4	0.7	0.1	0.2	0.6	29.5	2.2
12	14.4	31.2	3.5	15.0	2.4	0.7	0.1	0.1	0.7	29.2	2.4
13	14.7	31.3	3.4	15.0	2.4	0.6	0.1	0.1	0.6	29.3	2.3
14	14.6	31.4	3.5	14.8	2.4	0.6	0.1	0.1	0.7	29.4	2.4
15	14.6	31.2	3.4	14.6	2.4	0.6	0.1	0.1	0.7	29.0	2.5
16	14.5	31.1	3.6	14.7	2.4	0.7	0.1	0.1	0.7	29.5	2.4
17	14.6	31.3	3.6	14.8	2.3	0.7	0.1	0.1	0.6	29.4	2.4
18	14.5	31.4	3.5	14.9	2.3	0.7	0.1	0.2	0.7	29.3	2.4
19	17.7	33.0	3.2	11.9	1.7	0.3	0.1	0.1	0.9	29.3	1.7
20	17.7	32.5	3.1	11.9	1.6	0.3	0.1	0.1	0.9	29.2	1.6
21	17.7	32.4	3.3	12.2	1.7	0.4	0.0	0.1	0.9	29.2	1.7
22	17.7	32.3	3.0	11.6	1.6	0.4	0.1	0.2	1.0	29.1	2.6
23	17.0	32.3	3.4	12.2	2.0	0.9	0.1	0.1	1.0	29.2	2.2
24	17.3	32.7	3.3	11.9	1.7	0.4	0.1	0.1	0.9	28.9	1.8
25	17.4	32.8	3.3	12.3	1.6	0.4	0.1	0.2	0.9	29.2	1.8
26	16.9	32.2	3.1	12.3	1.7	0.4	0.1	0.2	0.9	29.2	2.2
27	16.6	29.8	2.9	11.1	1.7	0.5	0.0	0.5	1.4	29.0	5.7
28	16.9	30.0	3.0	11.3	1.7	0.5	0.0	0.5	1.5	29.2	5.6
29	16.6	29.6	2.8	11.6	1.7	0.4	0.0	0.4	1.4	29.1	5.4
30	16.3	30.7	3.3	12.6	1.9	0.6	0.1	0.3	0.9	29.2	3.5
31	16.8	29.8	2.9	11.2	1.8	0.3	0.0	0.5	1.4	28.9	5.8
32	14.1	29.8	3.3	13.4	2.4	0.7	0.1	0.2	1.3	29.3	4.9
33	14.0	28.3	3.2	12.9	2.0	0.6	0.2	0.3	1.7	29.4	6.7
34	14.2	29.4	3.1	13.6	2.3	0.6	0.2	0.2	1.3	29.5	4.9
35	14.0	28.2	3.2	12.6	2.0	0.7	0.1	0.3	1.8	29.5	7.3
36	14.1	29.5	3.1	13.4	2.2	0.8	0.2	0.2	1.3	29.6	5.2
37	14.1	29.3	3.1	13.4	2.3	0.9	0.1	0.2	1.4	29.6	5.6
38	13.9	27.8	3.0	12.4	2.0	0.6	0.1	0.4	1.9	29.5	7.7
39	14.0	28.9	3.0	13.2	2.2	0.6	0.1	0.3	1.5	29.6	6.0
40	13.8	27.2	3.0	12.1	1.9	0.4	0.1	0.4	2.2	29.2	9.0
41	13.6	26.9	2.9	11.8	1.9	0.5	0.1	0.5	2.3	29.0	9.5
42	17.1	32.9	3.4	12.5	1.8	0.4	0.0	0.1	0.7	29.6	1.3
43	14.9	33.2	3.6	14.8	2.2	0.5	0.1	0.1	0.4	29.6	0.7

Appendix 4.2 (continued) - Monazite Analyses

No.	La_2O_3 (wt %)	Ce_2O_3 (wt %)	Pr_2O_3 (wt %)	Nd_2O_3 (wt %)	Sm_2O_3 (wt %)	Gd_2O_3 (wt %)	Y_2O_3 (wt %)	SiO_2 (wt %)	CaO (wt %)	P_2O_5 (wt %)	ThO_2 (wt %)
44	17.3	32.8	3.3	12.4	1.8	0.5	0.0	0.1	0.8	29.8	1.3
45	17.7	32.4	3.0	11.8	1.7	0.3	0.1	0.1	0.9	29.6	1.8
46	18.1	32.6	2.9	11.3	1.7	0.3	0.1	0.2	0.9	29.4	2.0
47	17.2	32.7	3.3	12.5	1.7	0.3	0.1	0.2	0.8	29.5	1.3
48	14.7	32.9	3.5	15.0	2.2	0.5	0.1	0.1	0.4	29.5	0.7
49	17.5	33.1	3.1	12.3	1.7	0.5	0.1	0.2	0.8	29.3	1.5
50	17.9	29.3	2.7	9.7	1.4	0.2	0.0	0.3	2.0	29.2	6.5
51	17.5	28.8	2.6	9.7	1.4	0.3	0.0	0.3	2.1	29.1	6.8
52	17.8	29.3	2.6	9.8	1.4	0.3	0.0	0.4	1.8	29.2	6.4
53	17.8	29.5	2.7	10.0	1.4	0.3	0.0	0.3	1.8	29.1	6.5
54	17.5	29.1	2.6	9.7	1.5	0.3	0.1	0.4	2.1	29.1	7.0
55	17.5	28.8	2.7	9.9	1.5	0.2	0.1	0.3	1.9	29.2	6.8
56	13.7	25.7	2.6	10.8	1.7	0.4	0.1	1.9	2.7	27.8	8.2
57	15.1	29.4	3.2	12.3	2.2	0.9	0.2	0.3	1.2	29.2	4.1
58	14.8	29.1	3.0	12.3	2.4	1.4	0.3	0.3	1.0	29.3	4.2
59	15.1	30.0	3.0	12.0	2.0	0.7	0.1	0.4	1.8	28.9	2.6
60	16.6	31.5	3.3	12.7	2.0	0.6	0.1	0.2	0.9	29.1	2.7
61	16.0	29.5	3.0	12.2	2.1	0.8	0.2	0.4	1.1	28.9	4.7
62	16.3	29.2	3.0	11.8	2.0	0.6	0.1	0.5	1.2	28.9	5.5
63	15.5	29.8	3.3	13.1	2.5	1.1	0.2	0.3	0.9	29.2	3.4
64	14.6	27.9	3.0	11.9	2.0	0.9	0.2	2.6	2.6	28.1	3.4
65	13.8	29.2	3.2	13.1	2.0	0.5	0.1	0.3	1.6	28.8	6.1
66	14.1	30.5	3.6	14.4	2.2	0.6	0.1	0.2	1.0	29.3	3.6
67	14.0	30.1	3.4	14.2	2.5	0.7	0.1	0.2	1.0	29.2	3.8
68	14.0	29.9	3.4	14.4	2.4	0.7	0.1	0.1	1.0	29.2	3.7
69	16.8	30.3	3.1	11.6	1.9	0.5	0.1	0.4	1.1	29.1	5.1
70	17.0	30.1	2.8	11.7	1.9	0.7	0.1	0.3	1.0	29.3	4.5
71	16.5	29.0	2.9	11.2	1.7	0.4	0.1	0.5	1.4	28.9	6.9
72	13.8	29.5	3.1	14.1	2.4	0.7	0.1	0.2	1.2	29.2	4.6
73	14.8	31.7	3.5	14.6	2.3	0.6	0.1	0.1	0.7	29.4	2.4
74	16.4	31.9	3.2	12.6	1.9	0.5	0.1	0.2	0.9	29.2	2.4
75	17.3	31.5	3.1	11.6	1.8	0.4	0.0	0.2	0.9	29.3	2.7
76	17.2	30.3	2.8	10.9	1.7	0.5	0.0	0.2	1.5	29.1	4.7
77	16.9	32.5	3.2	12.3	1.7	0.3	0.0	0.2	0.9	29.0	2.2
78	16.5	32.8	3.3	12.8	1.8	0.4	0.0	0.2	0.8	29.3	1.7
79	14.6	31.9	3.7	14.7	2.3	0.6	0.0	0.2	0.5	29.5	1.7
80	14.4	31.6	3.4	14.8	2.3	0.6	0.1	0.2	0.6	29.5	1.8
81	15.8	32.4	3.2	13.4	1.8	0.4	0.0	0.2	0.7	29.1	1.8
82	14.6	31.5	3.6	14.0	2.2	0.6	0.1	0.3	0.8	28.9	2.8
83	15.5	30.4	3.6	15.3	3.0	0.9	0.5	0.1	0.2	29.6	0.2
84	15.5	30.6	3.3	15.2	2.8	0.9	0.5	0.2	0.2	29.4	0.2
85	16.0	30.8	3.4	14.4	2.6	0.8	0.3	0.2	0.3	29.4	0.8

Appendix 4.2 (continued) - Monazite Analyses

No.	L _a 2O ₃ (wt %)	Ce ₂ O ₃ (wt %)	Pr ₂ O ₃ (wt %)	Nd ₂ O ₃ (wt %)	Sm ₂ O ₃ (wt %)	Gd ₂ O ₃ (wt %)	Y ₂ O ₃ (wt %)	SiO ₂ (wt %)	CaO (wt %)	P ₂ O ₅ (wt %)	ThO ₂ (wt %)
86	16.5	31.7	3.2	13.3	2.2	0.7	0.1	0.4	0.5	29.1	1.3
87	16.3	30.9	3.2	12.8	2.1	0.6	0.1	1.1	0.6	28.5	1.3
88	15.6	31.3	3.5	15.0	2.8	0.8	0.3	0.2	0.3	29.3	0.2
89	14.9	29.7	3.1	12.4	1.8	0.4	0.1	0.2	1.5	29.7	6.0
90	14.7	29.2	3.2	12.5	1.9	0.4	0.1	0.2	1.5	29.6	6.2
91	14.7	29.4	3.1	12.5	1.8	0.5	0.1	0.2	1.5	29.5	6.1
92	14.7	29.3	3.1	12.5	1.8	0.4	0.1	0.2	1.6	29.3	6.0
93	14.6	29.4	3.1	12.3	1.8	0.6	0.1	0.3	1.6	29.4	6.4
94	14.7	29.6	3.2	12.6	1.7	0.3	0.1	0.3	1.5	29.5	6.0
95	14.9	29.7	3.2	12.5	1.9	0.5	0.1	0.2	1.4	29.3	5.9
96	14.9	29.9	3.0	12.5	1.8	0.6	0.1	0.2	1.5	29.4	6.0
97	14.6	29.4	3.2	12.6	1.8	0.4	0.1	0.2	1.5	29.4	6.2
98	14.6	29.8	2.9	12.5	1.9	0.5	0.1	0.3	1.5	29.2	5.9
99	16.7	30.8	3.1	11.9	1.9	0.6	0.1	0.2	1.1	29.4	4.1
100	16.7	31.1	2.9	12.5	1.9	0.3	0.1	0.2	0.9	29.3	3.1
101	16.9	30.5	3.1	11.4	1.7	0.5	0.0	0.3	1.3	29.0	4.7
102	16.8	30.1	2.7	11.3	1.6	0.4	0.0	0.4	1.5	28.8	5.4
103	16.3	31.0	3.1	12.4	2.0	0.5	0.1	0.3	0.9	29.1	3.6
104	15.1	29.5	3.0	12.0	1.7	0.4	0.1	0.3	1.5	29.0	6.3
107	15.1	31.7	3.5	15.0	2.6	0.8	0.4	0.0	0.2	29.2	0.3
108	14.9	31.5	3.3	14.9	2.8	0.9	0.6	0.1	0.2	29.3	0.3
109	14.6	30.7	3.3	14.8	2.8	1.1	0.6	0.1	0.3	29.2	0.3
110	14.9	30.8	3.5	14.6	2.6	1.1	0.5	0.1	0.5	29.8	1.1
111	14.9	30.9	3.4	14.7	2.7	0.9	0.5	0.1	0.4	30.1	1.2
112	15.0	30.9	3.4	14.8	2.6	1.1	0.5	0.1	0.4	29.8	1.2
113	14.8	30.3	3.4	14.4	2.7	1.2	0.6	0.2	0.6	29.7	1.3
114	14.7	31.1	3.4	15.3	2.9	0.8	0.4	0.1	0.4	29.8	0.5
115	14.7	30.8	3.4	14.9	2.8	0.9	0.7	0.1	0.3	29.9	0.7
116	14.5	31.0	3.6	15.3	2.8	1.0	0.6	0.1	0.3	29.9	0.8
117	14.7	31.0	3.7	15.4	2.8	1.0	0.5	0.1	0.4	30.3	0.6
120	6.5	18.6	2.7	12.0	3.0	1.8	0.2	20.0	6.2	16.3	0.1

Appendix 4.2 (continued) - Monazite Analyses

No.	UO ₂ (wt %)	PbO (wt %)	Total (wt %)	Th (ppm) (ppm)	U (ppm) (ppm)	initial time (Ma)	Initial Pb (ppm)	Th* (ppm)	Age (Ma)
3	0.1	0.2	100.7	12488	564	3174	2290	15104	2705
4	0.3	1.0	101.2	63309	2221	3046	10652	73374	2684
5	0.3	0.9	100.1	53660	2565	3165	9901	65533	2676
6	0.1	0.8	99.8	55620	458	2771	7580	57605	2686
8	0.0	0.9	98.7	59021	0	2980	8404	59021	2980
9	0.2	0.4	101.1	19905	2019	3621	5248	30149	2623
10	0.2	0.4	101.3	19316	1966	3794	5439	29695	2736
12	0.3	0.4	100.4	21364	2213	3689	5821	32765	2655
13	0.2	0.4	100.5	20344	1975	3730	5506	30614	2725
14	0.3	0.4	100.6	21144	2230	3725	5874	32729	2666
15	0.2	0.4	100.0	21601	2186	3652	5759	32772	2646
16	0.2	0.4	100.5	21434	2168	3703	5823	32643	2680
17	0.2	0.4	100.6	20968	2036	3736	5690	31575	2729
18	0.3	0.4	100.5	21276	2248	3712	5885	32918	2656
19	0.1	0.2	100.3	14940	696	3039	2617	18091	2584
20	0.1	0.2	99.3	14430	661	3114	2593	17462	2651
21	0.1	0.2	99.9	15230	608	3068	2632	17996	2662
22	0.1	0.3	99.9	22577	688	2986	3648	25660	2674
23	0.2	0.3	100.9	19299	1366	2971	3580	25410	2358
24	0.1	0.3	99.3	15739	688	3159	2854	18918	2705
25	0.1	0.3	100.0	15704	502	3120	2684	18011	2775
26	0.1	0.3	99.6	19255	688	3108	3324	22405	2732
27	0.1	0.7	100.2	50110	1005	2866	7428	54527	2661
28	0.1	0.7	100.9	48941	846	2826	7065	52637	2650
29	0.1	0.7	99.9	47421	899	2838	6922	51355	2645
30	0.2	0.5	100.0	30451	1807	3327	6225	39076	2711
31	0.1	0.7	100.3	50628	873	2803	7241	54426	2629
32	0.3	0.8	100.7	43273	2715	3346	9018	56279	2699
33	0.3	0.9	100.6	58661	2336	3126	10353	69395	2710
34	0.3	0.7	100.4	43448	2662	3313	8897	56119	2685
35	0.3	1.0	101.0	64065	2213	3043	10746	74086	2687
36	0.3	0.8	100.8	45311	2574	3293	9064	57516	2705
37	0.3	0.8	101.2	48888	2592	3224	9399	61015	2681
38	0.2	1.1	100.5	67906	2151	3003	11096	77579	2677
39	0.3	0.8	100.5	52342	2389	3132	9466	63334	2667
40	0.2	1.2	100.6	78952	1957	2912	12133	87619	2659
41	0.2	1.2	100.4	83786	2098	2894	12799	93050	2641
42	0.1	0.2	100.0	11266	564	3175	2104	13882	2666
43	0.1	0.1	100.4	6099	943	4228	2402	11677	2682

Appendix 4.2 (continued) - Monazite Analyses

No.	UO ₂ (wt %)	PbO (wt %)	Total (wt %)	Th (ppm) (ppm)	U (ppm) (ppm)	initial time (Ma)	Initial Pb (ppm)	Th* (ppm)	Age (Ma)
44	0.1	0.2	100.1	11143	441	3159	1990	13181	2741
45	0.1	0.3	99.8	15379	573	3192	2755	18045	2788
46	0.1	0.3	99.8	17655	450	3044	2860	19692	2769
47	0.1	0.2	99.8	11170	582	3136	2071	13849	2619
48	0.1	0.1	99.9	6231	934	4175	2369	11674	2678
49	0.1	0.2	100.3	13121	582	3196	2418	15829	2730
50	0.1	0.8	100.1	56964	494	2729	7649	59088	2641
51	0.1	0.8	99.7	59618	688	2744	8146	62583	2628
52	0.1	0.8	99.8	55840	749	2754	7718	59075	2620
53	0.1	0.8	100.4	56912	670	2722	7715	59790	2605
54	0.1	0.9	100.4	61877	661	2745	8429	64728	2637
55	0.1	0.9	99.8	59328	917	2800	8417	63316	2643
56	0.3	1.1	97.0	71957	2486	3087	12267	83301	2723
57	0.1	0.6	98.9	36014	1296	3034	6052	41872	2666
58	0.1	0.6	98.9	37218	1313	3054	6286	43177	2689
59	0.2	0.4	97.2	22638	1560	3436	4987	30250	2720
60	0.2	0.4	100.3	23631	1878	3401	5330	32725	2617
61	0.2	0.7	99.7	41524	1895	3081	7364	50164	2625
62	0.2	0.8	100.1	48554	2124	3170	8844	58397	2714
63	0.2	0.5	100.2	30293	1587	3349	6085	37899	2785
64	0.2	0.5	98.0	29976	2080	3233	6131	39728	2565
65	0.3	0.9	99.9	53827	2265	3086	9439	64164	2658
66	0.4	0.6	100.5	31523	3085	3632	8248	47217	2654
67	0.3	0.6	100.1	33131	2874	3618	8306	47705	2720
68	0.4	0.6	99.8	32094	3112	3709	8615	48200	2712
69	0.3	0.7	101.0	44415	2283	3230	8510	55111	2699
70	0.3	0.7	100.4	39107	2433	3352	8153	50777	2708
71	0.2	0.9	100.7	60480	2080	3014	10029	69854	2664
72	0.3	0.7	99.7	40012	2451	3371	8370	51810	2730
73	0.2	0.4	100.9	21399	1922	3578	5340	31058	2671
74	0.2	0.4	99.9	20696	1569	3400	4608	28295	2642
75	0.2	0.4	99.5	23508	1463	3266	4748	30411	2642
76	0.1	0.6	99.7	41067	1287	2884	6401	46741	2578
77	0.1	0.3	99.5	19448	740	3033	3294	22796	2648
78	0.0	0.2	99.8	14957	106	3060	2260	15438	2975
79	0.2	0.3	100.2	14826	1613	3612	3990	22994	2571
80	0.2	0.3	99.8	16126	1878	3725	4642	25880	2598
81	0.1	0.3	99.2	15511	1005	3259	3153	20245	2618
82	0.2	0.4	99.9	24668	2045	3484	5808	34745	2653
83	0.3	0.2	99.8	2030	2257	12346	2744603	3698016	2705
84	0.3	0.2	99.3	1960	2257	13459	8185269	9813620	2809
85	0.3	0.3	99.6	6670	2548	6721	18469	53212	2834

Appendix 4.2 (continued) - Monazite Analyses

No.	UO ₂ (wt %)	PbO (wt %)	Total (wt %)	Th (ppm) (ppm)	U (ppm) (ppm)	initial time (Ma)	Initial Pb (ppm)	Th* (ppm)	Age (Ma)
86	0.3	0.3	99.6	11091	2503	4978	7404	30076	2720
87	0.3	0.3	98.1	11135	2459	4858	6937	28964	2683
88	0.3	0.2	99.7	2030	2556	13542	10065529	11966049	2725
89	0.3	0.9	100.9	53098	2336	3142	9577	63864	2688
90	0.3	0.9	100.7	54117	2406	3117	9687	65159	2664
91	0.3	0.9	100.7	53985	2398	3114	9651	64981	2662
92	0.3	0.9	100.1	53054	2415	3124	9560	64150	2661
93	0.3	0.9	100.7	55883	2248	3112	9829	66189	2696
94	0.3	0.9	100.5	52649	2292	3136	9459	63202	2688
95	0.3	0.8	100.7	51463	2380	3151	9391	62450	2677
96	0.3	0.9	101.1	53054	2406	3104	9481	64069	2646
97	0.3	0.9	100.7	54258	2451	3109	9710	65486	2652
98	0.3	0.9	100.4	52087	2512	3202	9759	63794	2702
99	0.1	0.6	100.5	36163	1181	3022	5974	41493	2685
100	0.2	0.5	99.8	27516	1728	3300	5637	35718	2663
101	0.1	0.6	100.1	41243	820	2903	6197	44868	2696
102	0.1	0.7	99.8	47719	890	2871	7047	51636	2678
103	0.1	0.5	99.9	32024	1049	3114	5478	36835	2763
104	0.3	0.9	100.1	55040	2389	3153	9947	66073	2703
107	0.2	0.2	99.2	35469	2362	10187	291690	505096	2817
108	0.2	0.2	99.2	2663	2124	10774	556405	896560	2853
109	0.3	0.2	98.3	2830	2459	11018	816309	1277779	2793
110	0.2	0.2	99.8	9702	1322	4107	3442	17261	2716
111	0.1	0.2	100.1	10686	1287	3940	3380	17729	2709
112	0.1	0.2	100.2	10405	1164	4069	3358	16990	2847
113	0.2	0.3	99.6	11635	1675	4325	4606	21822	2799
114	0.1	0.1	99.5	4324	450	4105	1377	6893	2924
115	0.1	0.1	99.6	6556	908	4118	2352	11762	2709
116	0.1	0.1	100.1	6653	908	4012	2276	11714	2658
117	0.1	0.1	100.6	5018	529	3515	1287	7641	2527
120	0.2	0.1	87.6	1081	1957	11059	675304	1051978	1824

Appendix 4.3.1

Sample:9703-6365

Laser diameter: 20 μm																			
Analysis	^{234}Pb	^{206}Pb	$^{206}\text{Pb}/^{238}\text{U}$	Error	$^{207}\text{Pb}/^{235}\text{U}$	Error	$^{207}\text{Pb}/^{206}\text{Pb}$	Error	$^{206}\text{Pb}/^{238}\text{U}$ Age	Error	$^{207}\text{Pb}/^{235}\text{U}$ Age	Error	$^{207}\text{Pb}/^{206}\text{Pb}$ Age	Error	$^{207}\text{Pb}/^{235}\text{U}$ Age	Error	$^{207}\text{Pb}/^{206}\text{Pb}$ Age	Error	Discordance
Number	cps	cps rad	(2 σ)	(2 σ)	(2 σ)	(2 σ)	(2 σ)	(2 σ)	(Ma)	(2 σ)	(Ma)	(2 σ)	(Ma)	(2 σ)	(Ma)	(2 σ)	(Ma)	(2 σ)	(%)
1	0	81889	0.159	0.005	1.555	0.048	0.071	0.001	954	27	952	19	955	27	955	27	955	27	0.1
2	3	125978	0.191	0.006	2.110	0.064	0.080	0.001	1127	34	1152	21	1199	22	122	22	6.6		
3	0	285781	0.145	0.005	1.461	0.045	0.073	0.001	875	27	915	18	1004	21	13.8				
4	0	2730721	0.548	0.019	15.454	0.464	0.204	0.002	2815	78	2844	28	2861	16	2.0				
6	0	1094469	0.564	0.020	16.740	0.502	0.215	0.002	2883	83	2920	28	2942	16	2.5				
7	3	17419	0.539	0.023	15.712	0.471	0.211	0.003	2779	97	2859	28	2911	21	5.5				
8	0	20274	0.507	0.021	13.226	0.397	0.189	0.002	2645	88	2696	28	2732	20	3.9				
9	0	191372	0.640	0.028	18.845	0.566	0.213	0.002	3187	109	3034	29	2931	17	-11.1				
10	2	86917	0.551	0.025	14.773	0.443	0.196	0.002	2828	102	2801	28	2789	17	-1.7				
11	0	25948	0.541	0.026	14.929	0.448	0.201	0.003	2788	109	2811	28	2837	21	2.1				
12	0	38857	0.515	0.020	14.388	0.432	0.202	0.002	2678	86	2776	28	2844	18	7.1				
13	6	168076	0.528	0.024	14.056	0.422	0.192	0.002	2732	101	2753	28	2755	17	1.0				
14	0	274393	0.515	0.025	14.142	0.424	0.199	0.003	2678	105	2759	28	2816	21	6.0				
15	0	256705	0.495	0.022	13.564	0.407	0.198	0.003	2593	96	2720	28	2811	21	9.4				
16	0	467271	0.585	0.025	18.915	0.568	0.234	0.002	2970	103	3037	29	3078	16	4.4				
17	0	142525	0.509	0.021	13.614	0.409	0.194	0.002	2653	91	2723	28	2773	17	5.3				
18	262	104162	0.488	0.017	12.995	0.390	0.201	0.010	2563	73	2679	28	2831	79	11.5				
19	0	280583	0.583	0.025	17.354	0.521	0.215	0.002	2962	102	2955	28	2947	16	-0.7				
20	0	143600	0.479	0.021	12.620	0.379	0.191	0.002	2522	90	2652	28	2752	17	10.1				
21	0	72204	0.570	0.021	20.564	0.617	0.261	0.003	2909	86	3118	29	3255	17	13.2				
22	0	708942	0.620	0.026	21.254	0.638	0.248	0.003	3112	101	3150	29	3172	16	2.4				
23	318	1050207	0.430	0.028	9.671	0.290	0.162	0.002	2307	125	2404	27	2478	22	8.2				
24	5	33602	0.522	0.020	14.034	0.421	0.195	0.002	2709	82	2752	28	2786	20	3.4				
25	0	108036	0.535	0.026	14.470	0.434	0.197	0.002	2760	108	2781	28	2799	17	1.7				
26	0	47322	0.519	0.023	15.805	0.474	0.220	0.002	2696	96	2865	28	2984	17	11.8				

Appendix 4.3.1 (continued)

Analysis Number	^{204}Pb cps	^{206}Pb cps	$^{208}\text{Pb}/^{238}\text{U}$	Error (2 σ)	$^{207}\text{Pb}/^{235}\text{U}$	Error (2 σ)	$^{207}\text{Pb}/^{206}\text{Pb}$	Error (2 σ)	$^{208}\text{Pb}/^{235}\text{U}$	Error (2 σ)	$^{207}\text{Pb}/^{235}\text{U}$ Age (Ma)	Error (2 σ)	$^{207}\text{Pb}/^{206}\text{Pb}$ Age (Ma)	Error (2 σ)	$^{207}\text{Pb}/^{206}\text{Pb}$ Age (Ma)	Error (2 σ)	Discordance (%)
27	0	184214	0.508	0.023	13.547	0.407	0.193	0.003	2647	98	2719	28	2767	22	5.3		
27b	0	252620	0.608	0.024	17.415	0.523	0.208	0.002	3063	97	2958	28	2888	17	-7.6		
28	0	275888	0.549	0.024	13.941	0.418	0.184	0.002	2821	99	2746	28	2686	18	-6.2		
29	0	114826	0.549	0.021	14.521	0.436	0.191	0.003	2822	88	2784	28	2752	24	-3.2		
30	0	502779	0.566	0.032	14.746	0.443	0.188	0.009	2893	132	2799	28	2726	82	-7.6		
31	0	267408	0.570	0.036	14.746	0.443	0.186	0.003	2906	147	2799	28	2705	29	-9.2		
32	0	141287	0.529	0.019	13.681	0.411	0.187	0.002	2739	80	2728	28	2720	17	-0.9		
33	0	63579	0.508	0.025	13.826	0.415	0.198	0.002	2649	104	2738	28	2809	17	7.0		
34	0	74889	0.512	0.022	12.954	0.389	0.183	0.002	2664	94	2676	28	2683	22	0.9		
35	0	375389	0.553	0.075	14.176	0.425	0.185	0.004	2837	304	2762	28	2703	39	-6.1		
36	0	93209	0.504	0.045	13.033	0.391	0.187	0.003	2630	191	2682	28	2719	22	4.0		
37	0	91371	0.587	0.023	17.930	0.538	0.221	0.002	2976	94	2986	28	2986	17	0.4		
38	454	105963	0.515	0.022	12.434	0.373	0.181	0.002	2676	92	2638	28	2661	17	-0.7		
39	0	961778	0.510	0.022	14.798	0.444	0.208	0.003	2657	94	2802	28	2887	20	9.7		
40	0	766571	0.501	0.075	12.072	0.362	0.173	0.004	2620	312	2610	28	2588	41	-1.5		
41	0	411920	0.529	0.019	12.972	0.389	0.177	0.002	2737	80	2678	28	2625	17	-5.2		
42	5	330084	0.536	0.025	13.641	0.409	0.185	0.002	2766	104	2725	28	2697	17	-3.1		
43	0	129915	0.548	0.023	15.236	0.457	0.202	0.003	2817	95	2830	28	2842	21	1.1		
44	160	532266	0.722	0.076	19.634	0.589	0.188	0.004	3502	279	3074	29	2723	38	-37.3		
45	0	754728	0.555	0.046	14.955	0.449	0.196	0.003	2847	187	2812	28	2792	22	-2.5		
46	0	355063	0.574	0.023	16.530	0.496	0.208	0.002	2922	94	2908	28	2890	17	-1.4		
47	13	595793	0.563	0.023	14.951	0.449	0.192	0.002	2878	93	2812	28	2757	17	-5.5		
48	0	359481	0.569	0.026	16.253	0.488	0.207	0.002	2902	104	2892	28	2879	17	-1.0		
49	0	179855	0.628	0.024	20.699	0.621	0.239	0.003	3141	95	3125	29	3112	19	-1.2		
50	0	119211	0.503	0.022	12.207	0.367	0.177	0.002	2625	93	2620	28	2623	18	-0.1		
51	2	252450	0.509	0.018	12.967	0.389	0.184	0.002	2653	78	2677	28	2686	18	1.5		
52	0	433197	0.526	0.024	13.233	0.397	0.181	0.002	2723	102	2696	28	2665	18	-2.7		

Appendix 4.3.1 (continued)

Analysis Number	^{204}Pb cps	^{206}Pb cps	$^{206}\text{Pb}/^{238}\text{U}$	Error (2 σ)	$^{207}\text{Pb}/^{235}\text{U}$	Error (2 σ)	$^{207}\text{Pb}/^{206}\text{Pb}$	Error (2 σ)	$^{206}\text{Pb}/^{238}\text{U}$ Age (Ma)	Error (2 σ)	$^{207}\text{Pb}/^{235}\text{U}$ Age (Ma)	Error (2 σ)	$^{207}\text{Pb}/^{206}\text{Pb}$ Age (Ma)	Error (2 σ)	Discordance (%)
53	0	28562	0.537	0.025	13.595	0.408	0.183	0.002	2770	104	2722	28	2678	17	-4.2
54	0	68781	0.635	0.026	20.039	0.601	0.228	0.002	3171	102	3093	29	3037	16	-5.6
55	0	212176	0.541	0.026	13.603	0.409	0.182	0.002	2789	107	2722	28	2673	18	-5.4
56	0	383876	0.550	0.021	15.220	0.457	0.200	0.002	2826	85	2829	28	2825	17	-0.0
57	0	1039064	0.515	0.019	12.719	0.382	0.178	0.002	2680	80	2659	28	2634	18	-2.1
58	5	180066	0.501	0.021	13.112	0.394	0.189	0.002	2620	90	2588	28	2733	18	5.0
59	12	591804	0.546	0.023	14.502	0.435	0.192	0.002	2808	94	2783	28	2758	17	-2.2
60	8	771256	0.554	0.019	14.589	0.438	0.190	0.002	2843	79	2789	28	2741	17	-4.6
61	0	584738	0.522	0.019	13.080	0.393	0.182	0.002	2706	81	2685	28	2670	17	-1.7
62	0	404800	0.534	0.022	12.506	0.376	0.170	0.002	2757	93	2643	28	2559	18	-9.5
63	0	110255	0.500	0.019	13.612	0.409	0.197	0.002	2613	82	2723	28	2799	18	8.0
64	0	318305	0.524	0.023	13.068	0.392	0.180	0.002	2715	97	2685	28	2657	17	-2.7
65	5	129932	0.515	0.019	13.038	0.391	0.184	0.002	2679	82	2682	28	2686	18	0.3
66	3	94719	0.526	0.021	14.168	0.425	0.195	0.002	2724	89	2761	28	2789	17	2.9
67	0	61325	0.520	0.031	15.163	0.456	0.210	0.004	2700	131	2826	28	2904	32	8.6
68	0	129772	0.566	0.031	18.339	0.551	0.232	0.007	2893	126	3008	29	3069	49	7.1
69	0	95554	0.564	0.021	16.328	0.490	0.209	0.002	2882	86	2896	28	2898	19	0.7
70	0	293490	0.653	0.032	23.018	0.691	0.255	0.003	3240	123	3228	29	3214	17	-1.0
71	35	493985	0.682	0.028	23.676	0.711	0.252	0.003	3351	105	3255	29	3195	16	-6.3
72	0	176446	0.551	0.023	15.433	0.463	0.202	0.003	2828	97	2842	28	2843	20	0.7
73	0	416753	0.644	0.037	21.040	0.632	0.233	0.003	3204	143	3140	29	3074	21	-5.4
74	0	602224	0.483	0.034	13.195	0.397	0.197	0.010	2540	148	2594	28	2798	81	11.2
Average		243980		0.027		0.501		0.004							
STD (2 σ)				0.006		0.118		0.002							
STD (%)				23.339		23.486		68.932							

Appendix 4.3.2

Sample:9704-7069

Laser diameter: 40 μm																		
Analysis	^{204}Pb	^{206}Pb	$^{206}\text{Pb}/^{238}\text{U}$	Error	$^{207}\text{Pb}/^{235}\text{U}$	Error	$^{207}\text{Pb}/^{206}\text{Pb}$	Error	$^{208}\text{Pb}/^{238}\text{U}$	$^{207}\text{Pb}/^{235}\text{U}$ Age	Error	$^{207}\text{Pb}/^{235}\text{U}$ Age	Error	$^{207}\text{Pb}/^{206}\text{Pb}$ Age	Error	$^{207}\text{Pb}/^{206}\text{Pb}$ Age	Error	Discordance (%)
Number	cps	cps rad	(2 σ)	(2 σ)	(2 σ)	(2 σ)	(2 σ)	(2 σ)	(2 σ)	(Ma)	(2 σ)	(Ma)	(2 σ)	(Ma)	(2 σ)	(Ma)	(2 σ)	(%)
1	0	214408	0.504	0.017	12.904	0.387	0.186	0.002	2630	74	2673	28	2706	17	2706	17	3.5	
2	9	339261	0.520	0.017	13.239	0.397	0.185	0.002	2700	73	2697	28	2695	17	2695	17	-0.2	
3	6	494684	0.531	0.017	13.503	0.405	0.185	0.002	2744	73	2715	28	2695	17	2695	17	-2.2	
4	0	271175	0.517	0.018	13.204	0.396	0.186	0.002	2687	75	2694	28	2706	17	2706	17	0.9	
5	6	349530	0.528	0.018	13.503	0.405	0.185	0.002	2734	76	2715	28	2702	17	2702	17	-1.5	
6	0	296990	0.528	0.019	13.364	0.401	0.184	0.002	2733	80	2706	28	2686	17	2686	17	-2.1	
7	9	320457	0.534	0.018	13.591	0.408	0.185	0.002	2758	77	2722	28	2696	17	2696	17	-2.8	
8	2	84798	0.179	0.006	1.832	0.056	0.074	0.001	1060	32	1057	20	1044	23	1044	23	-1.7	
10	33*	525760	0.539	0.019	13.642	0.409	0.184	0.002	2779	81	2725	28	2692	17	2692	17	-4.0	
11	0	375193	0.534	0.018	13.594	0.408	0.185	0.002	2756	76	2722	28	2699	17	2699	17	-2.6	
12	0	448333	0.540	0.018	13.366	0.401	0.179	0.002	2785	74	2706	28	2648	17	2648	17	-6.4	
13	345*	545582	0.519	0.017	13.764	0.413	0.193	0.003	2693	72	2734	28	2771	22	2771	22	3.5	
14	0	390144	0.494	0.019	12.580	0.378	0.186	0.002	2587	80	2649	28	2704	17	2704	17	5.2	
15	0	736724	0.512	0.018	13.670	0.410	0.194	0.002	2663	77	2727	28	2774	17	2774	17	4.9	
16	12	848528	0.525	0.018	13.365	0.401	0.185	0.002	2719	76	2706	28	2702	17	2702	17	-0.7	
17	18	938147	0.518	0.017	13.311	0.400	0.186	0.002	2689	71	2702	28	2707	17	2707	17	0.8	
18	0	582255	0.508	0.018	13.089	0.393	0.187	0.002	2647	75	2686	28	2714	17	2714	17	3.0	
19	0	795402	0.513	0.019	13.070	0.392	0.185	0.002	2669	82	2685	28	2696	17	2696	17	1.2	
20	0	2404178	0.529	0.018	13.533	0.406	0.186	0.002	2736	76	2718	28	2703	17	2703	17	-1.5	
21	0	56840	0.500	0.018	12.721	0.382	0.185	0.002	2612	77	2659	28	2696	17	2696	17	3.8	
22	0	797209	0.510	0.017	13.043	0.391	0.185	0.002	2655	71	2683	28	2698	17	2698	17	1.9	
24	803*	816152	0.499	0.017	12.862	0.386	0.187	0.002	2608	73	2670	28	2717	17	2717	17	4.9	
25	803*	816152	0.497	0.017	12.698	0.381	0.186	0.002	2600	74	2657	28	2704	17	2704	17	4.7	
26	0	415002	0.492	0.016	12.714	0.382	0.187	0.002	2577	71	2659	28	2719	17	2719	17	6.3	

Appendix 4.3.2 (continued)

Analysis Number	^{204}Pb cps	^{206}Pb cps	$^{206}\text{Pb}/^{238}\text{U}$ (2 σ)	$^{207}\text{Pb}/^{235}\text{U}$ Error (2 σ)	$^{207}\text{Pb}/^{206}\text{Pb}$ Error (2 σ)	$^{206}\text{Pb}/^{238}\text{U}$ Age (Ma)	Error (2 σ) (Ma)	$^{207}\text{Pb}/^{235}\text{U}$ Age (Ma)	Error (2 σ) (Ma)	$^{207}\text{Pb}/^{206}\text{Pb}$ Age (Ma)	Error (2 σ) (Ma)	Error (2 σ) (%)	Discordance (%)	
27	0	271835	0.499	0.017	12.889	0.387	0.188	0.002	2608	74	2672	28	2722	17
28	26*	394534	0.507	0.017	12.975	0.389	0.186	0.002	2643	71	2678	28	2706	17
29	21*	209595	0.500	0.017	12.773	0.384	0.186	0.002	2614	73	2663	28	2704	17
30	0	255489	0.489	0.017	12.523	0.376	0.186	0.002	2568	73	2644	28	2705	17
31	0	194707	0.492	0.017	12.669	0.380	0.187	0.002	2579	72	2655	28	2717	17
32	25*	241413	0.494	0.017	12.662	0.380	0.186	0.002	2588	74	2655	28	2708	17
33	0	240836	0.510	0.019	13.043	0.392	0.186	0.002	2656	79	2683	28	2706	17
34	17*	574732	0.499	0.018	12.771	0.383	0.186	0.002	2609	76	2663	28	2706	17
35	0	300412	0.498	0.017	12.625	0.379	0.184	0.002	2607	71	2652	28	2688	17
36	21*	220435	0.508	0.018	12.977	0.389	0.186	0.002	2649	76	2678	28	2709	17
37	41*	146232	0.516	0.019	13.196	0.396	0.186	0.002	2681	79	2694	28	2705	17
38	3	204446	0.505	0.018	12.921	0.388	0.186	0.002	2634	76	2674	28	2705	17
39	28*	576630	0.504	0.017	12.773	0.383	0.184	0.002	2631	72	2663	28	2687	17
40	8*	297005	0.514	0.018	13.129	0.394	0.186	0.002	2674	76	2689	28	2707	17
41	0	339129	0.504	0.017	12.934	0.388	0.186	0.002	2630	73	2675	28	2710	17
42	2*	347335	0.519	0.018	13.317	0.400	0.186	0.002	2696	74	2702	28	2708	17
43	14*	380137	0.502	0.017	12.893	0.387	0.186	0.002	2622	73	2672	28	2710	17
44	4	591618	0.509	0.018	13.082	0.393	0.186	0.002	2651	78	2686	28	2706	17
45	1	285285	0.518	0.019	13.220	0.397	0.185	0.002	2692	78	2696	28	2698	17
46	1	166827	0.499	0.018	12.787	0.384	0.186	0.002	2609	75	2664	28	2706	17
47	0	729092	0.508	0.017	12.928	0.388	0.185	0.002	2646	73	2674	28	2697	17
48	6	267690	0.502	0.017	12.948	0.389	0.187	0.002	2621	73	2676	28	2717	17
49	0	445341	0.513	0.016	12.965	0.389	0.185	0.002	2669	69	2677	28	2695	19
50	0	312113	0.497	0.017	12.697	0.381	0.186	0.002	2599	73	2657	28	2704	17
51	241	623768	0.511	0.018	13.036	0.391	0.185	0.002	2659	76	2682	28	2703	17
52	4	222565	0.648	0.071	15.825	0.480	0.181	0.004	3219	271	2866	29	2663	34
53	0	501279	0.531	0.018	13.576	0.407	0.186	0.002	2744	75	2721	28	2704	17
54	0	158606	0.509	0.018	13.043	0.391	0.186	0.002	2652	78	2683	28	2707	17

Appendix 4.3.2 (continued)

Number	Analysis	^{204}Pb	^{206}Pb	$^{206}\text{Pb}/^{238}\text{U}$	Error	$^{207}\text{Pb}/^{235}\text{U}$	Error	$^{207}\text{Pb}/^{206}\text{Pb}$	Error	$^{206}\text{Pb}/^{235}\text{U}$ Age	Error	$^{207}\text{Pb}/^{235}\text{U}$ Age	Error	$^{207}\text{Pb}/^{206}\text{Pb}$ Age	Error	Discordance
		cps	cps	rad	(2 σ)	(2 σ)	(2 σ)	(2 σ)	(2 σ)	(Ma)	(2 σ)	(Ma)	(2 σ)	(Ma)	(2 σ)	(%)
55	37*	1712624	0.498	0.017	12.745	0.382	0.186	0.002	2604	71	2661	28	2705	17	4.6	
57	0	655263	0.192	0.007	2.103	0.063	0.080	0.001	1133	36	1150	20	1190	20	5.2	
58	0	391524	0.509	0.016	12.994	0.390	0.186	0.002	2653	70	2679	28	2706	17	2.4	
59	14*	886503	0.532	0.018	13.547	0.407	0.185	0.002	2749	75	2719	28	2698	17	-2.3	
60	17	566506	0.537	0.018	13.754	0.413	0.186	0.002	2771	76	2733	28	2705	17	-3.0	
61	0	1671861	0.500	0.018	12.824	0.385	0.186	0.002	2614	75	2667	28	2708	17	4.2	
62	10*	1923786	0.539	0.018	13.808	0.414	0.186	0.002	2781	75	2737	28	2706	17	-3.4	
64	0	322498	0.510	0.017	13.063	0.392	0.186	0.002	2657	72	2684	28	2706	17	2.2	
65	4	477160	0.527	0.019	13.519	0.406	0.186	0.002	2727	80	2717	28	2703	17	-1.1	
66	0	553343	0.523	0.017	13.426	0.403	0.186	0.002	2711	73	2710	28	2710	17	0.0	
67	0	1124922	0.496	0.017	12.249	0.368	0.179	0.002	2595	75	2624	28	2642	17	2.1	
68	0	892164	0.518	0.018	13.240	0.397	0.186	0.002	2690	75	2697	28	2704	17	0.6	
69	0	357015	0.503	0.018	12.853	0.386	0.186	0.002	2627	75	2669	28	2704	17	3.4	
70	0	622546	0.517	0.018	13.034	0.391	0.183	0.002	2688	74	2682	28	2685	17	-0.2	
71	0	533016	0.516	0.017	13.182	0.396	0.185	0.002	2684	73	2693	28	2702	17	0.8	
72	0	725502	0.501	0.017	12.810	0.384	0.186	0.002	2618	73	2666	28	2705	17	3.9	
73	0	602955	0.508	0.017	12.992	0.390	0.185	0.002	2650	71	2679	28	2699	17	2.2	
74	0	323607	0.501	0.017	12.748	0.383	0.185	0.002	2619	74	2661	28	2700	17	3.7	
75	0	549574	0.495	0.017	12.669	0.380	0.186	0.002	2591	74	2655	28	2707	17	5.2	
76	0	340710	0.504	0.017	12.928	0.388	0.186	0.002	2631	73	2674	28	2708	17	3.4	
77	0	326938	0.507	0.018	12.960	0.389	0.186	0.002	2643	76	2677	28	2705	17	2.8	
78	0	422879	0.509	0.018	13.094	0.393	0.187	0.002	2651	76	2686	28	2717	17	3.0	
79	0	358891	0.489	0.017	12.494	0.375	0.186	0.002	2568	74	2642	28	2704	17	6.1	
80	0	575115	0.504	0.020	13.025	0.391	0.186	0.002	2630	85	2681	28	2708	17	3.5	
81	0	305823	0.521	0.018	13.346	0.401	0.186	0.002	2704	77	2704	28	2707	17	0.1	
82	0	388537	0.330	0.011	5.088	0.153	0.112	0.001	1837	51	1834	25	1832	19	-0.3	
83	0	739264	0.500	0.017	12.805	0.384	0.186	0.002	2612	74	2665	28	2709	17	4.3	

Appendix 4.3.2 (continued)

Analysis Number	^{204}Pb cps	^{206}Pb cps rad	$^{206}\text{Pb}/^{238}\text{U}$ (2 σ)	$^{207}\text{Pb}/^{235}\text{U}$ Error	$^{207}\text{Pb}/^{206}\text{Pb}$ (2 σ)	Error	$^{206}\text{Pb}/^{238}\text{U}$ Age (Ma)	Error	$^{207}\text{Pb}/^{235}\text{U}$ Age (Ma)	Error	$^{207}\text{Pb}/^{206}\text{Pb}$ Age (2 σ) (Ma)	Error	Discordance (%)		
84	0	767685	0.489	0.018	12.477	0.374	0.185	0.002	2568	77	2641	28	2699	17	5.9
85	0	293058	0.540	0.025	13.629	0.409	0.185	0.002	2782	105	2724	28	2698	17	-3.8
86	0	224076	0.501	0.018	12.852	0.386	0.186	0.002	2620	76	2669	28	2709	17	4.0
87	0	617395	0.512	0.018	13.107	0.393	0.186	0.002	2666	77	2687	28	2703	17	1.7
88	0	348907	0.562	0.037	14.425	0.434	0.186	0.002	2873	150	2778	28	2710	17	-7.5
89	0	519856	0.493	0.017	12.584	0.378	0.185	0.002	2582	74	2649	28	2701	17	5.3
90	0	521319	0.499	0.018	12.752	0.383	0.186	0.002	2611	78	2661	28	2710	17	4.4
91	0	252339	0.514	0.018	13.164	0.395	0.186	0.002	2676	77	2692	28	2704	17	1.3
92	0	246194	0.508	0.018	12.852	0.386	0.184	0.002	2648	74	2669	28	2692	17	2.0
93	0	398093	0.505	0.018	13.008	0.390	0.186	0.002	2637	77	2680	28	2709	17	3.2
94	0	179826	0.499	0.018	12.776	0.383	0.185	0.002	2612	76	2663	28	2697	17	3.8
95	26*	453965	0.515	0.019	13.185	0.396	0.186	0.002	2678	78	2693	28	2705	17	1.2
96	0	442861	0.500	0.018	12.767	0.383	0.185	0.002	2614	76	2663	28	2700	17	3.9
97	0	685590	0.502	0.018	12.860	0.386	0.186	0.002	2624	76	2669	28	2704	17	3.6
98	43*	250697	0.504	0.017	13.155	0.395	0.189	0.002	2631	73	2691	28	2737	17	4.7
99	10*	268734	0.515	0.017	13.333	0.400	0.188	0.002	2676	73	2703	28	2727	17	2.3
358375.125															
Average	280047	0.019		0.392			0.002								
STD (2 σ)		0.005		0.014			0.000								
STD (%)		26.486		3.484			1.474								

Appendix 4.3.3

Sample: 9704-7069A

Laser diameter: 30μm										Laser diameter: 30μm									
	Analysis	^{204}Pb	^{208}Pb	$^{208}\text{Pb}/^{238}\text{U}$	Error	$^{207}\text{Pb}/^{235}\text{U}$	Error	$^{207}\text{Pb}/^{206}\text{Pb}$	Error	$^{205}\text{Pb}/^{206}\text{Pb}$	Error	$^{207}\text{Pb}/^{238}\text{U}$ Age	Error	$^{207}\text{Pb}/^{235}\text{U}$ Age	Error	$^{207}\text{Pb}/^{206}\text{Pb}$ Age	Error	Discordance	
Number	cps	cps	cps	(2σ)		(2σ)		(2σ)		(2σ)		(Ma)	(2σ)	(Ma)	(2σ)	(Ma)	(2σ)	%	
1	114*	302758	0.483	0.019	12.533	0.376	0.189	0.002	2539	84	2645	28	2729	17	2729	17	8.4		
3	53*	560950	0.471	0.025	12.168	0.366	0.188	0.002	2487	109	2617	28	2720	17	2720	17	10.3		
5a	127*	351713	0.464	0.019	12.129	0.364	0.189	0.002	2457	83	2614	28	2737	17	2737	17	12.3		
5b	122	53947	0.456	0.015	11.512	0.345	0.181	0.007	2423	67	2566	28	2657	60	2657	60	10.6		
6a	19*	212403	0.441	0.018	11.461	0.344	0.189	0.002	2354	81	2561	28	2731	17	2731	17	16.5		
6b-core	62*	214712	0.453	0.018	11.775	0.353	0.189	0.002	2410	77	2587	28	2730	17	2730	17	14.0		
6b-rim	18*	244272	0.450	0.016	11.639	0.349	0.188	0.002	2396	72	2576	28	2722	17	2722	17	14.3		
6c	60*	595582	0.490	0.024	12.392	0.372	0.184	0.002	2571	102	2635	28	2685	17	2685	17	5.2		
7	19*	290564	0.451	0.017	11.676	0.350	0.188	0.002	2400	76	2579	28	2724	17	2724	17	14.2		
8	4	124762	0.438	0.015	11.506	0.345	0.190	0.002	2344	65	2565	28	2743	17	2743	17	17.3		
10	124*	178627	0.438	0.014	11.462	0.344	0.190	0.002	2342	62	2562	28	2741	17	2741	17	17.3		
12	115*	687833	0.474	0.016	12.187	0.366	0.187	0.002	2502	71	2619	28	2712	17	2712	17	9.3		
13a	140*	312945	0.402	0.015	9.168	0.275	0.165	0.002	2180	70	2355	27	2508	20	2508	20	15.4		
13b	48*	458329	0.457	0.017	11.667	0.350	0.185	0.002	2424	76	2578	28	2695	17	2695	17	12.0		
Average		295146	0.460		11.879		0.187												
STD (2σ)		0.017			0.394		0.003												
STD (%)		3.714			3.315		1.578												

Appendix 4.3.4

Sample: 9704-7069b

Laser diameter: 30 μm																
Number	Analysis	^{204}Pb	^{206}Pb	$^{208}\text{Pb}/^{238}\text{U}$	Error (2 σ)	$^{207}\text{Pb}/^{235}\text{U}$	Error (2 σ)	$^{208}\text{Pb}/^{206}\text{Pb}$	Error (2 σ)	$^{207}\text{Pb}/^{238}\text{U}$ Age	Error (2 σ)	$^{208}\text{Pb}/^{235}\text{U}$ Age	Error (2 σ)	$^{207}\text{Pb}/^{206}\text{Pb}$ Age	Error (2 σ)	Discordance %
1	3	206152	0.458	0.020	11.765	0.353	0.187	0.002	2432	90	2586	28	2719	17	12.6	
3	68*	923470	0.476	0.018	12.337	0.370	0.188	0.002	2511	78	2630	28	2724	17	9.4	
4	45*	797025	0.480	0.019	12.296	0.369	0.186	0.002	2526	82	2627	28	2707	17	8.1	
5	0	268947	0.464	0.017	12.035	0.361	0.189	0.002	2458	72	2607	28	2730	17	11.9	
6a	0	463937	0.459	0.019	11.691	0.351	0.185	0.002	2436	82	2580	28	2697	17	11.6	
6b	9*	235899	0.449	0.018	11.657	0.350	0.188	0.002	2393	79	2577	28	2728	17	14.7	
7	38*	461483	0.475	0.020	12.284	0.369	0.188	0.002	2504	85	2626	28	2721	17	9.6	
8	57*	144589	0.444	0.017	11.366	0.341	0.187	0.002	2368	75	2554	28	2712	18	15.1	
10	114*	181970	0.457	0.020	12.008	0.361	0.190	0.002	2427	89	2605	28	2746	18	13.9	
Average		163279	0.451		11.687		0.189									
STD (2 σ)			0.009		0.454		0.003									
STD (%)			2.082		3.883		1.457									

Appendix 4.3.5

Sample: 9704-7054

Laser diameter: 30μm									
Analysis	^{204}Pb	^{206}Pb	$^{206}\text{Pb}/^{738}\text{U}$	Error	$^{207}\text{Pb}/^{235}\text{U}$	Error	$^{207}\text{Pb}/^{206}\text{Pb}$	Error	$^{208}\text{Pb}/^{232}\text{Th}$
Number	cps	cps rad	(2σ)	(2σ)	(2σ)	(2σ)	(2σ)	(2σ)	(2σ)
3a	5	25547	0.470	0.017	12.717	0.382	0.196	0.003	2485
3b	61*	50800	0.454	0.017	12.037	0.361	0.192	0.002	2412
4	6	63094	0.434	0.017	11.626	0.349	0.194	0.002	2325
5	38*	29820	0.425	0.016	11.647	0.350	0.198	0.003	2283
6	1	25218	0.435	0.018	11.958	0.359	0.199	0.002	2330
9	59*	22954	0.410	0.015	10.342	0.310	0.185	0.002	2214
11	61*	60968	0.432	0.017	11.483	0.345	0.192	0.002	2316
13	39*	40053	0.422	0.017	11.295	0.339	0.194	0.002	2269
14	7*	51596	0.429	0.017	11.404	0.342	0.193	0.002	2301
16	37*	29097	0.433	0.018	11.620	0.349	0.195	0.002	2319
17	69*	59525	0.425	0.015	11.258	0.338	0.192	0.002	2285
18	276	49641	0.428	0.017	10.762	0.323	0.180	0.004	2299
20a	40*	49166	0.425	0.017	11.173	0.335	0.191	0.002	2282
20b	34*	27031	0.418	0.018	11.193	0.336	0.193	0.002	2250
22a	63*	46144	0.425	0.018	11.306	0.339	0.193	0.002	2282
22b	52*	52206	0.393	0.017	9.563	0.287	0.176	0.002	2138
22c	4	26049	0.478	0.019	12.886	0.387	0.196	0.003	2517
Average		43384	0.428		11.241		0.190		
STD (2σ)		0.022			0.861		0.007		
STD (%)		5.108			7.663		3.647		

187

Appendix 4.3.6

Sample: GAR01

Laser diameter: 30μm																				
Analysis	^{204}Pb	^{206}Pb	$^{206}\text{Pb}/^{238}\text{U}$	Error	$^{207}\text{Pb}/^{235}\text{U}$	Error	$^{207}\text{Pb}/^{206}\text{Pb}$	Error	$^{208}\text{Pb}/^{232}\text{Th}$	Error	$^{207}\text{Pb}/^{235}\text{U}$ Age	Error	$^{207}\text{Pb}/^{206}\text{Pb}$ Age	Error	$^{207}\text{Pb}/^{235}\text{U}$ Age	Error	$^{207}\text{Pb}/^{206}\text{Pb}$ Age	Error	Discordance	
Number	cps	cps rad	(2σ)	(2σ)	(2σ)	(2σ)	(2σ)	(2σ)	(2σ)	(2σ)	(2σ)	(Ma)	(2σ)	(Ma)	(2σ)	(Ma)	(2σ)	(Ma)	(2σ)	%
1	70*	192288	0.453	0.020	12.009	0.360	0.192	0.002	2410	89	2605	28	2760	17	17	15.2				
2	87*	64963	0.417	0.016	11.165	0.335	0.194	0.002	2249	72	2537	28	2778	19	19	22.5				
5	58*	56819	0.460	0.018	12.454	0.374	0.197	0.002	2441	80	2639	28	2803	19	19	15.5				
6	3	121054	0.439	0.018	11.598	0.348	0.192	0.002	2344	79	2573	28	2739	18	18	17.9				
7	175*	220703	0.382	0.016	10.370	0.311	0.197	0.002	2085	74	2468	27	2802	19	19	29.9				
8	64*	217504	0.446	0.017	11.688	0.351	0.190	0.002	2375	77	2580	28	2745	17	17	16.1				
9	5	92824	0.434	0.016	11.649	0.350	0.195	0.002	2325	73	2577	28	2781	17	17	19.5				
10	8	210839	0.442	0.018	11.597	0.348	0.190	0.002	2361	80	2572	28	2745	17	17	16.7				
Average		173723	0.441		11.644		0.192													
STD (2σ)			0.006		0.045		0.002													
STD (%)			1.307		0.390		1.284													

Appendix 4.4 - Uranium-Lead Analyses by Thermal Ionization Mass Spectrometry

Sample number	Description	Weight (mg)	U (ppm)	Pb rad. (ppm)	$\frac{^{204}\text{Pb}}{^{235}\text{U}}$ Model (ppm)	$\frac{^{207}\text{Pb}}{^{238}\text{U}}$	$\frac{^{206}\text{Pb}}{^{238}\text{U}}$	$\frac{^{207}\text{Pb}}{^{235}\text{U}}$	$\frac{^{206}\text{Pb}}{^{238}\text{U}}$	$\frac{^{207}\text{Pb}}{^{206}\text{Pb}}$	discordance (%)	1σ error (Ma)		
9704-7122-1	4 lt pnk abr zr	17	25.17	13.91	11.60	0.247	12.45631	0.51725	0.17478	2687.5	2640.1	2604.0	-3.92	11.0
9704-7122-2	3 dk pnk abr zr	12	99.71	56.32	3.61	0.231	13.34276	0.52597	0.18398	2724.5	2704.2	2689.1	-1.61	0.9
9704-7134-1	3 clr abr zr	8	43.03	22.78	6.07	0.282	11.72762	0.49072	0.17333	2573.8	2582.9	2590.1	0.76	23.9
9704-7134-2	2 pnk abr zr	8	99.58	55.62	2.73	0.348	12.50195	0.50850	0.17831	2650.2	2642.9	2637.2	-0.60	1.7

abbreviations: lt = light, pnk = pink, abr = abraded, zr = zircon, dk = dark, clr = clear.